

Durham E-Theses

*Sequence stratigraphy of a pelagic chalk succession :
The Coniacian - Lower Campanian of the
Anglo-Paris Basin.*

Grant, Simon F.

How to cite:

Grant, Simon F. (1998) *Sequence stratigraphy of a pelagic chalk succession : The Coniacian - Lower Campanian of the Anglo-Paris Basin.*, Durham theses, Durham University. Available at Durham E-Theses Online: <http://etheses.dur.ac.uk/986/>

Use policy

The full-text may be used and/or reproduced, and given to third parties in any format or medium, without prior permission or charge, for personal research or study, educational, or not-for-profit purposes provided that:

- a full bibliographic reference is made to the original source
- a [link](#) is made to the metadata record in Durham E-Theses
- the full-text is not changed in any way

The full-text must not be sold in any format or medium without the formal permission of the copyright holders.

Please consult the [full Durham E-Theses policy](#) for further details.

**Sequence stratigraphy of a pelagic chalk succession:
The Coniacian – Lower Campanian of the Anglo-Paris Basin**

Simon F. Grant

*Department of Geological Sciences
University of Durham*

The copyright of this thesis rests
with the author. No quotation
from it should be published
without the written consent of the
author and information derived
from it should be acknowledged.

A thesis submitted to the University of Durham
in partial fulfilment of the degree of Doctor of Philosophy.

Volume 1



12 AUG 1998



The Seven Sisters, Sussex Coast, viewed from Seaford Head.

No part of this thesis has been submitted previously for a degree in this or any other university. The work described in this thesis is entirely that of the author, except where reference is made to previous published or unpublished work.

A handwritten signature in black ink that reads "Simon Grant". The signature is written in a cursive, flowing style.

Simon Grant

Department of Geological Sciences,

University of Durham

April, 1998

The copyright of this thesis rests with the author. No quotation from it should be published without his prior written consent and information derived from it should be acknowledged.

© 1998 Simon F. Grant

**Sequence stratigraphy of a pelagic chalk succession —
the Coniacian – Lower Campanian of the Anglo-Paris Basin**

The Upper Cretaceous Chalk of Northwest Europe was deposited in an open epi-continental sea during a period of high global eustatic sea-level. The sedimentary rocks preserved largely consist of a compacted, cemented, biogenically-precipitated coccolith ooze, chert layers and marl bands. At intervals in the succession, winnowing and reworking has led to the development of a range of nodular chalks, firmgrounds and hardgrounds, many of which can be traced over large areas of the Anglo-Paris Basin.

Sequence stratigraphical analysis of the Coniacian to Lower Campanian succession has identified twenty-nine third-order (short-term) cycles of relative sea-level change (~400 ka. duration), superimposed upon four second-order (longer-term) cycles (~3.2 Ma, ~2.8 Ma, ~3.2 Ma and ~2.4 Ma duration, respectively). Comparison of the sequence stratigraphical interpretation with independently derived carbon and oxygen isotope data shows a positive correlation. A relative sea-level curve is presented for the Coniacian, Santonian and Lower Campanian, and this is compared to published curves. A sequence stratigraphical model is defined for the Upper Cretaceous chalk.

The third-order cycles represent frequent, basin-wide oceanographic changes for which there are no known tectonic mechanisms. These cycles show a strong correlation with both the $\delta^{13}\text{C}$ and the $\delta^{18}\text{O}$ stable isotope curves, indicating a climatic control on sedimentation, probably linked to a Milankovitch eccentricity rhythm. The long-term trend in the $\delta^{13}\text{C}$ stable isotope values parallels the long-term relative sea-level curve, reflecting changes in productivity as the shelf area expands and contracts with relative sea-level change over the Coniacian to Lower Campanian interval. By contrast, the $\delta^{18}\text{O}$ stable isotope values show little change over the long-term during the Coniacian and Santonian, suggesting that tectonics rather than climate was the controlling factor on sedimentation and relative sea-level change. This is corroborated by the fact that the long-term cycle is coincident with a phase of increased activity at the mid-ocean ridges which is thought to allow for a 60 m rise in global sea-level during the Coniacian alone. The relationship between relative sea-level and $\delta^{18}\text{O}$ suggests that in a greenhouse salinity stratified ocean, the traditional relationship between $\delta^{18}\text{O}$ and temperature breaks down. Such a relationship is observed for the Coniacian and Santonian. During the Lower Campanian the relationship between $\delta^{18}\text{O}$ and relative sea-level curve is reversed. This suggests a change in ocean state, from a sluggish salinity stratified ocean to a more vigorous, thermally stratified one. This change is associated with upwelling and phosphorite deposition in the late Santonian.

Forty-six marl bands from the Coniacian to Lower Campanian of Southern England have been examined using geochemical analytical techniques to determine whether they are of volcanic or detrital origin. The results are compared to similar studies from the literature. Analysis by ICP-MS is found to be an effective technique in isolating volcanogenic marls from the chalk whilst analysis by XRD and XRF techniques is found to be inconclusive. The geochemical results are employed to resolve specific problems of correlation and strengthen the sequence stratigraphical analysis.

This work demonstrates the viability of sequence stratigraphy as a technique for subdividing the biogenic, pelagic sedimentary record of the Northwest European Upper Cretaceous, and demonstrates that, combined with stable isotope stratigraphy, sequence stratigraphy allows study of the underlying fundamental controls on deposition based upon often subtle changes in sedimentology, geochemistry and palaeontology.

This project was set up and supervised by Dr Angela Coe and Dr Gilbert Larwood and subsequently by Dr Howard Armstrong. Sadly, Gilbert passed away early in 1997. A constant source of boundless enthusiasm and a mine of interesting, though not always relevant, information, he was and is missed. I would like to take this opportunity to thank Angela for all her help over the course of this project and especially over the first eighteen months when the work on the sequence stratigraphy was done. Howard is thanked for all his help, especially during the last eighteen months when the wider implications of the research, considering stable isotopes and ocean states, were considered. Chalk sequence stratigraphy is a far cry from Lower Palaeozoic conodont biostratigraphy.

Professor Andy Gale is thanked for his devil's advocacy, helpful suggestions regarding suitable localities and for introducing me to Professor Jake Hancock. Jake is thanked for his generous hospitality and for guiding me around the chalk of Dorset and Wiltshire. Dr Hugh Jenkyns kindly supplied me with the stable isotope data for the English chalk, used herein. This data has enabled a productive and interesting distraction from pure chalk sequence stratigraphy. I would also like to thank Dr Dave Wray and Dr Dave Owen for useful discussions over the course of several BSRG conferences. Dr Mike Widdowson is thanked for his geochemical advice and Dr Jim Kennedy for his helpful suggestions regarding the French sections, leading to an enjoyably vinous month in Aquitaine. Dr Walter Gigon provided words of encouragement from afar.

In the department at Durham, I would like to thank Dr Neil Mitchell, Dr Mark Osborne, Dr Graham Pearson, Dr Christine Pierce, Dave Schofield, Dr Colin Scrutton, Dr Dick Swarbrick, Dr Ken Thomson, Professor Maurice Tucker and Dr 'Fred' Worrall for helping with the occasional question. Ken's seismic stratigraphy lectures don't go unrecommended for those seeking future gainful employment. Julie Southern has been more than patient in the face of rapidly dissolving chalk samples requiring thin-sectioning and Karen Aitkinson remarkably polite when faced with garishly-coloured diagrams. They are both thanked sincerely. Dave, Carole and Clare are thanked for their general helpfulness and friendliness and Dave Stevenson's help in trying to keep my computer on the rails has been appreciated.

Dr Chris Otley and Ron Hardy are both thanked for the many hours they have put in to aid, assist and enhance my rather meagre geochemical skills. Chris has operated the ICP-MS, patiently explained the sample preparation process and sorted out my mistakes. Ron was invaluable in the initial stages of the geochemistry, explaining the basics of the XRD and running the XRF. Their help has been greatly appreciated. Adrian Campbell-Smith is thanked for his help in crushing and preparing rock powders prior to analysis — quite a departure for a theoretical physicist. I would also like to thank the staff of the Geological Society Library, for their patient help over the course of my numerous visits, and Sarah Stafford at the Geologists' Association. Chris Wheatley assisted my study of the Trunch Borehole data during a visit to Keyworth, and the Director of the BGS kindly granted permission to publish work arising from this.

My fellow postgraduates in Durham are thanked for making the past years enjoyable ones. I would especially like to thank Dr Ziad Ahmadi for his friendly, abusive help and for plucking my locality maps out of a Unix machine somewhere. Dr Joanna Garland is thanked for her suggestions regarding sedimentary cyclicity and Jonny Imber for brightening up evening meals in the department. Above all I would like to thank Gail Radcliffe, my office-mate, for all her help, enthusiasm, useful and varied discussions and cake-consumption over the past years — a worthy fellow founder-member of the Cake, Coffee and Chocolate Research Group. Her assistance has been greatly appreciated.

I would also like to thank those non-geological friends who have provided welcome distraction from research as and when it has been required. Adrian Campbell-Smith, Sophy Jordan, George and Joyce Schlesinger and Anthony Zerillo have all filled this role admirably. I would also like to thank Martyn Barmby, Liz Burd, Adrian Carr, Dr Robert Hayward, Marilyn Hird, John Lofthouse, Dr Douglas Pocock and Tyne Tees Television for providing valuable help and support during the course of the trans-Atlantic fun and games on the Bailey. Helly Best-Shaw has provided greatly appreciated support over the past years, and welcome respite from Durham when it was needed, facilitating my visits to the Geological Society Library.

Last, but by no means least, this research would not have been possible without the generous funding of Margrit and Hanni Zwahlen. Their boundless generosity, and food parcels, have been greatly appreciated and have allowed complete freedom of research. Francis Grant has kindly translated many hundreds of pages of French and German text whilst Anne Grant has acted as field assistant and sherpa quite beyond the call of duty. Other than these cited examples, my parents have provided the continued and tireless support that only parents can. Thank you.

Frontis	ii
Declaration	iii
Abstract	iv
Acknowledgements	v
Table of Contents	vi
List of Figures	ix
Chapter 1 Introduction	1
INTRODUCTION	2
THESIS AIMS	2
THESIS OUTLINE	3
REGIONAL SETTING	3
STRATIGRAPHY	6
BIOSTRATIGRAPHY	6
Coniacian	6
Santonian	6
Campanian	7
LITHOSTRATIGRAPHY	7
ISOTOPE STRATIGRAPHY	10
MAGNETOSTRATIGRAPHY	11
SEQUENCE STRATIGRAPHY	11
TERMINOLOGY	11
ADAPTATIONS OF THE SEQUENCE STRATIGRAPHIC MODEL	13
IDEAL CHALK SEQUENCE	14
CORRELATION AND SEQUENCE DEFINITION	15
RELATIVE SEA-LEVEL CURVES	17
DEFINITION OF RELATIVE SEA-LEVEL CURVES	17
PUBLISHED RELATIVE SEA-LEVEL CURVES	19
STABLE ISOTOPES	20
OXYGEN	20
CARBON	22
Chapter 2 Coniacian	23
ABSTRACT	24
INTRODUCTION	24
STRATIGRAPHY	25
CORRELATION AND SEQUENCE DEFINITION	26
CONIACIAN SEQUENCE STRATIGRAPHY	26
SEQUENCE Co1	27
SEQUENCE Co2	30
SEQUENCE Co3	34
SEQUENCE Co4	35
SEQUENCE Co5	36
SEQUENCE Co6	38
SEQUENCE Co7	39
SEQUENCE Co8	40
CONIACIAN SECOND-ORDER SEQUENCE	41
STABLE ISOTOPE DATA	41
CARBON	42
OXYGEN	42
DISCUSSION AND UNDERLYING CAUSAL MECHANISMS	45
CONCLUSIONS	47

Chapter 3 Santonian	48
ABSTRACT	49
INTRODUCTION	49
STRATIGRAPHY	50
CORRELATION AND SEQUENCE DEFINITION	52
SEQUENCE STRATIGRAPHY	53
SEQUENCE Sa1	53
SEQUENCE Sa2	56
SEQUENCE Sa3	58
SEQUENCE Sa4	60
SEQUENCE Sa5	61
SEQUENCE Sa6	62
SEQUENCE Sa7	64
SECOND-ORDER SANTONIAN SEQUENCE	65
PUBLISHED SEA LEVEL CURVES	65
STABLE OXYGEN AND CARBON ISOTOPE DATA	68
THE ROLE OF TECTONICS	70
DISCUSSION	70
CONCLUSIONS	71
Chapter 4 Lower Campanian	72
ABSTRACT	73
INTRODUCTION AND STRATIGRAPHY	73
CORRELATION AND SEQUENCE DEFINITION	74
SEQUENCE STRATIGRAPHY	75
SEQUENCE Ca1	75
SEQUENCE Ca2	77
SEQUENCE Ca3	78
SEQUENCE Ca4	81
SEQUENCE Ca5	83
SEQUENCE Ca6	84
SEQUENCE Ca7	85
SEQUENCE Ca8	85
SEQUENCE Ca9	86
SEQUENCE Ca10	87
SEQUENCE Ca11	87
SEQUENCE Ca12	88
SEQUENCE Ca13	89
SEQUENCE Ca14	89
LONG-TERM SEQUENCES	90
PUBLISHED SEA-LEVEL CURVES	94
STABLE OXYGEN AND CARBON ISOTOPE DATA	95
TECTONICS	95
DISCUSSION AND CONCLUSIONS	97
Chapter 5 Geochemistry	99
ABSTRACT	100
INTRODUCTION	100
EXPERIMENTAL PROCEDURE	101
XRD	101
XRF	101

ICP-MS	102
REE APPLICATION	103
RESULTS	103
XRF AND XRD	103
ICP-MS	106
DISCUSSION	106
CONCLUSION	113
Chapter 6 Conclusions	114
INTRODUCTION	115
SEQUENCE STRATIGRAPHICAL MODEL	115
LONG-TERM RELATIVE SEA-LEVEL CURVE	116
COMPARISON WITH OTHER SEA-LEVEL CURVES	118
COMPARISON OF THE DATA WITH STABLE ISOTOPE CURVES	120
$\delta^{13}\text{C}$ CURVE	120
$\delta^{18}\text{O}$ CURVE	122
ICEHOUSE STATE	123
GREENHOUSE STATE	124
TRANSITIONAL STATE	126
RELATIVE SEA-LEVEL, STABLE ISOTOPES AND OCEAN STATE	126
DISCUSSION	129
POSSIBLE WIDER IMPLICATIONS	131
CONCLUSIONS	132

Volume 2 Appendices

Frontis	xii
Table of Contents	xiii
Appendix A Graphic logs	A1
Appendix B Cross-plots	B1
Appendix C ICP-MS Data	C1
Appendix D Sequence stratigraphical cross-section	Inside back cover

1.1	Basin structure and section location	4
1.2	Palaeogeography and depositional environments	5
1.3	Macrosfossil biozones	6
1.4a	Chalk with chert bands — photograph	8
1.4b	Chalk with marl bands — photograph	8
1.4c	Nodular, iron-stained sponge bed — photograph	9
1.4d	Chalk hardground — photograph	9
1.5	Lithostratigraphical schemes for southern England	10
1.6	Systems tracts and key surfaces	12
1.7	Ideal chalk sequence	14
1.8	Example cross-plot	16
1.9	Sequence definition flow-chart	17
1.10	Example sequence stratigraphical cross-section for the Coniacian	18
1.11	Relative sea-level curve definition	19
1.12	Stable oxygen and carbon isotope data	21
2.1	Coniacian locality map with basin structure	27
2.2	Summary cross-plots for the Coniacian	28
2.3	Key to graphic logs	29
2.4	Graphic log of Seaford Head for the Coniacian	30
2.5	Graphic log of Culver Cliff for the Coniacian	31
2.6	Graphic log of the Trunch borehole for the Coniacian	32
2.7	Graphic log of Shoreham Cement Works for the Coniacian	33
2.8	Graphic log of Reed for the Coniacian	34
2.9	Graphic log of Compton Abbas for the Coniacian	34
2.10	Graphic log of Charnage Down for the Coniacian	35
2.11	Graphic log of Pinhay for the Coniacian	35
2.12	Graphic log of the Loir Valley for the Coniacian	36
2.13	Graphic log of Triguères for the Coniacian	37
2.14	Triguères hardground — photomicrograph	38
2.15	East Kent Coast graphic log, relative sea-level and stable isotope curves	43
2.16	Sequence stratigraphical cross-section for the Coniacian	44
2.17	Schematic representation of the Railsback (1990) model	45
2.18	Ideal chalk sequence	46
3.1	Santonian locality map with basin structure	51
3.2	Santonian lithostratigraphy for southern England	51
3.3	Example Santonian cross-plots	52
3.4	Ideal chalk sequence - palaeontology and lithology	53
3.5	Graphic log of the Trunch borehole for the Santonian	54
3.6	Graphic log of the East Kent Coast for the Santonian	55
3.7	Graphic log of Seaford Head for the Santonian	56
3.8a	Graphic log of Culver Cliff for the Santonian	57
3.8b	Graphic log of Culver Cliff for the Santonian	58
3.9	Graphic log of Beauval for the Santonian	59
3.10	Graphic log of the Loir Valley for the Santonian	60
3.11	Graphic log of Coquelles for the Santonian	60

3.12	Graphic log of Taplow for the Santonian	61
3.13	Sequence stratigraphical cross-section for the Santonian	66
3.14	Comparison of Santonian relative sea-level curves	67
3.15	Upper Cretaceous transgressive episodes — Cooper (1977)	67
3.16	Santonian relative sea-level and stable isotope curves	68
4.1	Lower Campanian locality map with basin structure	74
4.2a	Graphic log of Culver Cliff for the Lower Campanian	76
4.2b	Graphic log of Culver Cliff for the Lower Campanian	77
4.3	Graphic log of Seaford Head for the Lower Campanian	78
4.4a	Graphic log of the Trunch borehole for the Lower Campanian	79
4.4b	Graphic log of the Trunch borehole for the Lower Campanian	80
4.5	Graphic log of Pr�cy-sur-Oise for the Lower Campanian	82
4.6a	Lower Campanian relative sea-level curve (Sequence CaA)	91
4.6b	Lower Campanian relative sea-level curve (Sequence CaB)	92
4.7	Lower Campanian sequence stratigraphical cross-section	93
4.8	Comparison of Lower Campanian relative sea-level curves	94
4.9	Lower Campanian relative sea-level and stable isotope curves	96
5.1	Typical chalk geochemistry	100
5.2	Analytical machines' operating parameters	102
5.3	Example XRD trace	104
5.4	Example XRD trace after expansion with ethylene glycol	104
5.5a	REE profile of sample CC35 (detrital)	105
5.5b	REE profile of sample H39 (bentonitic)	105
5.6	REE profiles from the Coniacian of Seaford Head	106
5.7a	REE profiles from the Lower Campanian of Seaford Head	107
5.7b	REE profiles from the Lower Campanian of Seaford Head	107
5.8	REE profiles from the Santonian – Lower Campanian of Culver Cliff	108
5.9	REE profiles from the Lower Campanian of Culver Cliff	109
5.10	Gd/Yb plotted against Eu/Eu* for marl band samples	111
5.11	La/Sm plotted against Eu/Eu* for marl band samples	111
5.12	Sr plotted against Ti/Zr for marl band samples	112
5.13	Th plotted against Ti/Zr for marl band samples	112
6.1	Ideal chalk sequence	115
6.2	Coniacian – Lower Campanian relative sea-level curve	117
6.3	Comparison of Coniacian – Lower Campanian relative sea-level curves	118
6.4	Upper Cretaceous transgressive episodes — Cooper (1977)	120
6.5	Coniacian – Lower Campanian stable isotope and relative sea-level curves	121
6.6a	Icehouse model of climatic deterioration (Vincent and Berger, 1985)	123
6.6b	Icehouse model ocean circulation	124
6.7a	Greenhouse model of climatic amelioration	125
6.7b	Greenhouse model ocean circulation	125
6.8	Flow chart showing ocean – climate – relative sea-level interaction	127
6.9	Stable carbon plotted against stable oxygen to determine climatic state	128
6.10	Ocean-state identified by carbon, oxygen and relative sea-level interactions	129

Chapter 1

Introduction

INTRODUCTION

Sequence stratigraphy has become established as a major technique for sub-dividing the rock record into packages of genetically related sediment (Hesselbo & Parkinson, 1996 & Howell & Aitken, 1996). This approach has proved particularly successful in shallow-water siliciclastic successions, the environment in which the technique was first applied (Mitchum, 1977; Vail, Mitchum & Thompson, 1977; van Wagoner *et al.*, 1988 & Vail *et al.*, 1991). Subsequent work has led to the evolution of sequence stratigraphical techniques for carbonate platforms (Sarg, 1988; Schlager, 1991 and Hunt and Tucker, 1993). However, little attention has been paid to largely biogenic, deeper-water, pelagic carbonates in basinal settings. Indeed, sceptics believe that these techniques are not applicable to deep-water sediments.

The Upper Cretaceous successions of southern England and northern France have previously been studied extensively with regard to palaeontology, sedimentology and traditional stratigraphy. Recent sequence stratigraphical studies have looked at the Cenomanian and the Turonian but, to date, the Coniacian – Lower Campanian has not been considered on a basin-scale. This study provides a sequence stratigraphical analysis of the Coniacian, Santonian and Lower Campanian chalks of the Anglo-Paris Basin and the Trunch borehole in the Anglo-Dutch Basin. A model has been defined which allows for the classification of the chalk succession in terms of key surfaces and systems tracts. Sections have been correlated at bed and marker horizon level, combining new information and published correlations. Second and third-order relative sea level curves have been derived from the sequence stratigraphical analysis and are considered in the light of lower resolution published curves from Northwest Europe and around the world.

Comparison with published stable carbon and oxygen isotope data has allowed the changes in relative sea level to be considered in terms of causal mechanism. These relationships are discussed on a long and short-term timescale. Fluctuations within a long-term Greenhouse climate are considered in the light of Greenhouse and Icehouse oceanic models (Railsback, 1990 and Vincent & Berger, 1985 respectively). Observations resulting from the data sets have led to the definition of a predictive model for the relationship between ocean state, sea-level change and stable isotope data. This model allows the separation of climatic and tectonic controls on sedimentation. The techniques developed herein are applicable to other chalk-dominated successions and provide a warning against the dogmatic interpretation of palaeotemperature from the $\delta^{18}\text{O}$ ratio.

THESIS AIMS

- To present a sequence stratigraphical model for the biogenic pelagic sediments of the Anglo-Paris Basin Upper Cretaceous.
- To analyse the Coniacian, Santonian and Lower Campanian with regard to sequence stratigraphy on a second (~2 – 5 Ma) and third-order timescale (~0.5 Ma).
- To present relative sea-level curves for the interval studied and compare these to curves available in the literature.
- To integrate stable carbon and oxygen isotope data to test the relative sea-level curves and elucidate controls on deposition and relative sea-level change.

- To examine marl bands from within the chalk geochemically, to refine correlations and test whether any of them are volcanogenic.
- To examine and explain changes in the relationship between relative sea level, stable carbon and stable oxygen isotope curves in terms of wider tectonic, climatic and oceanic processes.

THESIS OUTLINE

Chapter 1 deals with the background to the project in terms of regional setting, stratigraphy and sequence stratigraphy. The correlation criteria, sequence stratigraphical model and sea-level curve construction are detailed. Relevant tectonism and stable-isotope application to the problems at hand are discussed.

Chapters 2, 3 and 4 present a detailed sequence stratigraphical framework for the Coniacian, Santonian and Lower Campanian respectively. Relative sea-level curves are presented and considered in the light of published curves. Stable-isotope data are conflated with the sea level curves to elucidate mechanisms controlling relative sea-level change. These mechanisms are discussed for each stage.

Chapter 5 presents geochemical data, largely derived from ICP-MS analysis, for marl horizons within the chalk. Specific problems of correlation are tackled, and the clays are subdivided into either detrital or volcanic origin. These results have been utilised in the application of the sequence stratigraphical model to the sediments analysed in Chapters 2, 3 and 4 allowing greater precision when characterising systems tract by marl band.

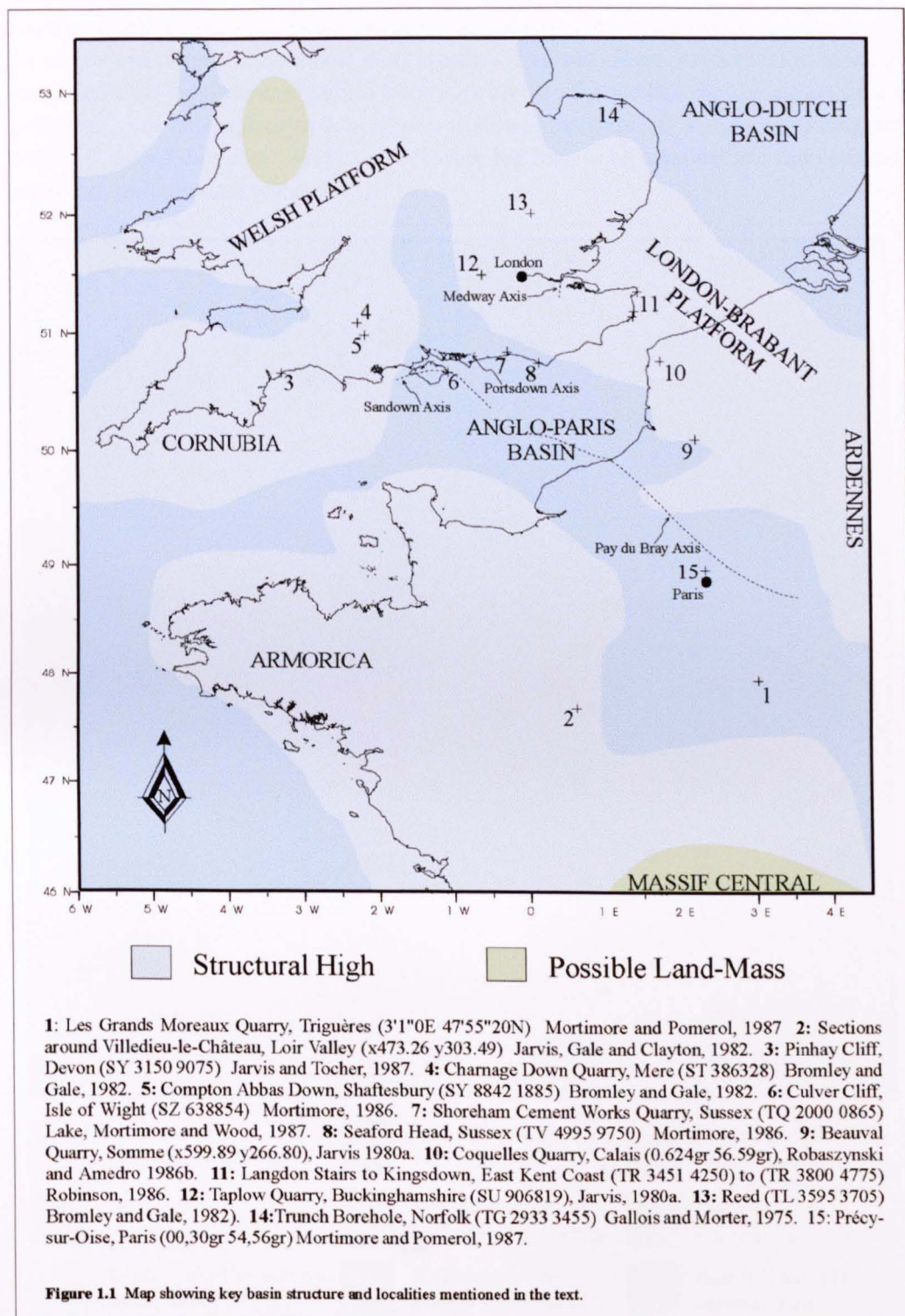
Chapter 6 presents the conclusions in terms of technique, results derived from each individual stage and analysis of longer-term trends. The short-and long-term trends in the data are analysed and considered in the light of existing ocean-state models. A predictive model for climate — ocean state interactions is suggested, based on the data utilised in this study.

REGIONAL SETTING

During the ^{Late}Upper Cretaceous, southern England and northern France were dominated by the Anglo-Paris Basin, stretching south to the Massif Central. (Figure 1.1). To the west, the structural highs of Cornubia and Armorica were divided by a connection to the deeper water of the Western Approaches whilst the Anglo-Paris Basin was separated from the Anglo-Dutch Basin to the east by the structural high of the London-Brabant Massif.

The Anglo-Dutch Basin represented the westerly margin of a large expanse of water stretching to Scandinavia in the north and as far as the Polish Trough to the east (Figure 1.2). Only the westernmost part of the basin is considered in this study.

This area, an epicontinental shelf sea on a passive margin, was tectonically relatively stable during the ^{Late}Upper Cretaceous. However, during the Coniacian – Lower Campanian, phases of activity affected tectonic lineaments such as the Pay-du-Bray Axis (Jarvis, 1980a, 1980b, 1980c; Jarvis and Woodroof, 1981; Mortimore and Pomerol, 1987, 1997), the Portsdown Axis (Gale, 1980), the Sandown Pericline (Smith and Curry, 1975; Mortimore, 1986), along the Normandy coast (Mortimore and Pomerol, 1987) and in south Dorset (Westhead and Woods, 1994). This activity



represented early phases of inversion, associated with the collision of Africa and Europe and development of divergent plate margins in the North Atlantic and Arctic region (Ziegler, 1990). Mortimore and Pomerol (1997) have detailed evidence from within the Anglo-Paris Basin for three discrete phases of tectonic activity over this interval — basal Coniacian, late-Santonian — early Campanian and latest early Campanian. The characteristic features of these phases are detailed with field evidence, showing lateral thickness and lithological variation across positive features and slumping and sliding into the deeper-water successions. Their work has been fol-

lowed up with a comparison between their observations of these tectonic movements in the Anglo-Paris Basin and Germany (Mortimore *et al.*, in press). The local effects of tectonics can be recognised within the sequence stratigraphic framework herein. The sections used herein are from a sufficiently wide geographical area to allow a sequence-stratigraphical analysis combining tectonic axis and off-axis data. An aim of this work has been to separate tectonic from climatic controls on sedimentation and cyclicity.

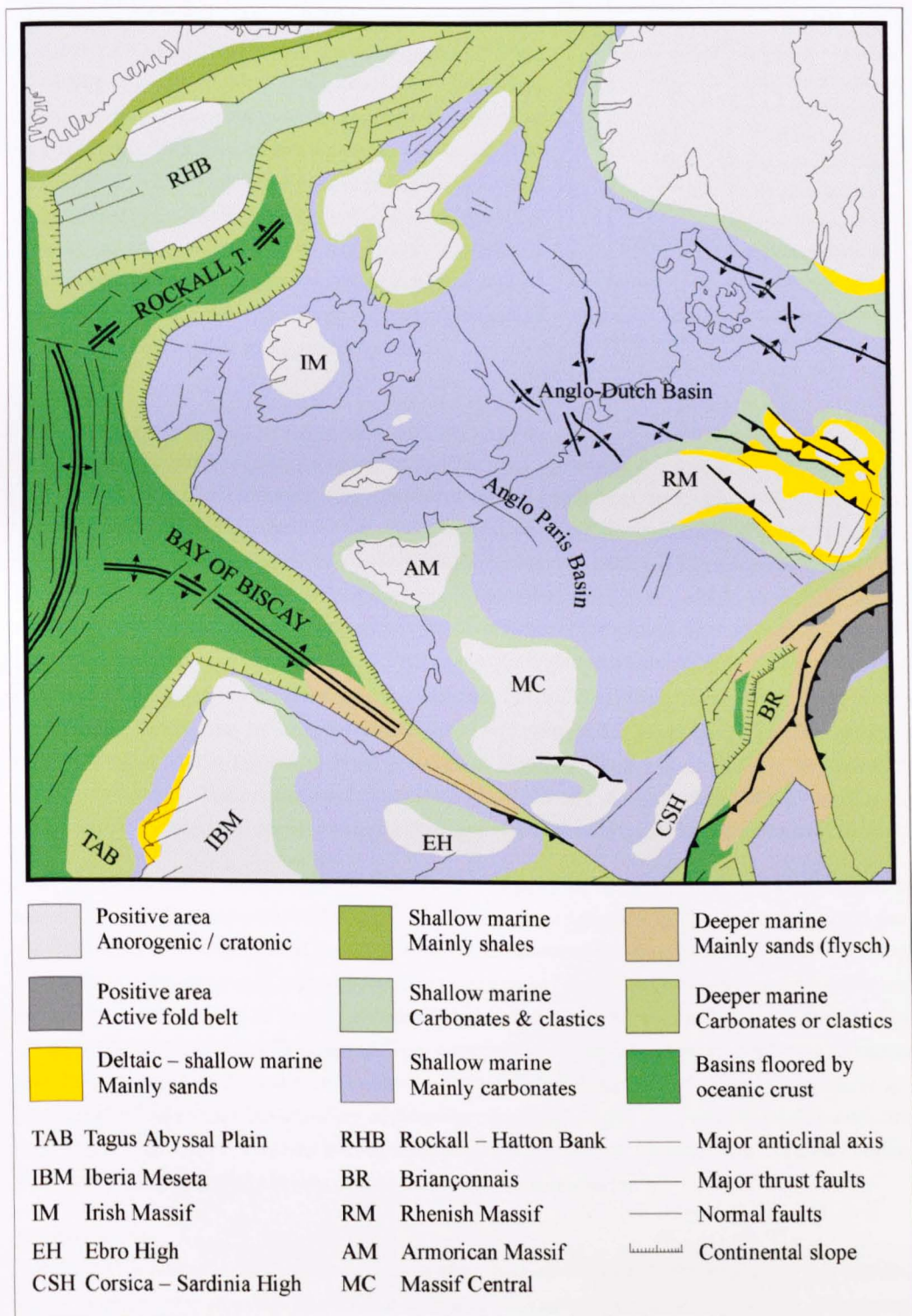


Figure 1.2 Map showing depositional environment, principal lithology and palaeogeography of the area around the Anglo-Paris Basin in late-Cretaceous times. From Ziegler, 1988.

STRATIGRAPHY

BIOSTRATIGRAPHY

The Anglo-Paris Basin formed at the triple junction between the Boreal, Tethyan and Atlantic Realms (Owen, 1996). This has resulted in a variety of biostratigraphical schemes across the area. A standard macrofossil biozonation is recognised for the United Kingdom, Figure 1.3 (Rawson *et al.*, 1978). Traditionally the Coniacian, Santonian and Campanian have been grouped together as the Senonian. The base of the Senonian corresponds to the base of the Coniacian. Bralower *et al.* (1995) presented an integrated microfossil biostratigraphy for the Upper Cretaceous, but this was not tied to any lithostratigraphical scheme, and does not appear to provide a higher resolution subdivision for the Coniacian – Lower Campanian interval than is available using macrofossils.

SENONIAN	CAMPANIAN	<i>B. mucronata</i>
		<i>G. quadrata</i>
		<i>O. pilula</i>
	SANTONIAN	<i>M. testudinarius</i>
		<i>U. socialis</i>
		<i>M. coranguinum</i>
	CONIACIAN	<i>M. cortestudinarium</i>

Figure 1.3 Macrofossil biozonation of the Senonian, after Rawson *et al.*, 1978

Coniacian

The Coniacian was erected by Coquand in 1857 based upon type sections around the town of Cognac in the Charente. Few useful fossils are now found in the glauconitic sands in this area and, now, ammonite assemblages from the Craie-de-Villedieu in the Touraine are used to indicate the base of the Coniacian in the southern part of the Anglo-Paris Basin. The ammonite *Barroisiceras haberfellneri* (Hauer) has been used as a marker for the base of the Coniacian in the type area since the last century (Birkelund *et al.*, 1984), though the specimens used have been assigned, subsequently, to *Forresteria (Harlites) petrocoriensis* (Coquand). Gale and Woodroof (1981) recorded a *Barroisiceras haberfellneri haberfellneri* (Hauer) from the Top Rock of Kent, providing ammonite evidence for the position of the basal Coniacian in southern England. However, as ammonites are extremely rare at this level in the English chalk, a variety of other fossils have been used in southern England (Bailey *et al.*, 1984). Inoceramids *Cremnoceramus? Waltersdorfensis hannovrensis* (Heinz), *C. deformis* (Meek) and/or *C. schloenbachi* (Böhm) are useful owing to their widespread occurrence across northwest Europe.

The base of the Coniacian, as indicated by these inoceramids, lies directly above a condensed or non-sequence, often represented by a hardground (Bailey *et al.*, 1984). Though other zonal fossils, both macro and micro, exist for the Turonian – Coniacian boundary interval, a combination of *F. (Harlites) petrocoriense* (Coquand) and *Cremnoceramus? waltersdorfensis hannovrensis* (Heinz) is taken to mark the base of the Coniacian (Birkelund *et al.*, 1984 and Bailey *et al.*, 1984). The *Micraster cortestudinarium* Goldfuss and lower part of the *Micraster coranguinum* Leske Biozones have been recognised over the last century for the Coniacian Stage in England (Rawson *et al.*, 1978), and are indicated alongside the sedimentary logs herein. For the purposes of this work, the base of the Coniacian is taken as the top surface of the Navigation Hardgrounds, though in effect the base is situated slightly lower, within the hardground complex.

Santonian

Named by Coquand in 1857, after Saintes in the Charente Maritime, the Santonian was divided into two ammonite biozones by de Grossouvre — *Texanites texanus* and *Placenticerus syrtales* (Rawson *et al.*, 1978). The base of the stage in southern England is marked by the first occurrence

of the inoceramid *Cladoceras undulatoplicatus* (Roemer), approximately coincident with the first appearance of *Texanites s. s.* (Birkelund *et al.*, 1984) and *Sigalia carpathica* Salaj (Lamolda and Hancock, 1996). Lamolda and Hancock (1996) report that there are no calcareous nannofossil events described in the literature that are sufficiently precise to define the Coniacian – Santonian boundary. In England, the upper part of *M. coranguinum* and the crinoid biozones *Uintacrinus socialis* (Grinnell) and *Marsupites testudinarius* (Schlotheim) give a tripartite subdivision of the stage. Rawson *et al.* (1978) record the rare occurrence of texanitid ammonites from the *M. coranguinum* Biozone in Kent but, otherwise, ammonites are of little correlative value in the English Santonian. Mortimore (1986) and Mortimore and Pomerol (1987) have suggested various correlative horizons within the Anglo-Paris Basin based upon the often subtle morphological changes in echinoid and inoceramid lineages. Christensen (1990) divided the Santonian of northern Germany into five belemnite Biozones based upon changes in the *Goniotoothis* lineage; however, belemnites are not sufficiently common in the English sections for this to be a practical method for subdivision. The consensus of opinion at the Second Symposium on Cretaceous Stage Boundaries (Brussels, September 1995) was that the Santonian could be divided into three. A possible marker for the base of the Middle Santonian was the extinction of *C. undulatoplicatus* and the base of the Upper Santonian might be marked by the first occurrence of *U. socialis*.

Campanian

The Campanian stage was erected by Coquand in 1857 based upon sections in Grande Champagne (Hancock and Gale, 1996). In the Anglo-Paris Basin, the base of the Campanian is taken to coincide with the extinction of the crinoid *Marsupites testudinarius* (Schlotheim). A quadripartite ammonite zonation was devised at the turn of the century by de Grossouvre using *Placenticeras bidorsatum* (Roemer) (also listed as *Diplacmoceras bidorsatum*), *Menabites (Delawarella) delawarensis*, *Hoplitoplacenticeras vari* and *Bostrychoceras polylocum*. *Scaphites leei* III (de Kay) and the genus *Submortonoceras* have also been used to mark the base of the Campanian stage outside Europe (Hancock and Gale, 1996). However, ammonites are not found over much of the Lower Campanian of southern England and it is therefore difficult to correlate with the type area in Aquitaine. Much of the correlation between English and French sections of the Anglo-Paris Basin has been achieved using echinoids, belemnites and inoceramids (Mortimore and Pomerol, 1987).

Two Biozones are established for the Lower Campanian in southern England: the echinoid *Offaster pilula* (Lamarck) and belemnite *Goniotoothis quadrata* (Blainville) are the eponymous zonal species (Rawson *et al.*, 1978). In the southern English sections, a Subzone of *Uintacrinus anglicus* (Rasmussen), is recognised at the base of the *O. pilula* Biozone covering the interval from the base of the Friars Bay Marl 1 to the top of Friars Bay Marl 3. The base of the Upper Campanian is coincident with the base of the *Belemnitella mucronata* (Schlotheim) Biozone.

LITHOSTRATIGRAPHY

The Coniacian – Lower Campanian sediments of the Anglo-Paris Basin consist largely of chalk. This is punctuated by horizons of chert (flint), marl, nodular and occasionally hardground chalk (Figure 1.4). Over the last fifteen years, a number of lithostratigraphical schemes have been introduced into the literature for the chalk of southern England. Mortimore (1986) suggested that the terms Middle and Upper Chalk, used by the Geological Survey since the turn of the century, could be replaced with that of Sussex White Chalk Formation. He named a number of members and beds in what was traditionally known as the Upper Chalk, revising some of the terms he had previously suggested (Mortimore, 1983), based upon sections in Sussex. This work was pub-



Figure 1.4a Photograph showing chalk with chert (flint) bands.



Figure 1.4b Photograph showing chalk with marl bands.



Figure 1.4c Photograph showing chalk with nodular, iron-stained sponge bed.



Figure 1.4d Photograph showing hardground chalk.

MAGNETOSTRATIGRAPHY

The Coniacian and the Santonian stages fall within the long Cretaceous Quiet Zone, magnetochron C34n (Gradstein *et al.*, 1995). The boundary between the end of C34n and C33r has traditionally been placed at or around the Santonian – Campanian boundary. In southern England this transition actually occurs in the Santonian *U. socialis* Biozone (Gale *et al.*, 1996). The Campanian is represented by a number of higher frequency reverse and normal polarity zones in chrons C33 and C32. The *G. quadrata* – *B. mucronata* Biozone boundary, marking the top of the Lower Campanian, falls within chron C33n (Montgomery in Gale *et al.*, 1996).

SEQUENCE STRATIGRAPHY

The sequence stratigraphic method of dividing the sedimentary record into packages of genetically related sediments resulting from relative sea-level change was developed in passive continental margin siliciclastic successions (e.g. Mitchum, 1977; Vail, Mitchum & Thompson, 1977; van Wagoner *et al.*, 1988; Vail *et al.*, 1991). A proliferation of research has followed which has included extending the concepts to carbonate facies, especially reefs and carbonate platforms (Sarg, 1988; Schlager, 1991; Hunt & Tucker 1993; Coe, 1996). Despite the powerful nature of sequence stratigraphy as a correlative and interpretative tool, relatively few studies have addressed deep-water pelagic carbonate facies. Recently, sequence stratigraphy has been applied to the relatively proximal chalk-marl alternations of the Cenomanian (Gale, 1990, 1995; Owen, 1996). Owen (1996) and Gale (1996) discuss the characterisation of key surfaces in the chalks of the Cenomanian and Turonian respectively.

TERMINOLOGY

Sequence stratigraphy divides the sedimentary record into a number of sequences bounded by unconformities and their correlative conformities, termed sequence boundaries (SB). A sequence represents sedimentary deposits or rocks deposited during one cycle of relative sea-level change. A sequence can be divided into separate parts, termed systems tracts, that define the parts of the sequence in terms of rising or falling relative sea-level. Systems tracts are demarcated by key surfaces. The lowermost systems tract (LmST) contains those sediments deposited during falling relative sea-level between the SB and transgressive surface (ts). The ts represents the first significant flooding of the basin margin during rising relative sea-level. The transgressive systems tract (TST) represents sedimentation between the ts and the maximum rate of relative sea-level rise which corresponds to the maximum flooding surface (mfs). Sediments deposited during the rising, highest and falling relative sea-level of the half-cycle between the mfs and successive SB are assigned to the highstand systems tract (HST). Smaller-scale packages of genetically related conformable sediments that are bounded by flooding surfaces are termed parasequences. These are the basic building blocks of sequences and stack to form systems tracts.

Van Wagoner *et al.* (1988, pp. 39 – 40), in their overview of the fundamentals of sequence stratigraphy, defined an unconformity as ‘a surface separating younger from older strata, along which there is evidence of subaerial erosional truncation or subaerial exposure, with a significant hiatus indicated’. They went on to say that ‘this definition restricts the usage of the term unconformity to significant subaerial surfaces and modifies the definition of unconformity used by Mitchum (1977)’. This earlier definition referred to both subaerial and submarine erosional truncations and was thought to be too broad by Van Wagoner *et al.* (1988). The terminology

developed from near-shore siliciclastic sequences recognises two types of sequence and sequence boundary, classified by erosional and basin-onlap architecture. These sequences are characterised by subaerial exposure and a downward shift in coastal onlap, with the more major type 1 sequences exhibiting concurrent subaerial erosion associated with stream rejuvenation and a basinwards shift in facies (van Wagoner *et al.*, 1988). The LmST is termed a Lowstand Systems Tract (LST) if overlying a type 1 SB and a Shelf-margin Systems Tract (SmST) if overlying a type 2 SB.

Within the TST individual parasequences and parasequence sets are retrogradational, onlapping the basin margin and consequently the SB. Consequently, the TST is composed of a package of sediments with a retrogradational architecture. The HST is characterised by an aggradational and subsequently progradational geometry with prograding clinoforms downlapping onto the underlying mfs.

Sequence stratigraphy recognises a number of orders of cyclicity (Vail *et al.*, 1991). The largest scale, or first-order, cyclicity also known as a ‘continental encroachment cycle’ represents major long-term transgressive – regressive facies shifts over periods of several hundred million years.

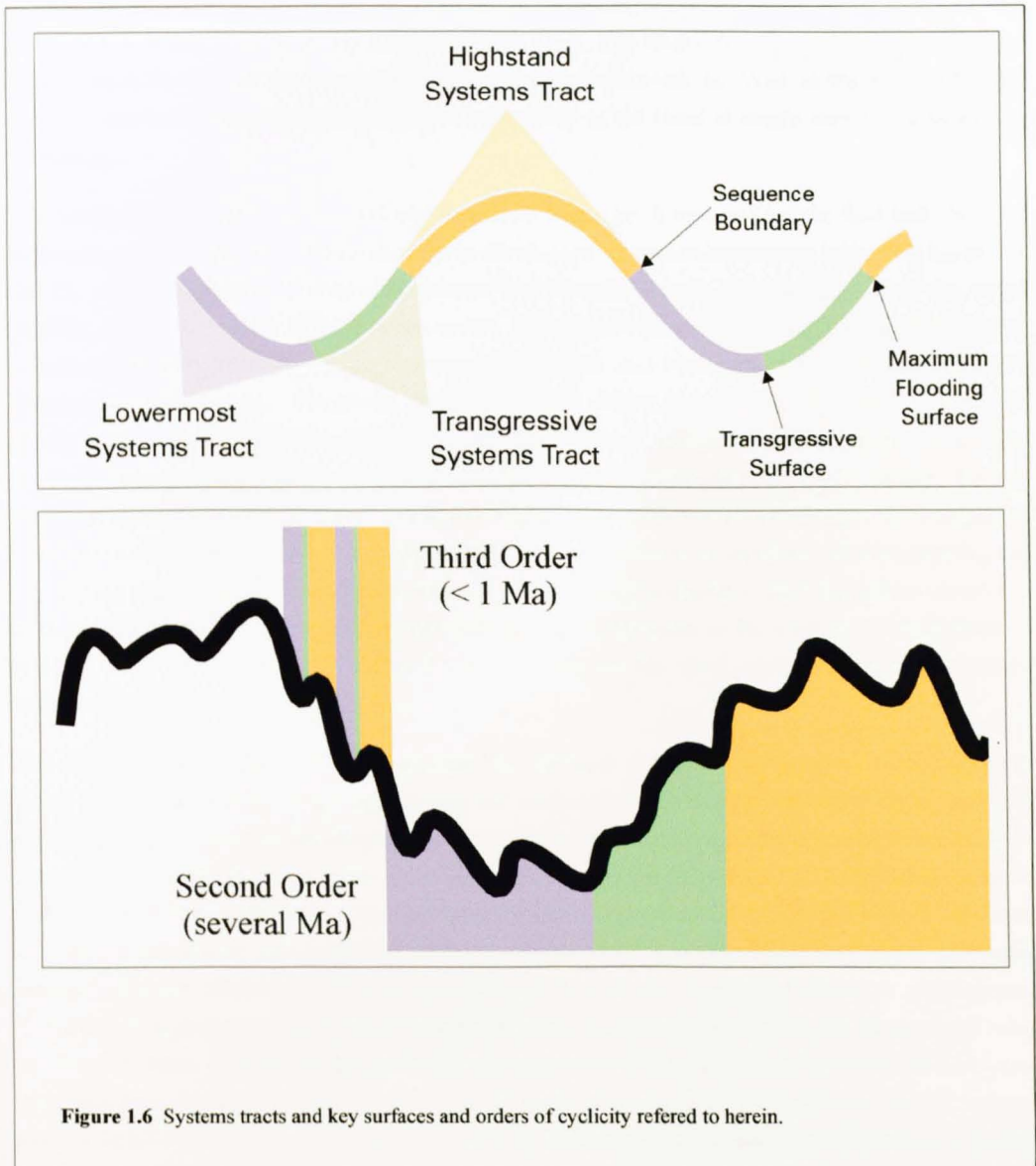


Figure 1.6 Systems tracts and key surfaces and orders of cyclicity referred to herein.

Consequently evidence exists for only a few of these cycles in the Phanerozoic record. Second-order cycles, the basic building blocks of continental encroachment cycles, have a duration varying from a couple of million to tens of millions of years, and represent significant accumulations of sediment. Third-order cycles, from half a million years to several million years, are the basic components of second-order cycles and are divisible into systems tracts reflecting deposition during specific parts of a cycle of relative sea-level change (Figure 1.6). Smaller-scale, fourth-order cycles are recognised to sub-divide third-order cycles. These have durations of a few tens of thousand to a hundred thousand years and are akin to parasequences. Typical cycles would be those resulting from Milankovitch precession and obliquity cyclicity (House & Gale 1995).

ADAPTATIONS OF THE SEQUENCE STRATIGRAPHIC MODEL

The chalk of the Coniacian – Lower Campanian was deposited in an unique depositional environment — most of the Northwest European landmass being submerged during a period of high eustatic sea level. Consequently the epicontinental shelf seas, depocentres for the chalk, were characterised by water depths several hundred metres greater than those observed at the present day, with Hancock (1975) suggesting a maximum figure of up to 600m. The deeper water sections studied herein are a considerable distance from the nearest exposed landmass with only the clay fraction transported and deposited from the land. The water depth and distance from land require modification of the sequence stratigraphical framework as, even in the most marginal sections studied, subaerial exposure is not seen, even at the most strongly developed sequence boundaries.

The traditional sequence stratigraphical approach is further hampered by the fact that the bulk sediment in the Anglo-Paris Basin during the Coniacian – Lower Campanian interval is biogenic. CaCO_3 was precipitated by coccolithophores and foraminifera in the photic zone of the water column, across the whole of the marine realm. Consequently, rather than a depositional setting dominated by terrigenously-derived sediments, the chalk seas were experiencing a largely evenly distributed calcite rain. However, several factors affect deposition, allowing a sequence stratigraphical framework to be defined. Current activities associated with changes in relative sea-level have led to variation in depositional geometry, dependant upon basin setting. For instance, proximal settings are more winnowed, and show considerable condensation with sequence boundaries down-cutting and transgressive packages of sediment onlapping and overstepping the underlying sediments. Differences in water depth caused by position in the basin allow variations in depositional geometry combined with lithological expression to be used in the definition of systems tract. This approach is detailed in the sections on the 'ideal chalk sequence' and 'correlation and sequence definition' below.

The definition of an unconformity proposed by Mitchum (1977) is used herein. Submarine erosional surfaces and hiatuses are apparent in the marginal sections, over structural highs, and into relatively deep water. In the deepest-water settings, the sequence boundary is represented by a correlative conformity, or an influx of terrigenously derived detrital material interpreted to represent a fall in relative sea-level and consequently, increased subaerial exposure. Where sequence boundaries are traced into marginal sections, severe condensation and down-cutting erosional relationships are observed. This is especially evident in the marginal Coniacian successions. However, though the extent to which sequence boundaries have developed can be assessed relative to each other, working in deeper-water successions it is not possible, or relevant, to designate sequence boundaries type 1 or type 2. Consequently, the LmST is referred to as LmST herein, and not as LST or SmST. An indication of the geometries of individual systems tracts, showing

condensation and onlap — downlap relationships is obtained from the simple basin-wide cross-sections in Appendix D.

Here, the longer-term sequences identified are assigned to the second-order and the shorter-term cycles to the third-order. Though the cycles herein are at the lower limits of duration generally accepted as second and third-order, their lithological and geometrical expressions reflect the order of magnitude and status implied by this terminology.

IDEAL CHALK SEQUENCE

An idealised chalk depositional sequence has been derived (Figure 1.7) from a combination of field observations, correlations from the literature and the cross-plot method of graphical correlation, discussed below. These definitions support and build upon those recently proposed for chalk successions by Gale (1996) and Owen (1996).

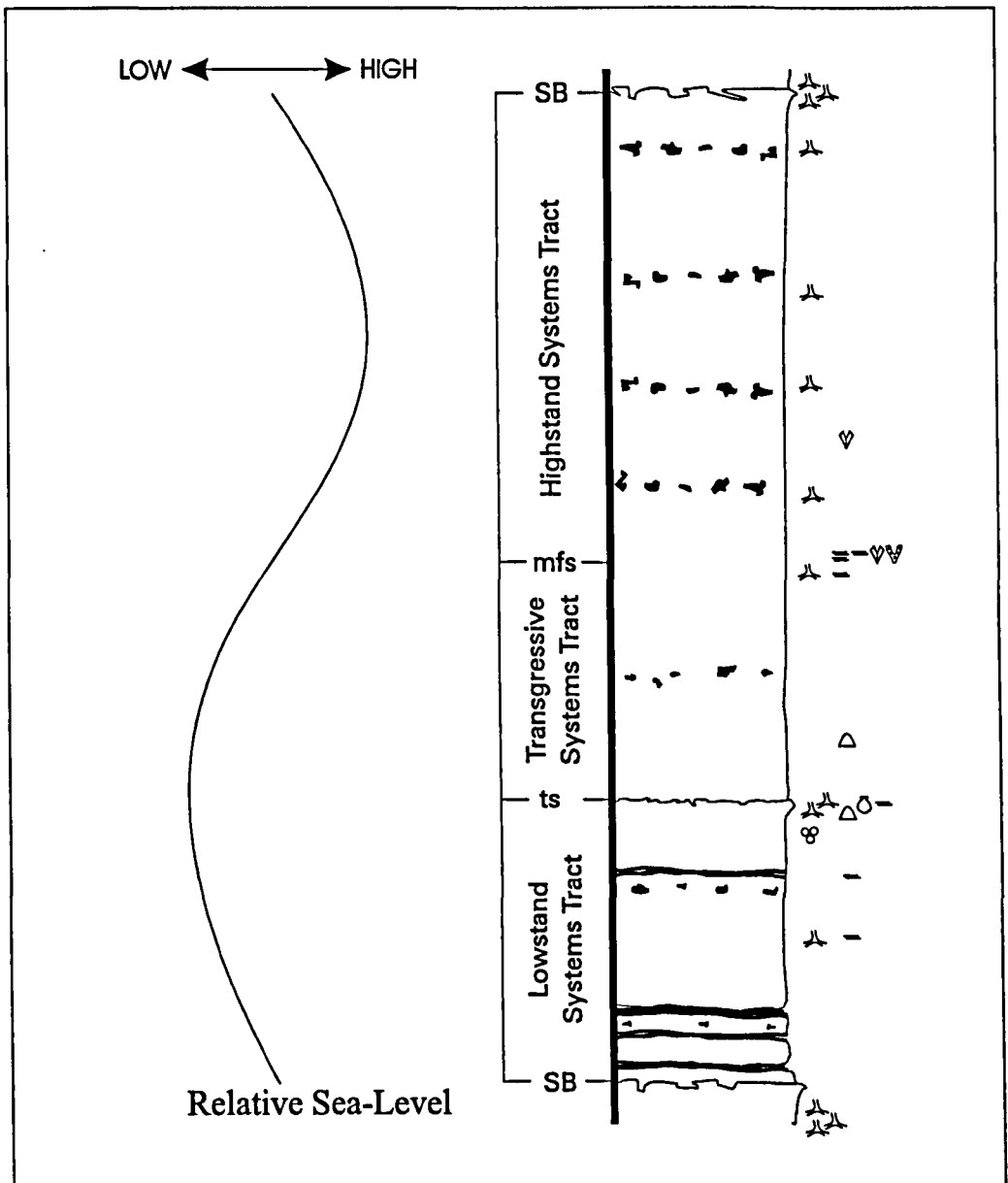


Figure 1.7 Ideal chalk sequence. See Figure 2.3 and inside front cover for key to log. Up to 20m in thickness

A hardground surface, passing basinwards into nodular chalks represents the SB. The SB hardground is usually characterised by a relatively planar surface with *Thalassinoides* burrows descending from the surface between lithified nodular chalk. The surface and burrow linings may be mineralised, often with an iron-stained patina. Iron mineralisation can extend several centimetres to tens of centimetres beneath the surface depending upon the period of ^{non-deposition} exposure at the sea floor and the availability of mineral-rich fluids. Fossils on the hardground surface are usually relatively scarce and often consist of inoceramid debris or echinoid tests out of life position. During periods of higher long-term relative sea-level, the SB may be far less pronounced or represented by a correlative conformity in the deeper sections. In these cases, the SB is placed *a priori* at the base of the lowest marl band — this represents an increase in the detrital influx associated with increased landmass exposure. The LmST is characterised by chalk, rich in marl horizons.

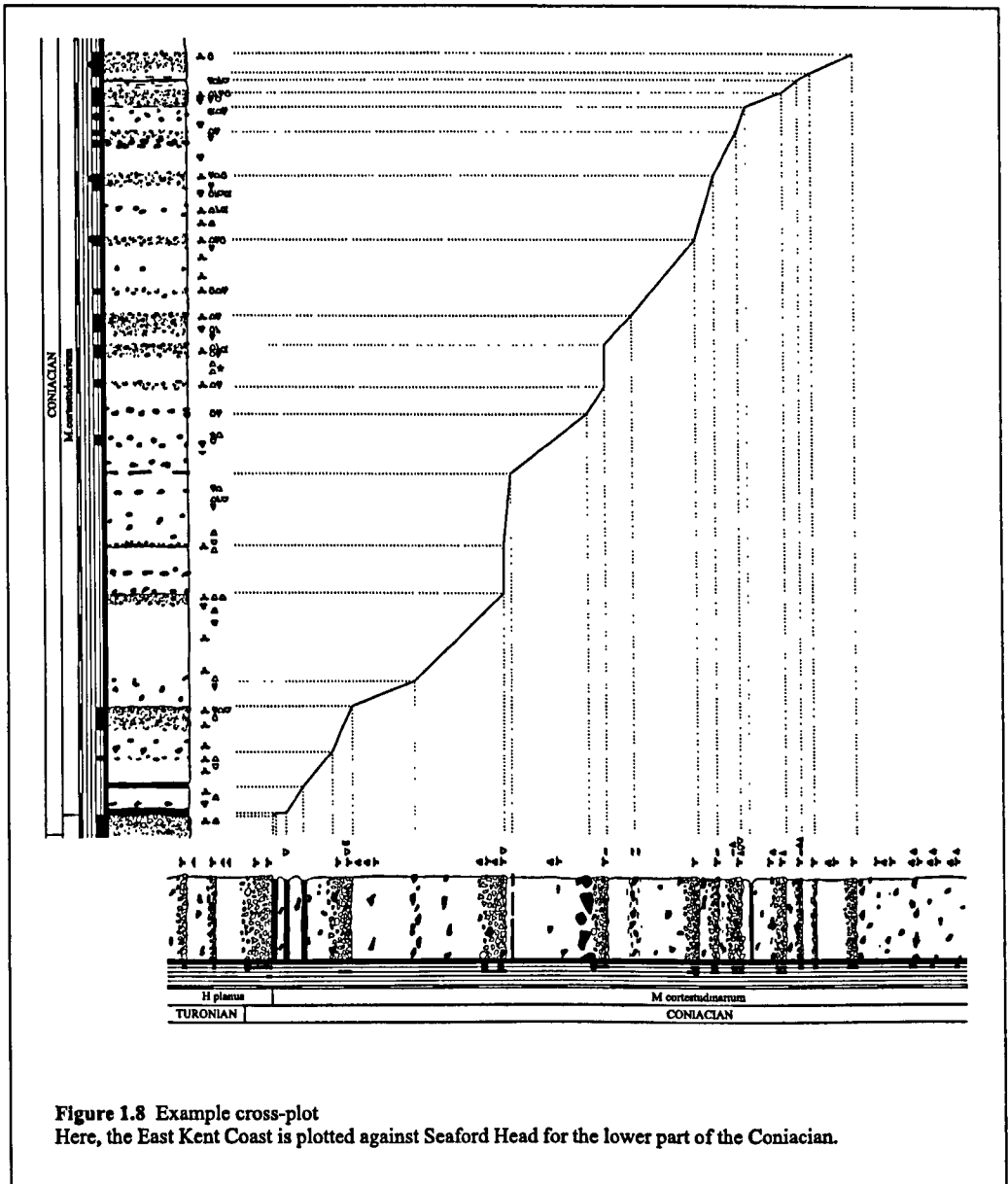
Hardgrounds and nodular chalks also mark the ts, characteristic of higher energy environments and winnowing as the basin margins are flooded. Hardgrounds at the ts are often more fossiliferous, with better preserved and more varied fauna than seen at the SB. Phosphatic and glauconitic mineralization is often common, coupled with a reduction in iron-staining compared with SB hardgrounds. Though phosphate and glauconite usually extend beneath the surface to a depth of several centimetres, mineralization is most prominent as a surface patina. In deeper-water sections, fossiliferous horizons may replace nodular chalks at the ts. The TST may be punctuated, additionally, by nodular chalks and fossiliferous horizons related to transgressive pulses.

The mfs is variously represented by a winnowed and fossiliferous horizon, nodularity or the onset of typical HST deposits which comprise homogenous white chalk, usually with regularly-spaced flint bands. It is often hard to define the mfs in chalk successions. Marl horizons may be preserved in the HST owing to reduced reworking of the sediment by current activity and an increase in detrital input as the next SB is approached. Such marls are less well-developed than those that occur in the LmST.

CORRELATION AND SEQUENCE DEFINITION

Selected, well-exposed sections in southern England and northern France (Figure 1.1) have been graphically logged (Appendix A) and broadly correlated using the key lithological horizons and published biozonations traceable across the basin. Detailed correlations have been made using the cross-plot graphical method (Carney & Pierce, 1995; Neal, Stein & Gamber, 1995) to match specific horizons such as marl bands, fossil-rich horizons, sponge beds, chert bands, nodular chalks and hardgrounds (Figure 1.8 and Appendix B). In some sections this has allowed a number of alternate lines of correlation to be investigated within the broader framework of established tie-points from the literature. Elsewhere only one correlation solution has presented itself. In all cases the simplest solution has been chosen.

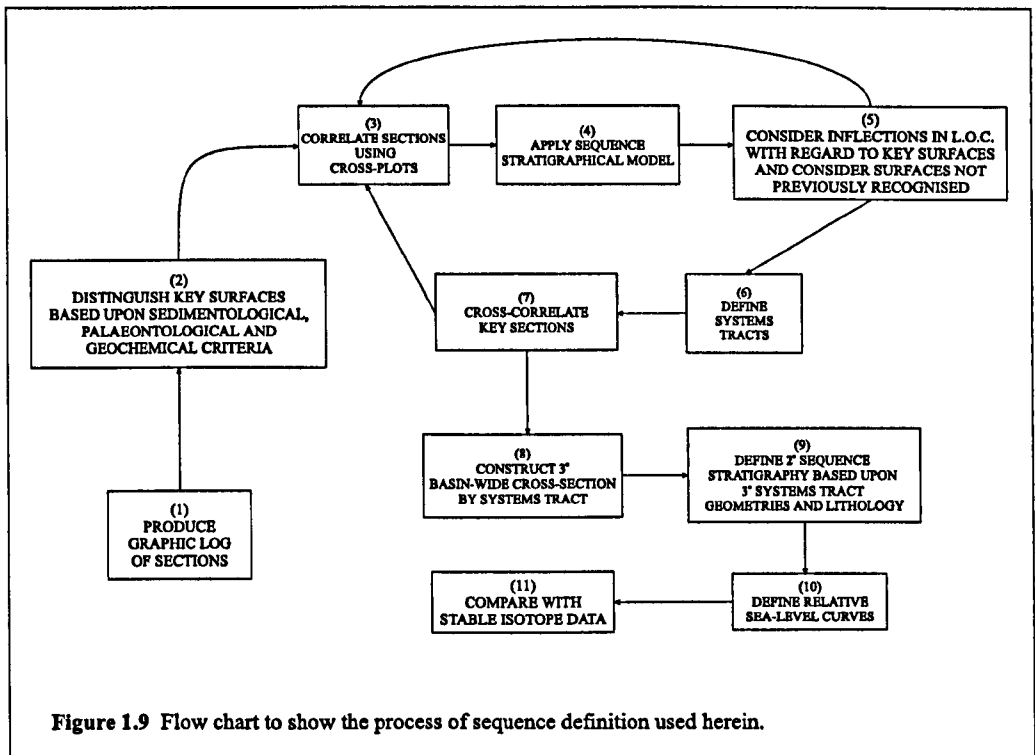
The most complete, deeper-water successions — Seaford Head, East Kent Coast, Trunch Borehole, and Culver Cliff — have been cross-plotted with each other. After these sections were correlated one against the other, they were back-correlated, through the line of correlation, to test the sequence stratigraphical analysis — key surfaces and other markers correlate from one section to the next and so on back in to the original section. This simple test of correlating section A:B, B:C, C:D and D:A, ending up with the same key surface or marker horizon in the final 'A' section as was started with in the initial 'A' section demonstrates the consistency of the correlation between sections. This process is summarised in Figure 1.9.



Key sequence stratigraphical surfaces have been identified by combining lithological and palaeontological field data with the cross-plots. Inflections in the gradient of the line of correlation indicate a change in the depositional rate between the two sections, with major inflections and identified hiatuses usually corresponding to third-order sequence stratigraphical key surfaces. Where a section does not contain a hiatus, the cross-plots have enabled the respective correlative conformity to be identified in the non-condensed section.

After the definition of a sequence stratigraphical framework for the Anglo-Paris Basin using cross-plots and the ideal chalk sequence for the four main sections, the other, more minor, sections were cross-plotted with the key sections, within the framework of previously identified marker horizons, biozone and stage boundaries, allowing the extension of the sequence stratigraphical analysis to more marginal and less continuous sections across the Anglo-Paris Basin.

The sections have been put together to form a broad cross-section through the basin using the third-order key surfaces as tie-points (Figure 1.10 and Appendix D). The area between the sec-



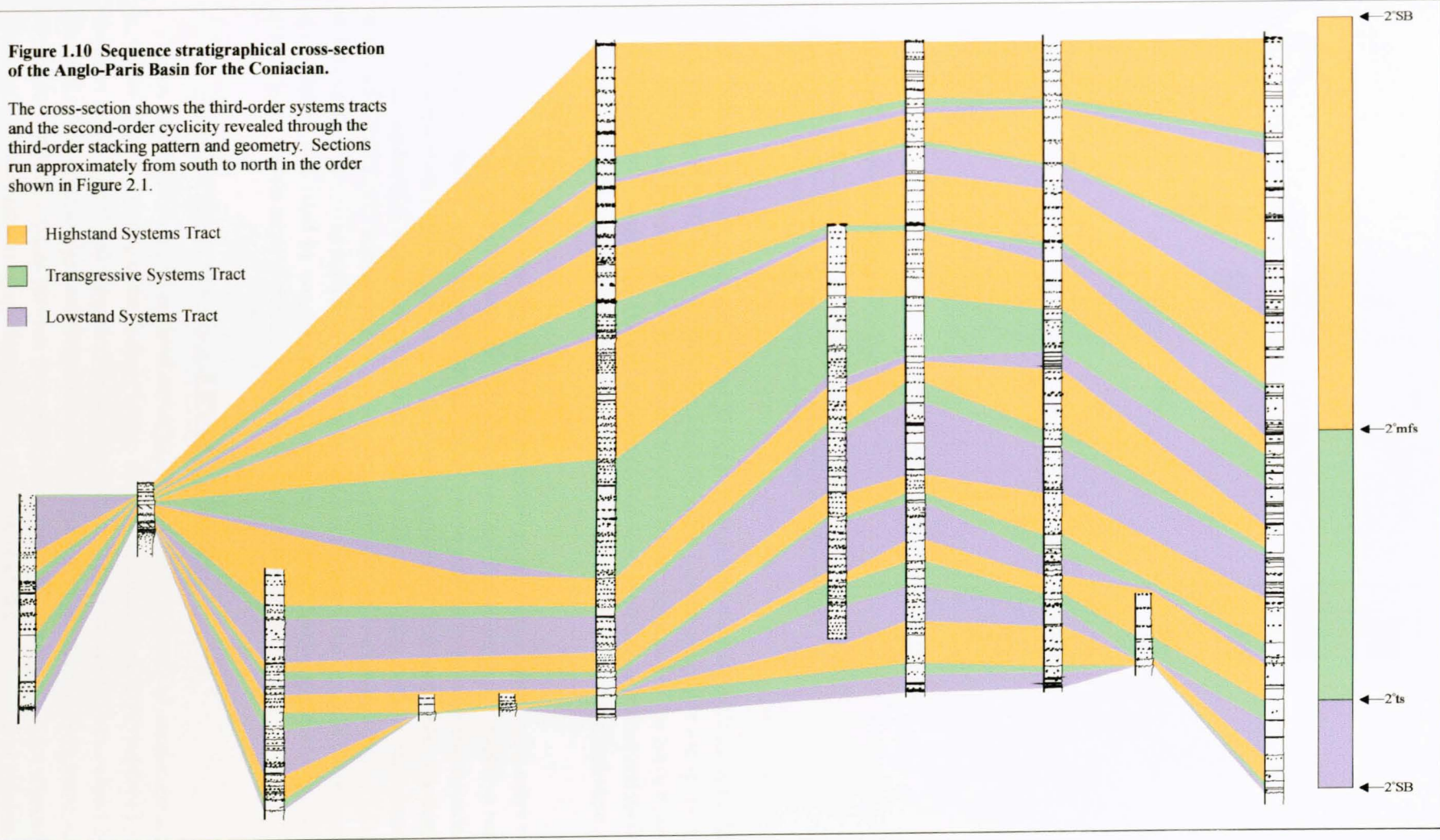
tions has been shaded to show the relative spatial and temporal development of individual third-order systems tracts. This has allowed a longer-term, second-order, cyclicity to be identified in the Anglo-Paris Basin. The second-order systems tracts are characterised by more prominent corresponding third-order systems tracts (i.e. second-order LmST by more prominent third-order LmSTs). The individual third-order systems tracts show less variation in thickness across the basin structure during second-order TSTs and HSTs, a consequence of higher relative sea-level and, consequently, more uniform depositional conditions between the sections. Similarly, during the second-order LmST, the marginal sections and those over structural highs are characterised by condensation not as apparent as in the deeper-water sections. A significant transgression over the basin margins corresponds to the longer-term transgression with shorter-term, third-order, cycles of transgression – regression superimposed upon this.

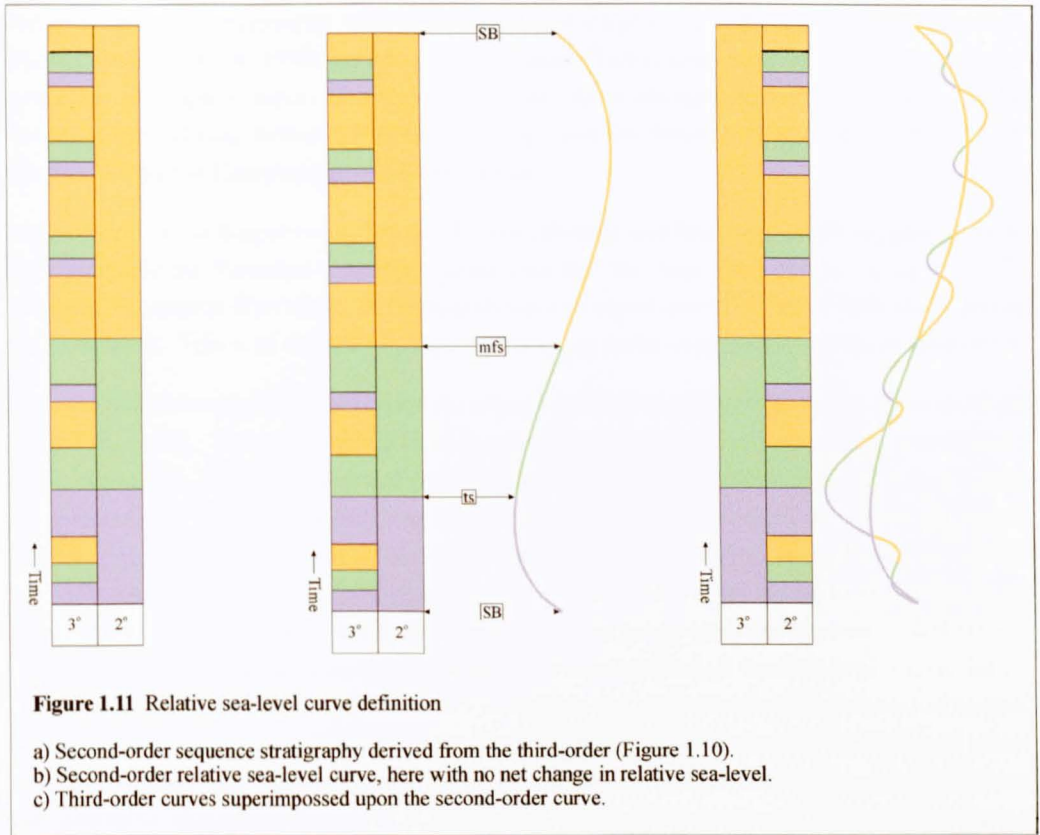
RELATIVE SEA-LEVEL CURVES

The sequence stratigraphical analysis has allowed the definition of relative sea-level curves for the Anglo-Paris Basin, over the second and third-orders, of the Coniacian – Lower Campanian interval of the Upper Cretaceous. These have then been compared to a number of published curves for the same area and wider afield.

DEFINITION OF RELATIVE SEA-LEVEL CURVES

After the definition of the sequence stratigraphical framework for the chalk sections studied, a natural spline (Bezier) curve, representing a cycle of longer-term relative sea-level was plotted alongside a sedimentary log subdivided by second and third-order systems tract, using the CorelDraw6 graphics package (Figure 1.11). The beginning and end of the curve correspond to





the second-order sequence boundaries. The falling and low part of the curve correspond to the second order LmST. The curve was plotted so that the initial increase after the low-point coincided with the second-order *ts*, and the steepest gradient on the rising part of the curve corresponded to the second-order *mfs*. The half wave-length between the maximum positive and maximum negative gradients corresponds to the second-order HST, between the *mfs* and subsequent SB.

The positions of the third-order key surfaces were marked on the Bezier curve, and a series of smaller curves were plotted between the SBs to represent the third-order cycles of relative sea-level change. These were plotted such that the initial positive gradient in the curve corresponded to the position of third-order *ts* and the maximum positive gradient to third-order *mfs*. The third-order sequence boundaries, transgressive surfaces and maximum flooding surfaces were plotted to lie on the Bezier curve representing the second-order of relative sea-level change (Figure 1.11). Relative magnitudes of the third-order curves were plotted according to the degree of relative sea-level change suggested by condensation, winnowing, sedimentology, palaeontology and geochemistry, and the relative gradient of the second-order curve.

PUBLISHED RELATIVE SEA-LEVEL CURVES

A number of published relative sea-level curves have been used for purposes of comparison and to test the wider application of the findings herein. Hancock and Kauffman (1979) published on the great transgressions and regressions of the Cretaceous. This was subsequently refined by Hancock (1990) using hardgrounds and nodular chalks as indicators of regression with transgressive peaks placed equidistant between these regressive points. Though similar to the approach used herein, no account was taken of hardgrounds and nodular chalks as indicators of transgres-

sion or the possible asymmetry of some cycles, a fact acknowledged by the author in the paper. This account (Hancock, 1990) based upon the British chalk is used for purposes of comparison herein. A subsequent paper (Hancock, 1993) used these changes in sea level, thought to be eustatic, in correlating between Northwest Europe and the Western Interior Seaway of North America during the Campanian and Maastrichtian.

Recent work on the Kaiparowits Plateau of Utah (Shanley and McCabe, 1995) suggests a base-level curve for the Turonian – earliest Campanian that has been used herein. Cooper (1977) compiled an account of evidence for transgression and regression on a world-wide scale during the Cretaceous. This is of sufficiently high resolution to make comparisons on the second-order.

The sea-level curves that have generated the most discussion are those of Haq and his co-workers (Haq *et al.*, 1988). They generated a chart detailing patterns of coastal onlap, presumed eustatic sea-level changes, calibrated ages and various biozonations for the Mesozoic and Cenozoic. This compilation used a number of erroneous tie-lines for the Cretaceous data, detailed by Hancock (1993b). Hancock's conclusion is that most of the second-order cycles in the Haq *et al.* (1988) curve are suspect and that it is difficult to relate many of their third-order cycles to the stratigraphy. Miall (1992) calculated that a series of events generated using random numbers would have a minimum of a 70% chance of correlating with the events depicted on the Haq *et al.* curve. However, as Hancock (1993b) points out, Miall's work does not take into account the order of magnitude of each event, and consequently his conclusion that any comparison with the Haq *et al.* curve is worthless might be considered harsh. However, the real problems of comparing events are seen here with three versions of the Haq *et al.* curve used, giving different results. The original version is plotted with the Haq *et al.* stage boundaries against the relevant stage boundaries herein. Subsequent versions have been plotted, firstly with calibrated age used by Haq *et al.* (1988) against the Gradstein *et al.* (1995) calibrated ages used herein and, secondly, by direct comparison of biozone boundaries.

These curves from the literature are compared to the curves generated herein on a stage by stage basis in Chapters 2, 3 and 4, and over the longer-term in Chapter 6.

STABLE ISOTOPES

OXYGEN

During evaporation of sea-water, the lighter ^{16}O fraction is preferentially evaporated, enriching the liquid fraction in ^{18}O . The $\delta^{18}\text{O}$ ratio of calcite precipitated by marine organisms is dependent upon the $\delta^{18}\text{O}$ ratio in the sea water, and temperature. The $\delta^{18}\text{O}$ ratio has been used extensively in the determination of palaeotemperature, and is a sensitive indicator of climatic change (Epstein *et al.*, 1951; Urey *et al.*, 1951; Teis, Chupakhin & Naidin, 1957; Spaeth, Hoefs & Vetter, 1971; Anderson & Arthur, 1983; Arthur, Dean & Schlanger, 1985 and Williams, 1988). The inverse relationship between temperature and the $\delta^{18}\text{O}$ ratio is enhanced during glacial intervals when ^{16}O becomes trapped in land-ice after precipitation, and has been used extensively in Quaternary studies. During periods of salinity-stratified ocean-state, evaporation leads to ^{18}O -heavy water sinking and becoming trapped beneath the pycnocline. Precipitation returns the ^{16}O to the surface waters, with a net lightening of the surface water oxygen isotope composition (Railsback, 1990).

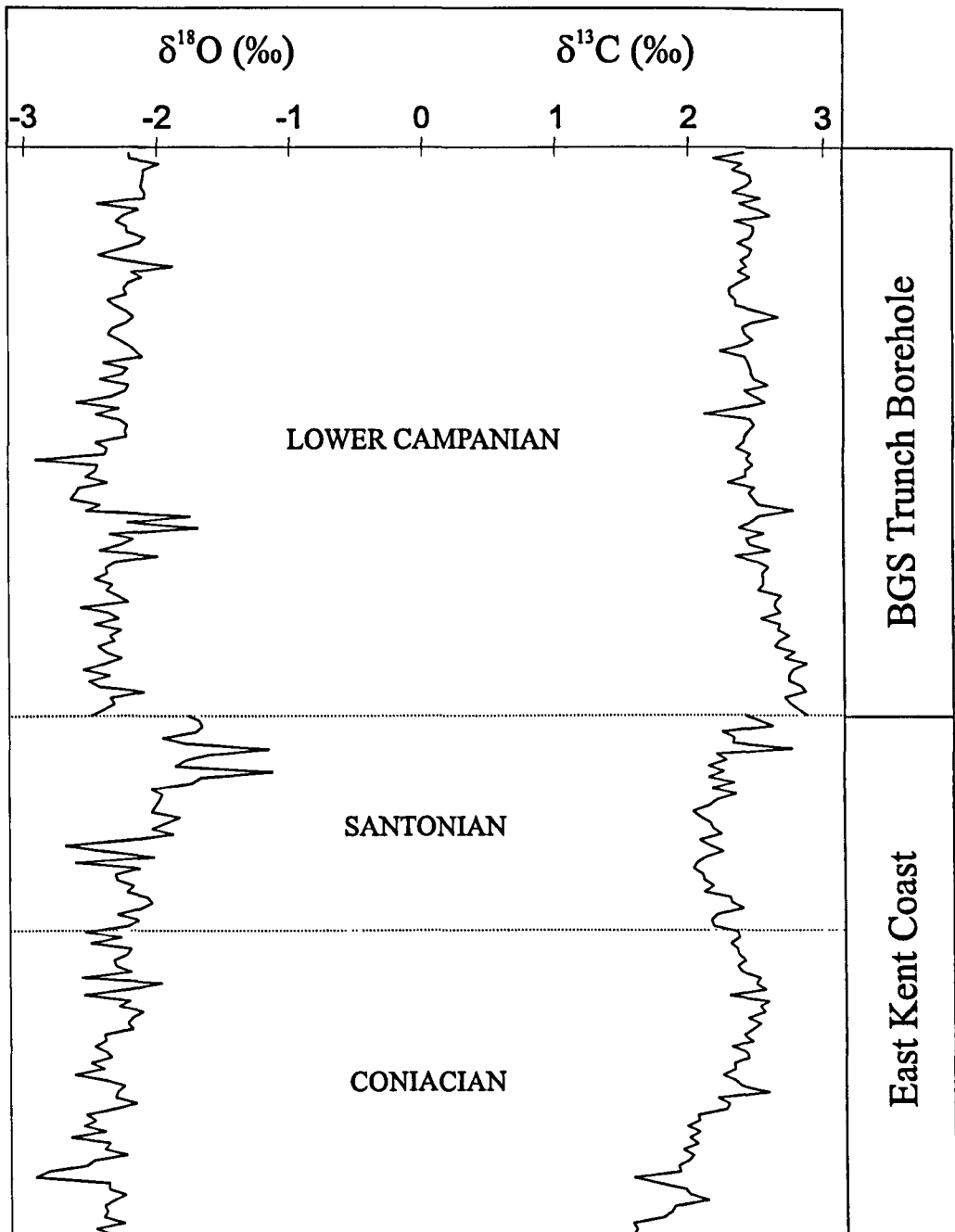


Figure 1.12 Stable oxygen and carbon isotope data. After Jenkyns, Gale and Corfield, 1994.

Jenkyns, Gale & Corfield (1994) thought that more negative $\delta^{18}\text{O}$ values were associated with clay-rich and organic-carbon rich sediments. Here, the $\delta^{18}\text{O}$ ratio is compared with the relative sea-level curves, to test whether changes are caused by climatic factors, indicated by an in-phase relationship. The $\delta^{18}\text{O}$ ratio is susceptible to the effects of diagenesis, especially the addition of isotopically light cement. However, as reported by Jenkyns, Gale and Corfield (1994) the data used here are free of a monotonic lightening with increased burial depth, characterised by clear positive and negative excursions (Figure 1.12).

CARBON

The $\delta^{13}\text{C}$ ratio reflects the fractionation between the ^{12}C and ^{13}C isotopes of carbon in the biosphere during photosynthesis, indicating biosphere and especially marine productivity, as ^{12}C is concentrated preferentially into organic carbon. These processes are climatically driven and operate on both short and long timescales (Berger & Vincent, 1986). As the majority of organic carbon is synthesised in the shallow shelf seas, an increase in the $\delta^{13}\text{C}$ ratio has been used as a proxy for a rise in sea level and a decrease as a proxy for a fall in sea level (Scholle & Arthur, 1980; Arthur, Schlanger & Jenkyns, 1987; Mitchell, Paul & Gale, 1993; Jenkyns, Gale & Corfield, 1994).

The $\delta^{13}\text{C}$ ratio is less prone to diagenetic alteration than the $\delta^{18}\text{O}$ ratio. Mitchell, Paul and Gale (1993) examined successions with demonstrably different burial and diagenetic histories but $\delta^{13}\text{C}$ curves similar enough to be used for correlation. Variation in chalk $\delta^{13}\text{C}$ directly reflects changes in the oceanic carbon reservoir. Interactions between those with significantly different isotopic compositions will appreciably alter the ratio, whilst the interaction of two reservoirs with similar compositions will have a negligible net effect (Mitchell, Paul and Gale, 1993). Increased relative sea level enlarges the area of the shallow shelf seas, and the ocean in general, where the majority of organic carbon is synthesised and enriches them in nutrients, previously locked up on the landmasses. This and the reverse process lead to a direct link between the $\delta^{13}\text{C}$ ratio and changes in relative sea level, discussed in some depth by Mitchell, Paul and Gale (1993) and Jenkyns, Gale and Corfield (1994).

Trends in the $\delta^{13}\text{C}$ ratio, therefore, can provide an independent test of the relative sea-level curves. The published carbon and oxygen stable isotope data sets (Jenkyns, Gale & Corfield, 1994) have been compared with the interpreted relative sea-level data in order to test whether they are related to the sequence stratigraphy and to investigate possible causal mechanisms for the observed changes.

Chapter 2

Coniacian

ABSTRACT

The Upper Cretaceous Chalk of Northwest Europe was deposited in an open epi-continental sea during a period of high global eustatic sea level. The sedimentary rocks preserved largely consist of a compacted and cemented biogenically precipitated coccolith ooze, bands of chert and marl beds. At intervals in the succession, winnowing and reworking have led to the development of a range of nodular chalks, firmgrounds and hardgrounds, many of which can be traced across the Anglo-Paris Basin.

Sequence stratigraphical analysis of the Coniacian succession has identified eight third-order (short-term) cycles of relative sea-level change (~400 ka. duration), superimposed upon a second-order (longer-term) cycle (~3.2 Ma. duration). The third-order cycles represent frequent, basin-wide oceanographic changes for which there are no known tectonic mechanisms. These cycles show a strong correlation with both the $\delta^{13}\text{C}$ and the $\delta^{18}\text{O}$ stable isotope curves, indicating a climatic control on sedimentation, probably linked to a Milankovitch eccentricity rhythm. The relationship between relative sea-level and $\delta^{18}\text{O}$ suggests that in a greenhouse salinity-stratified ocean, the traditional relationship between $\delta^{18}\text{O}$ and temperature breaks down.

The long-term trend in independently derived $\delta^{13}\text{C}$ stable isotope values parallels the long-term relative sea-level curve, reflecting increased productivity as the shelf area expands. By contrast, the $\delta^{18}\text{O}$ stable isotope values show little change over the long-term, suggesting tectonics rather than climate as the controlling factor on sedimentation. This is corroborated by the fact that the long-term cycle is coincident with a phase of increased activity at the mid-ocean ridges which is thought to allow for a 60 m rise in global sea-level.

INTRODUCTION

After the pioneering work of Rowe (1902, 1903, 1904, 1905, 1908) on the biostratigraphy of the English chalk, work virtually ceased. More recently, Hancock (1975) detailed chalk petrology; and lithostratigraphic and biostratigraphic schemes developed through the work of Bailey *et al.* (1983), Mortimore (1983, 1986 & 1987), Mortimore and Pomerol (1987), Robinson (1986 & 1988), Gale, Wood and Bromley (1987). Aspects of the Coniacian Top Rock have been tackled in some detail by Gale and Woodroof (1981) and Bromley and Gale (1982) whilst stable isotope studies have been published for carbon and oxygen (Jenkyns, Gale & Corfield, 1994) and strontium (McArthur *et al.*, 1992 & 1993).

The Anglo-Paris Basin of Northwest Europe formed at the junction between the Tethyan, Boreal and Atlantic Realms (Owen, 1996). The basin actively infilled from Permian times (Chadwick, 1986), with a major marine incursion during the Aptian (Owen, 1996 and references therein). Localised tectonically controlled sedimentation was reported across the area (Lake & Karner, 1987) and specifically, over the Pays du Bray Axis (Jarvis, 1980a, 1980b & 1980c; Jarvis & Woodroof, 1981 and Mortimore & Pomerol, 1987), on the Normandy coast (Mortimore & Pomerol, 1987) and over the Portsdown Axis (Gale, 1980) and the Sandown Pericline (Smith & Curry, 1975 and Mortimore, 1986), and in south Dorset (Westhead & Woods, 1994). Mortimore and Pomerol (1997) discussed tectonism in the Anglo-Paris Basin as a whole. Subsequent to the basal Coniacian, large areas of the basin were generally tectonically stable. To the northeast of the London – Brabant Massif, the Anglo-Dutch Basin marked the edge of a deeper reach of open water that extended to Scandinavia and the Danish – Polish Trough further to the east (Figure 2 of Hancock, 1975).

STRATIGRAPHY

The Coniacian Stage in southern England and northern France is represented by a succession of white pelagic coccolith packstones with regularly-spaced bands of chert, rare hardgrounds and marl horizons (Hancock, 1975) that were deposited in an open epicontinental sea during a period of high global eustatic sea level.

The standard macro-fossil biozonation for the Coniacian of the United Kingdom (Rawson *et al.*, 1978) recognises the *Micraster cortestudinarium* Goldfuss and the lower part of the *Micraster coranguinum* Leske biozones within the Coniacian. The stage can be divided into the *Barroisiceras haberfellneri* de Grossouvre and *Paratexanites emscheris* de Grossouvre ammonite zones based on the type locality, Cognac, France (Rawson *et al.*, 1978). A higher resolution ammonite biostratigraphy is available for the Tethyan Realm (Robaszynski & Amédro, 1980; Amédro, 1981 and Kennedy, 1984). Unfortunately there are virtually no ammonites recorded from southern England. There is also a tripartite inoceramid zonation for the Coniacian (Tröger, 1989), though this has not been linked to lithostratigraphy. Work in the Loir Valley has attempted a correlation between the marginal Craie-de-Villedieu Formation of the Touraine (Jarvis, Gale & Clayton, 1982 and Pomerol, 1985) with the main depocentre of the Anglo-Paris Basin using echinoids, inoceramids and ammonites. Although some work has been published on the chalk of southern England utilising microfossils (Barr, 1961; Hart *et al.*, 1989), and a detailed integrated microfossil scheme has been drawn up for the Cretaceous based on ODP results (Bralower *et al.*, 1995), these are not accurately tied to onshore lithostratigraphy. Various fossil ranges have been discussed extensively in connection with proposals for Upper Cretaceous stage boundaries (Birkelund *et al.*, 1984 and Bailey *et al.*, 1983, 1984).

In general, a number of distinct lithological and palaeontological horizons can be traced through much of the English part of the Anglo-Paris Basin (Mortimore, 1986 and Mortimore & Pomerol, 1987), though local variation is evident (e.g. Isle of Wight, Mortimore & Pomerol, 1987 and Devon, Gallois *pers. com.*). The white chalk facies of France and England are readily correlatable using lithological and palaeontological criteria (Robaszynski & Amédro, 1986 and Mortimore & Pomerol, 1987). The basin margins exhibit relatively condensed, lithified successions, with hardgrounds often representing major erosive surfaces. In the Touraine of France these hardgrounds exhibit mixed carbonate-siliciclastic lithofacies (Jarvis, Gale & Clayton, 1982).

Jenkyns, Gale and Corfield (1994) have published stable carbon $\delta^{13}\text{C}$ and oxygen $\delta^{18}\text{O}$ isotope curves based on outcrops in southern England which they correlated with data from Gubbio, Italy. Sampling points are clearly identified on sedimentary logs and these data are incorporated below. A Sr-isotope curve has been published for the Trunch borehole in Norfolk and cliff sections in Dorset (McArthur *et al.*, 1992, 1993).

The Turonian – Coniacian boundary is taken as 89 Ma. \pm 0.5 Ma. and the Coniacian – Santonian boundary as 85.8 Ma. \pm 0.5 Ma., giving a stage duration of 3.2 Ma. (Gradstein *et al.*, 1994, 1995). The Coniacian falls within the quiet magnetochron C34.

The sequence-stratigraphic method of dividing the sedimentary record into packages of genetically related sediments resulting from relative sea-level change was developed in passive continental margin siliciclastic successions (e.g. Mitchum, 1977; Vail, Mitchum & Thompson, 1977; van Wagoner *et al.*, 1988 and Vail *et al.*, 1991). A proliferation of research has followed which has included extending the concepts to carbonate facies, especially reefs and carbonate platforms (Sarg, 1988; Schlager, 1991; Hunt & Tucker 1993 and Coe, 1996). Despite the powerful nature

of sequence stratigraphy as a correlative and interpretative tool, relatively few studies have addressed deep-water pelagic-carbonate facies. The sequence-stratigraphic model needs to be adapted to take into account the unique features of pelagic chalks — a biogenic precipitate formed in the photic zone, minimal input of terrigenous material, and large distances from the landmasses. Recently, sequence stratigraphy has been applied to the relatively proximal chalk-marl alternations of the Cenomanian (Gale, 1990, 1995 and Owen, 1996). Gale (1996) and Owen (1996) discuss the characterisation of key surfaces in the purer chalks higher in the Upper Cretaceous succession.

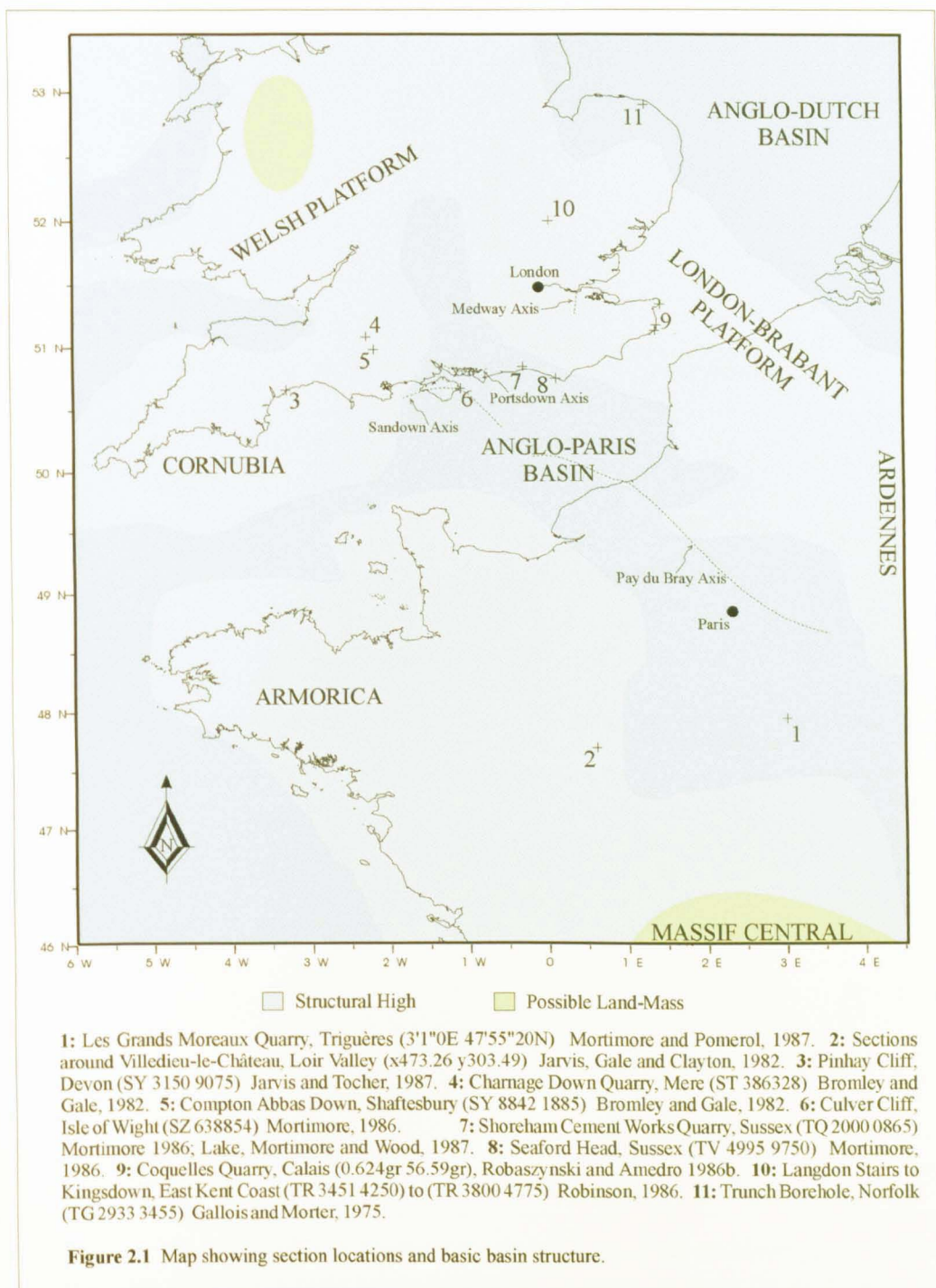
CORRELATION AND SEQUENCE DEFINITION

Selected, well-exposed sections in southern England and northern France (Figure 2.1) have been graphically logged (Figures 2.4 – 2.13, 2.15, 2.16 & Appendix A) and broadly correlated using the key lithological horizons and published biozonations traceable across the basin. Detailed correlations have been made using the cross-plot graphical method (Chapter 1; Carney & Pierce, 1995 and Neal, Stein & Gamber, 1995) to match specific horizons such as marl bands, fossil-rich horizons, sponge beds, chert bands, nodular chalks and hardgrounds (Figure 2.2 and Appendix B). In some sections this has allowed a number of alternate lines of correlation to be investigated within the broader framework of established tie-points. Elsewhere only one correlation solution has presented itself. In all cases the simplest solution has been chosen. The sections have been back-correlated through the line of correlation to test the sequence stratigraphical analysis.

Key sequence stratigraphical surfaces have been identified by combining lithological and palaeontological field data with the cross-plots. Inflections in the gradient of the line of correlation indicate a change in the depositional rate between the two sections, with major inflections and hiatuses corresponding to sequence-stratigraphical key surfaces.

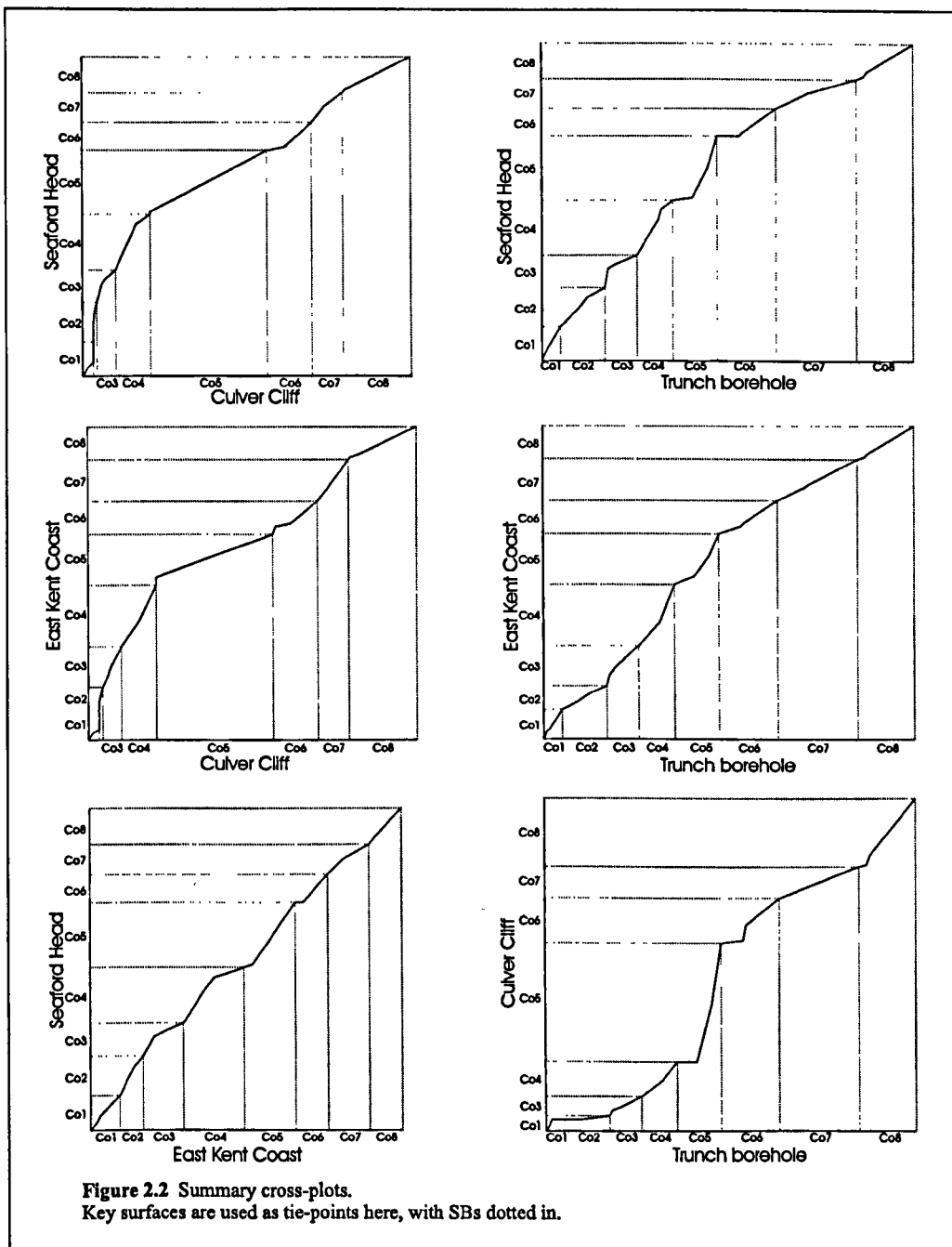
CONIACIAN SEQUENCE STRATIGRAPHY

Eight shorter-term cycles of relative sea-level change have been identified. These are superimposed upon a longer-term cycle corresponding to the entire stage (3.2 Ma. duration). The shorter-term cycles vary in thickness and in lithological characteristics, the more condensed sequences are often associated with distinct hiatuses and the relatively expanded cycles exhibit typical white chalk lithologies. The short-term sequences are defined as third-order and herein referred to as 'Co1' to 'Co8' inclusive, and the longer-term sequence is defined as second-order. The sequences are separated by sequence boundaries (SB) and each sequence can be divided into lowermost systems tract (LmST), transgressive systems tract (TST) and highstand systems tract (HST), separated by the respective key surfaces — transgressive surface (ts) and maximum-flooding surface (mfs). Calculation of the duration of individual sequences is beyond the resolution of the available radiometric and biostratigraphical data; however, based upon the absolute dating of the Coniacian Stage by Gradstein *et al.* (1994, 1995), the mean duration is 400Ka.



SEQUENCE Co1

Co1 is at its most complete and typical in the Seaford Head section (Figure 2.1, Locality 8 & Figure 2.4). The base of the Coniacian is an erosive surface developed as a nodular firmground cutting down into the Turonian chalk. This develops into a fully lithified hardground towards the basin margins and has been named variously as the Navigation Hardgrounds in Sussex (Mortimore, 1983 & 1986); South Foreland Hardgrounds in Kent (Robinson, 1986); and the lowest of the Top Rock suite of hardgrounds (Bromley & Gale, 1982 and Gale, 1996). In the Trunch borehole this corresponds to the hardground at 432.03 m. The erosive surface is interpreted as SB Co1. Where

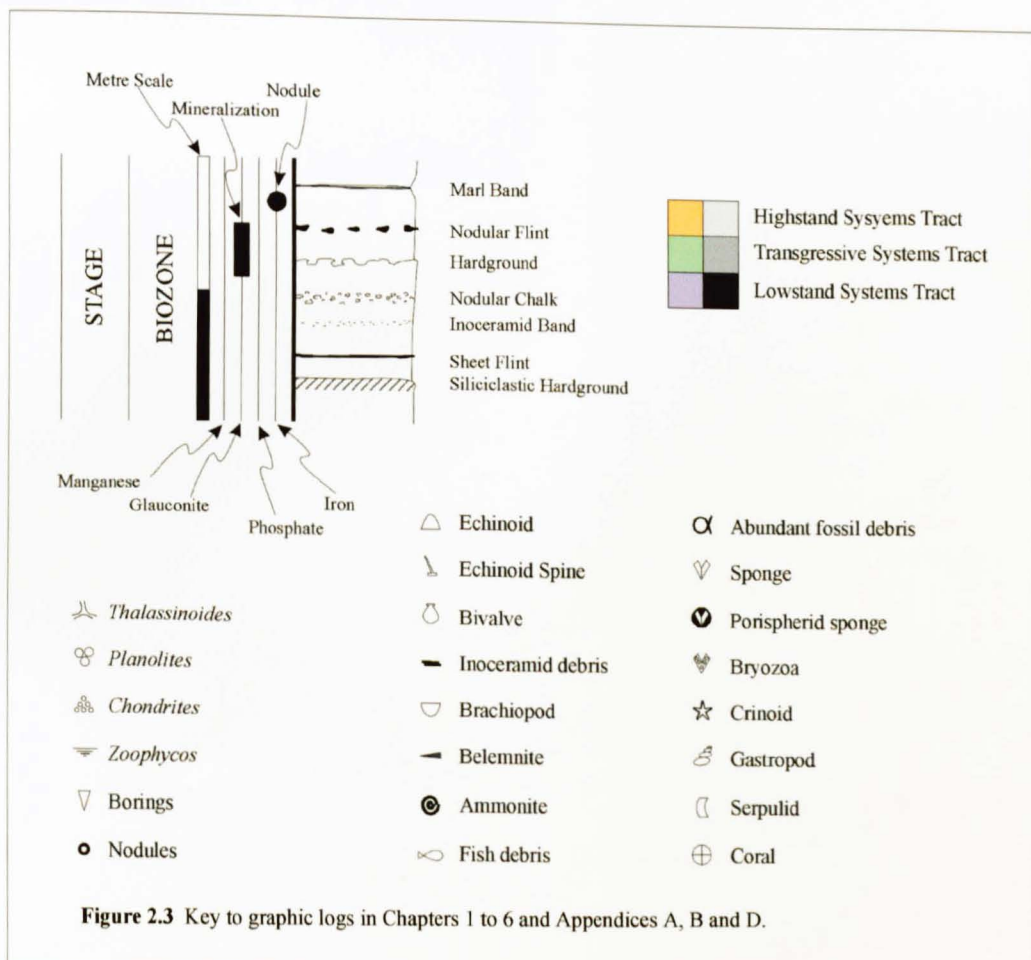


this surface is indurated it is highly mineralised with iron staining and associated pyrite nodules cemented into the chalk directly below the surface. Borings penetrate the hardground and *Thalassinoides* burrows are clearly developed with the mineralization extending downwards in the burrows as linings. Inoceramid fragments are frequently cemented into the lithified chalk. A thin package of chalk with several distinctive marl bands and localised flints overlies the hardground and represents LmST Co1. These marls are missing in the more marginal sections at Reed (Figure 2.1, Locality 10 & Figure 2.8), Compton Abbas (Figure 2.1, Locality 5 & Figure 2.9), Charnage Down (Figure 2.1, Locality 4 & Figure 2.10), Pinhay (Figure 2.1, Locality 3 & Figure 2.11) and the Loir Valley (Figure 2.1, Locality 2 & Figure 2.12).

The transgressive surface (ts Co1) is placed directly above these detrital marls, the reduction in terrigenous material is interpreted as indicative of rising relative sea-level. On the basin margins,

ts Co1 is erosive, cutting down to coalesce with the underlying SB. At Seaford Head the ts is marked by a level of nodular burrow-fill flint. Above this, the chalk is fossiliferous, with echinoids and brachiopods common. This horizon has been intensely bioturbated, with *Thalassinoides* abundant. Langdon Stairs, Kent (Figure 2.1, Locality 9 & Figure 2.15) preserves a slightly condensed, nodular, iron-stained chalk culminating in a hardground interpreted as the mfs. The Culver Cliff (Figure 2.1, Locality 6 & Figure 2.5) and Pinhay sections are flint-free during this interval, with the former containing abundant *Thalassinoides*. At Reed, Charnage Down, Compton Down, and in the Loir Valley the ts is superimposed upon the underlying SB Co1. In the Anglo-Dutch Basin at Trunch (Figure 2.1, Locality 11 & Figure 2.6) a thin package of flint-free chalk is preserved (Gallois & Morter, 1975).

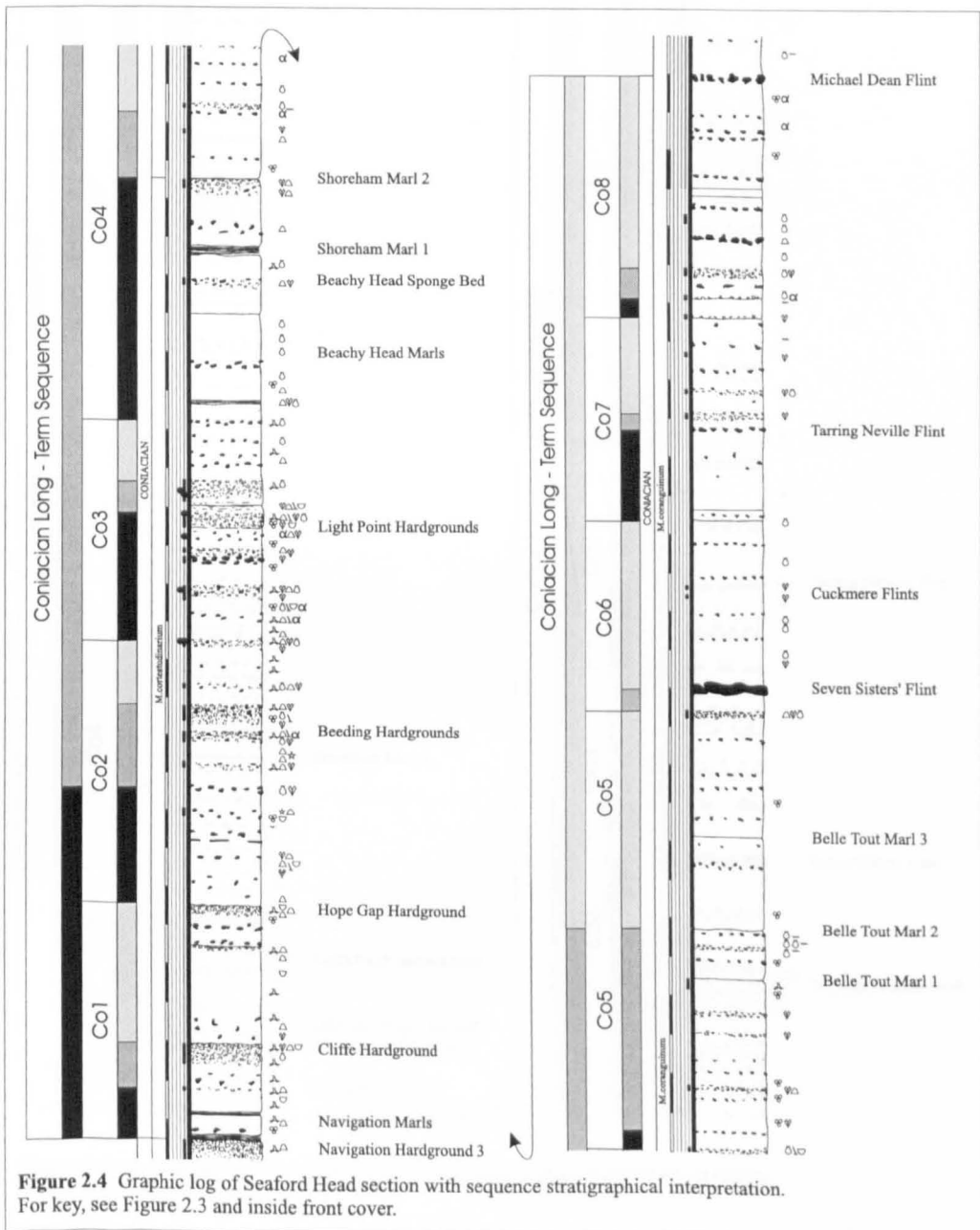
A winnowed, nodular horizon preserved in all the sections studied is interpreted as representing the mfs. This coalesces with SB and ts Co1 in the marginal sections giving a strongly indurated composite hardground (Reed, Charnage Down, Compton Down, and in the Loir Valley). A thicker succession of white chalk with bands of chert is taken as representing the HST across the basin. This has not been preserved at Culver Cliff, probably owing to movement associated with the Isle of Wight fault system (Karner, Lake & Dewey, 1987 and Mortimore & Pomerol, 1991a and 1997). On the Sussex and Kent coasts a typical chalk and flint rhythmicity indicates the HST. This is capped by a nodular chalk horizon associated with the overlying sequence boundary. At Trunch a largely flint-free succession with a marl band is interpreted as the HST. At Reed, 50 cm of white chalk is present above the hardground of coalesced SB, ts and mfs Co1. This chalk is relatively unfossiliferous with no flints. The pit on Compton Abbas Down exposes 17 cm of white chalk (HST), the top of which is indurated, linked to the formation of the hardground above. This



HST package is bioturbated with distinctive small *Thalassinoides* burrows and is absent at Charnage Down. The Loir Valley succession is slightly less condensed, with a few centimetres of soft glauconitic calc-arenite preserved and interpreted as the HST. At Pinhay a thin marl band and two nodular hardgrounds within a nodular, sandy-chalk facies are interpreted as forming an anomalous HST succession, topped by a hardground associated with the overlying SB (Co2). These lithologies are characteristic of the high-Turonian and low-Coniacian in the area.

SEQUENCE Co2

This sequence is noticeably thicker than Co1 in all the deeper water sections, except for Culver Cliff, where the entire sequence is represented by only 30 cm of semi-indurated chalk. The Sussex Coast exposes the complete sequence clearly, as does the Langdon Stairs section on the Kent coast. However, in the latter section, some considerable condensation is evident at the level of the ts when compared to sections inland (Robinson, 1986), and the exposure beneath Seaford Head is



preferred as a reference section. In all the sections studied an indurated and strongly nodular chalk passing laterally into a distinctive hardground on the basin margins represents SB Co2. This is at a depth of 428.76 m in the Trunch borehole and correlates with the Hope Gap Hardground in Sussex and the Pines Garden Hardground in Kent. At Compton Abbas the correlative hardground is fairly massive, with burrows penetrating the underlying HST; the surface is phosphatic and exhibits a glauconitic veneer interpreted as being associated with the ts, superimposed upon SB Co2. In Charnage Down Quarry the SB is also represented by a composite (mfs Co1 – ts Co2) hardground near the base of the Coniacian succession. Above SB Co2 in the Trunch borehole a succession of relatively flint-free chalk is preserved, representing the LmST, whilst this unit is flinty in Kent and Sussex. At Pinhay Cliff, a thick package of flinty, nodular chalk with two thin

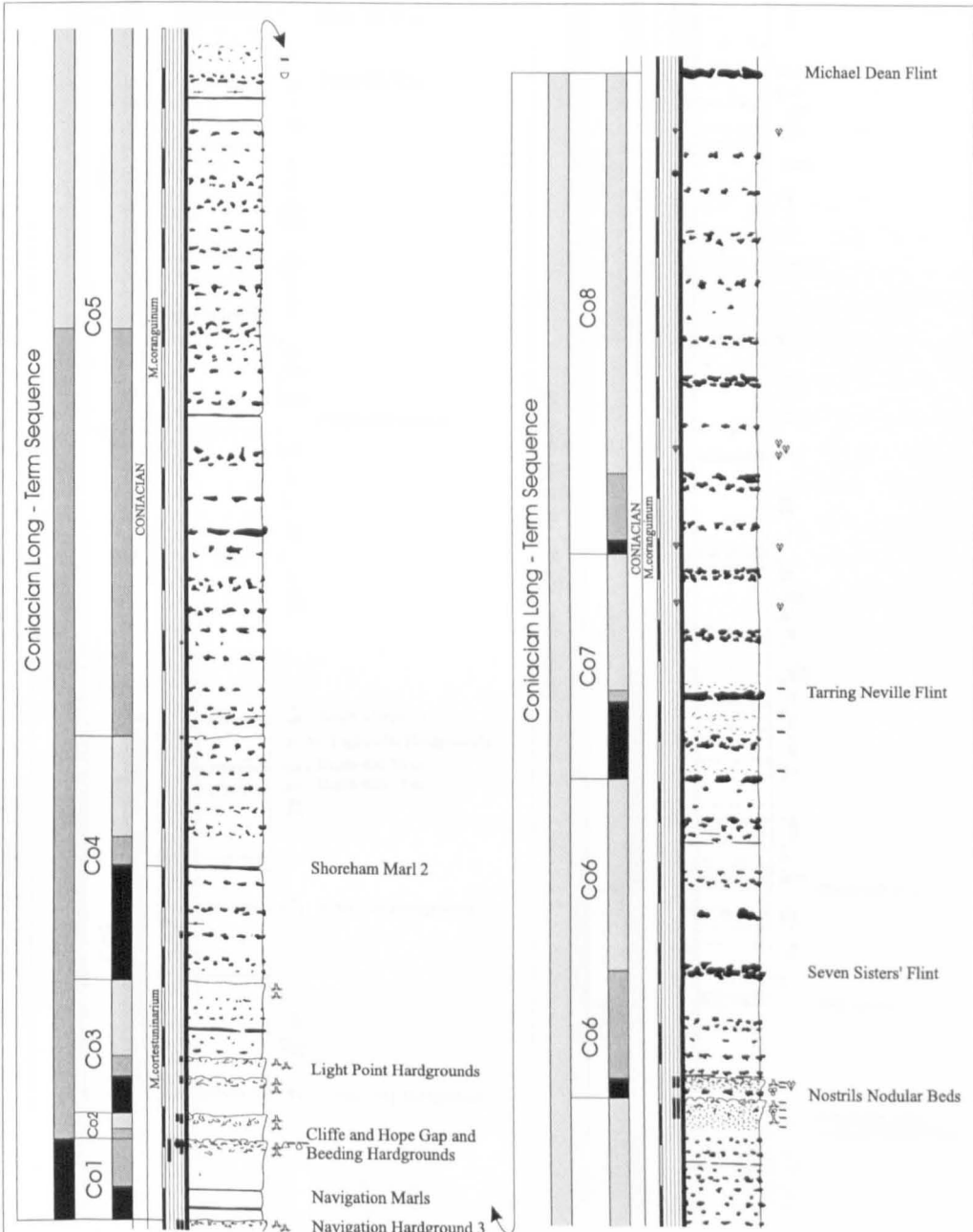


Figure 2.5 Graphic log of Culver Cliff section with sequence stratigraphical interpretation. For key, see Figure 2.3 and inside front cover.

marl bands is present and interpreted to represent the LmST. The chalk in the cliffs here varies considerably locally (Gallois *pers. com.* 1996) and the correlation with the main sections at Culver Cliff, Seaford Head and on the East Kent Coast must remain tentative at the current time. At Culver Cliff the LmST is not preserved, again probably related to local tectonic activity. This systems tract has also been removed at Reed and in the Loir Valley by current winnowing associated with ts Co2.

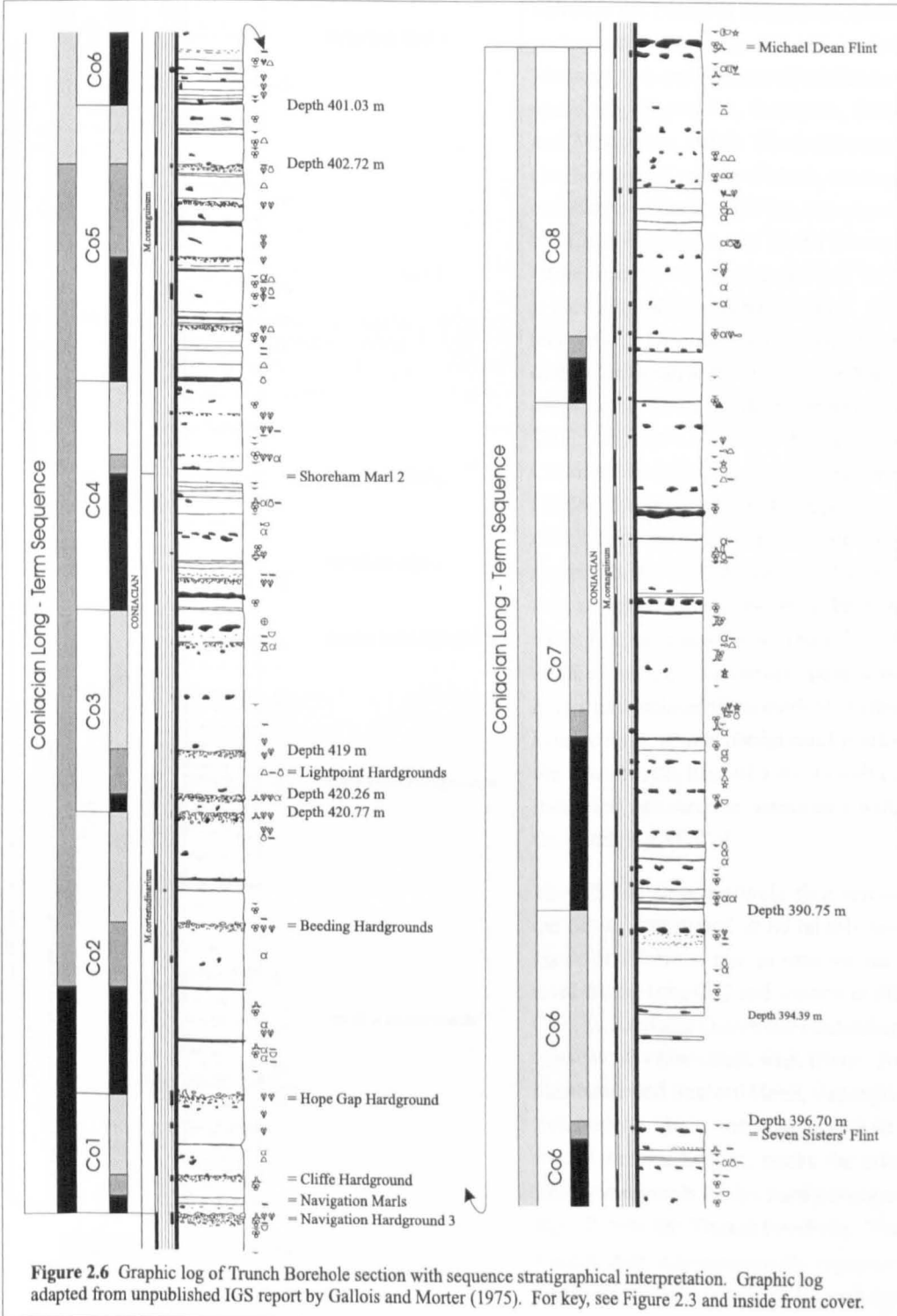


Figure 2.6 Graphic log of Trunch Borehole section with sequence stratigraphical interpretation. Graphic log adapted from unpublished IGS report by Gallois and Morter (1975). For key, see Figure 2.3 and inside front cover.

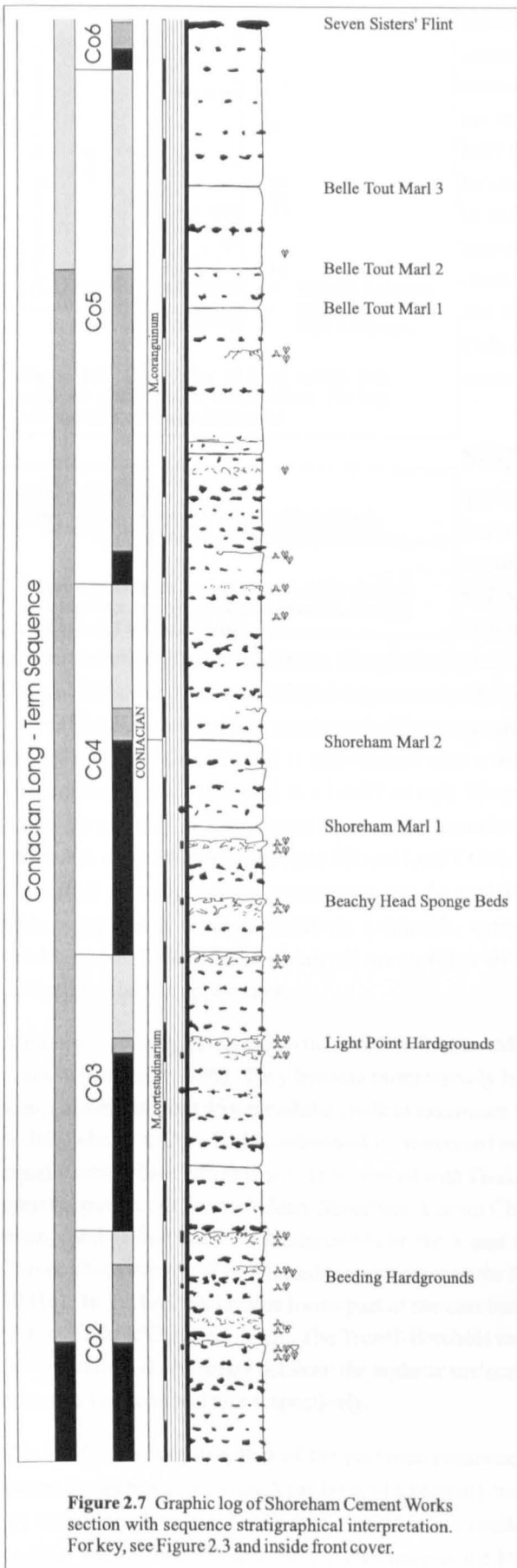


Figure 2.7 Graphic log of Shoreham Cement Works section with sequence stratigraphical interpretation. For key, see Figure 2.3 and inside front cover.

A return to more nodular chalk marks the ts in the main depocentres. This is especially clear in the Kent, Seaford Head and Shoreham Cement Works (Figure 2.1, Locality 7 & Figure 2.7) sections where several winnowed, nodular horizons are interpreted as transgressive pulses. Longer hiatuses are observed in the Langdon Stairs and Culver sections related to movement on the Medway Axis and Sandown Pericline respectively (Figure 2.1; Robinson, 1986 and Mortimore, 1986). The former section has several metres of chalk missing at the level of the Stroud Flint, compared to inland sections in the North Downs (Robinson, 1986). At Culver, a thin TST is preserved above the hardground. After considerable condensation at the base of the Coniacian at Reed, 1.5 m of flinty chalk and inoceramid debris marks the TST. In the Compton Abbas and Charnage area, the succession remains condensed, preserving a 30 cm package of more strongly indurated chalk that represents the TST. In Devon, a distinctive nodular horizon below a broken sheet flint indicates the ts. The 1.3 m of chalk above this is relatively pure with only small isolated flints evident. In the Loir section, a thin hardground marks the ts within the base of a 40 cm unit of indurated calc-arenite associated with the overlying SB Co3.

The HST is comparatively thin across the basin, interpreted to be largely the result of a limited rise in relative sea-level during time Co2 and erosion at SB Co3. In Kent and Devon the succession consists of white chalk with flints. At Shoreham and Seaford Head, a sponge-rich nodular chalk, the highest of a series of three in Sussex, marks the mfs. This corresponds to the hardground at 423.82 m in the Trunch borehole. The Reed section is comparatively expanded with 3.5 m of white chalk with regularly

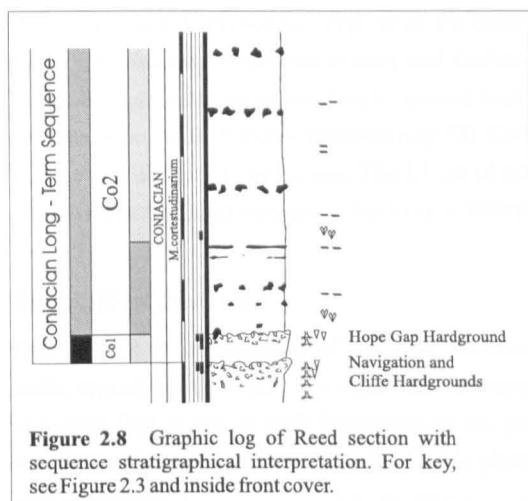


Figure 2.8 Graphic log of Reed section with sequence stratigraphical interpretation. For key, see Figure 2.3 and inside front cover.

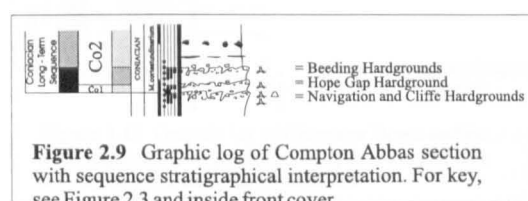


Figure 2.9 Graphic log of Compton Abbas section with sequence stratigraphical interpretation. For key, see Figure 2.3 and inside front cover.

spaced flint bands, before the section is obscured by slipped ground. After the period of tectonically-induced condensation and the 20 cm thick TST at Culver Cliff, a 40 cm thick HST terminates in a unit of bioturbated, nodular chalk beneath SB Co3. The HST is thinner in the Loir Valley where it forms part of the heavily indurated, coarse-grained, silica-rich chalkstone with intense *Thalassinoides* beneath the Ribochère Massive Hardground (Jarvis, Gale & Clayton, 1982). A typically flinty HST succession is preserved at Charnage Down.

SEQUENCE Co3

This is the first sequence in the Coniacian that has a degree of lithological uniformity across the main sections examined in the Anglo-Paris and Anglo-Dutch Basins though it remains condensed in the Loir Valley. The most complete

reference section is at Seaford Head, though the slightly condensed sections at Langdon Stairs and Culver Cliff exhibit better developed sequence stratigraphical key surfaces. The succession in the Trunch Borehole is relatively condensed with hardgrounds forming the SB (420.77 m), ts (420.26 m) and mfs (419 m). The SB is iron-stained with a dense network of *Thalassinoides* burrows. This condensation is reflected in a LmST of only 76 cm; thickening into the deeper parts of the Anglo-Paris Basin. In Kent, several nodular hardgrounds (Corn Hill Hardgrounds 1–3 of Robinson, 1986) and a marl band characterise SB and LmST Co3. The nodular chalks are iron-stained and have small phosphatic nodules cemented into the hardground surfaces. The chalk is fossiliferous, with conspicuous borings, bivalves, echinoids, echinoid spines, inoceramids, sponges and brachiopods. *Thalassinoides* burrows are in-filled with indurated chalk, giving the horizons a distinctive nodular appearance.

A number of hardgrounds outcrop on the London-Brabant Massif in Kent (Corn Hill Hardgrounds 4–7, *sensu* Robinson 1986). They become progressively less winnowed and pronounced up-succeSSION, culminating in a 45 cm nodular chalk at maximum flooding. The onset of phosphate-stained nodular chalk, at Corn Hill Hardground is interpreted as the ts. The overlying nodular chalks are equally mineralised and extensively burrowed with *Thalassinoides* and represent subsequent transgressive pulses. At Seaford Head, Shoreham, Culver Cliff and Pinhay the TST is less than a metre thick, sandwiched between hardgrounds at the ts and mfs. The ts is particularly prominent at Culver where it may still be affected by movement on the Sandown Pericline (Mortimore & Pomeroy, 1991a). In the Loir Valley this forms part of the unit beneath the Ribochère Massive Hardground (Jarvis, Gale & Clayton, 1982). The Trunch Borehole records 1.26 m of chalk with isolated flints, inoceramids and *Micraster* between the nodular surfaces at 420.26 m and 419 m which are interpreted to be the ts and mfs respectively.

The HST is thicker than that of the previous sequence, and demonstrates greater variation between the sections. At Trunch the level of a partially indurated, iron-stained sponge bed (419.00 m) represents the mfs. Above this, 4 m of white chalk with occasional flint bands and another nodular sponge bed towards the top characterise the HST. In Kent, a similar thickness of more

chert-rich chalk is preserved, typical of the other sections in the English part of the Anglo-Paris Basin. At Seaford Head, Shoreham and Culver Cliff, the HST is thinner, still containing flint bands, though these are more closely-spaced than in Kent. In these sections the HST is terminated by a nodular chalk horizon representing SB Co4. Though more condensed, this level does not display any nodularity in Devon. The 25 cm of indurated sediment directly beneath the Ribochère Massive Hardground surface in the Loir is interpreted as the HST.

SEQUENCE Co4

This is the lowest sequence of uniform thickness and distribution across the main parts of the basin, signifying the onset of a significant transgression, inundating the basin margins. Typically, sequence Co4 is not as well developed as the previous ones. It is best developed in the Trunch borehole reference section. Here SB Co4 is placed at 415.17 m directly beneath the lowest of the

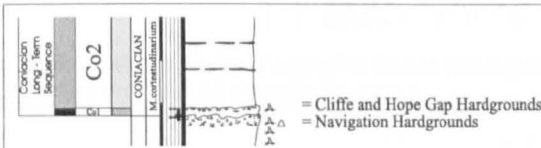


Figure 2.10 Graphic log of Charnage Down section with sequence stratigraphical interpretation. For key, see Figure 2.3 and inside front cover.

marls which characterise the LmST at this level. In the Anglo-Paris Basin a similar influx of clay is not seen at SB Co4, suggesting an isolated source area to the north or north-east of the Anglo-Dutch Basin. LmST Co4 in the Anglo-Paris Basin is the thickest of the Coniacian Stage. Pinhay Cliff, Culver Cliff and the Kent coast exhibit a series of regularly-spaced flint bands. This heralds a return to ‘normal’ sedimentation over the Isle of Wight, after a period of relative condensation during Co1 – Co3. In Sussex, two prominent marl bands are developed within the LmST, with a third preserved at the ts. The LmST chalk is slightly nodular in Sussex, though thicker than elsewhere. In the Loir Valley reworking has led to a clastic lag of sponge-bored nodules which is interpreted as the LmST. The LmST attains a considerable thickness, up to 6.25 m, across the deeper sections examined, though is only partially preserved on the basin margins.

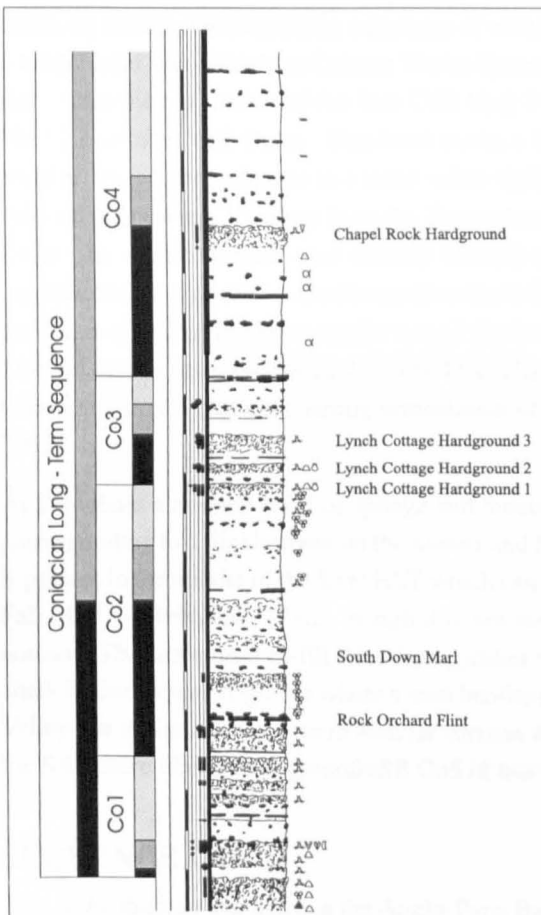
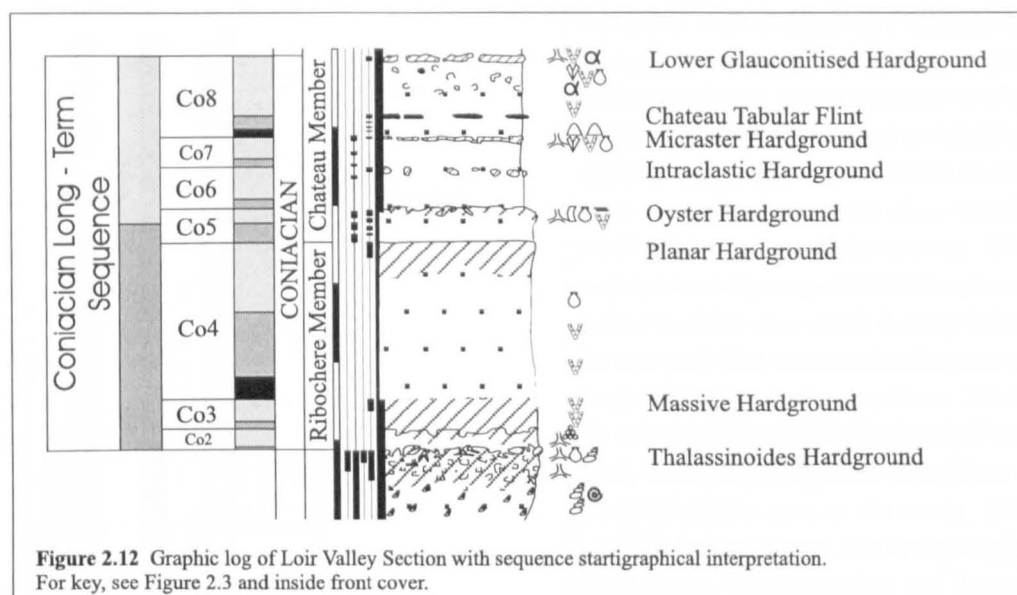


Figure 2.11 Graphic log of Pinhay Cliff section with sequence stratigraphical interpretation. For key, see Figure 2.3 and inside front cover.

The ts coincides with the onset of the major long-term transgression, and at Pinhay this is marked by the glauconitic and phosphatic Chapel Rock Hardground (Jarvis & Tocher, 1987). At Triguères (Figure 2.1 Locality 1 & Figure 2.13), a hardground also characterises the ts. Here it is well-developed with phosphatic mineralization, a glauconitic patina and extensive surface borings (Figure 2.14), though in the field, details are obscured by liesegang rings. It is overlain by a horizon rich in echinoids encrusted by serpulids and bryozoa passing upwards into



flint-free chalk. The ts corresponds to the base of the *M. coranguinum* Biozone. In the main part of the Anglo-Paris Basin a bentonite is present directly beneath the ts (Shoreham Marl 2 of Mortimore, 1986). This bentonite is present at Culver Cliff where it is overlain by 80 cm of white chalk. In Sussex it is overlain by a package of white chalk truncated by erosion that culminates in a hardground. At Shoreham Cement Works Quarry this hardground represents the mfs. On the Kent coast the top surface of the East Cliff Marl 2 (Robinson, 1986), a correlative of Shoreham Marl 2, coincides with the ts. This level marks a basin-wide change in lithology from partially nodular, winnowed sediment to a purer softer chalk associated with increased water-depths and reduced winnowing. The core from the Trunch borehole is missing in what is presumed to be the lower part of this systems tract directly beneath a flint; the upper portion of the systems tract consists of flint-free chalk. On the south-western flank of the Anglo-Paris Basin, the Loir Valley section is a similar thickness to the rest of the basin, highlighting the long-term transgression. This has locally reworked the LmST. The TST is largely represented by a finer grained bioturbated calcareous sand lacking the strong cementation of the nodular horizon (Jarvis, Gale & Clayton, 1982).

At Shoreham a nodular level of sponge and inoceramid debris 70 cm above Shoreham Marl 2, corresponding to a flint horizon on the Sussex and Kent coasts, marks the mfs. An indistinct marl is present in the middle of the Kent HST which can be traced throughout the North Downs (White Fall Marl — Robinson, 1986), though it is not seen in the sections outside Kent. A more pronounced *Thalassinoides* in-fill flint distinguishes the mfs at Culver Cliff. The change to flinty chalk is also seen at Triguères where a marl band is preserved directly beneath the mfs. In the Loir Valley this is signified by a more nodular horizon within the strongly lithified unit culminating in the Riboichère Planar Hardground (SB Co5 of this scheme) of Jarvis, Gale and Clayton (1982).

SEQUENCE Co5

This is the thickest sequence in the Anglo-Paris Basin. The most typical exposure can be seen at Langdon Stairs on the Kent coast, though here it is more condensed than in other sections. The thickest development of the sequence is at Culver Cliff, but only the HST is preserved here. At Culver Cliff, an iron-stained hardground, rich in sponge debris marks the SB. In Sussex this

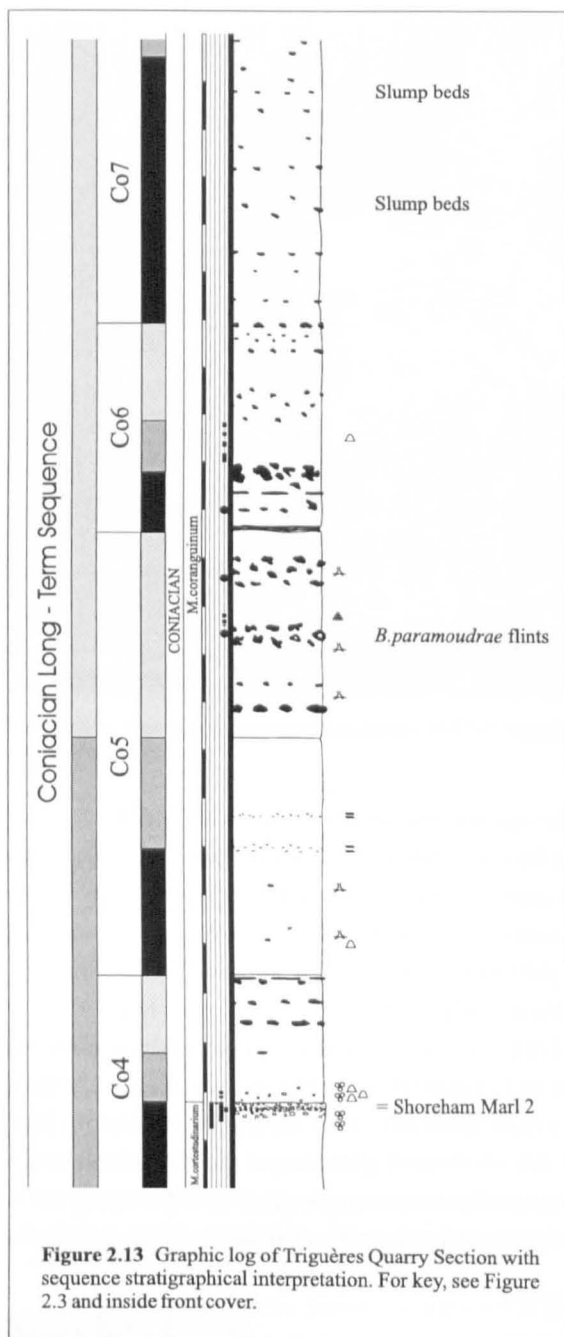


Figure 2.13 Graphic log of Triguères Quarry Section with sequence stratigraphical interpretation. For key, see Figure 2.3 and inside front cover.

correlates with a winnowed horizon of sponge, echinoid, inoceramid and brachiopod debris. In the Trunch borehole, a nodular horizon is preserved at 407.25 m within a succession of marl bands at this level. No further evidence of winnowing is preserved here or on the Kent coast. The correlative conformity of SB Co5 is placed at the top of the white chalk directly below the first marl that characterises the base of LmST Co5 in both these sections. Marls are not seen at this horizon in the other sections, indicating terrigenous input from a probable source area to the north. The LmST is generally very thin in the Anglo-Paris Basin, thickening into the Anglo-Dutch Basin. To the south-east, at Triguères a marl band is preserved 2.5 m above the hardground. The correlative of SB Co5 lies directly beneath this marl. Above this, the chalk is characteristically flint-free and indicative of the LmST. A major hiatus occurs in the Loir sections — the Ribochère Planar Hardground, representing the SB above which no LmST is preserved.

The TST is well preserved in the main sections of the Anglo-Paris and Anglo-Dutch Basins, attaining a considerable thickness throughout. This is indicative of peak flooding coincident with the interval directly below the long-term mfs. At Trunch a sponge-rich, iron-stained hardground (405.36 m) characterises the ts. A further hardground in the middle of this package (403.80 m), similar to that of the ts, identifies another transgressive pulse. At Culver Cliff the ts

is locally erosive, cutting down to merge with the hardground surface interpreted as SB Co5. The thick (11 m) package of chalk with flint bands overlying this forms the TST. Elsewhere in the English sections there is no evidence for erosion, and a correlative conformity is placed at the first flint band above the SB at Seaford Head. This correlates with the return to chalk directly above the uppermost marl band at this level on the Kent coast. Above the ts, the Loir sections preserves a thin horizon of fossiliferous calc-arenite sediment forming the TST. Oysters (*Ceratostreon* — Jarvis, Gale & Clayton, 1982), inoceramids, bryozoa and serpulid casts are abundant, and the upper surface of this unit forms an indurated horizon named the Château Oyster Bed (Jarvis, Gale & Clayton, 1982). At Triguères the base of the lower of two bands of inoceramid debris is identified as representing the ts with the overlying flint-free package forming the TST.

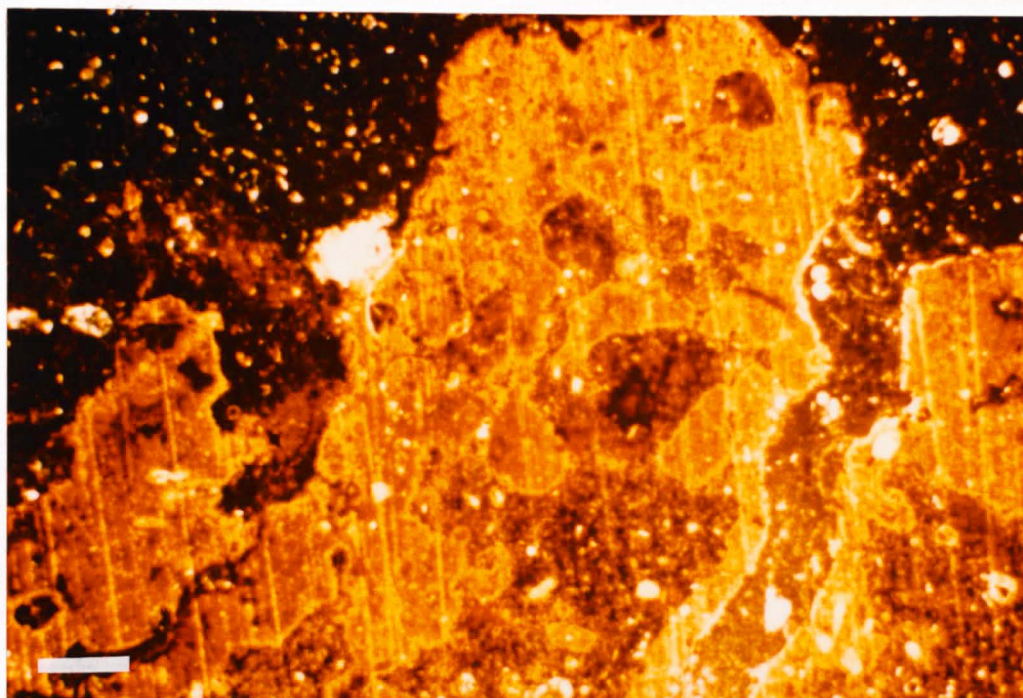


Figure 2.14 Photograph of hardground surface (ts Co4) Triguères Quarry. Scale bar is 2mm.

In the Trunch borehole a well-developed hardground (402.72 m), rich in sponges, and slightly iron-stained is formed at the mfs. Abundant *Zoophycos*, bioturbating 20% of the rock alongside occasional *Thalassinoides* and *Planolites* burrows, characterises the overlying HST. This unit thickens into the Anglo-Paris Basin, reaching its maximum thickness in the deeper-water sections. At Culver Cliff, the succession is now considerably expanded, and, above sequence Co5 represents the most complete section studied. There is little lithological variation in the chalk between the main sections, with regularly-spaced flint bands and the occasional marl being typical. In Kent and Sussex, the top surface of the upper of two marl bands marks the mfs. In Sussex a third marl is preserved within the HST. The flinty succession is also characteristic of Triguères where a marl horizon occurs immediately beneath the mfs and the return to HST chalk. The thick HST is not preserved in the Loir where current-activity associated with the longer-term maximum rate of relative sea-level rise is interpreted to have extensively winnowed the sediment.

SEQUENCE Co6

This sequence is well developed throughout the Anglo-Paris Basin and was deposited during the onset of the long-term relative sea-level maximum. None of the locations provides an ideal reference section. The most complete sequence is preserved in the Trunch borehole, with a well-developed though more condensed section visible at Culver Cliff. The HST is most typical at Seaford Head whilst the SB and ts are best preserved at Culver Cliff. In these two sections an erosive surface marks the SB. This forms a distinctive yellow, iron-stained hardground associated with inoceramid debris at Culver Cliff, clearly visible on the southern side of the White Horse promontory (SZ 638854). Above this, 40 cm of LmST is preserved before another distinctive hardground marking the ts. The Seaford Head succession is less indurated; SB Co6 is represented by a sponge-rich nodular horizon above which no LmST is preserved. In the Loir the top of the indurated Oyster Hardground (Jarvis, Gale & Clayton, 1982) represents the SB. At Shoreham a flint band, two below the distinctive Seven Sisters Flint (*sensu* Mortimore 1983, 1986), is corre-

lated with an erosive nodular level at Seaford Head that is interpreted as SB Co6. Compared with Seaford Head, the succession at Shoreham is slightly expanded preserving a thin LmST. At Langdon Stairs a succession similar to that at Shoreham is observed, though here it is slightly more expanded. The succession thickens into the Anglo-Dutch Basin where a unit of poorly-fossiliferous marl-rich chalk at Trunch represents the LmST. The correlative conformity is placed directly beneath the lowest of these marl bands (401.03 m). This horizon is fossiliferous with fish remains, sponges, brachiopods, *Micraster* with some *Inoceramus* debris. A pyrite₂ nodule is preserved above the main unit of marls. Trace fossils are also present, with *Zoophycos*, *Planolites* and *Thalassinoides* all evident. At Triguères a thick, limonite-stained marl band marks the base of the LmST, above which a thin package of flinty chalk is preserved, characterised by distinctive *Paramoudrae bathichnus* flints (Bromley, Schulz & Peake, 1975), possibly indicating rapid deposition (Mortimore & Pomerol, 1987).

At Seaford Head the SB Co6 and ts are coincident at the top of a nodular chalk. A more pronounced hardground is evident at Culver Cliff and this is iron-stained and associated with abundant inoceramid debris. The TST is relatively expanded here and comprises 2.5 m of flinty chalk, but in Trunch, Sussex, Triguères and on the East Kent Coast its maximum thickness is 40 cm. At Kent, Shoreham and Triguères this is as a thin package of white chalk without flint. This horizon consists of white chalk with a band of flint directly below 231 cm of missing core in the Trunch borehole (396.70 – 394.39 m). The sediment in the Loir is partially indurated around oyster shells above the Oyster Hardground, becoming more lithified towards the top of the unit.

A major semi-tabular flint traceable throughout the main part of the Anglo-Paris Basin (East Cliff Flint of Bailey *et al.*, 1983, 1984; Gale, Wood & Bromley, 1987; Oldstairs Bay Flint of Robinson, 1986 and Seven Sisters Flint of Mortimore, 1983, 1986), coinciding with a level of missing core in the Trunch borehole (394.39 m) marks the mfs. Above this, a package of white chalk with regularly-spaced flints characterises the HST of equal thickness throughout the sections studied. This level marks the top of the accessible section at Shoreham Cement Works, though the flint bands in the chalk are clearly visible up to the lower Santonian. At Triguères a return to the distinctive chalk-flint rhythms marks the mfs and HST in the east wall of the upper part of the quarry. At Culver, Seaford Head and on the Kent coast, white chalk with four flint bands characterises the HST.

SEQUENCE Co7

Seaford Head provides the best reference section for this sequence. In the Trunch borehole an influx of marls marks the base of the LmST. SB Co7 is placed directly beneath the lowermost of these at 390.75 m. In the deeper parts of the Anglo-Paris Basin such as Culver Cliff, this level is lithologically monotonous, and the correlative conformity can only be placed within the succession of white flinty chalks at a level identified by the cross-plots. Similarly on the London-Brabant Massif along the Kent coast SB Co7 has been placed at a slightly irregular flint band at the base of a thin package of chalk defining the LmST. At Seaford Head this corresponds to a level directly beneath the lower of two faint bands of marl. The LmST is thicker than in sequences Co5 and Co6 and of more uniform thickness the Anglo-Paris Basin, thickening into the Anglo-Dutch Basin at Trunch. At Triguères, several metres of irregular flint slump beds, dipping at low angles, represent the LmST. The chalk above this is partially obscured by staining from recent weathering. In the Loir Valley the succession is condensed. SB Co7 coincides with the reworked Intraclastic Hardground (Jarvis, Gale & Clayton, 1982). This is highly limonitic and contains immature quartz grains in a micritic matrix. No LmST is preserved.

The TST is very thin throughout the sections studied. In Trunch the change from chalk with marls to purer chalk defines the ts which is placed directly above the marl band at depth 385.95 m. At Seaford Head, Culver Cliff and on the Kent coast, the TST commences at the level of the Tarring Neville Flint (Figures 2.4, 2.5 & 2.15 and Mortimore, 1986), directly beneath a sponge bed at Seaford Head. In Triguères quarry a return to chalk-flint rhythms towards the top of the exposure without evidence for further slump disturbance marks the ts. In the Loir Valley, an increase in the level of glauconite in the sediment directly above the Intraclastic Hardground indicates the TST whilst a horizon of reworked nodules reported by Jarvis, Gale and Clayton (1982) indicates the ts associated with current activity and winnowing.

A flint-dominated chalk HST is seen in deeper ^{water} sections. The HST thickens northwards over the London-Brabant massif into the Anglo-Dutch Basin. At Seaford Head a slightly nodular sponge-rich horizon marks the mfs. Otherwise the mfs is placed by cross-plotting within the flint-chalk succession directly above the major flint band associated with the TST. In the Trunch borehole, this corresponds to a horizon of fossiliferous white chalk (385.12 m), containing sponges, *Inoceramus* fragments, bryozoa, asteroids, *Spondylus* and sharks teeth (Gallois & Morter, 1975). In Kent and at Culver Cliff two distinctive flint bands in uniform chalk distinguish the HST.

SEQUENCE Co8

The most typical exposure of sequence Co8 is that at Seaford Head which can be used as a reference section. Here and at Trunch, a reduction in the flint content of the chalk and an influx of marl defines the LmST. At Seaford Head, a nodular, iron-stained sponge bed is preserved directly beneath the lower marl band and this is marks SB Co8. In Kent and at Culver the cross-plots indicate a correlative level within the flinty chalk succession. The glauconitic and limonitic surface of the *Micraster* Hardground (Jarvis, Gale & Clayton, 1982) defines SB Co8 in the Loir. This is overlain by reworked limonite-stained clasts forming the LmST.

A thin TST is preserved across the Anglo-Paris Basin. In the reference section the appearance of a marly sponge bed (6.3 m below the Michael Dean Flint) defines the ts. Elsewhere the ts is indistinguishable in the field and is placed within a monotonous unit of chalk with regularly-spaced flints as determined by the line of correlation. In the Loir Valley succession the reworked limonitic clasts that overlie the *Micraster* Hardground have been disturbed by the transgressive pulse. The ts is coincident with the top surface of this bed. A distinctive feature here is a laterally persistent tabular flint that occurs within the softer sediment of the TST. This varies locally, occurring at a slightly higher horizon at some of the outcrops around Villedieu-le-Château in the Loir Valley (Château Tabular Flint — Jarvis, Gale & Clayton 1982). Jarvis, Gale and Clayton (1982) have interpreted this to be a diagenetically-altered bed of sponge debris.

In Sussex, the occurrence of a nodular sponge bed marks the mfs. This surface is less distinct elsewhere in the main sections at Culver Cliff, Trunch and on the east Kent Coast. A thick succession of white chalk marks the last HST of the Coniacian. The HST thickens into the deeper basinal settings where several marl bands appear and are thought to be indicative of the longer term relative sea-level fall. In the Loir, the softer glauconitic sediments of the TST pass upwards into partially lithified clasts associated with the hardground that defines the upper boundary of sequence Co8. At Trunch there are four slightly nodular fossiliferous horizons, with abundant *Zoophycos*, blue-grey manganese-stained sponges and bryozoa; and specimens of *Orbirhynchia*

and *Micraster*. These occur within the middle part of the HST. Above this level the chalk contains up to 30 % *Inoceramus* fragments, *Micraster*, serpulids and bryozoa. At Culver Cliff a thick succession of chalks with regularly-spaced bands of flint, and the occasional *Ventriculites chonoides* (Mantell) represent the HST. A similar, though thinner, succession is seen on the Kent coast.

CONIACIAN SECOND-ORDER SEQUENCE

Sequences Co1 – Co8 stack to form a longer term, second-order cycle of relative sea-level change which occurred over the entire Coniacian. The second-order SB is coincident with SB Co1 at the base of the stage (Figure 2.15) which is a major hiatus. The erosive surface cuts down into the Turonian-age chalk sediments. The thin packages of marly chalk separated by hardground horizons which define sequence Co1 and the LmST of Co2 represent the LmST of the second-order cycle.

The first significant flooding of the basin margin occurs at the ts of Co2 and this level is interpreted as the ts of the second-order sequence (Figure 2.15). This increase in sedimentation at the basin margin is seen at Reed (Figure 2.8) on the north edge of the London-Brabant Massif; at Compton Abbas (Figure 2.9) and Charnage Down (Figure 2.10) on the north-western flank of the Anglo-Paris Basin; and to the south-west of the basin in the Loir Valley (Figure 2.12). The transgression is also characterised by an increase in sediment thickness during individual third-order systems tracts across the Anglo-Paris Basin, and ultimately the accumulation of a thick succession of pure chalks with regularly-spaced bands of chert. Nodular chalks and localised current activity within the basin represent subsequent, subsidiary transgressive pulses. The second-order rise in relative sea-level produced the accommodation space for the third-order LmST deposits to be preserved.

The second-order mfs is placed at the same horizon as mfs Co5. This level marks the thickest-developed TST and HST pairing (Figure 2.16), above which systems tracts are more uniformly developed across both the distal and proximal sections. The second-order HST is coincident with the thickest development of HST chalk in the third-order cycles. The white chalk punctuated with flint bands typical of the second-order HST preserved in the deeper sections is indicative of increased biogenic precipitation during high relative sea-level.

As relative sea-level started to fall, approaching the end-Coniacian sequence boundary, minor influxes of marl are recorded in the main Anglo-Paris basin sections. In the Anglo-Dutch Basin (Trunch borehole) a greater marl content throughout the second-order TST and HST indicates that a landmass may have been exposed to the north or west providing sediment throughout the Coniacian. The localisation of marls to the Anglo-Dutch Basin at some levels also suggests restricted transport of sediment across the London-Brabant massif. During the second-order LmST virtually no marl is preserved in the Trunch borehole, suggesting more vigorous current activity than in the Anglo-Paris Basin at this level. These basin-wide spatial and temporal variations in systems tract are illustrated by Figure 2.16.

STABLE ISOTOPE DATA

The $\delta^{18}\text{O}$ ratio has been used extensively in the determination of palaeotemperature, and is a sensitive indicator of climatic change (Epstein *et al.*, 1951; Urey *et al.*, 1951; Teis, Chupakhin & Naidin, 1957; Spaeth, Hoefs, & Vetter, 1971; Anderson & Arthur, 1983; Arthur, Dean &

Schlanger, 1985 and Williams, 1988). Jenkyns, Gale and Corfield (1994) noted that more negative $\delta^{18}\text{O}$ values appear to be associated with marl-rich and organic-carbon rich sediments.

The $\delta^{13}\text{C}$ ratio reflects the fractionation between the ^{12}C and ^{13}C isotopes of carbon in the biosphere during photosynthesis, indicating that biosphere productivity as ^{12}C is concentrated preferentially into organic carbon. These processes are climatically driven and operate on both short and long timescales (Berger & Vincent, 1986). With the majority of organic carbon being synthesised in the shallow shelf seas an increase in the $\delta^{13}\text{C}$ ratio has been used as a proxy for a rise in sea level and a decrease as a proxy for a fall in sea level (Scholle & Arthur, 1980; Arthur, Schlanger & Jenkyns, 1987; Mitchell, Paul & Gale, 1993 and Jenkyns, Gale & Corfield, 1994).

Variation in the $\delta^{13}\text{C}$ ratio can therefore provide an independent test of our relative sea-level curves. The published carbon and oxygen stable isotope data sets (Jenkyns, Gale & Corfield, 1994) have been compared with our interpreted data (Figure 2.15) in order to test the sequence stratigraphy and to investigate possible causal mechanisms for the observed relative sea-level changes.

CARBON

Comparison of the second-order $\delta^{13}\text{C}$ curve with the second-order relative sea-level curve shows a strong positive correlation. At the base of the stage, $\delta^{13}\text{C}$ values are approximately 1.6‰ , rising steadily with increasing relative sea-level to a peak of just over 2.5‰ . The $\delta^{13}\text{C}$ values fall to 2.3‰ at SB Co8. Fluctuations in $\delta^{13}\text{C}$ from SB Co2 to ts Co3 show a weaker correlation and are harder to interpret. Jenkyns, Gale and Corfield (1994) collected their samples from the East Kent Coast where this interval is condensed with nodular chalks and hardgrounds common, suggesting diagenetic overprint at this level. The increase of $\delta^{13}\text{C}$ to a maximum of 2.6‰ during Co4 coincides with the major transgressive phase at this time. This $\delta^{13}\text{C}$ peak is interpreted as representing a release of nutrients into the basin during the first significant flooding of the exposed landmasses combined with the effect of the increase in area of the shelf sea. The stable carbon curve parallels the relative sea-level curves in the second-order HST, with third-order systems tracts corresponding to smaller variations, for example, the pronounced LmST of Co7 corresponds to a significant negative excursion in the $\delta^{13}\text{C}$ curve.

OXYGEN

The correlation between the $\delta^{18}\text{O}$ curve and the relative sea-level curve is less obvious. Over the long-term, $\delta^{18}\text{O}$ levels remain stable, rising by only a fraction of a ‰ over the entire stage. However, values do fluctuate over the duration of a short-term cycle by up to 1‰ . In general, more negative $\delta^{18}\text{O}$ values are associated with periods of lower relative sea-level and more positive $\delta^{18}\text{O}$ values with times of high relative sea-level e.g. Co4. Rising $\delta^{18}\text{O}$ values characterise TSTs, though some fluctuations are evident. The relationship between less negative $\delta^{18}\text{O}$ values and high relative sea-level is exaggerated in sequences Co1 to Co3 and a major negative excursion coincides with the LmST and TST of Co3. It is likely that, though partially a primary signal, $\delta^{18}\text{O}$ values have been affected by diagenesis associated with the formation of the many hardgrounds at this level. Above mfs Co3 the correlation between the $\delta^{18}\text{O}$ curve and the relative sea-level curve is much stronger. However, some variations persist; in sequence Co4 values fluctuate in the LmST and TST, though absolute values are clearly lower than those seen in the HST. Above these horizons, during sequences Co4 to Co8 the $\delta^{18}\text{O}$ curve parallels the relative sea-level curve.

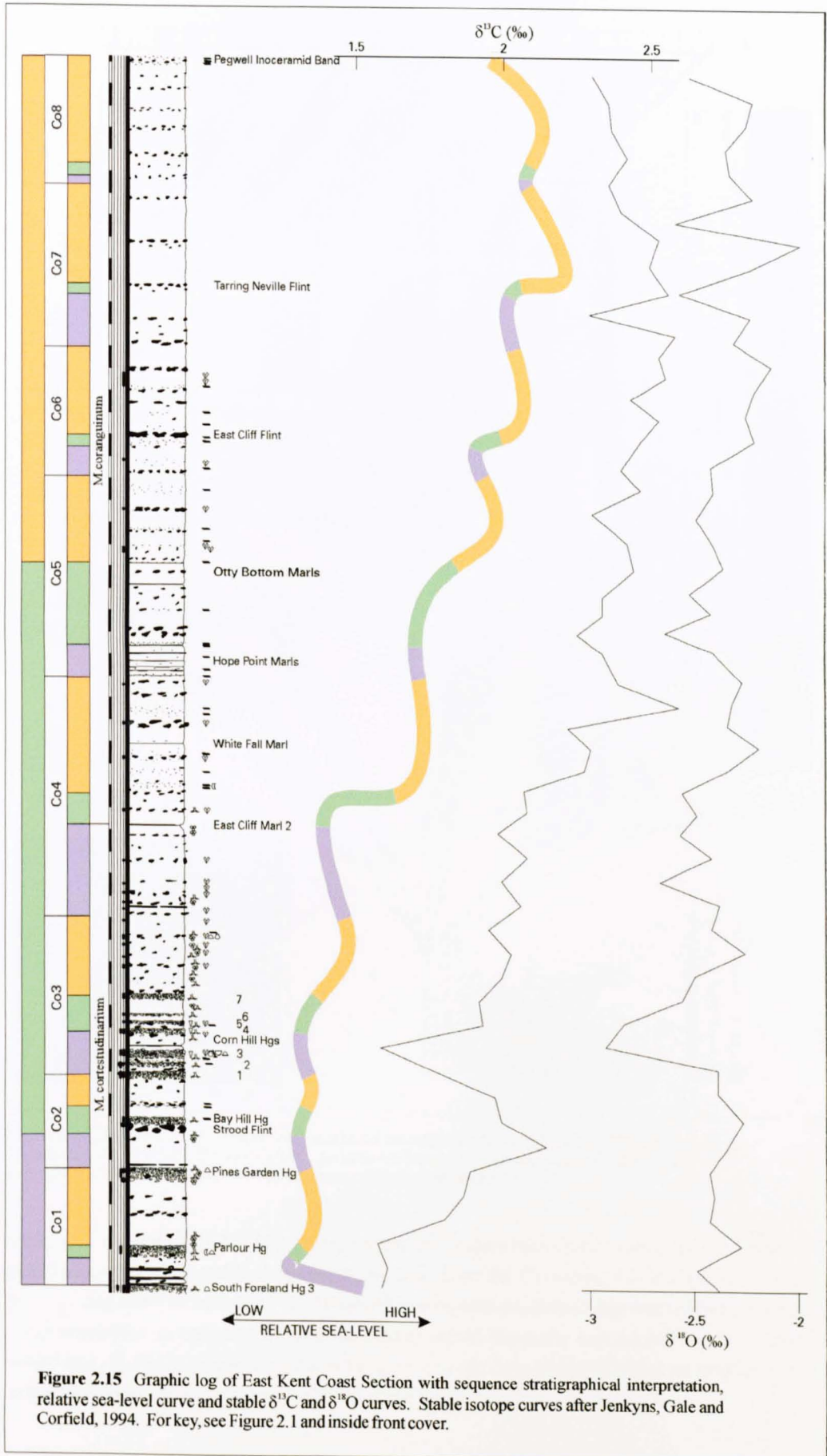


Figure 2.15 Graphic log of East Kent Coast Section with sequence stratigraphical interpretation, relative sea-level curve and stable $\delta^{13}\text{C}$ and $\delta^{18}\text{O}$ curves. Stable isotope curves after Jenkyns, Gale and Corfield, 1994. For key, see Figure 2.1 and inside front cover.

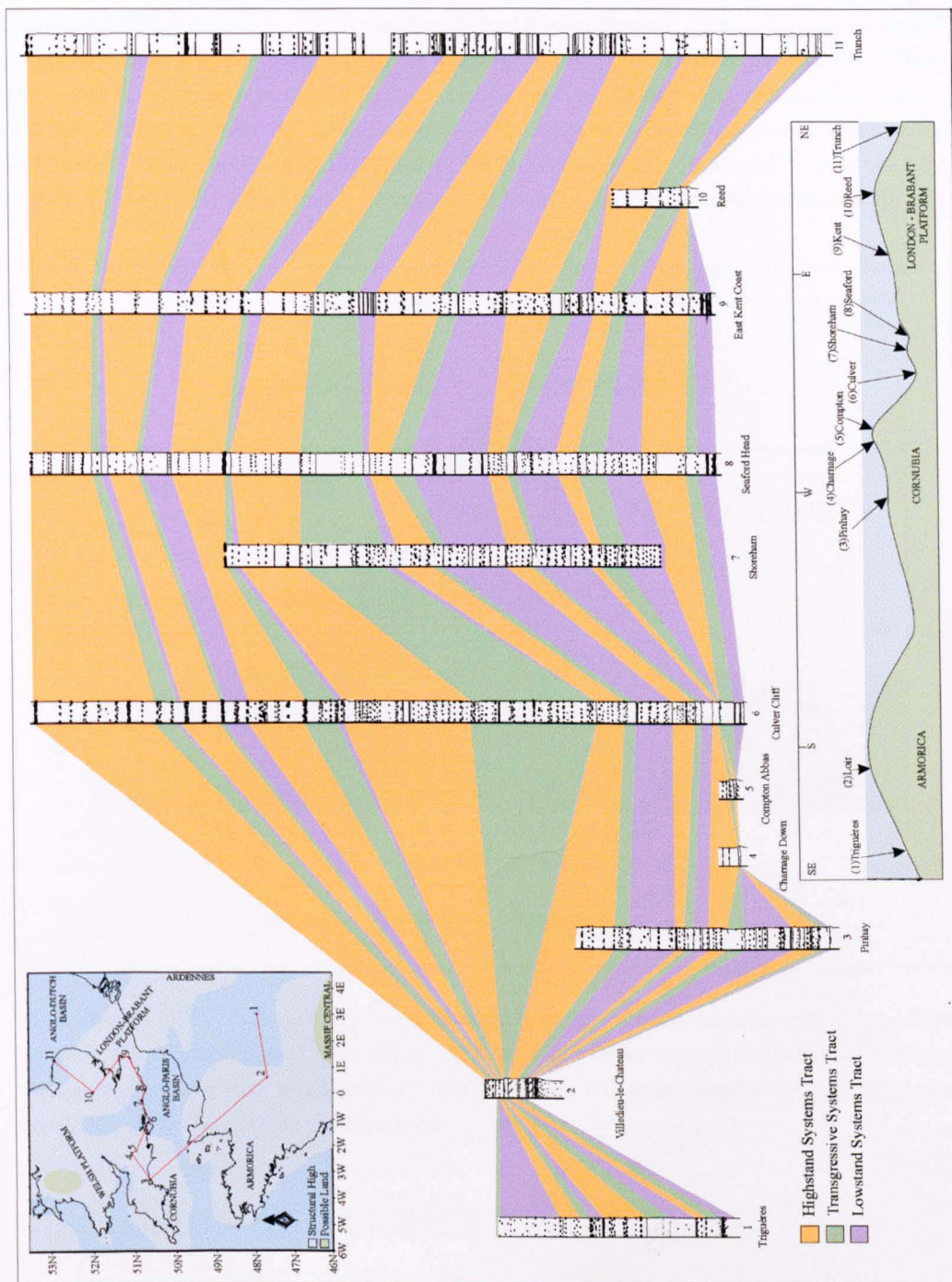


Figure 2.16 Sequence stratigraphical cross-section of the Anglo-Paris Basin for the Coniacian. Sections are tied by third-order key surface. Sections are located on a smaller version of Figure 2.1 and a schematic cross-section is included to show relative water depths.

Jenkyns, Gale and Corfield (1994) have generated a palaeotemperature curve for the ^{late} Upper Cretaceous based on their stable oxygen-isotope data. Over the Coniacian this indicates minor long-term cooling of approximately 1 °C. If the $\delta^{18}\text{O}$: temperature relationship was to hold for the third order sequences, as temperature rose the oceans would thermally expand and relative sea-level would rise. In fact, we observe the exact opposite in our data, suggesting that no simple relationship exists between temperature and $\delta^{18}\text{O}$ at the third-order.

Railsback (1990) developed a model which explained this problematic relationship. In this model, enhanced warming at the equator intensifies warm saline deep-water circulation (WSDW — Brass *et al.*, 1982). Changes in oxygen isotope composition of sea water affects salinity. Hence, WSDW circulation preferentially sequestered ^{18}O in the deep ocean during greenhouse climatic conditions. The corresponding depletion of ^{18}O in surface waters ($0.5 - 1.5 \text{‰}$) would have resulted in lower $\delta^{18}\text{O}$ values in marine biogenic carbonates deposited on the continental shelves.

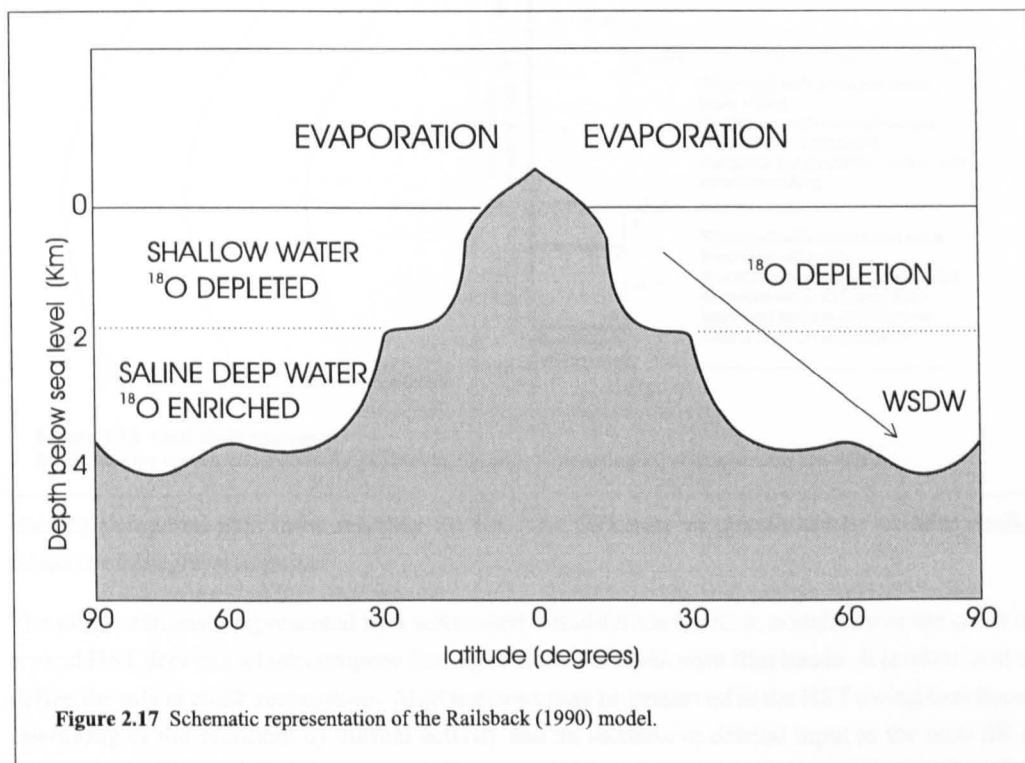


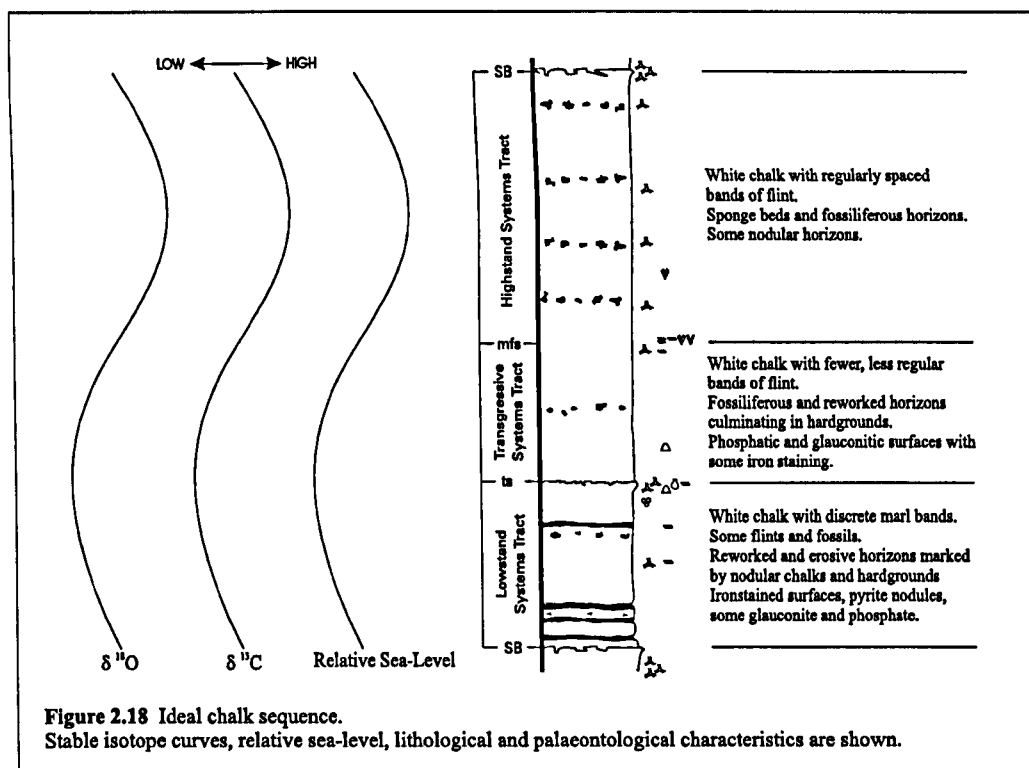
Figure 2.17 Schematic representation of the Railsback (1990) model.

The Railsback (1990) data-set suggests the ocean may have reached a stable greenhouse condition over the period of millions of years. However, our observations suggest the WSDW circulation could have been sensitive to temperature changes of a few degrees, similar to the thermohaline circulation (cold deep-water) during icehouse conditions.

DISCUSSION AND UNDERLYING CAUSAL MECHANISMS

The sequence stratigraphical model presented here enables the elucidation of an idealised chalk depositional sequence (Figure 2.18). A hardground surface which passes basinwards into nodular chalks represents the SB. During periods of higher long-term relative sea-level the SB may be far less pronounced or represented by a correlative conformity in the deeper sections. In these cases the SB is placed *a priori* at the base of the lowest marl band as this represents a slight increase in the detrital influx. The LmST is characterised by chalk, rich in siliciclastic clay and marl horizons.

Hardgrounds and nodular chalks also mark the ts which is characteristic of higher energy environments and winnowing as the basin margins are flooded. Hardgrounds at the ts are often more fossiliferous and characterised by phosphatic and glauconitic mineralization and reduced iron-



staining compared with those marking the SB. The TST may be punctuated by nodular chalks related to transgressive pulses.

The mfs is variously represented by a winnowed, fossiliferous horizon, nodularity or the onset of typical HST deposits which comprise homogenous white chalk with flint bands. It is often hard to define the mfs in chalk successions. Marl horizons may be preserved in the HST owing to reduced reworking of the sediment by current activity and an increase in detrital input as the next SB is approached. These definitions support those recently proposed for chalk successions by Gale (1996) and Owen (1996).

Studies have shown that chalk-marl rhythms in the Upper Cretaceous follow the Milankovitch orbital forcing timescales (Ditchfield & Marshall, 1989; Gale, 1990 and 1995 and de Boer & Smith, 1994). Ditchfield and Marshall (1989) and Gale (1990, 1995) have recognised the precession (19-23 Ka.) and obliquity (41 Ka.) cycles in chalk-marl rhythms of the Cenomanian. Berger and Loutre (1994) and House (1995) highlighted the dominance of the 106 Ka. and 410 Ka. eccentricity cycles in the geological record. The eight shorter-term cycles of relative sea-level change identified herein have an average duration of 400 Ka. (based on the timescale of Gradstein *et al.* 1994, 1995) and reflect the 400 Ka. eccentricity cycle.

There is no apparent correlation between second-order relative sea-level changes and $\delta^{18}\text{O}$. Over the timescale of the entire Coniacian (c. 3 Ma) tectonic processes could provide a suitable mechanism for changing relative sea-level and producing cyclicity in the sedimentary record (Cloetingh, 1988; Cande & Kent, 1995; Knott *et al.*, 1993; Kristoffersen, 1978; Roest & Srivastava, 1991; Srivastava, & Tapscott, 1986; Watts, 1982 and Wei, 1995). Of these processes, increased spreading at the mid-ocean ridges is considered to have a major influence on global sea-level. Hays and Pitman (1973) have calculated that increased ridge-building activity accounted for a rise of approximately 60 m in global sea-level for the period 85 — 80 Ma. It would seem plausible therefore that increased rates of sea-floor spreading over the Coniacian could have resulted in the second-order cycle of relative sea-level change reported herein.

CONCLUSIONS

Sequence-stratigraphic analysis is a powerful technique for recognising different scales of cyclicity in deep water hemi-pelagic successions. Combined with independent stable isotope data it is possible to elucidate climatic and tectonic controls on sedimentation and relative sea-level change. Owing to its biogenic nature, chalk is an extremely sensitive climatic indicator, and variations detected through the isotope data are clearly mirrored in the sedimentary response. The eight short-term, third-order sequences are suggested to be eccentricity-driven. A longer-term, second-order sequence spanning the entire Coniacian appears to be related to changes in plate kinematics and ridge-building processes. Our data support the model proposed by Railsback (1990), that during warming, enhanced WDSW circulation sequestered ^{18}O into the deep ocean resulting in marine coccoliths displaying a lower than predicted $\delta^{18}\text{O}$ ratio. This has implications for the determination of palaeotemperature from $\delta^{18}\text{O}$ values during greenhouse-climate conditions.

Chapter 3

Santonian

ABSTRACT

The Upper Cretaceous Chalk of Northwest Europe was deposited in an open epicontinental sea during a period of high global eustatic sea level. The bulk sediment consists largely of a white coccolith ooze with common bands of chert and temporally localised bands of marl. At intervals in the succession, current-induced winnowing and reworking has led to the development of a range of nodular chalks, firmgrounds and hardgrounds, many of which can be traced across the Anglo-Paris Basin.

A sequence stratigraphical analysis of the Santonian succession has identified seven short-term, third-order cycles of relative sea-level change superimposed upon one longer-term, second-order cycle. Comparison of the sequence stratigraphical interpretation with independently derived carbon and oxygen isotope data shows a positive correlation. A relative sea-level curve is presented for the Santonian, and this agrees closely with other published curves.

The long-term change in $\delta^{13}\text{C}$ correlates strongly with the long-term relative sea-level curve, reflecting increased productivity as the shelf area expands. This is coincident with a phase of increased activity at the mid-ocean ridges. It is proposed that variations in ocean-ridge activity control this longer-term relative sea-level change.

Sequence stratigraphic analysis is a powerful technique for recognising different scales of cyclicity in deep water pelagic successions, and combined with independent data it allows the possible differentiation between climatic and tectonic causal mechanisms. This research builds on published work to suggest that ^{Late}Upper Cretaceous oceans were salinity-stratified, and that the $\delta^{18}\text{O}$ stable isotope ratio is not a reliable indicator of temperature under such circumstances.

INTRODUCTION

A number of publications have focused on various aspects of chalk stratigraphy and correlation. Mortimore (1983) provides a lithostratigraphic nomenclature for the outcrops in Sussex, which he revised and expanded to cover a wider area in 1986. Robinson (1986) presented a detailed stratigraphy for the chalk of the North Downs in Kent. Correlations within the chalk succession have been made across the Channel by Robaszynski and Amédéo (1986a, 1986b) whilst Mortimore and Pomerol (1987) extended marl band correlation over a wider area using electrical resistivity and gamma ray wire-line log data.

Barron, Arthur and Kauffman (1985) have linked Cretaceous cyclical bedding to Milankovitch rhythms. Hart (1987), Ditchfield and Marshall (1989) and Gale (1990) concentrated on the chalk of southern England and identified cycles which they linked to Milankovitch obliquity and precession rhythms. Fischer (1993) recognised eccentricity-rhythms in chalk successions from the Albian of Italy, the Senonian Niobrara Formation of Colorado and from the Turonian – Coniacian of Germany using field evidence and borehole data. The 100ka eccentricity rhythm totally dominated the spectrum whilst the 400ka rhythm, though identified visually, was not apparent in the spectra.

Owen (1996), Gale (1996) and Chapter 2 herein, presented sequence stratigraphic interpretations of the Cenomanian, Turonian and Coniacian of southern England respectively. These Coniacian cycles were linked to the 400ka eccentricity cycle (Chapter 2).

The effects of tectonic activity on chalk deposition in the southern part of the Anglo-Paris Basin have been documented by Pomerol (1989). This was extended to the Anglo-Paris Basin as a whole by Mortimore and Pomerol (1991, 1997) who identify a period of reactivation along existing tectonic lineaments commencing during the late-Santonian. Mortimore *et al.* (1997) compare the tectonic activity in the Anglo-Paris Basin with that from northern Germany.

Jenkyns, Gale and Corfield (1994) generated stable carbon and oxygen curves for the whole Upper Cretaceous from sections in southern England and demonstrated the potential of correlating excursions on a regional scale by comparing curves from the Italian Scaglia with those from the English Chalk. McArthur *et al.* (1993) presented a strontium-isotope curve from the English Chalk.

This paper presents a sequence stratigraphical analysis of the Santonian chalks of the Anglo-Paris and Anglo-Dutch Basins, and integrates these interpretations with independently-derived stable oxygen and carbon data (Jenkyns, Gale and Corfield, 1994), to elucidate the relative importance of climatic and tectonic mechanisms as the underlying control on sedimentation in this deep-water setting.

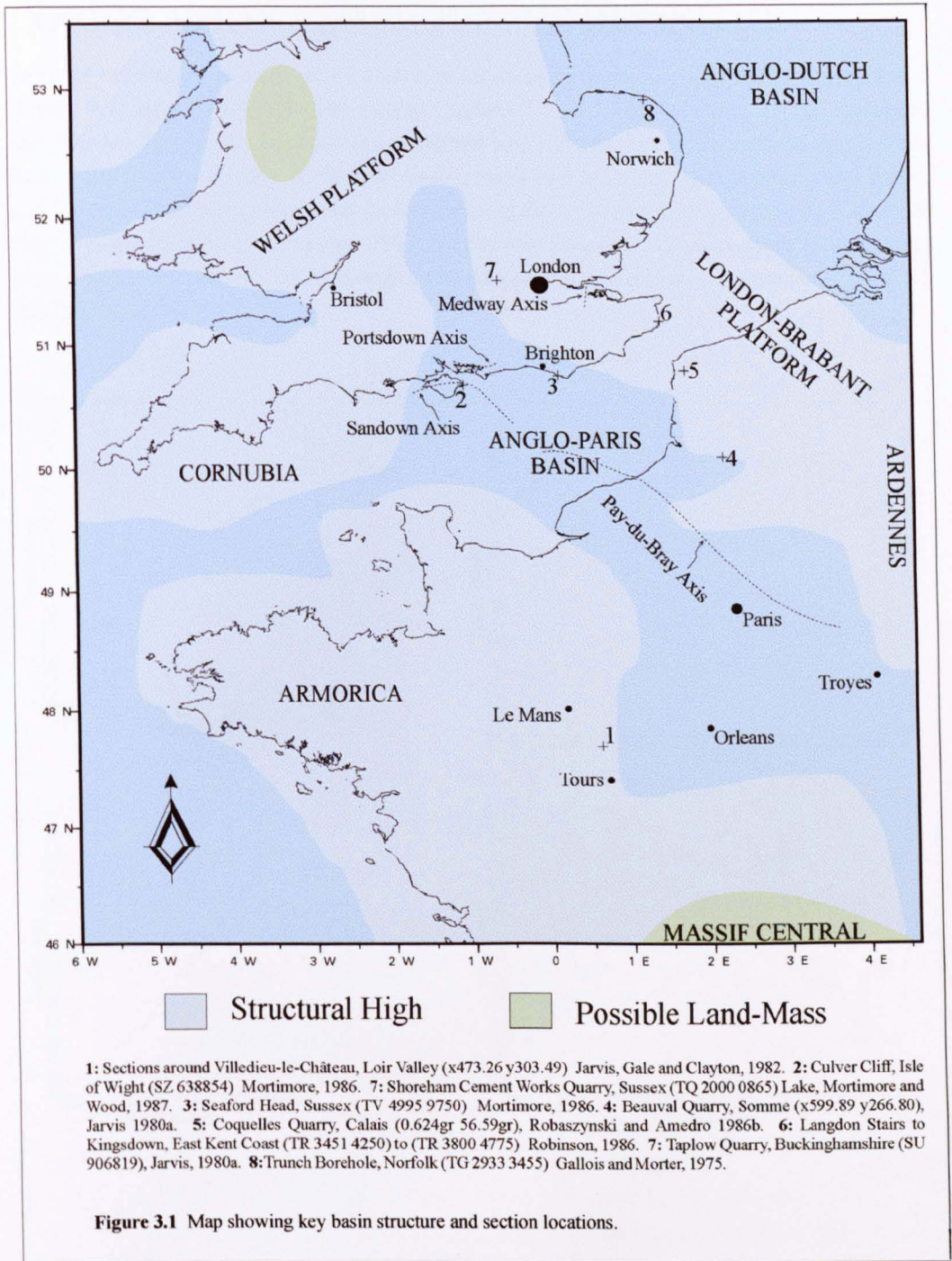
STRATIGRAPHY

Santonian strata outcropping in southern England and northern France (Figure 3.1) typically comprise white coccolith chalks with regularly-spaced bands of chert and less common marl horizons. Several lithostratigraphical schemes, mentioned above, have been introduced to cover the Santonian chalk of southern England. A comparison of the schemes is given in Figure 3.2 for locally-varying names referred to in the sequence-stratigraphical description below.

The base of the stage is marked by the incoming of the bivalve *Cladoceramus undulatoplicatus* (Roemer) across the Anglo-Paris Basin (Bailey *et al.*, 1984). This was correlated with the Pegwell Inoceramid Band in Kent, occurring 1.5 m below the Chartham Flint (Bailey *et al.*, 1983; Robinson, 1986) and at the level of the Michael Dean Flint in Sussex (Mortimore, 1986). A tripartite macrofossil biozonation has been established for the Santonian of England (Rawson *et al.* 1978). The lower to middle Santonian contains the upper part of the echinoid biozone *Micraster cortestudinarium* (Goldfuss). The Upper Santonian is divided into the *Uintacrinus socialis* (Grinnell) and *Marsupites testudinarius* (Schlotheim) crinoid zones.

The *M. coranguinum* Biozone is characterised by a thick succession of white chalk with regularly-spaced flint bands. A number of these flints have been named and can be traced across southern England (Mortimore, 1983, 1986). The lowest recorded occurrence of texanitid ammonites in the English successions occurs at the Chartham Flint (Bailey *et al.*, 1983). A major faunal turnover coincides with the upper band of *Cladoceramus* in Kent (Bailey *et al.*, 1983) at the level of a distinctive *paramoudrae* flint (Bedwell's Columnar Flint).

The base of the *U. socialis* Biozone in southern England coincides with a basin-wide change in lithology, from white chalk with regular flint bands to chalk with fewer, less regular flints and a reappearance of discrete marl bands after their virtual absence above the lowest few metres of the *M. coranguinum* Biozone. This reduction in flint is more pronounced along the East Kent Coast section which is also anomalous owing to the virtual absence of marl during the Santonian. The uppermost Santonian Biozone of *M. testudinarius* is lithologically similar to the *U. socialis* Biozone. Gradstein *et al.* (1994, 1995) reported a duration of 2.3 Ma for the Santonian, with calibrated absolute ages of 85.8 Ma \pm 0.5 Ma for the base of the stage and 83.5 Ma \pm 0.5 Ma for the top.



Mortimore, 1986 — Sussex	Robinson, 1986 — Kent	BGS Memoirs
Rough Brow Flint Flat Hill Flint	Whitaker's 3 Inch Flint Bedwell's Columnar Flint	Whitaker's 3 Inch Flint Bedwell's Columnar Flint Flat Hill Flint
Baily's Hill Flint Michael Dean Flint	Chartham Flint Pegwell Inoceramid Band	

Figure 3.2 Table showing the various lithostratigraphic nomenclatures used for the Santonian of southern England.

CORRELATION AND SEQUENCE DEFINITION

Selected, well-exposed outcrops of Santonian strata in southern England and northern France (Figure 3.1) have been graphically logged (Figures 3.5 –3.12 & Appendix A) and correlated using the key lithological horizons and published biozonations traceable across the Anglo-Paris Basin. Detailed correlation of the marl bands, fossil-rich horizons, sponge beds, chert bands, nodular chalks and hardgrounds was facilitated using the cross-plot graphical method (Carney & Pierce, 1995; Neal, Stein & Gamber, 1995 and Chapter 1 herein). Cross-plotting various correlation hypotheses allowed the definition of the most parsimonious line of correlation (Figure 3.3 and Appendix B).

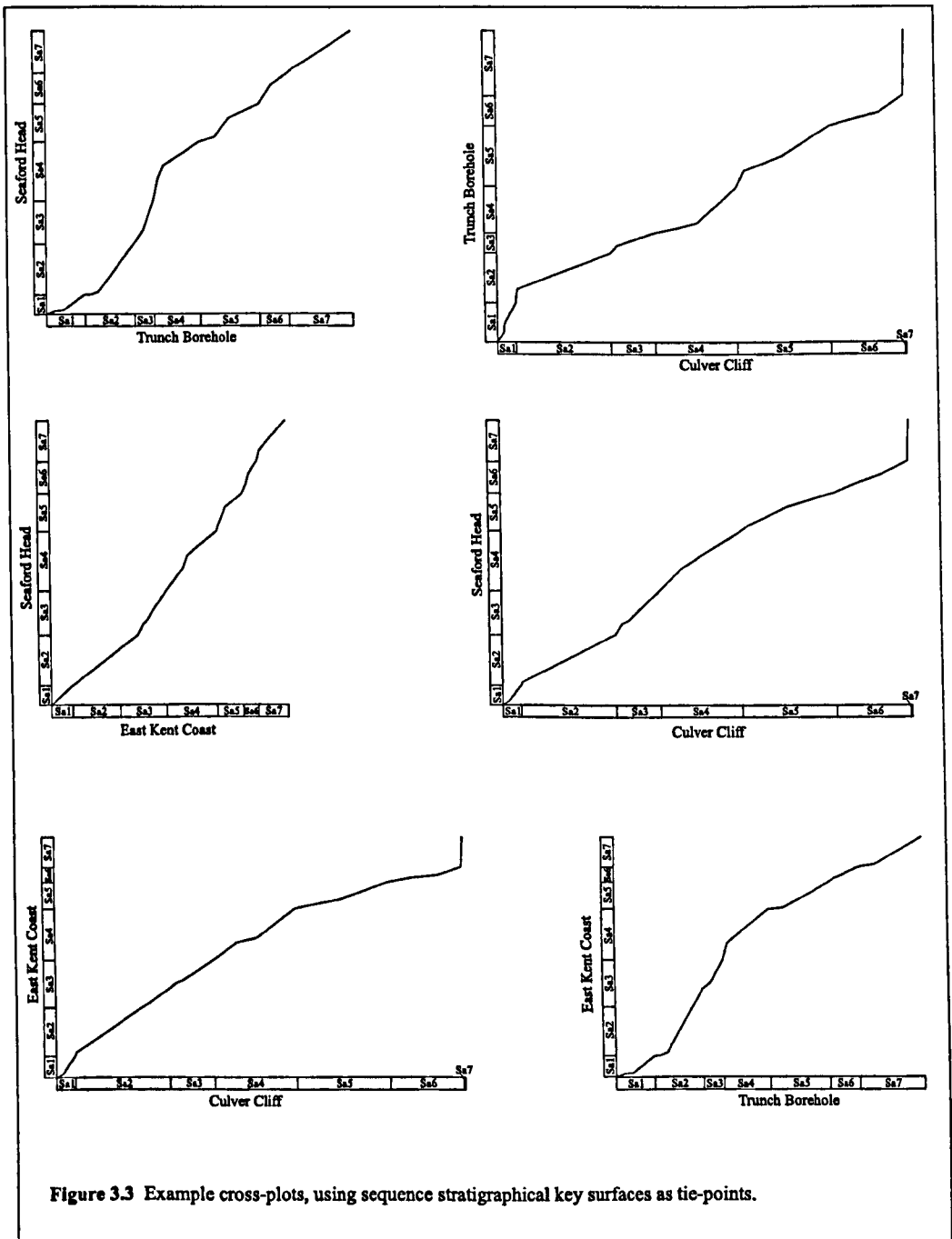
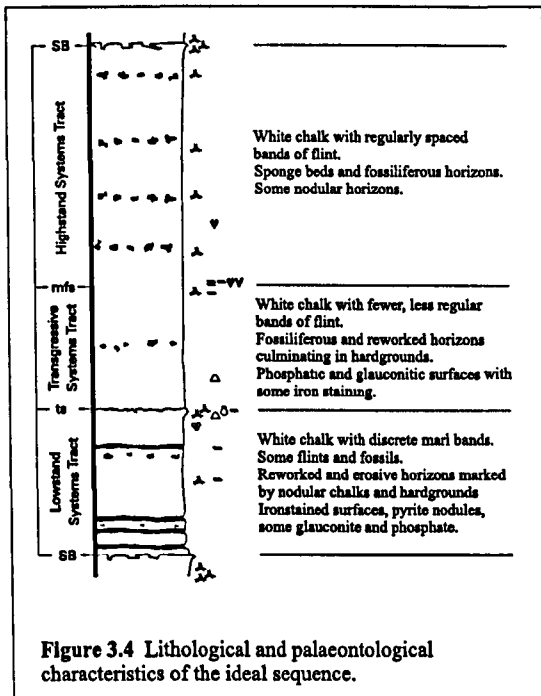


Figure 3.3 Example cross-plots, using sequence stratigraphical key surfaces as tie-points.



Key sequence stratigraphical surfaces were defined using a combination of lithological, palaeontological and geochemical data from the sections where they were best developed, following the 'idealised chalk sequence' model (Figure 3.4). Where field and published data were insufficient to allow the definition of key surfaces, these were placed using the line of correlation. Inflections in the gradient of the line of correlation indicate a change in the rate of deposition between the two sections, with major inflections and hiatuses interpreted as corresponding to the better-developed sequence stratigraphical key surfaces.

SEQUENCE STRATIGRAPHY

The Santonian has been divided into seven short-term cycles of relative sea-level change based upon the idealised chalk sequence, that stack to form a longer-term, second-order cycle. During the Santonian, the less-nodular lithologies preserved are interpreted to represent deposition under conditions of higher relative sea-level than during the Coniacian, with water depths during the LmST equivalent to those during the TST of the Coniacian second-order cycle. In addition, the late-Santonian HST is more pronounced than that of the Coniacian, with a sharper rise in relative sea-level during the TST and a sharper fall during the latter part of the HST. Towards the basin margins in the Loir Valley this major transgression is reflected by Santonian sediments directly overlying Turonian strata (Jarvis, Gale and Clayton, 1982). The average duration of the third-order cycles is 330 ka, based on a calibrated duration of 2.3 My for the stage (Gradstein *et al.*, 1994, 1995).

SEQUENCE Sa1

Sequence Sa1 is only thinly developed in the Anglo-Paris Basin, thickening over the London – Brabant Massif into the Anglo – Dutch Basin where it is at its thickest in the Trunch Borehole (Figure 3.5). At Trunch, a succession of grey bioturbated chalks with five discrete marl bands contrasts with the main Anglo-Paris Basin sections (East Kent Coast, Figure 3.6; Seaford Head, Figure 3.7 and Culver Cliff, Figure 3.8) that are less marly and characterised by regularly-spaced flint bands. The SB is placed at the base of the influx of marls in the Trunch borehole, lying just above the base of the Santonian (depth 365.01 m). This corresponds to the thin flint band a metre beneath the Chartham Flint on the Kent Coast. At Seaford Head, this SB lies at the base of the marly horizon 110 cm above the Michael Dean Flint. This correlates conformably with the top of the second flint band above the Michael Dean Flint at Culver Cliff and outcrops in the south-western corner of Horse Shoe Bay (SZ 63850 85455). At Beauval (Figure 3.9) on the Pay-du-Bray Axis, the Cavernous Hardground (*sensu* Jarvis, 1980a) marks the SB. On the south-western

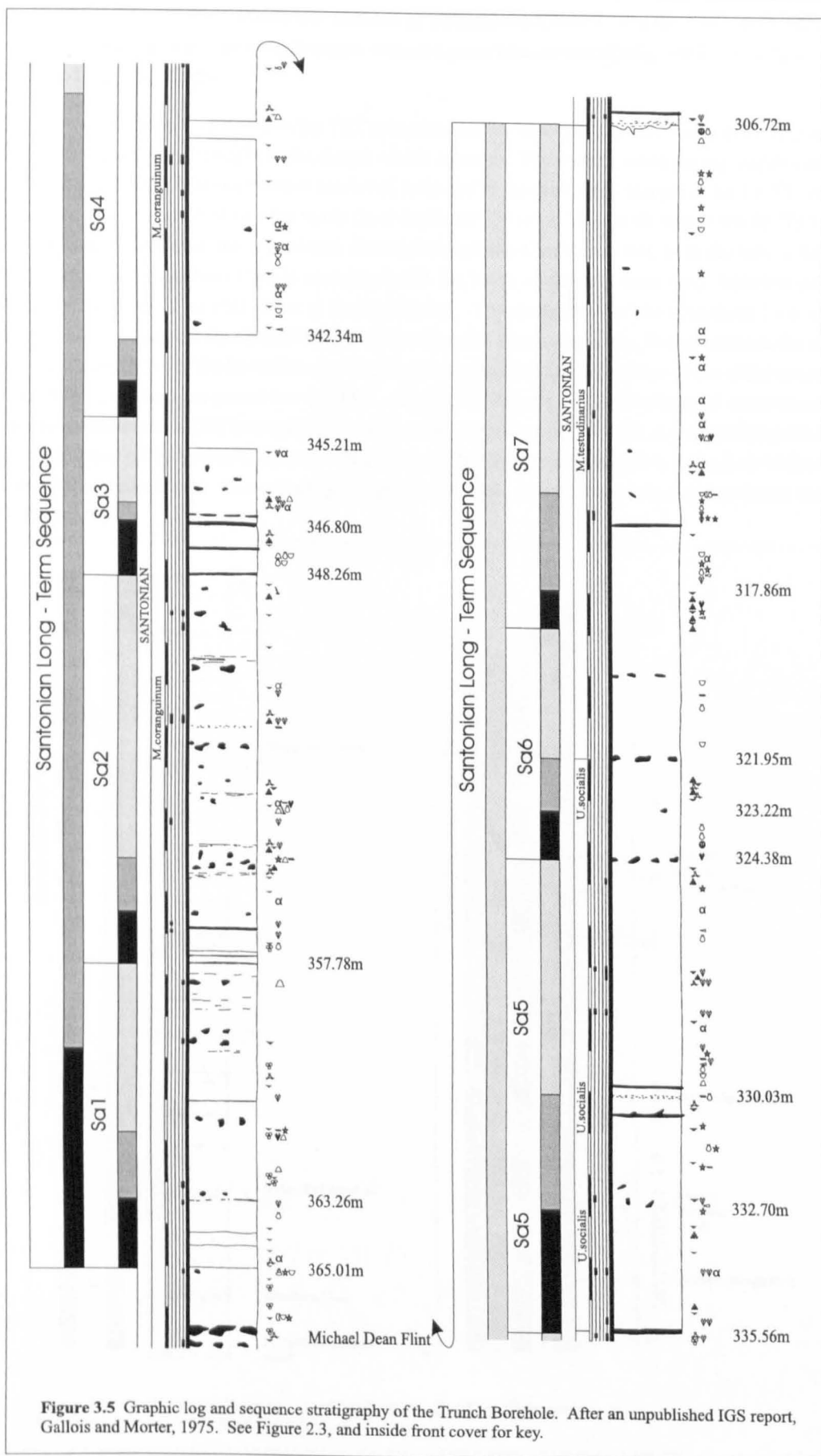
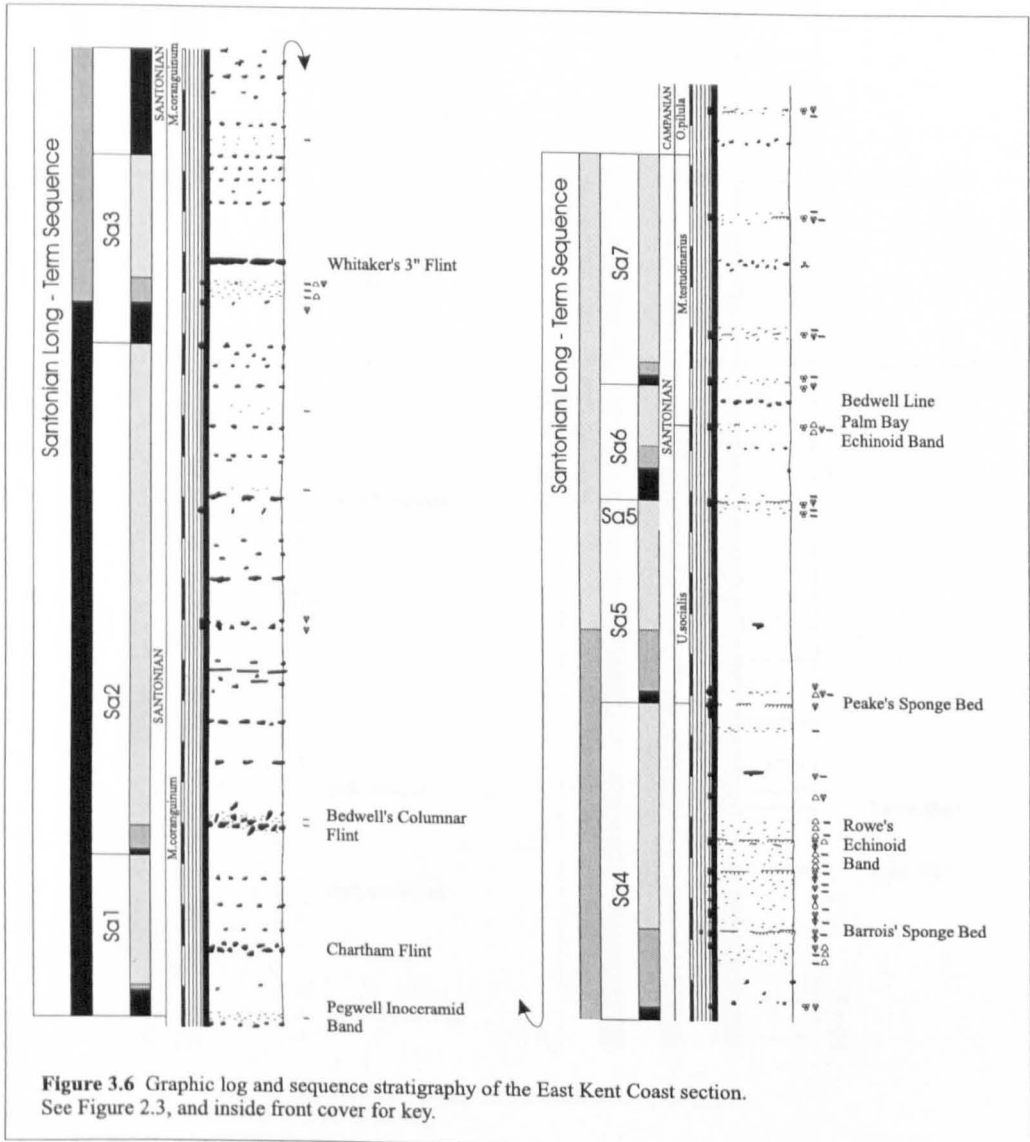


Figure 3.5 Graphic log and sequence stratigraphy of the Trunch Borehole. After an unpublished IGS report, Gallois and Morter, 1975. See Figure 2.3, and inside front cover for key.

margin of the Anglo-Paris Basin, the sections at Villedieu-le-Château (Figure 3.10) are highly condensed; the SB is placed at the limonite stained Lower Glauconitic Hardground (*sensu* Jarvis, Gale and Clayton, 1982).

Throughout the Anglo-Paris Basin the TST is represented by homogenous chalk which is thin and of uniform thickness throughout the deeper-water sections. The overall trend during sequences Sa1 and Sa2 is one of falling relative sea-level, reflected in the prolonged second-order LmST. A thin succession of chalk above the marls (ts at depth 363.26 m) in Trunch characterises the TST. On the East Kent Coast, the ts is placed directly beneath the Chartham Flint, with the mfs at the flint band. The Chartham Flint is correlated with the lower of the two main flints between the Michael Dean and Flat Hill Flints at Seaford Head. The correlative of the Chartham Flint at Culver Cliff is a double flint band with a smaller, irregular flint in-between. In this instance the ts is placed at the base of the lower band whilst the mfs is placed at the top surface of the upper band. This thin flinty horizon preserves the TST. At Beauval Quarry, a thin package of inoceramid debris characterises a TST beneath the *Thalassinoides*-burrowed HST chalk. A glauconitic patina on the surface of the Lower Glauconitic Hardground (SB Sa1) represents the ts in the Loir Valley. Above this a condensed 40 cm package of glauconite-rich, fossiliferous calc-arenites forms the TST and HST.



Above the mfs, the HST thickens from the Anglo-Paris Basin northeastwards into the Anglo-Dutch Basin. At Trunch an influx of disseminated clay material is preserved towards the top of the HST. This is interpreted as representing increased terrigenous erosion and run-off as relative sea-level started to fall. In the Anglo – Paris Basin the HST comprises flinty, white chalk, suggesting a possible source area for the clay limited to the margins of the Anglo – Dutch Basin. At Beauval, the HST is characterised by *Thalassinoides* burrows in-filled with phosphatic chalk.

SEQUENCE Sa2

This sequence is much thicker than Sa1, largely the result of a thicker HST. In the Trunch Borehole, a change from disseminated clay to discrete marl horizons marks the onset of sequence Sa2. The SB is placed directly beneath the lowermost marl band (depth 357.78 m). On the Kent Coast an

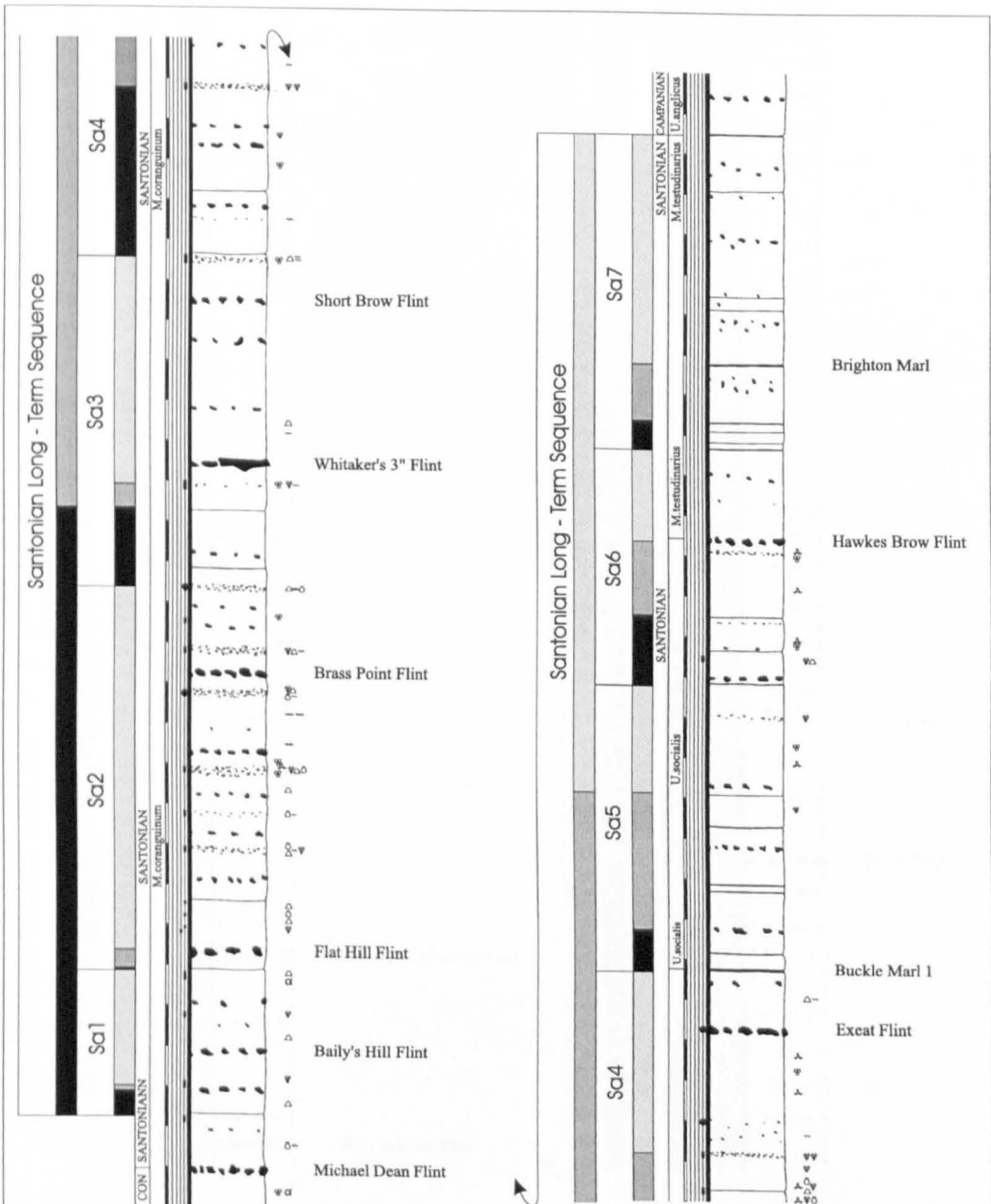


Figure 3.7 Graphic log and sequence stratigraphy of the Seaford Head section. See Figure 2.3, and inside front cover for key.

intermittent minor omission surface at this level (Robinson, 1986) marks the SB. At Seaford Head this is correlated with the base of the marl band, 5 m above the Michael Dean Flint. In the main sections of the Anglo-Paris Basin correlative conformity SB Sa2 lies within white chalk directly beneath Bedwell's Columnar Flint. At Beauval an iron-stained parting within a unit of

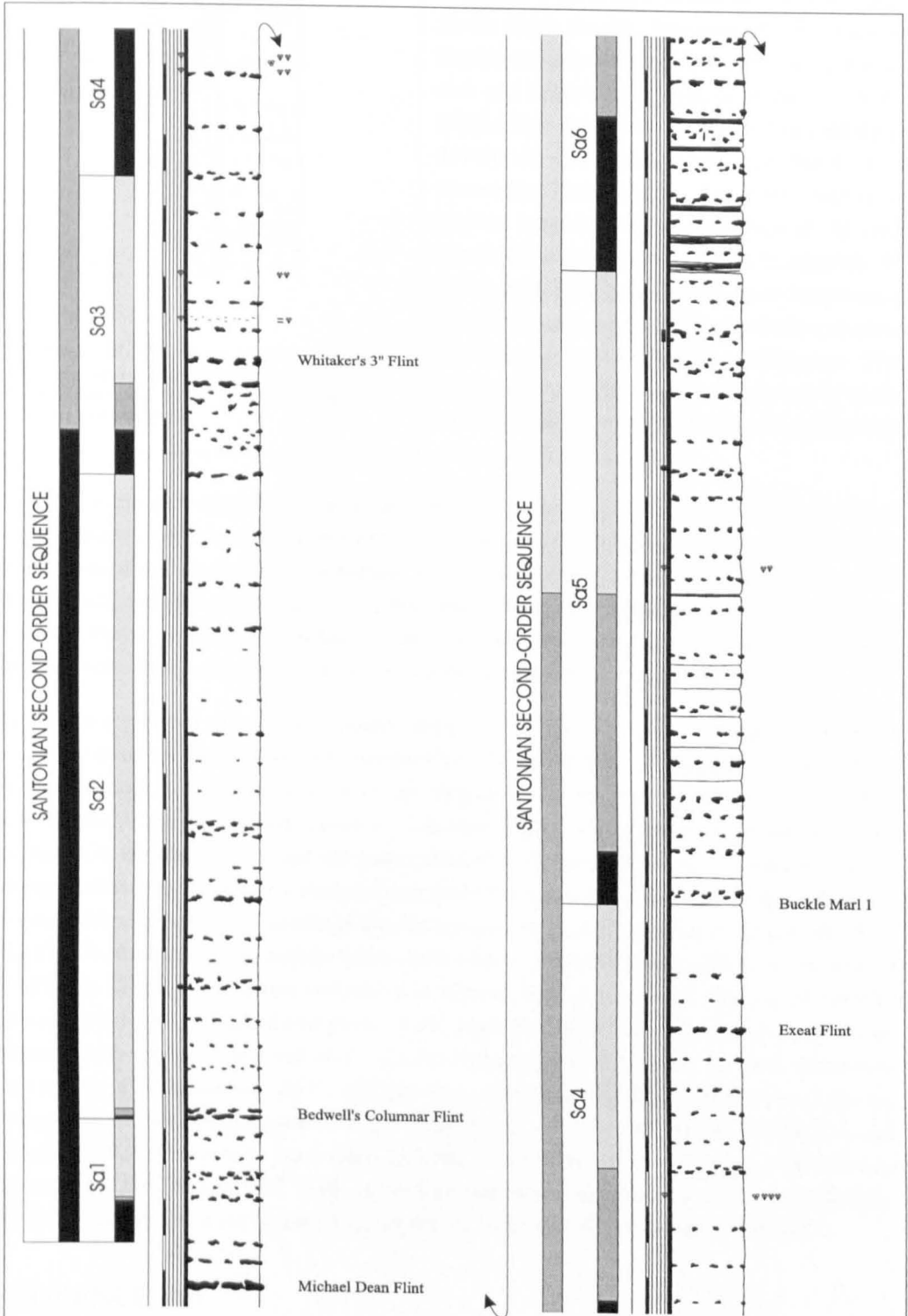
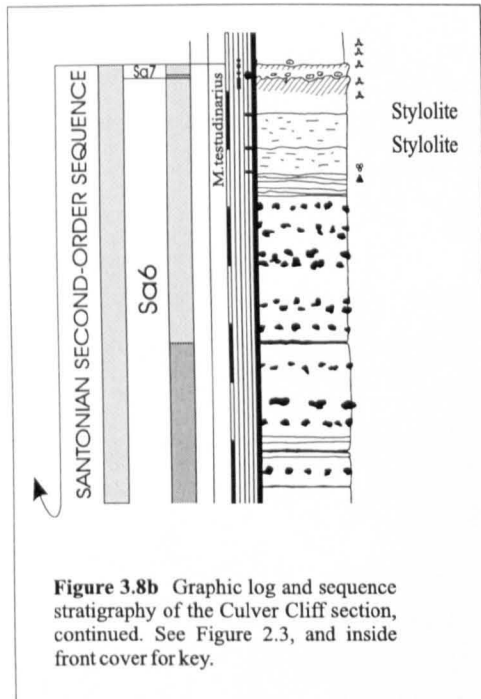


Figure 3.8a Graphic log and sequence stratigraphy of the Culver Cliff section. See Figure 2.3, and inside front cover for key.



harder chalk above the phosphatic, burrowed horizon marks SB Sa2. A LmST is not preserved at this locality. At Villedieu-le-Château in the Loir Valley, a hardground (Upper Glaucanitic Hardground, *sensu* Jarvis, Gale and Clayton, 1982) clearly marks the SB. The hardground surface is fragmented and exhibits evidence of extensive erosion and reworking (Jarvis, Gale and Clayton, 1982). This Upper Hardground is more strongly developed and mineralised than the Lower Glaucanitic Hardground. The lower Santonian exhibits considerable local variation in the area (Jarvis, Gale and Clayton, 1982), interpreted to be the result of differential erosion and deposition over the palaeotopography during the low relative sea-level characteristic of the basal Santonian. The correlative of SB Sa2 can be seen directly beneath Bedwell's Columnar Flint in the upper quarry wall at Coquelles, Figure 3.11.

The TST is thinly developed throughout the Anglo-Paris Basin and in the Trunch Borehole where it is associated with only a few centimetres of chalk directly beneath Bedwell's Columnar Flint in the main sections. In the Loir, this horizon is characterised by a shell lag of bored, oyster-encrusted and glauconitic clasts that overlie the Upper Glaucanitic Hardground (Jarvis, Gale and Clayton, 1982). At Beauval on the Pay-du-Bray Axis a 50 cm thick horizon of phosphatic *Thalassinoides* in-fills forms the TST overlying the iron-stained parting of SB Sa2.

The mfs is associated with a level of major faunal turnover in the Anglo-Paris Basin (Bailey *et al.*, 1983) at the level of Bedwell's Columnar Flint. Sequence Sa 2 is dominated by a thick HST. At its maximum development at Culver Cliff, 18 m of chalk with regularly-spaced bands of flint and occasional sponge beds are recorded. The other sections in the Basin-centre are up to 50% thinner. On the East Kent Coast the sediments attain a thickness of 12 m. At Seaford Head a sponge bed and associated erosive surface are preserved at the mfs. The Trunch succession is of similar thickness to that at Seaford and the mfs is placed above a flint band at a depth of 355.37 m. The HST is characterised by slightly marly chalk with well-defined bands of flint. At Beauval on the Pay-du-Bray Axis, a thinner succession of flintless chalk is preserved. The top of the HST contains winnowed, reworked phosphatic chalk, piped down through *Thalassinoides* burrows associated with the overlying sequence. On the basin-margin in the Loir, the thin, glauconitic successions are characterised by the addition of a major burrow-fill flint and associated pyrite. An erosive surface characterised by *Pycnodonte* oysters caps the HST where Jarvis, Gale and Clayton (1982) provisionally placed the Coniacian-Santonian boundary. The accumulation of a considerable thickness of HST chalk, increasing basinwards, suggests a prolonged, gradual decrease in relative sea-level which characterises the major part of the second-order LmST.

SEQUENCE Sa3

At Seaford Head, a minor erosive surface associated with a sponge bed is evident, marking the SB. Above this, two marl bands representing an influx of clay are preserved. The LmST thickens slightly into the deeper-water sections; the base of the sequence being placed at a level of correla-

tive conformity at the top of a chalk unit with regularly spaced flint bands in the Culver Cliff succession. The LmST is characterised by a horizon of irregularly bedded flint. On the East Kent Coast the SB lies directly above a thick band of flints; flint-free chalk with inoceramid debris characterising the LmST. In the Trunch Borehole the SB is placed directly below the lowest of two marl bands (depth 348.26 m) that delimit the LmST. At Coquelles this level is represented by

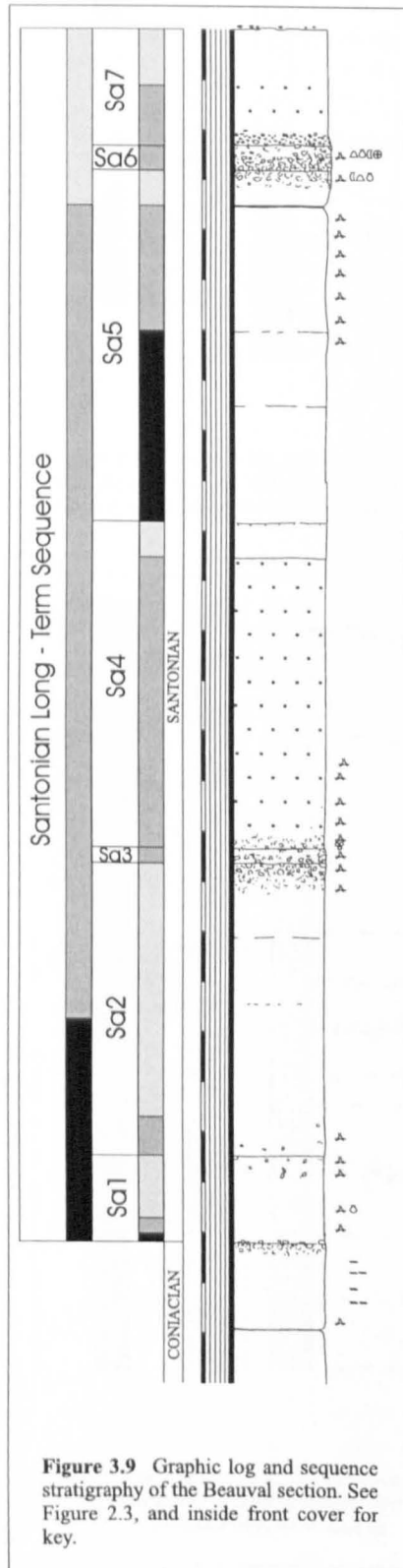


Figure 3.9 Graphic log and sequence stratigraphy of the Beauval section. See Figure 2.3, and inside front cover for key.

a correlative conformity towards the top of the exposure. Sequence Sa3 is highly condensed at Beauval, only preserving 42 cm of sediment. A *thalassinoides*-burrowed hardground surface marks the SB. This is undulose and characterised by iron-stained phosphatic intraclasts, the burrows in-filled with phosphatic chalk. In the Craie-de-Villedieu Formation an erosion surface directly below the horizon of *Pycnodonte vesicularis* oysters (Jarvis, Gale and Clayton, 1982) identifies the SB. The oysters persist into the LmST within a poorly consolidated calcarenite. LmST Sa3 represents the lowest relative sea-level of the Santonian in the Anglo-Paris Basin. Relative sea-level is interpreted as having been only slightly lower than during sequence Sa2, this protracted, minor fall in relative sea-level having left little evidence for an erosive SB.

The TST is of uniform thickness throughout the area studied and characterises a marked transgression onto the south-western margin of the Anglo – Paris Basin. This sequence is conspicuously thicker than Sa1 and Sa2 around Villedieu-le-Château, here a sponge-flint associated with glauconitic sediment marks the ts. Over the Pay-du-Bray Axis at Beauval a shiny phosphatic veneer, superimposed upon the SB hardground, marks the ts, thus the TST rests directly upon the SB. The TST is characterised by *Thalassinoides*-burrowed chalk, in-filled with phosphatic chalk, and towards the top of the unit, by phosphate and glauconite. At Seaford Head the ts is placed directly above the marl band that underlies Whitaker's 3 Inch Flint. On the East Kent Coast a level of sponges and inoceramid fragments associated with a band of dispersed, small irregular flints marks the ts. Here, a fossiliferous package of white chalk rich in inoceramid debris and echinoids forms the TST. At Culver Cliff the ts occurs at the upper limit of the chaotic-flints. In the TST the flints remain slightly anomalous, but are horizontally bedded. TST Sa3 corresponds to the onset of the second-order Santonian transgression.

In the main successions of the Anglo – Paris Basin and at Trunch in the Anglo – Dutch Basin the mfs is placed just beneath the prominent Whitaker's 3 Inch Flint. The upper surface of an inoceramid, echinoid and sponge-rich

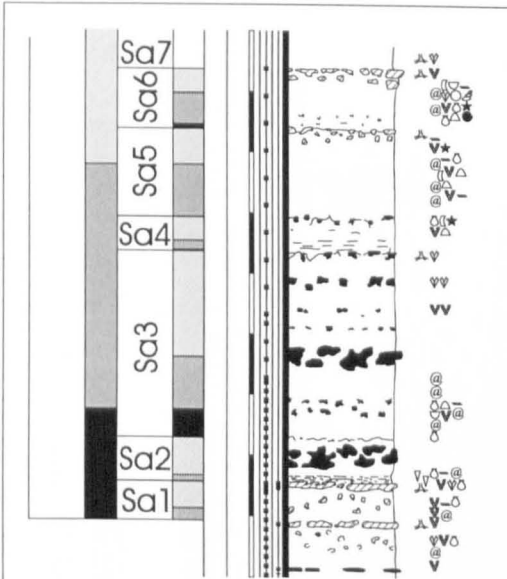


Figure 3.10 Graphic log and sequence stratigraphy of the Loir Valley section. See Figure 2.3, and inside front cover for key.

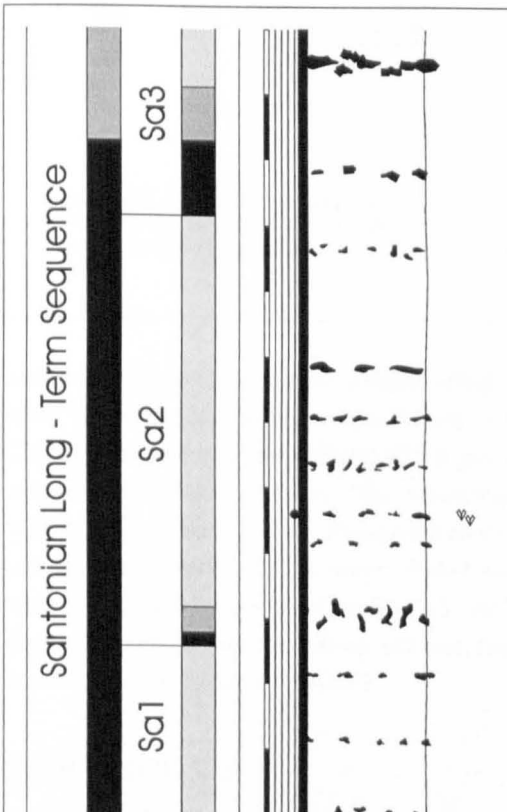


Figure 3.11 Graphic log and sequence stratigraphy of the Coquelles section. See Figure 2.3, and inside front cover for key.

horizon defines this level at Seaford Head and along the Kent Coast. This correlates with a fossiliferous horizon at 346.80 m in the Trunch Borehole. This level is less fossiliferous at Culver Cliff, marked by a flint band 70 cm beneath the correlative of Whitaker’s 3 Inch Flint. In the Loir Valley the Wine-cave Flint (*sensu* Jarvis, Gale and Clayton, 1982) marks the mfs. Here the HST is comparatively well preserved, attaining a thickness of 2 m, and, as in the rest of the Anglo-Paris Basin, it is dominated by a typical succession of chalk with regularly-spaced flints. At Beauval, erosion associated with SB Sa4 has removed the HST.

SEQUENCE Sa4

In the Trunch Borehole, SB Sa4, the LmST and TST are presumed to coincide with a section of missing core (depth: 345.21 – 342.34 m). On the Kent coast, a package of irregular and unevenly bedded flints characterises the LmST; the SB is placed at the base of this unit. At Seaford Head this level is characterised by more regular flint bands and two faint marl horizons that are not recorded in the other sections examined. An erosion surface beneath the lower of these marls marks the SB. In the deepest-water section at Culver Cliff a correlative conformity Sa4 is placed at a flint band six metres above Whitaker’s 3 Inch Flint. At Beauval, a hardground forming the base of the main Lower Phosphatic Chalk (Jarvis, 1980a, 1980b) marks SB Sa4. This hardground exhibits evidence of considerable winnowing, and the LmST is not preserved. Here, as in the Loir, current activity associated with the second-order rise in relative sea-level has resulted in marked condensation. The omission surface associated with the Lower Burrow Flint (*sensu* Jarvis, Gale and Clayton, 1982) is interpreted as representing SB Sa4 in the Loir.

A metre of flint-free chalk on the East Kent Coast indicates a period of more rapid and continuous deposition associated with the TST; the ts is coincident with the top of the LmST flints. The TST is rich in inoceramid debris and echinoids. A nodular sponge bed defines the

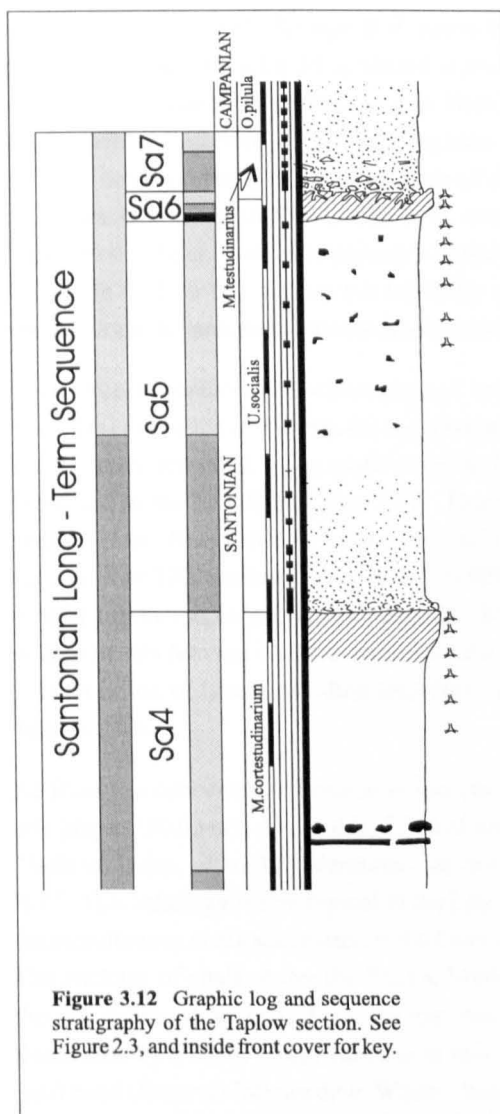


Figure 3.12 Graphic log and sequence stratigraphy of the Taplow section. See Figure 2.3, and inside front cover for key.

nodular sponge bed overlain by a double-band of small flints marks the mfs with the HST dominated by a large flint band towards the top — the Exeat Flint of Mortimore (1986). At Culver Cliff the succession is more flinty, with a prominent band in the middle of the HST correlating with the Exeat Flint in Sussex. The condensed HST succession in the Loir is represented by a well-developed burrow-flint. Phosphatic chalk, terminating at a limonitic parting, forms the majority of the Beauval HST. A metre of HST sediment is preserved above this; another limonitic omission surface is interpreted as SB Sa5. At Taplow (Figure 3.12) a level of phosphatic chalk piped-down *Thalassinoides* burrow systems, from the phosphatic hardground forming the overlying SB, defines the top of the HST.

SEQUENCE Sa5

Sequence Sa5 in the Trunch Borehole is characterised by a largely flint-free succession. A marl encompassing the biozone boundary between *M. coranguinum* and *U. socialis* directly overlies the SB (depth 335.56 m); two iron-stained sponge beds (335.20 and 334.35 m) with associated body fossils are preserved in the LmST. Over this interval, the trace-fossil assemblage is dominated by *Zoophycos* and *Chondrites*. On the East Kent Coast a locally developed, erosive, nodu-

ts at Seaford Head with the TST containing a thin marl band here which was not observed in the Culver Cliff section — the TST consisting of chalk with regularly-spaced flints. The ts is arbitrarily placed within a section of missing core (depth: 345.21 – 342.34 m) in the Trunch Borehole, accounting for the whole of the TST. At Beauval a significant unit of phosphatic chalk rests directly on the SB hardground, characterising the TST. This unit is interpreted to be the result of deposition under conditions of high productivity, probably associated with dynamic upwelling and associated current activity over the Pay-du-Bray Axis (Jarvis, 1980a, 1980b, 1980c). The mfs is placed within the upper part of the phosphatic chalk. In the Loir sections a thin TST is preserved above the slightly marly LmST.

Chalk with the occasional, rare, flint characterises the HST in the Trunch Borehole and East Kent coast sections. At Trunch the mfs coincides with the top of a section of missing core. In Kent a low-relief glauconitised sponge-rich hardground, locally known as Barrois' Sponge Bed (Robinson, 1986) defines the mfs. Several distinctive, though laterally impersistent sponge beds and echinoid-rich horizons with the occasional isolated burrow-fill flint are preserved within the HST. Elsewhere throughout the main sections, a more typical flint and chalk succession thickens basinwards. At Seaford Head a

lar sponge bed (Peake's Sponge Bed, *sensu* Robinson 1986) marks the SB. Where this is not present, the base of the LmST is placed, *a priori*, at a level of correlative conformity within the white flint-free chalk. In the main Anglo-Paris Basin at Culver Cliff and Seaford Head the Buckle Marls (*sensu* Mortimore, 1986) mark the base of sequence Sa5. At Taplow, a distinctive erosion surface forming a hardground at the base of the Lower Phosphatic Chalk (*sensu* Jarvis, 1980a) marks the SB. The LmST consists of a reworked and winnowed phosphatic lag. SB Sa5 is interpreted to be at a limonitic parting at Beauval, a metre above the top of the Lower Phosphatic Chalk. In the Loir this sequence is relatively expanded. A minor erosion surface marks the SB, above which the sediment becomes more marly and bryozoa-rich characterising the LmST.

In the Trunch Borehole an horizon of small irregular flints, sponge, crinoid and fish debris (depth 332.70 m) marks the ts. Above, the succession is relatively fossiliferous with *Zoophycos*, crinoids and bivalves recorded. The marls seen in the deeper parts of the Anglo-Paris Basin are not preserved in the East Kent Coast TST. This unit is only a metre thick and unfossiliferous. At Seaford Head, Buckle Marls 3 and 4 lie within the TST with the under-surface of marl 5 marking the mfs. The TST thickens towards Culver Cliff where five thin marl bands are preserved and the base of a sixth, thicker marl marks the mfs. White chalk characterises the TST at Beauval, whilst at Taplow this horizon is characterised by the deposition of the Lower Phosphatic Chalk. In the Loir an influx of fauna including serpulids, sponges, bivalves, crinoids, bryozoa and echinoids defines the ts.

At Trunch, a concentrated horizon of inoceramid debris between two tabular flints identifies the mfs (depth 330.03 m). Above this, 5.5 m of fossiliferous white chalk with *Zoophycos*, *Chondrites*, *Thalassinoides*, crinoids, belemnites, echinoids, sponges and brachiopods are recorded in the HST. This lithology is also typical of the East Kent Coast, where the mfs is placed *a priori* within the monotonous chalk succession at the level of an isolated flint in the absence of other indicators. The package of chalk above the Buckle Marls forms the HST at Seaford Head. At Culver Cliff the mfs is placed directly above the uppermost Buckle Marl, and the overlying systems tract is dominated by a chalk – flint succession that attains a thickness of just over 9 m. At Beauval, a marl band (Beauval Intermediate White Chalk Marl, *sensu* Jarvis, 1980a) is preserved at the mfs. Above this, the HST has been largely removed by the erosion associated with the hardground at the base of the next phosphorite deposit. A return to a typical chalk facies with regularly-spaced flint bands characterises the HST at Taplow. In the Loir the HST is represented by 1.5 m of glauconite-rich fossiliferous calc-arenite.

SEQUENCE Sa6

Throughout the Anglo-Paris and Anglo-Dutch basin sections, sequence Sa6 is considerably thinner than Sa5. The sediments in the deeper-water sections of the Anglo-Paris Basin are characterised by discrete bands of marl interpreted to represent the flushing of detrital material from the landmasses as relative sea-level reached its maximum for the Santonian. Lithologically, the sequences of the later Santonian are very similar. An iron-stained, inoceramid-rich, sponge bed in the upper part of the *U. socialis* Biozone marks the SB on the Kent coast. This correlates with a flint horizon (depth 324.38 m) in the Trunch Borehole. The conspicuous lack of marl at Trunch and along the East Kent Coast at this level suggests that the source area of the clay minerals was to the west of the Anglo-Paris Basin. Lack of marl at Trunch and along the Kent Coast may be the result of interaction of water masses between the Anglo – Paris and Anglo – Dutch Basins agitating the water column over the London-Brabant Massif, preventing gravity settling of fine sediment. Marl bands were deposited here during the lower relative sea-level of the Coniacian; a

consequence of higher levels of detrital material in the water. The LmST at Seaford Head is dominated by three distinctive marl bands separated by flinty chalk. At Culver Cliff five marl bands are developed, forming prominent, weathered-out grooves in the cliff face on the north-east side of Horse Shoe Bay. The SB is represented by a well-developed phosphatic chalk hardground at Beauval. The ts is also erosive; in parts of the quarry this surface lies slightly above the SB, represented by a separate hardground (*sensu* Jarvis, 1980a) whilst elsewhere it is coincident with the SB. At Taplow the SB lies at the top of the flint-chalk rhythms of sequence Sa5 and marks the base of the nodular, phosphatic hardground chalk associated with the base of the Upper Phosphatic Chalk (Jarvis, 1980a). This part of the succession is highly condensed and the LmST has not been preserved. The Craie-de-Villedieu Formation is also condensed at this level; a consequence of the levelling-off of the long-term relative sea-level rise. The SB is marked by the Lower Limonitic Hardground of Jarvis, Gale and Clayton (1982) who described the overlying bioclastic gravels as the most fossiliferous horizon in the late Turonian to late Santonian exposures in the area. This reworked horizon represents the LmST and contains reworked fragments of the SB hardground.

The ts in the Trunch Borehole (depth 323.22 m) and on the East Kent Coast is placed at a small flint within the chalk succession. At Seaford Head this surface lies directly above the top of the three LmST marls; the TST comprises two metres of chalk with a sponge bed a few centimetres from the top. At Culver Cliff, the ts is placed at the top of the sequence of marls; the TST is characterised by a further complex of thin marls within flinty chalk. In the Loir, the ts marks a reduction in the amount of coarse bioclastic material. The TST comprises a thin package of coarse-grained phosphatic chalk, including clasts of the underlying phosphatic hardground up to 30 cm in length floating within the sediment. This fossiliferous horizon is characterised by serpulids, corals, echinoids and inoceramids. On the Pay-du-Bray Axis at Beauval, the ts is superimposed upon SB Sa6 and is overlain by a coarse-grained lag of reworked phosphatic blocks and fragments of hardground, up to 30 cm long, abundantly fossiliferous and characterised by a chocolate-brown phosphorite. At Taplow the TST forms part of the lithified chalk at the base of the Upper Phosphatic Chalk.

The mfs coincides with the *U. socialis* – *M. testudinarius* Biozone boundary. In the Anglo-Dutch Basin at Trunch this is at a depth of 321.95 m. The HST above this is characterised by white chalk and occasional flint-bands. This level is very fossiliferous with *Zoophycos*, *Chondrites*, belemnites, crinoids, sponges, brachiopods, fish remains and inoceramid fragments recorded. In Kent the mfs is marked by the Palm Bay Echinoid Band (*sensu* Robinson, 1986), a horizon of *Echinocorys elevata* Brydone. In Sussex the HST comprises the two metres of chalk above the mfs, placed at the Hawkes Brow Flint. The mfs is placed at the top surface of the upper marl band within the TST at Culver. Here, the HST is characterised by a package of flinty chalk that becomes marly towards the top. Two anastomosing stylolites are developed within the marly chalk. At Beauval, the mfs is interpreted to be at the top of the unit of TST phosphorite breccia. This level is again condensed and forms a hardground surface. The overlying HST is missing, with SB Sa7 and ts Sa7 interpreted as being coincident with hardground surface mfs Sa6. Condensation is also evident at Taplow, where the HST is represented by the winnowed and lithified sediment forming the hardground chalk below the Upper Phosphatic Chalk. In the Loir the thin HST is dominated by lithification extending from the hardground above. Clasts from this hardground have collapsed into the underlying softer sediment.

SEQUENCE Sa7

In the Anglo-Dutch Basin at Trunch and on the East Kent Coast over the London-Brabant Massif the chalk is lithologically undifferentiated. However, the section at Seaford Head is characterised by a higher marl content than sequence Sa6, represented by four discrete bands. The SB lies directly beneath the lowest of these. In the Culver Cliff succession a well-developed hardground forms the SB. This is characterised by iron nodules cemented into the hardground surface, and a strong glauconitic veneer. Glauconitisation extends down twenty centimetres from the surface. At Taplow and Beauval, distinctive phosphatic chalk hardgrounds mark the SB; these are interpreted to represent the final stage of current-reworking and winnowing prior to deposition of the Upper Phosphatic Chalk (Jarvis, 1980a, 1980b, 1992; Jarvis and Woodroof, 1981). At Beauval this erosion cuts down to the TST of sequence Sa6, whilst at Taplow it has resulted in non-deposition or erosion of LmST Sa7. Here, ts Sa7 is interpreted to be coincident with SB Sa7. The lithified hardground at Taplow represents levels down to the HST of Sa5. At the top of the Craie-de-Villedieu Formation, erosion and non-deposition associated with the fall in relative sea-level has led to the formation of the Upper Limonitic Hardground, (*sensu* Jarvis, Gale and Clayton, 1982) marking the SB. At Trunch a level of increased *Chondrites* and *Zoophycos* activity marks the base of Sa7 (depth 318.88 m).

The ts is placed above the first package of marls in the main depocentres, with a thin TST characterised by flinty chalk. In the Trunch Borehole a change from the marly, *Zoophycos* and *Chondrites*-rich sediment to purer chalk highlights the ts (317.86 m). In addition to purer chalk, the TST is characterised by an increase in body-fossils. At Culver Cliff, this level is highly condensed, the ts being superimposed upon the SB hardground, and represented by a glauconitic patina. The TST is characterised by reworked glauconitic nodules floating above the hardground surface. The top surface of a marly unit marks the ts at Seaford Head; the overlying TST comprising a thin package of chalk with flint bands. This corresponds to the deposition of phosphatic chalk at Beauval and Taplow. A horizon of inoceramid debris is preserved at the ts on the Kent Coast with a thin package of white chalk forming the TST.

A relatively thick HST is preserved throughout the Anglo – Paris and Anglo – Dutch Basins, resulting from deposition during a slow and protracted fall in relative sea-level. As relative sea-level fell a number of discrete marls indicative of detrital influx were deposited in the basin centre. The top of the Santonian is marked by a distinctive burrowed omission surface in Trunch at a level (306.72 m) some way below the top of the *M. testudinarius* Biozone (Wood and Morter, in Arthurton *et al.*, 1994). At Culver Cliff the HST is largely unrepresented, represented by a thin package of chalk beneath the overlying hardground marking the base of the Campanian. This horizon becomes less condensed laterally, with the hardground horizons dying out at Downend in the centre of the Isle of Wight (Osborne-White, 1921). This condensation is associated with movement along the Isle of Wight fault system that runs sub-parallel to the chalk (Mortimore and Pomerol, 1997). The East Kent succession reveals a typical HST assemblage of chalk with flints and sponge horizons. In Sussex, a similar succession is seen with the addition of a number of discrete marl bands. The mfs is placed at the level of the Brighton Marl. At Beauval and Taplow, the HST is represented by phosphorite. The top of the Santonian is not preserved in the sections around Villedieu-le-Château. A late-Santonian net fall in relative sea-level is indicated by sequence Sa7.

SECOND-ORDER SANTONIAN SEQUENCE

The seven Santonian third-order sequences stack to form a second-order cycle of relative sea-level change (Sa). The Sa SB is placed at SB Sa1. Sa LmST is characterised by thin third-order LmSTs and TSTs, with only the HSTs preserved to any extent during a gradual fall in relative sea-level. Thick HST Sa2 is indicative of a virtual stillstand.

The Sa ts is placed at ts Sa3. A more rapid rise in relative sea-level is evident during Sa4 time, highlighted by the significantly thicker third-order systems tracts. During this transgression the basin-margins were rapidly inundated, and consequently middle Santonian sediments rest directly upon Turonian in the southwest of the Loire Valley (Jarvis, Gale and Clayton, 1982). This also is reflected in the main depo-centres by an increase in detrital clay — flushed from the landmasses during the rapid Santonian transgression.

Sa mfs coincides with mfs Sa5, at the top of the thickest and most extensively developed third-order TST across the Anglo – Dutch and Anglo – Paris Basins. During this time, relative sea-levels were significantly higher than during Coniacian peak-transgression. The Sa HST is characterised by an increase in the number of marl bands. This is the result of the inundation of the south-western basin margins releasing sediment to the main depocentre of the Anglo – Paris Basin. Current activity over the London – Brabant Massif and greater distances to the margins of the Anglo – Dutch Basin is thought to account for the purer chalks in the Kent and Trunch sections studied.

This presents a paradox whereby, during the Santonian, both second-order HST and third-order LmSTs are characterised by abundant detrital material. It would appear that terrigenous run-off is effective in transporting detritus to the depo-centres during both second and third-order lowstands, but it is only over a longer period of transgression that sediment is flushed effectively from the landmasses by rising sea level. Global evidence for a transgressive-cycle during the Santonian and other published sea-level curves are discussed below. The correlation diagram (Figure 3.13) shows lateral and temporal variations between the third-order cycles and within the second-order cycle.

PUBLISHED SEA LEVEL CURVES

A number of sea level curves have been published for the ^{Late}Upper Cretaceous, often tied to the 'Exxon curve' of Haq *et al.* (1988). Hancock (1993b) argued that there are considerable problems associated with this curve and consequently with subsequent, dependent correlations. Miall (1992) tested the Exxon curve against a randomly generated succession, and found a 70% fit. He concluded that any correlation with the Exxon curve will invariably succeed, but was pointless. None-the-less the Exxon work has inspired considerable research into global, eustatic sea-level changes. Hancock (1990) constructed a relative sea-level curve based upon hardgrounds and nodular chalks as indicators of regressive troughs. This approach is not dissimilar to that used herein with regard to the identification of sequence boundaries. However, we also recognise the formation of nodular chalks and hardgrounds at some transgressive surfaces, often characterised by phosphatic or glauconitic mineralization. The Hancock (1990) curve and that presented herein correspond closely, with Hancock recognising a significant peak during the mid *U. socialis* Biozone characterised by relative sea-levels higher than previously in the Cretaceous. The *U. socialis* peak corresponds to the highest Santonian relative sea-level identified herein. These curves are compared to the relative sea-level curve herein in Figure 3.14.

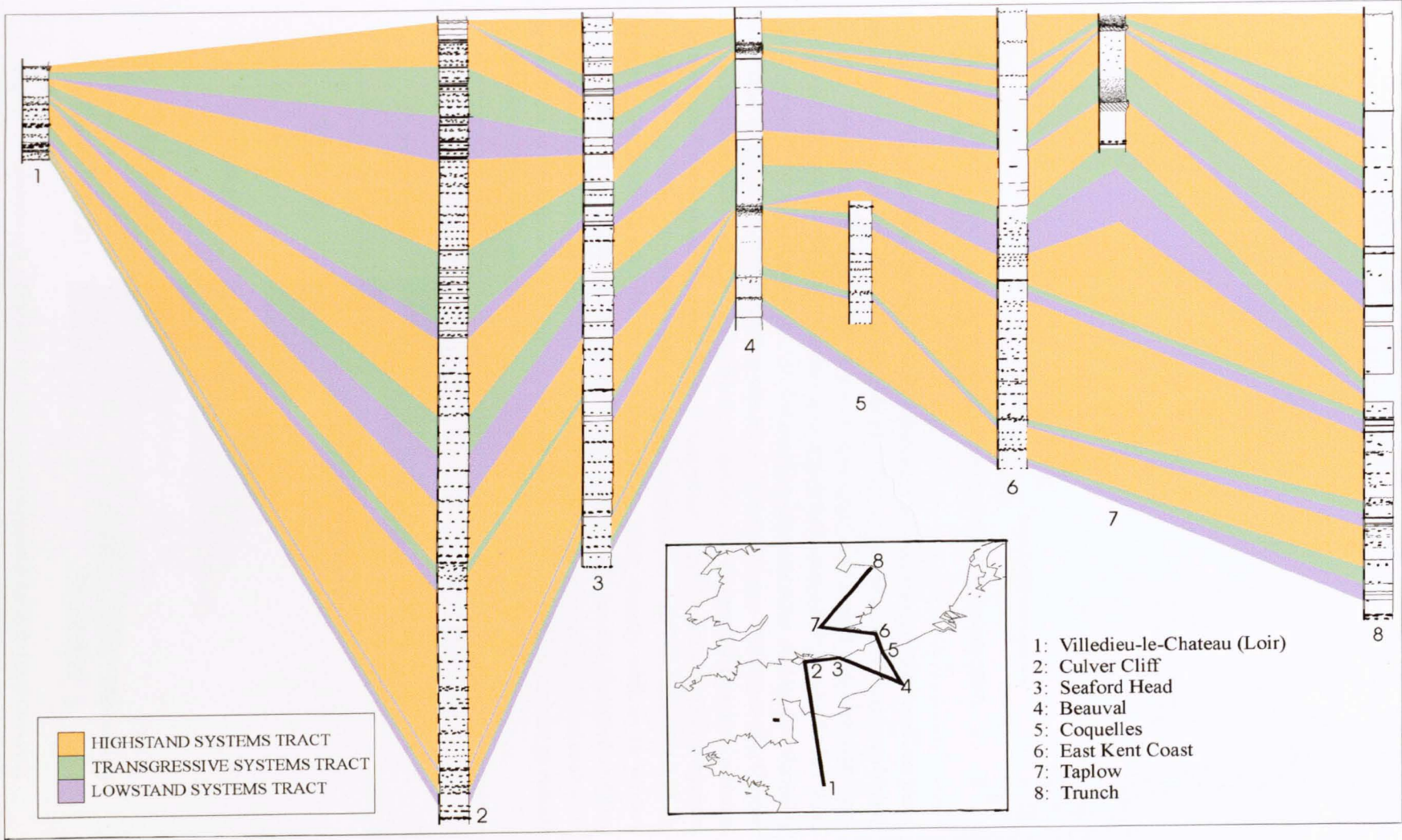


Figure 3.13 Sequence stratigraphical cross-section for the Santonian. Sections run approximately south to north.

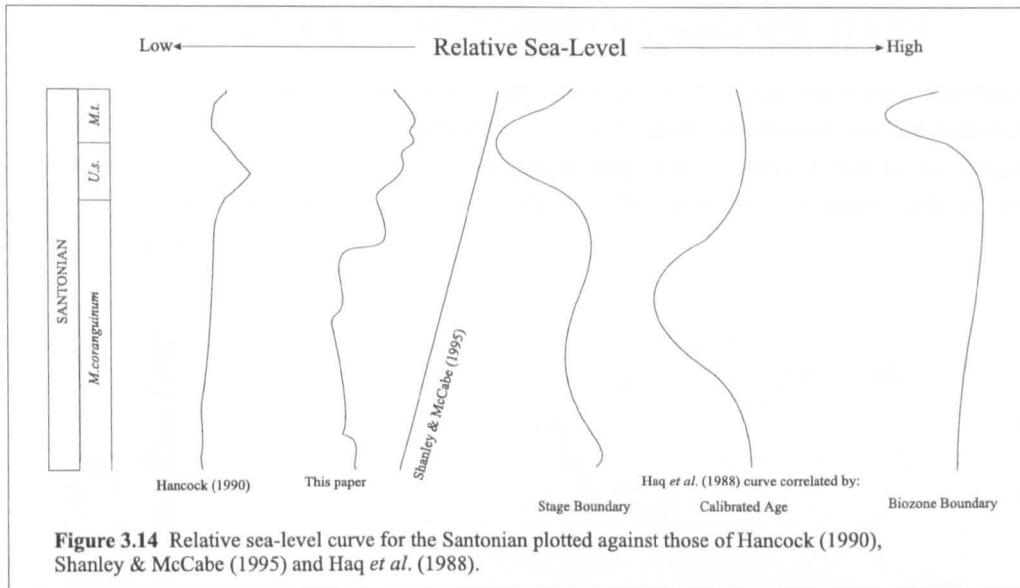


Figure 3.14 Relative sea-level curve for the Santonian plotted against those of Hancock (1990), Shanley & McCabe (1995) and Haq *et al.* (1988).

Cooper (1977) lists the localities world-wide from which data indicating a mid-Santonian transgression has been collected. His global data-set can be interpreted in terms of a sequence boundary at the Coniacian-Santonian boundary, a prolonged LmST, and a rapid mid-Santonian transgression culminating in a sequence boundary at the top of the Santonian (Figure 3.15). In Poland (Marcinowski, 1974) and in Libya (Barr, 1972) Santonian sediments onlap, resting unconformably on Turonian rocks. The base of the Dessau Limestone in Texas (Young, 1963 reported in Cooper, 1977) is unconformable with the underlying rocks, and this unconformity is thought to correlate with the basal Santonian sequence boundary defined herein — SB Sa. Jeletzky (1971) reported that the mid-Santonian was strongly transgressive, and represented the maximum extent of the Cretaceous Sea in the Canadian Western Interior Seaway. More recently, work on the Western Interior Seaway of North America by Shanley and McCabe (1995) has also identified a relative sea-level rise that is coincident with the Santonian stage. Our sequence stratigraphical analysis of the Santonian of the Anglo-Paris and Anglo-Dutch Basins further supports the case for an eustatic transgression during this period.

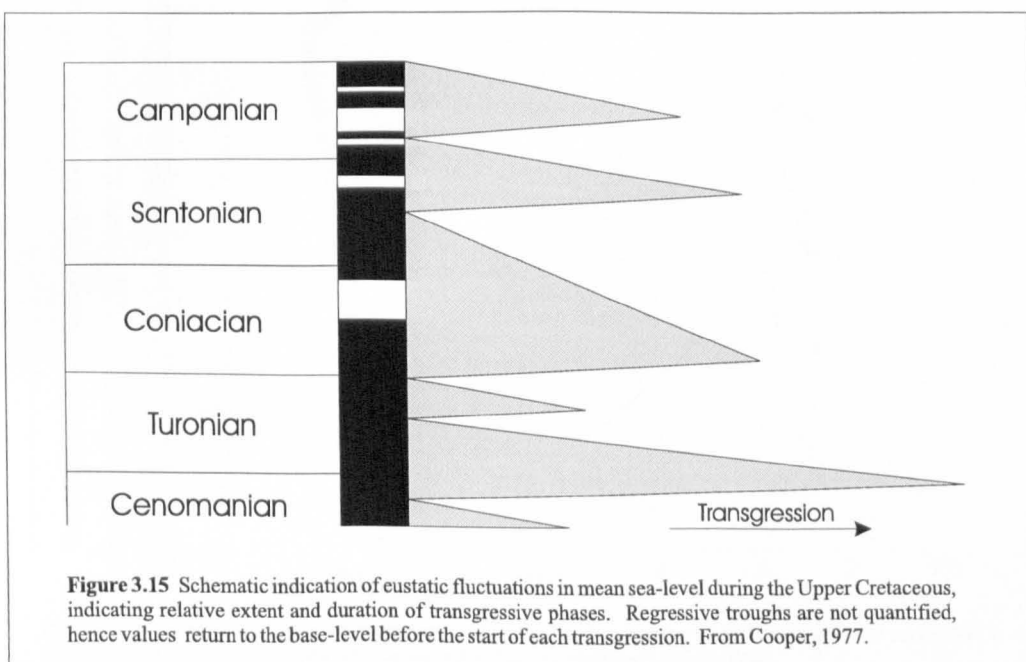


Figure 3.15 Schematic indication of eustatic fluctuations in mean sea-level during the Upper Cretaceous, indicating relative extent and duration of transgressive phases. Regressive troughs are not quantified, hence values return to the base-level before the start of each transgression. From Cooper, 1977.

STABLE OXYGEN AND CARBON ISOTOPE DATA

Assuming that $\delta^{13}\text{C}$ is related to productivity and extent of the shelf seas, variation in the stable $\delta^{13}\text{C}$ curve can provide a useful independent test of the relative sea-level curves and sequence stratigraphical interpretation of the Santonian presented herein. Published carbon and oxygen stable isotope data sets (Jenkyns, Gale and Corfield, 1994) have been compared with our sequence stratigraphical data (Figure 3.16).



Figure 3.16 Graphic log, Sequence stratigraphy, relative sea-level curves and stable $\delta^{13}\text{C}$ and $\delta^{18}\text{O}$ curves for the East Kent Coast section. Stable isotope data after Jenkyns, Gale and Corfield, 1994.

Comparison of the second-order relative sea-level curve and the $\delta^{13}\text{C}$ curve reveals a strong correlation. Values of $\delta^{13}\text{C}$ are in the range 2 – 2.8 ‰. The initial rise in $\delta^{13}\text{C}$ values can be seen to correlate with the significant rise in relative sea-level during TST and early in the HST of Sa4, representing the main phase of transgression. Stable $\delta^{13}\text{C}$ values decrease during the early to middle Santonian, rising to a high point immediately below the *U. socialis* – *M. testudinarius* Biozone boundary. Above this point, values decline slightly through the rest of the stage. The point of maximum excursion coincides with the highest relative sea-level, derived from the sequence-stratigraphical model.

Within the $\delta^{13}\text{C}$ data a higher resolution cyclicity can be seen to correlate broadly with the third-order sequence stratigraphy. In general, LmSTs correspond to lower relative values for $\delta^{13}\text{C}$, and HSTs to increased $\delta^{13}\text{C}$ values. The TSTs show a general rising $\delta^{13}\text{C}$ trend, though thinly developed TSTs were not always apparent in the $\delta^{13}\text{C}$ data. Falling $\delta^{13}\text{C}$ values are generally observed, within the upper part of individual HSTs, from the relative sea-level maximum to the SB at the end of each sequence. This is not the case as for HST Sa4, and this may be the consequence of the slow rate of relative sea-level rise rather than the absolute levels of change (Jenkyns, Gale and Corfield, 1994). The positive correlation between an increase in $\delta^{13}\text{C}$ values and a rise in relative sea-level shows a dynamic link between marine transgression and an increase in organic-carbon synthesis and storage. This follows the relationship discussed by Jenkyns, Gale and Corfield (1994) and described for the Coniacian in Chapter 2.

The stable $\delta^{18}\text{O}$ ratio has appeared extensively in the literature as a means of calculating palaeotemperature. More recently it has been used as an indication of salinity stratification in greenhouse oceans (Railsback, 1990). This relationship has been invoked to explain the relationship between $\delta^{18}\text{O}$ values and relative sea level during the Coniacian (Chapter 2). The correlation between $\delta^{18}\text{O}$ values and relative sea-level during the Santonian is slightly less obvious than that between $\delta^{13}\text{C}$ and relative sea-level. Though considerable short-term fluctuation in the values is seen (-2.8 to -1 ‰), the long-term shift in values during the Santonian is less pronounced (-2.4 to -1.75 ‰). At the base of the stage, values become more negative, after an initial increase, to a negative excursion coinciding with the lowest relative sea level. As the second-order transgression begins, $\delta^{18}\text{O}$ values become less-negative, rising to a positive excursion that corresponds to maximum relative sea level during Sa6 time. Short-term fluctuations in the $\delta^{18}\text{O}$ data can be matched to specific third-order systems tracts. Lower $\delta^{18}\text{O}$ values correspond to third-order LmSTs, rising and high $\delta^{18}\text{O}$ to TSTs and HSTs. During periods of higher second-order relative sea-level this relationship becomes more clearly defined. The HSTs of Sa5 – Sa7 are clearly marked by less-negative $\delta^{18}\text{O}$ values, and the LmSTs by more-negative values. This relationship follows that observed for the Coniacian, suggesting that thermal expansion and contraction of the water column, caused by climatic change, is a mechanism for both short-term and long-term relative sea-level fluctuations in the Santonian chalk seas. Thermal expansion and contraction is likely to be superimposed upon a more dominant, tectonic, mechanism. The stable $\delta^{13}\text{C}$ and $\delta^{18}\text{O}$ data correlate strongly with the relative sea-level curve, indicating shelf-sea expansion and supporting the salinity-stratified ocean models.

THE ROLE OF TECTONICS

Mortimore and Pomerol (1997) related variations in the style of sedimentation during the late Santonian and Early Campanian to the Wernigerode tectonic phase. Localised lithological changes were noted in the *U. socialis* Biozone, typified by non-preservation of marl bands over structural highs. The Culver Cliff succession represented a relatively deep water setting during much of the late Cretaceous, with thick packages of sediment preserved, such as during the mid-Santonian. However, prominent hardgrounds, especially associated with SB Sa7 and the overlying end-Santonian SB, developed from time to time. Here development of a palaeo-high associated with periodic reactivation along the Isle of Wight – Pay-du-Bray Axis (Mortimore, 1986; Mortimore and Pomerol, 1991, 1997) coincided with a more widespread fall in relative sea-level and resulted in pronounced winnowing, and hence the development of the hardgrounds. These effects die out laterally away from the tectonic axis. These tectonic movements are also evident at the southernmost extent of the Pay du Bray Axis. Here, the prominent hardgrounds at Beauval represent periods of intense condensation. This phase of tectonic activity was widespread, and can be traced out of the Anglo-Paris Basin to Germany (Mortimore *et al.*, in press) during the ~~upper~~ Santonian – ~~lower~~ Campanian. Reductions in accommodation space resulting from tectonic movements provide a depositional environment where eustatic sea-level falls result in more pronounced erosion at the sequence boundaries and rises in relative sea-level lead to more intensive winnowing at the ts.

The second-order cycle of relative sea-level change can be seen to be independent of climatic control, the $\delta^{18}\text{O}$ curve remaining stable over this time period. A probable explanation for the observed second-order cycle is an increase in activity at the mid-ocean ridges. Hays and Pitman (1973) show that the volume of the world's oceans was increasing during the Coniacian and Santonian, with increased rates of spreading documented by Cande and Kent (1995), Knott, Burchell, Jolley and Fraser (1993), Pitman (1978) and Srivastava and Tapscott (1986). This eustatic increase in relative sea-level is invoked to explain the Santonian second-order cycle, with the mid-Santonian represented by transgressive facies world-wide, and the end-Santonian – early-Campanian by regressive-facies (Cooper, 1977).

DISCUSSION

A number of calibrated age scales giving differing durations for the Santonian have been published over the last twenty years. Obradovich and Cobban (1976) assigned the Coniacian a duration of 1 Ma based upon biozone data and the Santonian 4.5 Ma. These figures were duplicated by Harland *et al.* (1982) though they later revised this (Harland *et al.*, 1989), reducing the duration of the Santonian to 3.5 Ma and increasing that of the Coniacian to 2 Ma. Odin (1983) suggested a duration of 3 Ma for the Santonian compared with 2 Ma for the Coniacian. Successive schemes demonstrate a trend towards reducing the duration of the Santonian stage relative to the Coniacian. Gradstein *et al.* (1994, 1995) reported a duration of 3.2 Ma \pm 0.5 Ma for the Coniacian and 2.4 Ma \pm 0.5 Ma for the Santonian. Observations resulting from the sequence stratigraphical analysis of the Santonian presented here, and the Coniacian (Chapter 2) suggest that the Santonian was of shorter duration than the Coniacian, but that the succession is less condensed. Consequently, the dates suggested by Gradstein *et al.* (1994 and 1995) are preferred here as more realistic. Eight cycles were recognised in the Coniacian and, assuming a Coniacian duration of 3.2 Ma, this gives a cycle duration of 400 ka, coincident with the prominent Milankovitch 400 ka eccentricity cycle. The third-order cycles are thus interpreted to be related directly to a climatic control.

Here in the Santonian, seven such cycles are reported and consequently, assuming that these are also 400 ka in duration, it is suggested that the Santonian is at the upper limit of the Gradstein *et al.* (1994 and 1995) dates at approximately 2.8 Ma duration. The relative sea-level curve constructed using the sequence stratigraphical model, herein, agrees closely with others' curves published for Santonian sections world-wide on a second-order scale. The third-order curves herein are an order of magnitude above those available from the literature.

Fluctuations in incident solar radiation as the result of the Milankovitch 400 Ka eccentricity cycle have varied rates of evaporation in the low-latitudes during geological time. In turn, following the Railsback model (1990) for a salinity-stratified greenhouse ocean, this has resulted in changes in the $\delta^{18}\text{O}$ ratio of the ocean water, a consequence of heavy ^{18}O -rich water being trapped beneath the pycnocline. This process appears a consistent feature of the ~~Upper~~^{lake} Cretaceous epicontinental chalk seas (Coniacian — Chapter 2), a corollary being that the $\delta^{18}\text{O}$ can not be used as a reliable indicator of palaeotemperature in such environments. A growing body of work from the Cretaceous Western Interior Seaway of the United States supports the salinity stratification model. Baron, Arthur and Kauffman (1985) associate increased run-off during wetter periods with a dilution of the surface waters, and a subsequent build-up of ^{18}O -rich water beneath the pycnocline. Wright (1987) envisages an increased run-off scenario from the western margin of the Seaway, with a return flow of warm saline bottom water generated through increased evaporation on the eastern margin. The Railsback (1990) model supports this explanation for the Western Interior stable isotope curves, and is invoked to explain the ^{18}O curves plotted alongside the sequence stratigraphy herein. Pratt *et al.* (1993) highlights the sensitivity of the Western Interior Seaway to salinity changes during periods of prolonged isolation from the world's oceans, and argues that strong stratification would have reduced the effects of wind-driven currents and turbulent mixing of the water column. Hay, Eicher and Diner (1993) support the salinity-stratification model for the Western Interior Seaway. Pratt *et al.* (1993) argue that orbital fluctuations would result in variations in the effect of low-latitude incident solar radiation. This could have caused zones of intense precipitation, especially along the northern margins of Tethys. This would have further enhanced the dilution of the upper, ^{18}O -depleted waters. Fischer (1993) recognises a persistent 400ka Milankovitch eccentricity cycle in densitometer and %-carbonate borehole data alongside a weaker 400ka cyclicality in the gamma ray log from Upper Cretaceous chalk – marl sequences from the Western Interior.

CONCLUSIONS

Seven short-term, third-order sequence stratigraphical cycles of relative sea-level are identified in the Santonian. Comparison of these data with published stable-isotope data suggests a 400 ka Milankovitch eccentricity rhythm controlling mechanism. These cycles stack to form a longer-term, second-order cycle of relative sea-level change controlled by variations in the rate of mid-ocean ridge spreading. A duration of 2.8 Ma is suggested for the Santonian stage based upon the assumption that the third-order cycles are related to thermal expansion and contraction of the water column related to Milankovitch cyclicality. The second-order cycle is linked to a tectonic mechanism linked to spreading at the ocean ridges, with a climatic overprint. Independent stable isotope data and a world-wide identification of mid to ~~Upper~~^{lake} Santonian relative sea-level change strengthens the sequence stratigraphical model (Chapters 1 & 2) utilised here. This also suggests that the second-order cycle is eustatic. The correlation between the stable isotope data and sequence stratigraphical cycles presented highlights the potential usefulness of stable isotope curves in sequence stratigraphical analysis.

Chapter 4

Lower Campanian

ABSTRACT

The Upper Cretaceous chalk of Northwest Europe was deposited in an open epicontinental sea during a period of high global eustatic sea level. The bulk sediment consists of a white coccolith ooze with bands of chert and marl. At intervals in the succession, winnowing has led to the development of nodular chalks and hardgrounds, often correlatable across the basin.

A sequence stratigraphical analysis of the Lower Campanian succession has led to the identification of fourteen short-term, third-order, cycles of relative sea-level change superimposed upon two longer-term, second-order, cycles. Comparison of the sequence stratigraphical interpretation with independently derived stable isotope data shows a good correlation. A relative sea-level curve has been produced from the sequence stratigraphical analysis and is compared with similar curves from the literature. The relative sea-level curve shows a positive correlation with the independent $\delta^{13}\text{C}$ curve and an inverse correlation with the $\delta^{18}\text{O}$ curve.

The longer-term change in the $\delta^{13}\text{C}$ curve is interpreted to represent fluctuations in the area of the shallow shelf seas controlled by changes in relative sea-level. The relationship between $\delta^{18}\text{O}$ and the relative sea-level curves suggests a climatic control on relative sea-level fluctuations in a thermally stratified ocean with good circulation. This represents a change, associated with upwelling in the late-Santonian, from the salinity-stratified, sluggish oceans of the Coniacian and Santonian (Chapters 2, 3 & 6).

This work demonstrates the viability of sequence stratigraphy as a technique for subdividing the biogenic, pelagic sedimentary record of the Northwest European Upper Cretaceous, and demonstrates that combined with stable-isotope stratigraphy, sequence stratigraphy allows study of the underlying fundamental controls on deposition based upon often subtle changes in sedimentology, geochemistry and palaeontology.

INTRODUCTION AND STRATIGRAPHY

During the ~~Lower~~^{Early} Campanian, the Anglo-Paris Basin lay at the triple junction of the Boreal, Tethyan and Atlantic realms (Owen, 1996). The Campanian Stage was erected by Coquand in 1857 based upon sections in Grande Champagne, Aquitaine (Hancock and Gale, 1996). In the Anglo-Paris Basin, the base of the Campanian is taken to coincide with the extinction of the crinoid *Marsupites testudinarius*. Two biozones have been established for the Lower Campanian in southern England, utilising the echinoid *Offaster pilula* and belemnite *Goniot euthis quadrata*. In the southern English sections, a Subzone of *Uintacrinus anglicus* is recognised at the base of *O. pilula* covering the interval from the base of the Friars Bay Marl 1 to the top of Friars Bay Marl 3. The base of the Upper Campanian is placed at the base of the *Belemnitella mucronata* Biozone. Ammonites are not found over much of the Lower Campanian of southern England and it is therefore difficult to correlate with the type area of Aquitaine. Much of the correlation between English and French sections has been achieved using echinoids, belemnites and inoceramids (Mortimore and Pomerol, 1987).

The Lower Campanian sediments of the Anglo-Paris Basin are dominated by a coccolith chalk, equivalent to part of the Upper Chalk Formation of southern England, and are characterised by regularly-bedded burrow-fill cherts and discrete bands of clay material, though locally, both of these may be absent. Several lithostratigraphical schemes have been introduced, subdividing the chalk into members and named horizons, (Mortimore, 1986; Gale, Wood and Bromley, 1987;

Lake *et al.*, 1987, 1988; Shephard-Thorn, 1988; Arthurton, 1994 and Bristow, Mortimore and Wood, 1997) but none of these have met with universal acceptance. The lithostratigraphical nomenclature employed here largely follows that of Jarvis (1980a) and Mortimore (1986) for the English sections and Jarvis (1980a) and Mortimore and Pomerol (1987) for the French sections.

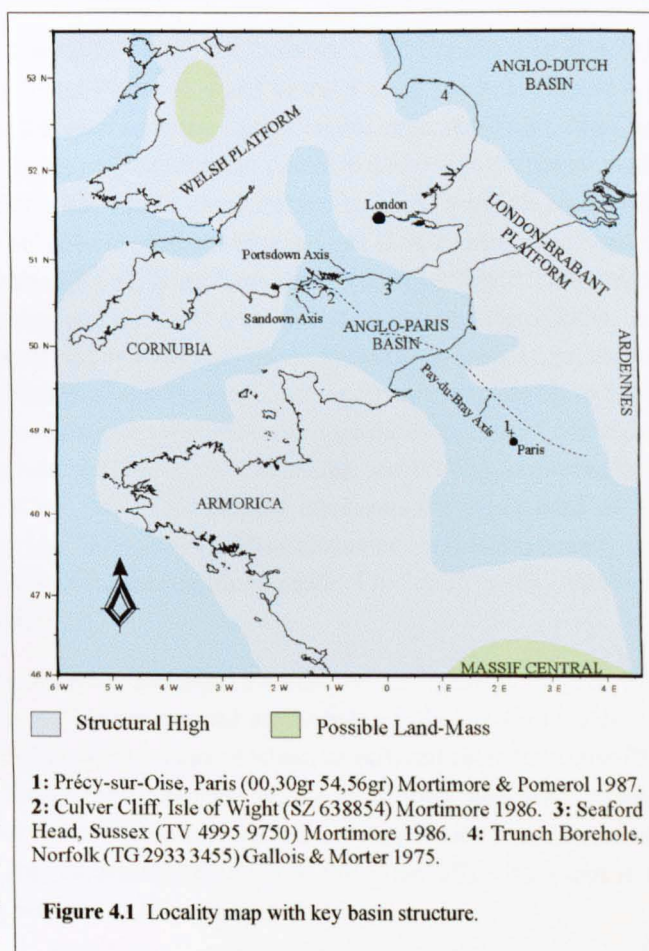
Stable carbon and oxygen isotope stratigraphies (Jenkyns, Gale and Corfield, 1994) and a strontium isotope curve (McArthur *et al.*, 1993) exist for this interval. The Santonian – Campanian boundary is taken, generally, to coincide with the base of magnetochron 33r, though some workers have placed it in the early Campanian (discussion in Gale *et al.*, 1995). The Santonian – Campanian boundary is taken as 83.5 +/- 0.5 Ma and the top of the Lower Campanian at 78 Ma, giving a duration of 5.5Ma (Gradstein *et al.*, 1995).

Evidence for localised tectonism can be found within the Anglo-Paris Basin, especially prominent over the Portsdown Axis (Gale, 1980), Sandown Pericline (Smith and Curry, 1975; Mortimore, 1986) and Pay-du-Bray Axis (Jarvis, 1980a, 1980b, 1992; Jarvis and Woodroof, 1981; Mortimore and Pomerol, 1987, 1997; Mortimore *et al.*, in press). To the northeast, the Anglo-Dutch Basin is thought to have extended to Scandinavia and the Danish-Polish Trough (Hancock, 1975), Figures 4.1 and 1.2.

In this paper, sequence stratigraphical analysis is employed to refine regional correlations and elucidate climatic and oceanographic *versus* tectonic controls on sedimentation during the Lower Campanian. This work builds upon the application of sequence stratigraphical principles to open-marine pelagic facies of Chapters 2 and 3.

CORRELATION AND SEQUENCE DEFINITION

Well-exposed sections in southern England and northern France (Figure 4.1) have been graphically logged (Figures 4.2a – 4.5 & Appendix A) and broadly correlated using the key lithological horizons and published biozonations, traceable across the Anglo-Paris to Anglo-Dutch Basins. Detailed correlations have been made using the cross-plot graphical method (Carney & Pierce, 1995; Neal, Stein & Gamber, 1995 and Chapter 1 herein) to match specific horizons such as marl bands, fossil-rich horizons, sponge beds, chert bands, nodular chalks and hardgrounds (Appendix B). In some sections this has allowed a number of alternate lines of corre-



lation to be investigated within the broader framework of established tie-points. Elsewhere only one correlation solution has presented itself. In all cases the simplest solution has been chosen. The sections have been back-correlated through the line of correlation to test the sequence stratigraphical analysis.

Key sequence stratigraphical surfaces have been identified by combining lithological and palaeontological field data with the cross-plots following the methodology outlined in Figure 1.9. Inflections in the gradient of the line of correlation indicate a change in the depositional rate between the two sections, with major inflections and hiatuses corresponding to sequence stratigraphical key surfaces.

SEQUENCE STRATIGRAPHY

The Lower Campanian can be divided into fourteen short-term cycles of relative sea-level change following the model for sequence definition of Figure 1.9. Initial sedimentation in the lower Campanian is indicative of a dramatic relative sea-level fall with evidence for severe attenuation. Tectonic activity has locally affected sedimentation along tectonic axes. The fourteen short-term, third-order cycles stack to form two longer-term, second-order cycles of relative sea-level change. Gradstein *et al.* (1995) suggested a duration of 5.5 Ma for the Lower Campanian (*O. pilula* and *G. quadrata* Biozones). Standard abbreviations for key surface and systems tract are used throughout.

SEQUENCE Ca1

This sequence is recognised at Culver Cliff (Figure 4.1 Locality 2 and Figures 4.2a & 4.2b), Seaford Head (Figure 4.1 Locality 3 and Figure 4.3) and in the Trunch borehole (Figure 4.1 Locality 4 and Figure 4.4a & 4.4b). It is most complete and accessible at Seaford Head. Here, an influx of clay marks the base of the sequence, with SB Ca1 placed at the base of the lowest marl. A package of three marl bands (Friar's Bay Marls) characterises the LmST which is coincident with the *U. anglicus* (Rasmussen) Subzone in southern England. At Culver Cliff, a moderately glauconitised hardground characterises SB Ca1, lying 20cm above a more prominent hardground (SB Sa7). The relatively planar hardground surface is cross-cut by an anatomising stylolite. As at Seaford Head, the LmST is characterised by three marl bands; here the upper marl represents a heavily bioturbated horizon, with *Planolites* and *Thalassinoides* burrows extending up to 50cm into the chalk beneath. Flecks of glauconite are disseminated through the chalk in the 1.5 m above the hardground. In the Trunch borehole, the base of the Campanian, and SB Ca1, is marked by a burrowed erosion-surface (depth 306.72 m). This horizon represents the upper third of the Santonian *M. testudinarius* Biozone (Arthurton, 1994). The Campanian chalk is more marly and bioturbated than the soft, white chalk of the Santonian beneath. The LmST is very thin here (11cm), the result of erosion at the SB.

At Seaford Head, the upper surface of Friar's Bay Marl 3 marks the transgressive surface. The TST is characterised by a decrease in clay content and an absence of discrete flint bands. A similar succession is seen at Culver Cliff where a metre of white, bioturbated chalk forms the TST beneath a prominent hardground. The ts lies at the upper surface of the third marl band. A band of inoceramid debris 11cm above the base of the Campanian indicates the ts in the Trunch borehole (depth 306.61m). Above this, 1.36m of unbioturbated chalk forms the TST. This unit is of relatively uniform thickness throughout the sections examined.

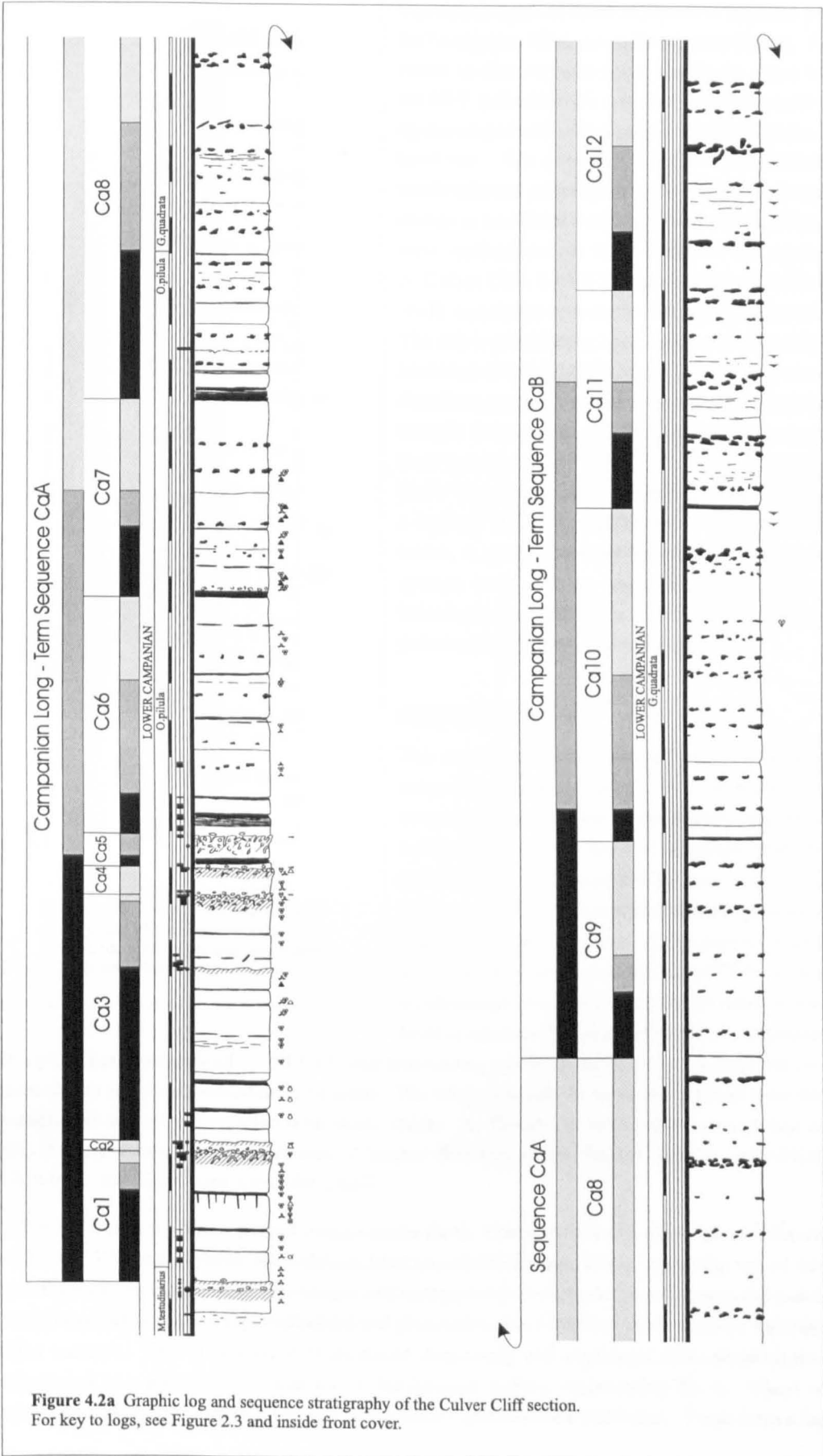


Figure 4.2a Graphic log and sequence stratigraphy of the Culver Cliff section. For key to logs, see Figure 2.3 and inside front cover.

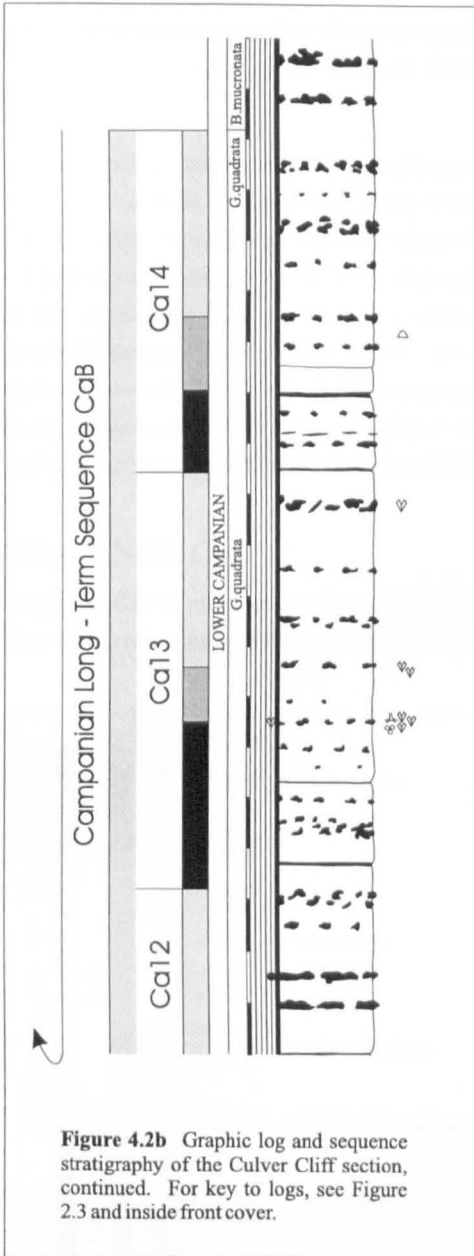


Figure 4.2b Graphic log and sequence stratigraphy of the Culver Cliff section, continued. For key to logs, see Figure 2.3 and inside front cover.

The mfs at Seaford Head is placed at the base of the Ovingdean Marl, *sensu* Mortimore (1986). A return to discrete marl bands marks the onset of the HST, indicative of a reduction in current activity associated with a slowing down of relative sea-level rise. The reappearance of continuous flint bands indicates punctuation in the relative sea-level change as maximum water depths for sequence Ca1 were reached and sea level started to fall again. At Culver Cliff, the HST is dominated by lithified chalk associated with the overlying hardground. The mfs is placed at the base of this unit of heavily bioturbated and lithified chalk. The severe condensation recorded by the hardground surface is thought to have spanned the fall in relative sea-level from the early HST of Ca1 to the ts of Ca2. In the Trunch borehole, a slender *Gonioteuthis* at a depth of 305.25m, overlain by a horizon of fish scales, is used to indicate the mfs. Iron-stained sponge beds and the reappearance of heavy bioturbation are indicative of the return to a more punctuated HST depositional regime.

SEQUENCE Ca2

This sequence is best-preserved and most readily accessible at Seaford Head. Here, the more pronounced Blackrock Marl, *sensu* Mortimore (1986) indicates the onset of the next sequence, with SB Ca2 placed at the base of this horizon. Above the Blackrock Marl, two thin marl bands are preserved in a 1.5 m of flint-free chalk. A flint horizon marks the top of this LmST unit. At Culver Cliff, severe condensation associated with a fall in relative sea-level at this level has resulted in the development

of a prominent hardground — SB Ca2, characterised by pyrite nodules on the surface and cemented into the chalk immediately beneath. The *Thalassinoides* burrows descending from the hardground surface are filled with marly chalk. At Trunch, an iron-stained sponge bed at 303.36m represents SB Ca2. A unit of largely flint-free chalk characterised by clay-filled *Chondrites* and *Zoophycos* forms the LmST.

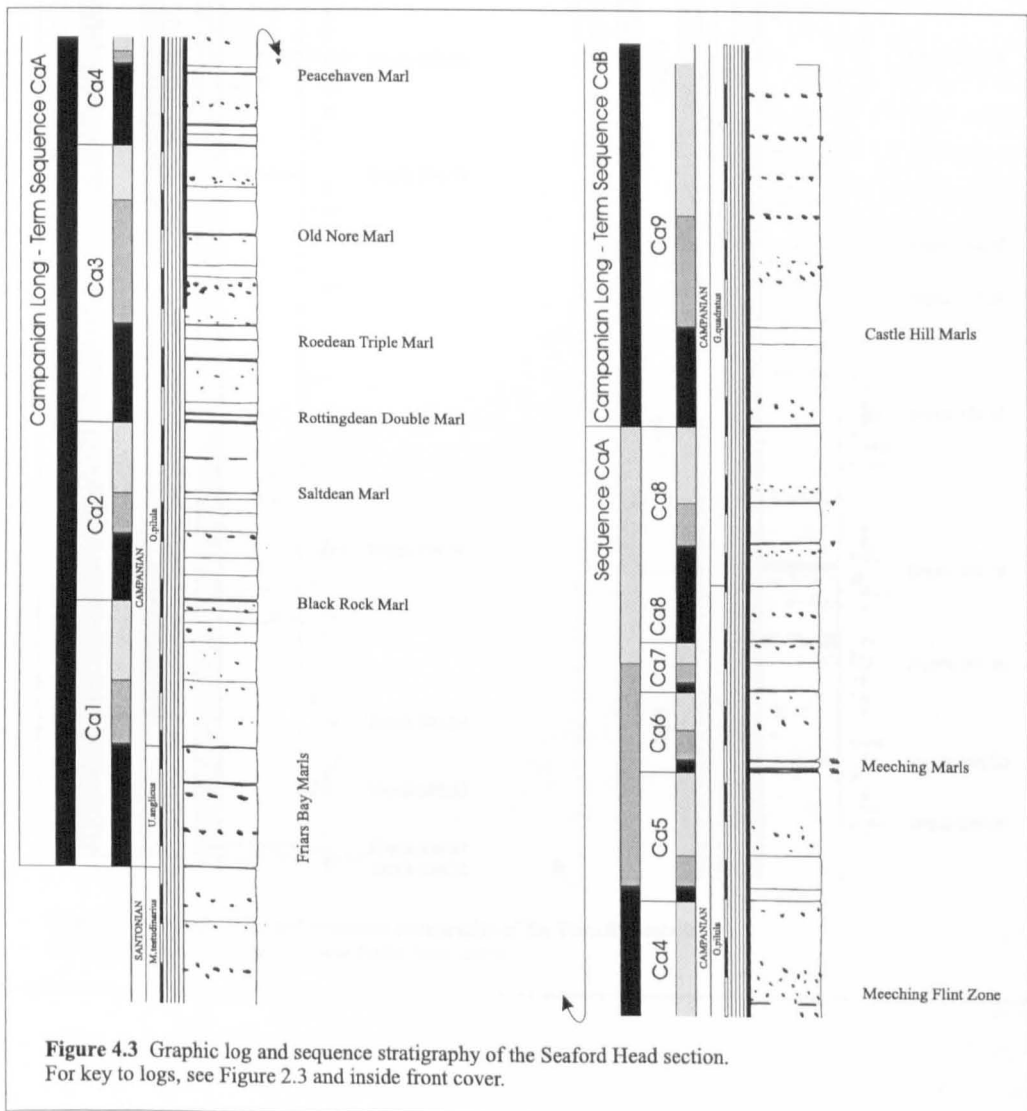
A flint horizon in the Seaford Head section marks the ts. This is overlain by three thin marl bands within the TST and a fourth, the Saltdean Marl (*sensu* Mortimore, 1986), marks the top of this systems tract. At Culver Cliff, inoceramid and sponge debris is cemented into the serpulid-bored hardground surface which is phosphatised and glauconitised to a depth of 12cm between the clay-filled burrows. This is indicative of increased winnowing and associated mineralization that culminated in a glauconitic veneer on the hardground surface, representing the ts. Clasts of hardground chalk became detached and subsequently glauconitised and bored. These form a lag

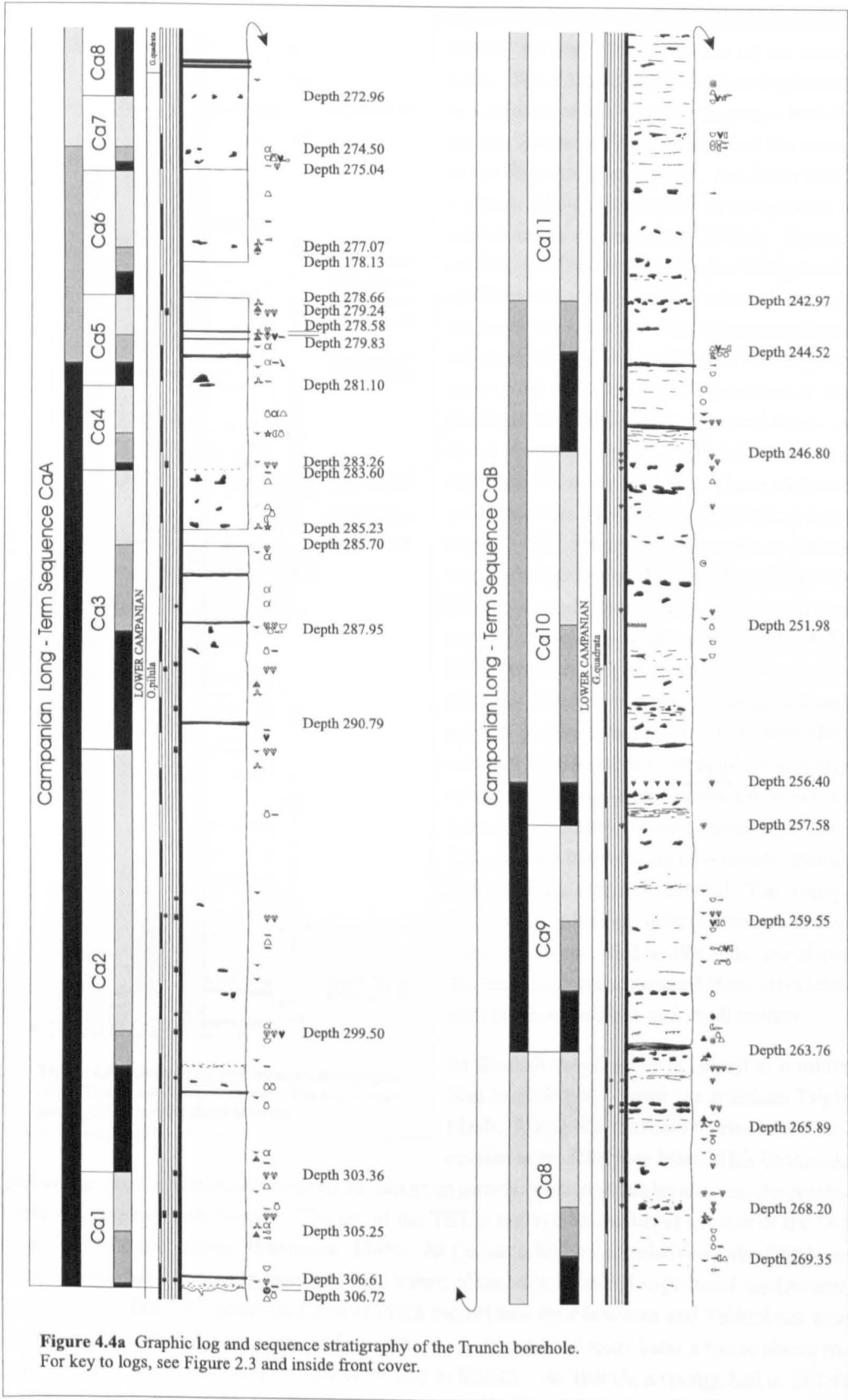
above the hardground surface that is interpreted as representing the TST. This is correlated with an horizon of inoceramid debris in the Trunch borehole that marks the *ts*. The TST comprises fossiliferous chalk.

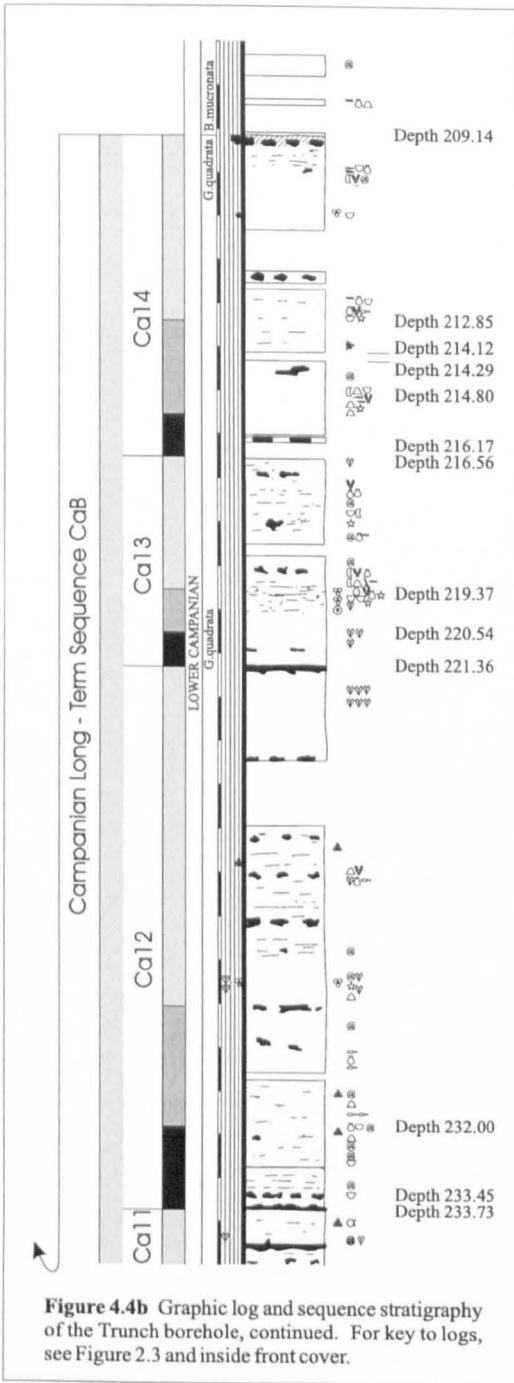
The base of the Saltdean Marl marks the *mfs* at Seaford Head, above which the HST is characterised by purer chalk. A sheet flint, along a fracture, is located in the middle of the HST. At Culver Cliff the glauconitised and reworked clasts floating in the chalk above the hardground surface are interpreted as representing the TST. The top surface of these clasts marks the position of the *mfs* in this condensed section which is overlain by 21cm of indurated HST chalk. An horizon of pyritised sponges (depth 299.50 m) is used to identify the *mfs* in the Trunch borehole. The HST in Trunch is virtually flint-free and comprises 8 m of bioturbated and fossiliferous chalk. Breaks in deposition are recorded by occasional, iron-stained sponge-beds. This is by far the thickest systems tract preserved in the *O. pilula* Biozone from the sections studied.

SEQUENCE Ca3

Sequence Ca3 is most accessible at Seaford Head where the most typical sequence is preserved. The onset of sequence Ca3 is marked by the development of a pair of thicker marl bands







(Rottingdean Paired Marls *sensu* Mortimore, 1986). SB Ca3 lies at the base of the lower band. The 2.5m of LmST chalk is dominated by a number of discrete marl horizons, including the Roedean Triple Marls, and the occasional dispersed flint horizon. At Culver Cliff, a planar, slightly glauconitised hardground is interpreted as representing SB Ca3. Pyrite nodules are cemented within the hardground, and flecks of pyrite are disseminated through the overlying sediment. The hiatus associated with formation of the hardground is thought to correspond to the period of deposition of the Rottingdean Paired Marls at Seaford Head. A metre above the hardground, the first of two major marl bands is recorded. These marls are correlated with the Roedean Triple Marls from Sussex. The upper of these marls at Culver was correlated with the Old Nore Marl by Mortimore and Pomerol (1997) and with less certainty by Jenkyns, Gale and Corfield (1994). REE geochemical analyses of these marls (Chapter 5) has demonstrated that such a correlation is unsustainable. The Old Nore Marl sampled from Seaford Head displays a clearly volcanogenic signature ^{whereas} whilst the horizons from Culver demonstrates a detrital signature. In the Trunch borehole, an iron-stained sponge bed is taken to represent SB Ca3. The overlying chalk is relatively unfossiliferous. A thin sheet-flint is recorded at 290.79m, and above this there are several isolated flints associated with inoceramid chips and small oysters.

At Seaford Head, the ts is placed at a minor flint band directly above the Roedean Triple Marls. Above this the main feature of the succession is the Old Nore Marl. This bentonitic

horizon (as discussed above) represents an important marker-horizon at this level across the Anglo-Paris and Anglo-Dutch Basins. The top of the TST is marked by the lower surface of the Old Nore Pair of marls (*sensu* Mortimore, 1986). At Culver Cliff, the correlative of the Old Nore Marl, a condensed section represented by a minor, glauconitised and phosphatised hardground, forms the ts. The TST comprises 2 m of chalk bioturbated by *Planolites* and *Techichnus* with flecks of disseminated glauconite and phosphate. A pronounced marl band a metre above the hardground is correlated with the Old Nore Pair in Sussex. At Trunch, a sponge bed at 287.95 metres is interpreted as the ts. This is overlain by an horizon of brachiopods, oysters and fish remains. The Old Nore Marl is recorded at the bottom of the lower quarry at Précy-sur-Oise (Figure 4.5) at the eastern end of the Pay-du-Bray Axis (Mortimore and Pomerol, 1987). The

chalk beneath this distinctive horizon is assigned to LmST Ca3 with the under-surface of the marl marking the ts. Mortimore and Pomerol (1987) suggested that the succession above the Old Nore Marl at Précý-sur-Oise was considerably attenuated, an assertion that is borne out by the sequence stratigraphical analysis herein.

At Seaford Head the mfs is placed at the bottom surface of the lower marl of the Old Nore Pair. A thin, irregular horizon of flints overlies this with a metre of white chalk forming the remainder of the HST. This level marks the onset of another period of condensation at Culver Cliff. The HST has largely been removed by erosion associated with the formation of the major hardground representing SB Ca4 at Culver Cliff. The *Planolites* and *Thalassinoides*-burrowed, lithified chalk beneath the hardground surface is interpreted as representing the HST, with the mfs placed at the lower limit of lithification 40cm below the surface. In the Trunch borehole the mfs is interpreted as being coincident with a level of core loss at a depth of 285.23 – 285.70m. Above this the succession is relatively fossiliferous and flintier than previous levels. At Précý-sur-Oise a horizon of slightly more bioturbated chalk characterised by *Planolites* is taken to represent the mfs, above which, a thin package of sponge and echinoid-rich chalk forms the HST.

SEQUENCE Ca4

Sequence Ca4 is at its most accessible and representative at Seaford Head owing to severe attenuation at Précý-sur-Oise and in the Trunch borehole. These sequences thicken into the deeper-water Culver Cliff section, though here, localised syn-sedimentary tectonic activity has accentuated condensation associated with the development of the hardgrounds in sequences Ca4 and Ca5. At Seaford Head, the base of sequence Ca4 is marked by a unit of three marl bands with the SB placed directly beneath the lowest. These are overlain by a flint band and two further marls, constituting the LmST. The lowest and best developed of the upper marls is the Peacehaven Marl *sensu* Mortimore, 1986. At Culver Cliff the LmST is interpreted to be missing, the result of condensation and erosion associated with the formation of the prominent hardground representing SB Ca4. The undulose hardground is iron-stained and contains pyrite nodules; a glauconitic and phosphatic patina coats the surface. Glauconite mineralization is evident for 8cm beneath the surface, whilst phosphate penetrates to a depth of 20cm. This hardground is more strongly developed than those preserved during sequences Ca1 – Ca3 above. A horizon of inoceramids at 283.60m marks SB Ca4 in the Trunch borehole. The thin LmST overlying this is representative of the attenuation evident at this level. This unit is not correlated with Précý-sur-Oise at the eastern end of the Pay-du-Bray Axis. Relative sea-level (see below) is interpreted as low during this sequence, and it is thought that this and the position of the Précý-sur-Oise section over a tectonically controlled palaeo-high, accentuated current activity, constantly winnowing and reworking the sediment.

At Seaford Head a sponge bed directly above the marls of the LmST marks the ts. Here the TST is interpreted to be thin, with the top marked by a second sponge bed 40cm above the first. The hardground at Culver Cliff represents a hiatus that has resulted in little preservation of TST sediments. The glauconitic patina on the hardground surface represents the ts and the reworking and glauconitisation of the clasts overlying the hardground surface is interpreted to have occurred during the TST. At Trunch an iron and manganese-stained sponge bed at a depth of 283.26m is taken to indicate the ts. The ts is overlain by a unit of relatively unfossiliferous chalk that represents the TST. The attenuation at this level is more pronounced at Précý-sur-Oise where TST Ca4 is interpreted to be missing altogether. There is no evidence indicating an hiatus or syn-sedimentary lithification, and it is thought that rates of coccolith production must have declined drastically

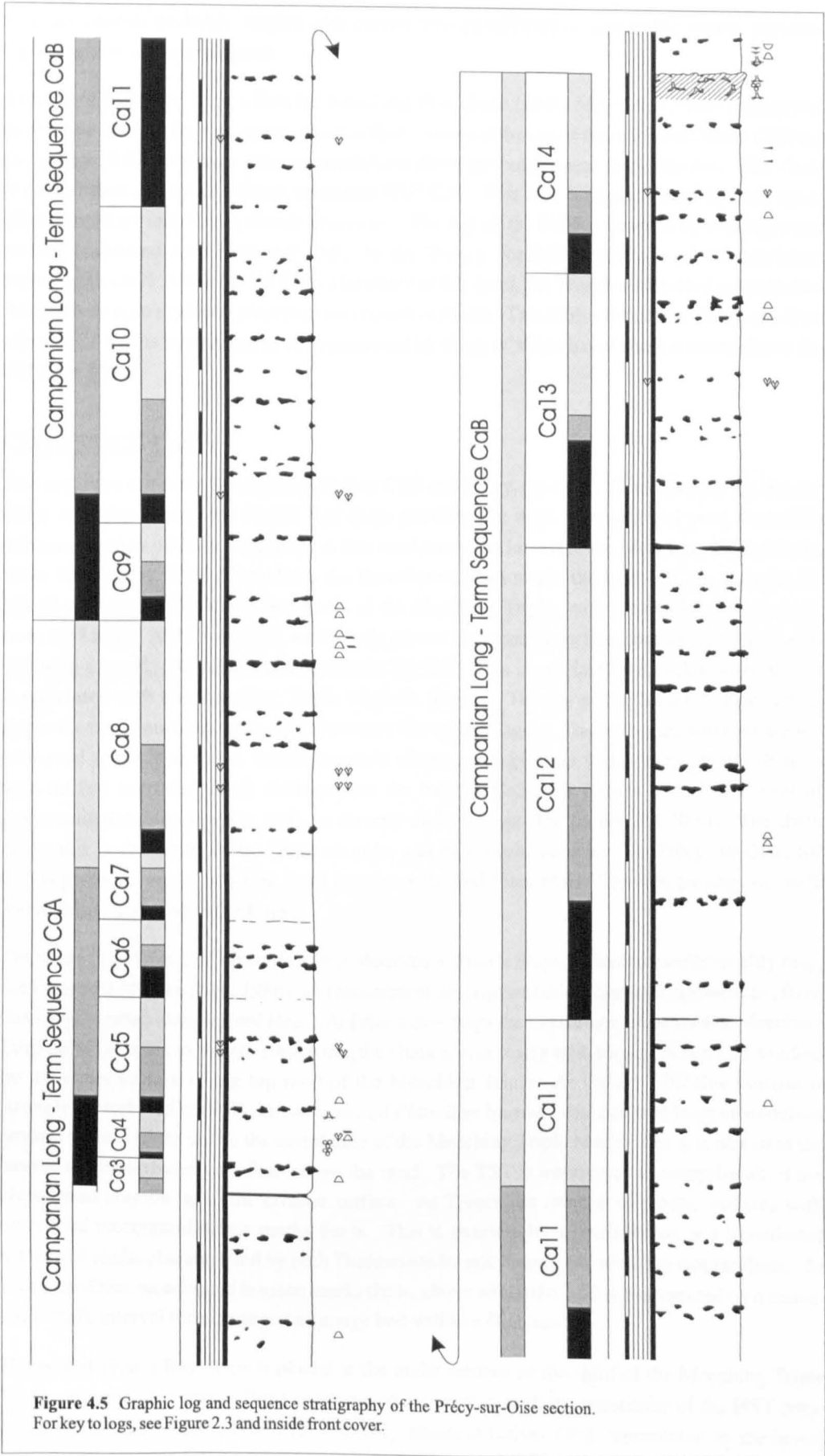


Figure 4.5 Graphic log and sequence stratigraphy of the Précý-sur-Oise section. For key to logs, see Figure 2.3 and inside front cover.

over this interval, probably coupled with current activity sufficient to agitate the waters, preventing deposition or mineralization.

At Seaford Head and Friar's Bay, the Meeching Flint Zone (*sensu* Mortimore, 1986) comprises most of the HST. A further, narrow band of flints is seen at the top of the HST. At Culver Cliff the top surface of the reworked, glauconitised clasts above the hardground marks the mfs. The 72cm of bioturbated chalk above these represents HST Ca4. This unit is characterised by dark marl-filled *Planolites* and *Thalassinoides* burrows. The top of the HST is marked by a hardground surface associated with Sequence Ca5. In the Trunch Borehole, a package of unbioturbated fossiliferous chalk marks the HST. As elsewhere at this level, the Trunch succession is attenuated though there is no evidence preserved for erosion or hiatus. This is also the case at Pr cy-sur-Oise where HST Ca4 is interpreted to be represented by 80cm of bioturbated chalk a metre above the Old Nore Marl.

SEQUENCE Ca5

This sequence is poorly developed at Culver Cliff and Pr cy-sur-Oise. Consequently the Sussex Coast at Seaford Head and Friar's Bay Steps provides the most complete and most accessible reference section of those examined. A thin marl band (the lowest of the Meeching Triple Marls, *sensu* Mortimore, 1986) 3.9m above the Peacehaven Marl marks the base of Ca5, with the SB placed at its base. The lower two marls of the Meeching Triple, with the chalk between them, form the LmST. At Culver Cliff, a relatively planar hardground surface containing pyrite nodules with a weakly phosphatic coating marks SB Ca5. This is overlain by a thick marl band that is correlated with the Meeching Triple Marls in Sussex. The top of the LmST is placed 5cm above the marl band where the chalk becomes bioturbated again. Discrete marl horizons are not preserved at this level in the Trunch borehole where a change from fossiliferous, white chalk to marl-infilled burrowed chalk distinguishes the base of Ca5. SB Ca5 is placed at a level of inoceramid debris and pyritic surfaces directly under a large flint (depth 281.10 m). The chalk above this is characterised by *Thalassinoides* and *Zoophycos* burrows. At Pr cy-sur-Oise, SB Ca5 is placed, *a priori*, at a flint band 2m above the Old Nore Marl. The thin package of chalk above this is assigned to the LmST.

The succession from Ca5 upwards is best observed at Friar's Steps, Peacehaven (for locality map, see Figure 22 of Lake *et al.*, 1988), and subsequent descriptions of the Sussex exposures are from this locality rather than Seaford Head. At Friar's Bay Steps the top surface of the middle Meeching Triple Marl is taken as the ts. Above this the chalk is less marly with the top of the TST marked by the under-surface of the top marl of the Meeching Triple. At Culver Cliff this horizon is strongly bioturbated with *Thalassinoides* and *Planolites* burrows that descend from an undulose erosion surface 65cm above the correlative of the Meeching Triple Marls. The ts is placed at the base of the bioturbated unit, 5cm above the marl. The TST is interpreted to comprise all of the bioturbated horizon up to the erosion surface. At Trunch, an interval of pyritic surfaces with associated inoceramid debris marks the ts. This is overlain by a fossiliferous and bioturbated horizon of chalk, characterised by both *Thalassinoides* and *Zoophycos* with two tabular flints. At Pr cy-sur-Oise, an echinoid horizon marks the ts, above which the TST is represented by a metre-thick chalk interval terminating at a sponge bed within a flint band.

The mfs at Friar's Bay Steps is placed at the under-surface of the third of the Meeching Triple Marls. A band of scattered flints is preserved above this, with the remainder of the HST composed of flint-free chalk. This level is largely absent at Culver Cliff, represented by the hiatus

associated with the formation of the bioturbated erosion surface. A glauconitic patina coats this surface, and is interpreted as representing the mfs. A light grey marl in-fills the burrows, contrasting with the darker grey of the LmST marl. At Trunch, a fossiliferous horizon between two tabular flints (279.83 and 278.58m) marks the mfs. Above this the chalk is characterised by *Zoophycos* and *Thalassinoides* though other than a sponge bed at 279.24 metres is ^{at 278.58m}unfossiliferous. The top of the HST coincides with a level of missing core (278.66 – 278.13m). A sponge bed within a broad flint band is taken as the mfs at Précý-sur-Oise and above this a metre of white chalk characterises the HST, terminating at an iron-stained parting.

SEQUENCE Ca6

As in the previous sequence, the best reference section is that on the Sussex Coast at Friar's Bay Steps. A more expanded succession is preserved at Culver Cliff, but this is anomalously thick as a result of tectonically-induced slumping. Mortimore and Pomerol (1997) reported that this part of the succession did not display a typical marl band succession as a consequence of slumping. The appearance of a pair of thicker, bioturbated marls (Meeching Paired Marls, *sensu* Mortimore, 1986) in the Seaford Head section marks the base of sequence Ca6 with the SB at the under-surface of the lower Meeching Marl. These marls are iron-stained and characterised by abundant *Zoophycos* and *Planolites*. The top surface of the upper marl marks the top of the LmST. At Culver Cliff, the hiatus associated with erosion surface mfs Ca5 is interpreted to have persisted through the HST, representing SB Ca6. This is overlain by a metre of chalk dominated by two thick marl bands forming the LmST. The lower marl was correlated with Telscombe Marl 1 by Mortimore and Pomerol (1997). Herein, however, they are correlated with the Meeching Paired Marls. Mortimore and Pomerol (1997) reported an horizon of flat laminae and intraclasts within their correlative of the Telscombe Marl 1. At Culver Cliff, this is a broad flaser horizon, the base marked by a 3cm thick, more concentrated, marl horizon with a similar, 9cm layer at the top. The 23cm of intermediate marly chalk contains approximately 5% glauconite and granular phosphate (250—375mm grade) and is heavily bioturbated with chalk-filled *Planolites*. Forty-three centimetres of LmST chalk are preserved above this marl. In the Trunch borehole, the missing core (depth 278.66 – 278.13m) is thought to coincide with the SB, LmST and ts of sequence Ca6. At Précý-sur-Oise, the base of a marly horizon 4.75m above the Old Nore Marl is taken as SB Ca6. This is overlain by a thin package of LmST chalk beneath a major flint band.

At Friar's Bay Steps, a metre of flintless chalk is preserved above the upper of the Meeching Paired Marls. This is interpreted as representing the TST with the ts directly above the Meeching Paired Marls. At Culver Cliff a thin lime-green, glauconitic, nodular horizon marks the ts. Above this, a package of chalk with marl bands is interpreted as indicative of a more pronounced transgressive event than seen during sequences Ca1 – Ca5. A further omission surface is recorded 84cm above this by Jenkyns, Gale and Corfield (1994). Above, flint bands reappear within the chalk after an absence during the earlier Campanian. In the Trunch borehole, the ts is interpreted to coincide with the level of core loss (depth 278.66 – 278.13m). Above this, a thin package of chalk beneath a pair of flints is thought to represent the upper portion of the TST. A prominent, broad flint band is seen at Précý-sur-Oise, and the iron-stained, sponge-rich base of this is thought to mark the ts. The 80cm of flinty chalk above the ts forms the TST.

Above the purer chalk of the TST, a broad flint horizon (110 cm) marks the HST at Friar's Bay Steps. At Culver Cliff, an horizon of *Thalassinoides*, in-filled with grey marl, is thought to represent the mfs. Above this, 2.5 m of bioturbated chalk, with a marl band just above the mfs, characterises the HST with a sheet flint preserved 80cm from the top. In the Trunch borehole, a pair of

isolated flints at 277.07m, associated with abundant fish debris and serpulids, marks the mfs whilst the HST is comprised of fossiliferous chalk. The top surface of the broad flint band at Pr cy-sur-Oise marks the mfs, with the HST composed of a thin band of white chalk terminating in a marly parting.

SEQUENCE Ca7

Sequence Ca7 is relatively condensed in all the sections except for Culver Cliff, which is preferred, therefore, as a reference section. The base of the first Telscombe Marl (*sensu* Mortimore, 1986) marks SB Ca7. The thin package of chalk between this and the second Telscombe Marl is taken to represent the LmST and the TST — the top of the ts placed, *a priori*, equidistant between the marl bands. At Culver Cliff, the correlative of Telscombe Marl 1 is an 18cm thick marl horizon that is directly overlain by a horizon of chalk pebbles and clasts within a light-green marly chalk. This slump-horizon is succeeded by 1.67m of heavily bioturbated chalk with discreet flint bands that represent the LmST. *Thalassinoides*, *Planolites* and *Chondrites* dominate the chalk, clasts of *Thalassinoides* in-fill chalk often heavily burrowed by *Chondrites*. This part of the succession is far less expanded in the Trunch Borehole where no evidence for slumping is seen. A thin marl band marks the base of sequence Ca7, with the SB at its lower-surface (depth 275.04m). At Pr cy-sur-Oise, the succession is similar to that at Trunch; 1.6m of undifferentiated chalk, divided *a priori*, above the basal marl band into LmST, TST and HSTs of equal thickness.

In Sussex, the ts in the Friar's Bay Steps succession is placed equidistant between the lower two Telscombe Marls. The thin TST terminates against the mfs represented by the under-surface of the second marl. The base of an additional marl band in the Culver Cliff succession, 1.7m above Telscombe Marl 1 marks the ts. This is overlain by a flint band, and a further, thinner marl horizon a metre above this. The latter marl is correlated with the wispy Telscombe Marl 2 in Sussex. The Trunch succession is devoid of marl, and the ts is placed at a fossiliferous horizon coincident with the base of a band of flints. The thin TST is comprised entirely of this flint band.

The base of the HST at Friar's Bay Steps is represented by the mfs directly beneath the second Telscombe Marl. This is overlain by a thin unit of chalk, capped by a narrow flint band, forming the HST. The correlative systems tract at Culver Cliff is thicker, comprising 2.55m of chalk with two flint bands. The mfs lies at the under-surface of the thin Telscombe Marl 2. In the absence of a marl band stratigraphy, the top of the flint band at 274.50m marks the mfs overlain by 1.54m of HST chalk.

SEQUENCE Ca8

Sequence Ca8 is significantly thicker than Ca4 – Ca7 in all the sections studied. The succession at Culver Cliff is preferred as the reference section owing to its relative completeness and exposure. At Friar's Bay, SB Ca8 lies at the under-surface of Telscombe Marl 3. The LmST includes a flint band and terminates at the upper surface of Telscombe Marl 4. At Culver Cliff the correlative of Telscombe Marl 3 is a thick griotte marl, 35cm thick, with a more concentrated marl at the base. The 4m of chalk with marls and flint bands above the SB comprise the LmST, distinguished by a horizon of iron-stained and glauconitic debris 1.4 m above SB Ca8. In the Trunch succession, SB Ca8 is placed at an iron-stained flint band overlain by fish debris (depth 272.96 m). This is overlain by a distinctive twin-tabular flint, in turn succeeded by iron-stained and stylolitic marly chalk forming the LmST. At Pr cy-sur-Oise a marly parting marks SB Ca8. The 1.5 m of powdery chalk and flint band above this are interpreted as representing the LmST. Gallois and

Morter (1975) placed the *O. pilula* – *G. quadrata* Biozone boundary directly below the lower tabular flint at Trunch. This biozone was tentatively placed at a level corresponding to the top of the LmST Ca8 at Culver Cliff and Friar's Bay Steps by Jenkyns, Gale and Corfield (1994) and Mortimore (1986) respectively. Mortimore and Pomerol (1987) placed it at a level at Précý-sur-Oise that corresponds to SB Ca8.

The top-surface of the correlative of Telscombe Marl 4 at Culver Cliff marks the ts at Culver Cliff. Above this, five flint bands within slightly marly chalk make up the TST. At Trunch, a sudden increase in body fossils at 269.35 metres is interpreted to represent the ts. The chalk above this is fossiliferous and partially silicified, distinguished by a conchoidal to hackly fracture. The top of the TST is marked by an iron-stained flint band at 268.20m. At Précý-sur-Oise, a prominent iron-stained sponge bed marks the ts; this is overlain by a thin package of white chalk, terminating at another sponge bed.

The fifth flint band of the TST at Culver Cliff contains a fractured sheet flint, with the mfs placed at the upper-surface of the flint horizon. The overlying chalk represents the first HST exhibiting a significant thickness in the Lower Campanian succession at Culver Cliff. Ten metres of monotonous, regularly-spaced flint bands, ^{commonly} often as complex *Thalassinoides* in-fills, dominate a marl-free HST. In the Trunch borehole the HST is thicker than the previous Campanian sequences other than Ca2. An iron-stained flint and sponge horizon at 268.20 metres indicates the mfs. Above this, the chalk is characterised by a number of flint bands, bioturbation (*Thalassinoides*, *Chondrites* and *Zoophycos*) and iron-stained sponge horizons. Above 265.89 m the clay content of the chalk increases with the HST terminating at the base of a discreet marl (depth 263.76 m). At Précý-sur-Oise the upper of two iron-stained sponge beds marks mfs. Above this, the chalk is less attenuated than in the previous sequences, and a broad band of echinoids and inoceramids is recorded towards the top of the sequence.

SEQUENCE Ca9

This sequence is well exposed and easily accessible at Culver Cliff, which is taken as the reference section. In the deeper-water sections the base of Ca9 is marked by a marl band, with the SB placed at its under-surface. At Culver Cliff, this marl is thin, its base marking the SB, overlain by 1.8m of chalk with a flint band. Above this, the chalk becomes more flint-rich. This marl is more significant in the Trunch borehole (base at depth 263.76 m), and is overlain by 1.36 m of marly and iron-stained chalk forming the LmST. The section at Précý-sur-Oise is devoid of marl above sequence Ca8, and here the top surface of the flint above the echinoid horizon is taken to represent the correlative level of SB Ca9.

The TST is less substantial across the logged sections than that of sequence Ca8, attaining a thickness of 2 m at its maximum in the Trunch borehole. A unit of marly, *Zoophycos*-rich chalk with occasional body-fossils characterises the TST at Trunch. At Culver Cliff, the lower surface of a unit of three flint bands is taken as the ts, with the TST entirely represented by the flint unit. The TST thins onto the Pay-du-Bray structural high with attenuation, compared to the other sections, evident at Précý-sur-Oise. Here some 80cm of powdery chalk above a flint band, representing the ts, pass without distinction into the HST characterised by a flint band. The mfs is placed, *a priori*, equidistant between the ts and the flint band within the HST.

At Culver Cliff, the top surface of the flints representing the TST is taken as the mfs. The 3 m of typical white chalk and regularly-spaced flint bands beneath the next influx of marl represent the

HST. In the Trunch borehole, a fossiliferous horizon (depth 259.55 m) represents the mfs. The chalk above this is more marly and poorly fossiliferous compared with that of the TST in addition to being flintier. At Précý-sur-Oise, the mfs lies equidistant between the ts and the flint band that dominates the HST. The chalk above and below the flint is soft and powdery, typical of this part of the succession at Précý-sur-Oise.

SEQUENCE Ca10

Sequence Ca10 records near-uniform depositional conditions from Norfolk, through the Anglo-Paris Basin to Paris. The Trunch borehole and Culver Cliff are representative of a typical deep-water chalk sequence, with marls characteristic of detrital input, and rhythmic flints of deeper-water transgressive and highstand conditions. Culver Cliff is preferred as a reference section for its accessibility. At Culver Cliff, the base of a 5cm thick marl, forming a distinctive notch in the cliff-profile, indicates SB Ca10. This is overlain by a thinner marl and a further 64cm of chalk above this representing the LmST. In the Trunch Borehole, an influx of marl at a depth of 257.58 metres marks SB Ca10. Here, clay minerals account for up to 50% of the sediment with some iron-staining also evident. There is a gradual decrease in clay content through the LmST to approximately 20% beneath the ts. The trace-fossil assemblage is dominated by *Zoophycos*. At Précý-sur-Oise, SB Ca10 is placed within the powdery chalk 50cm above the flint band of HST Ca9. A sponge bed, associated with small forms of *Echinocorys* (Mortimore and Pomerol, 1987), marks the upper limit of the LmST.

At Culver Cliff the flint band directly above the LmST marls is taken to mark the ts. This is overlain by 3.5 m of flinty chalk containing a marl band 127cm above the ts. At a depth of 256.40 m in the Trunch Borehole, a prominent, iron-stained hexactinellid sponge bed represents the ts. This is overlain by 4.42m of irregular and often isolated flints within a marly, fossiliferous chalk representing the TST. At Précý-sur-Oise, an iron-stained sponge-bed marks the ts, above which 2.3m of chalk with flints forms the TST.

At Culver Cliff an increase in the frequency of the flint bands above a dense burrow in-fill flint (mfs) marks the HST. The flints occur in two distinct groups in this systems tract, with the top of the lower unit marked by a sponge horizon. At Trunch, a prominent concentration of oysters at 251.98m represents the mfs, above which a 5.14m package of chalk with regularly-spaced flints characterises the HST. The lower part of the HST contains *Thalassinoides* burrows in-filled with *Zoophycos*, passing up into a creamy-white moderately fossiliferous chalk with iron-stained sponges at the top. A succession of powdery chalk with regularly-spaced flint-bands identifies the HST at Précý-sur-Oise, representing a return to 'normal' deeper-water chalk sedimentation, albeit marl-free. HST Ca10 is of uniform thickness across the sections examined.

SEQUENCE Ca11

This sequence is most typically developed in the Trunch Borehole, and best exposed at Culver Cliff. A 10cm thick, prominent marl band marks the base of Ca11, with the under-surface marking the SB, at Culver Cliff. Above this, 1.98m of marly chalk with flints represents the LmST. The influx of marl, initially as burrow in-fills, in the Trunch Borehole marks SB Ca11 (depth 246.80 m). The overlying chalk includes a sheet flint with calcite core, and a more substantial semi-tabular flint that marks the top of the LmST. A laterally impersistent flint band overlain by chalk with less-frequent, regularly-spaced flints is taken as the correlative of SB Ca11 in the Précý-sur-Oise succession.

The top surface of a prominent, burrow-fill flint marks the ts at Culver Cliff. This is overlain by a metre of chalk with a moderate marl content. Above this, a 50cm thick *Thalassinoides* flint delimits the top of the TST, the mfs placed in the centre of this flint band. In the Trunch Borehole a fossiliferous horizon immediately above the semi-tabular flint at 244.52 metres marks the ts. Above this, the chalk is moderately fossiliferous, more lithified and contains small, pyrite-filled burrows. At Précý-sur-Oise, a prominent flint at the base of a 3 m package of chalk with more closely-spaced flint bands than those recorded during the LmST marks the ts. The package of regularly-spaced flints above this represents the TST.

The HST at Culver Cliff is characterised by slightly marly, *Zoophycos*-rich chalk. The flint bands become more prominent through the systems tract, with the top surface of a broad, double band marking the top of the sequence. At Trunch the reappearance of flint bands in the succession marks the mfs at 242.97 metres, directly above a green, marly horizon with pyrites nodules. A thick unit (9.24m) of HST flinty chalk is preserved above this, with the succession becoming more marly above a depth of 238m. A slight break in the spacing of the flint bands at Précý-sur-Oise is taken to represent the base of the HST, with the mfs placed at the top surface of the more closely-spaced flints beneath.

SEQUENCE Ca12

Sequence Ca12 is the most laterally consistent across the sections studied with little variation in thickness and lithology. As with Ca11, the most lithologically typical succession is seen at Trunch, and the most accessible is at Culver Cliff. Here, the SB is placed at the upper surface of a double-flint and is overlain by 1.5m of LmST chalk, dominated by a major flint 30cm from the top. In the Trunch borehole, a closely-spaced double-flint at 233.73 – 233.45m marks the base of sequence Ca12. Heavy iron-staining between the two layers marks SB Ca12 which is overlain by marly chalk. At Précý-sur-Oise, a sheet flint at the top of a unit of chalk with regular, closely-spaced flint bands marks the base of Ca12. Above this level, the flint bands exhibit a wider-spacing, with 3 m of chalk containing two flint bands forming the LmST.

At Culver Cliff, 2 m of chalk, rich in marl-filled *Zoophycos*, marks the TST. The ts is placed at a weakly developed flint, directly beneath the *Zoophycos*-rich unit. At 232 m in the Trunch Borehole, a fossiliferous layer, marking the change from marly to purer chalk, represents the ts. The overlying chalk becomes less marly with fewer body-fossils, and towards the top of the TST, discrete flint bands reappear. At Précý-sur-Oise, the ts lies at the top surface of a prominent flint band, with a unit of flint-free white chalk forming the TST. This unit contains a broad band of echinoids, identified by Mortimore and Pomerol (1987) as *Echinocorys* c.f. *E. marginata* and *Galeola* sp, and belemnites.

At the top of the Culver Cliff TST, the main layer of a 65cm thick *paramoudrae* flint marks the mfs. This is overlain by 6 m of chalk, containing a prominent double flint band above a weakly developed marl horizon, that form the HST. At Trunch, an iron-stained, branching, tubular flint marks the mfs; this is overlain by fossiliferous chalk containing numerous manganese-coated sponges. Above, the clay content increases, concentrated in *Chondrites* burrows, whilst the fossil content decreases. Regularly-spaced flint bands characterise the succession. At Précý-sur-Oise, after an initial period of purer chalk deposition, a regularly-spaced flint succession characterises the HST.

SEQUENCE Ca13

Culver Cliff is preferred as a reference section owing to its ease of access and typical succession. Here, a marl band marks the base of the sequence, with the SB placed at the top-surface of the underlying flint-band. Two flint bands and a second, thinner marl band is preserved 1.5 m above the first. Above the marls, a further metre of flinty chalk is preserved in the LmST. In the Trunch borehole, the top-surface of an iron-stained semi-tabular flint (221.36) marks SB Ca13. A thin unit of relatively unfossiliferous chalk characterises the LmST above the flint. At Précý-sur-Oise, a prominent shattered-flint horizon (the Grey Shatter Bed, *sensu* Mortimore and Pomerol, 1987) is interpreted to represent the SB. This horizon of flint shards and chalk was interpreted by Mortimore and Pomerol to represent a plane of *décollement* associated with the formation of the hardground towards the top of the succession (SB Ca15 in this study). This horizon marks a change from regularly-spaced HST flints, to less flinty, LmST-type sedimentation.

At Culver Cliff, an iron-stained sponge-bed with associated *Thalassinoides* and *Planolites* marks the ts. This is overlain by a 1.1cm of relatively flint-free chalk representing the TST. An horizon of hexactinellid sponges at 220.54m marks the ts in the Trunch Borehole. Moderately fossiliferous chalk containing shark's teeth, fish remains, sponges and sponge-filled burrows represents the TST. At Précý-sur-Oise, the ts is placed at the underside of a broad layer of flints, with the top surface, 80cm above, marking the mfs. The TST is of fairly uniform thickness across the sections, thinning slightly onto the Pay-du-Bray Axis at Précý-sur-Oise.

A further sponge horizon characterises the mfs at Culver Cliff, overlain by 4.2m of chalk with regularly-spaced flints. The succession at Trunch directly beneath a depth of 219.37m is extremely rich in body fossils, and this level marks the mfs. Above 219.37m, the chalk is up to 50% bioturbated with marly burrows, often entrapping large foraminifera, bryozoa and bivalves. This passes up into marly chalk with occasional flints. At Précý-sur-Oise, the 4 m of flinty chalk above the ts is interpreted to represent the HST. The flint bands are less regularly-spaced than those characterising the previous HSTs. The lower band is associated with iron-stained sponges, and the upper with small *Echinocorys* (Mortimore and Pomerol, 1987).

SEQUENCE Ca14

A typical deep-water chalk sequence is preserved at Culver Cliff which is preferred as the reference section. A marl band marks the base of the sequence; this is overlain by two flint bands and a further two marls, the top one very thin. The two flint horizons are separated by a broken sheet-flint. The SB is placed at the under-surface of the lowest marl, and the ts directly above the second, prominent, marl. In the Trunch Borehole, SB Ca14 is interpreted to coincide with a level of core loss (216.56 – 216.17m). This is overlain by a flint and a further level of core loss (7cm), collectively interpreted as representing a thin LmST. At Précý-sur-Oise, this level is correlated with the lowest of three relatively closely-spaced flints, the SB placed, *a priori*, in the chalk beneath the flint, and the ts in a similar position beneath the successive flint.

The ts at Culver Cliff lies at the upper surface of the second marl band, and this is overlain by progressively less marly and more flinty chalk, preserving echinoids. A flint, 95cm above the faint marl band, is interpreted to represent the mfs. This correlates with a fossiliferous horizon (214.85m) in the Trunch borehole. An increase in preserved body fossils at 214.80m marks the ts. At Précý-sur-Oise, the ts is placed in soft chalk beneath the middle flint of a group of three, the top surface of the uppermost of these flints representing the mfs.

Above the marls and minor flints of the LmST and TSTs, the succession at Culver Cliff passes into more substantial, regularly-spaced flint bands. The mfs is placed at the top surface of the first of the more massive flints, 1.45m above the ts. At Trunch, the fossiliferous horizon at 212.85m represents the mfs, overlain by fossiliferous and flinty chalk representing the HST. At 209.14 m, a phosphatic-coated hardground-surface is recorded, overlain by a more prominent hardground with abundant marcasite. This hardground surface is taken as the *G. quadrata* – *B. mucronata* Biozone boundary (Gallois & Morter, 1975 & 1976 and Arthurton^{et al.} 1994). This correlates with the hardground in the Pr cy-sur-Oise succession, below, and the Main Downend Hardground in Hampshire (Gale, 1980; Mortimore and Pomerol, 1997). At Pr cy-sur-Oise, the top surface of a group of flints represents the mfs, and this is overlain by less flinty chalk capped by a prominent hardground 3 m above the mfs. The hardground-surface is glauconitic, with iron-staining descending down to 10cm beneath the surface. This surface is taken to represent the *G. quadrata* – *B. mucronata* Biozone boundary by Mortimore and Pomerol (1997), who link the formation of the hardground to movement along the Pay-du-Bray Axis as a result of Basin-wide tectonic realignments, causing the Downend Hardgrounds in Hampshire. They invoked a similar explanation for the condensation in the lower Campanian at Culver Cliff, though a similar lithological expression is not seen during the end *G. quadrata* Biozone at Culver Cliff.

LONG-TERM SEQUENCES

The fourteen third-order cycles of relative sea-level change stack to form two second-order cycles of relative sea-level change (Figures 4.6 & 4.7). The base of the lower sequence, CaA, is defined by the base of the Campanian Stage. This sequence equates to the whole of the *O. pilula* and the lower few metres of the *G. quadrata* Biozones. The second sequence, CaB, has its base towards the bottom of the *G. quadrata* Biozone, and extends upwards to the *G. quadrata* – *B. mucronata* boundary. CaA comprises third-order sequences Ca1 – Ca8 whilst CaB is made up of sequences Ca9 – Ca14.

SB CaA is represented by a hardground in the sections examined, coinciding with SB Ca1. The upper-third of the Santonian *M. testudinarius* Biozone in the Trunch borehole is absent relative to German sections (Arthurton^{et al.} 1994), indicative of a period of pronounced non-deposition and erosion during the end-Santonian – initial-Campanian. This coincides with a period of hardground formation, and anomalous sequences of marl bands (Mortimore and Pomerol, 1997) at Culver Cliff. LmST CaA is characterised by relatively flint-free deposition in the Trunch borehole, correlating with an highly condensed, anomalous sequence at Culver Cliff. Here a number of hardgrounds represent considerable hiatuses. In the lower part of LmST CaA, corresponding to LmSTs Ca1, Ca2 and Ca3, thick marly-units are preserved in the Anglo-Paris Basin, interpreted to represent increased erosion and run-off from terrigenous sources during lower relative sea-level. Seaford Head reflects a more typical marl-band succession, characteristic of a deep-water environment, whilst the succession at Culver Cliff is more complex, with a syn-sedimentary tectonic overprint (Mortimore and Pomerol, 1997) preserved. The LmST is relatively prolonged, ts CaA not recognised until ts Ca5. TST CaA encompasses one complete and two partial third-order sequences (ts Ca5 – mfs Ca7). Relative sea-level is interpreted to be at its highest, for the Coniacian – Lower Campanian interval, during sequence CaB. Over this interval, net relative sea-level is thought to have risen, albeit with significant fluctuations. Longer-term patterns of relative sea-level change are discussed in Chapter 6.



Figure 4.6a Graphic log, sequence stratigraphy and relative sea-level curve for Lower Campanian Long-Term Sequence A (CaA) in the Trunch borehole.

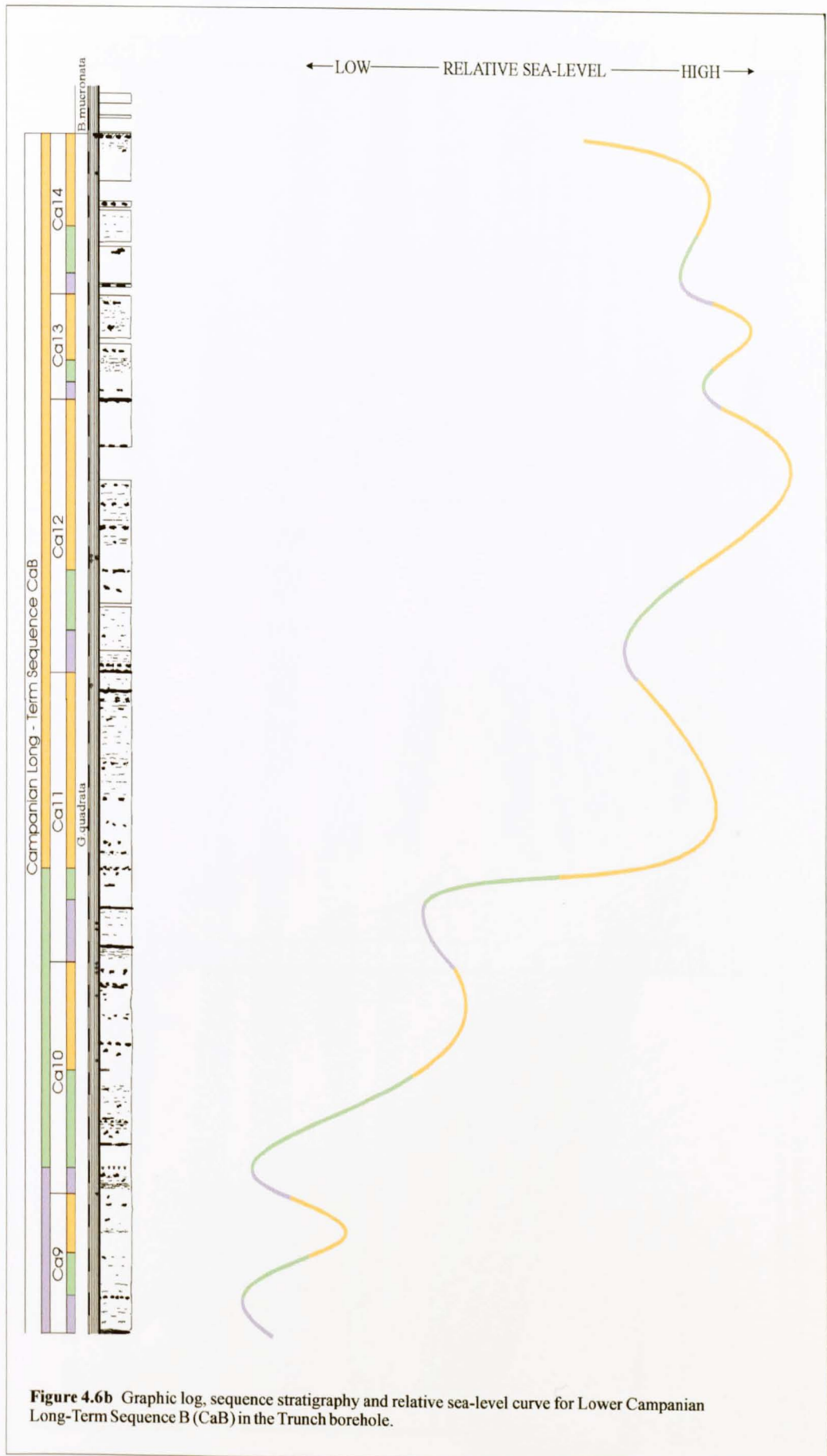
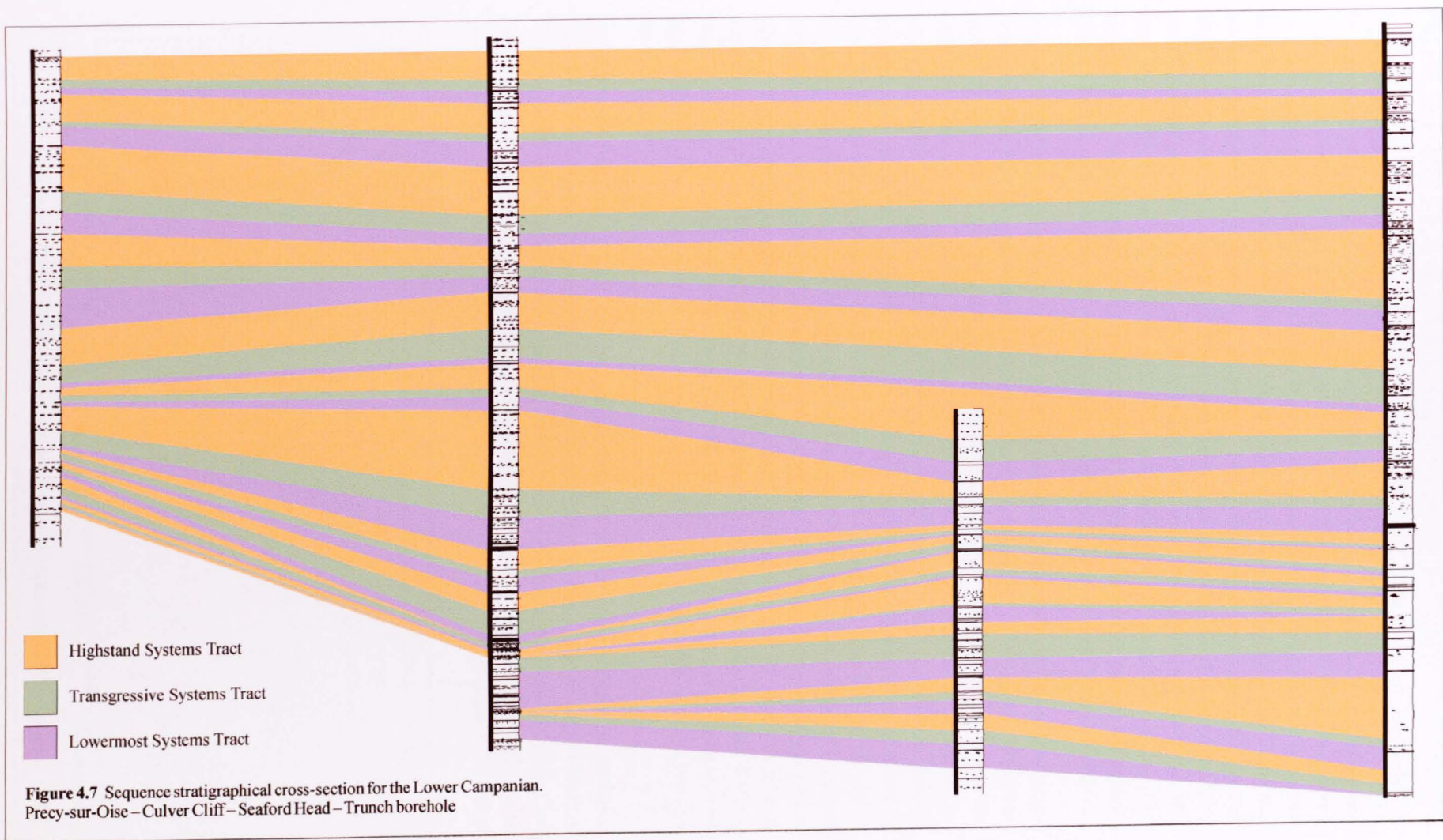


Figure 4.6b Graphic log, sequence stratigraphy and relative sea-level curve for Lower Campanian Long-Term Sequence B (CaB) in the Trunch borehole.



PUBLISHED SEA-LEVEL CURVES

A number of relative sea-level curves have been published for the ^{late} Upper Cretaceous, ^{commonly} often tied to the 'Exxon curve' of Haq *et al.* (1988). For a detailed critique of the Exxon curve, readers are referred to Hancock (1993b). Miall (1992) has also highlighted problems with the Exxon curve. As a consequence of the difficulties inherent in using the Exxon curve for comparison, it is plotted using three sets of criteria for correlation with the relative sea-level curves herein (radiometric, biostratigraphical and stage boundary), Figure 4.8. These curves show a reasonable fit with the relative sea-level data presented here. In all cases the peak in relative sea-level of sequence CaA is more exaggerated in the Haq *et al.* (1988) curve than that herein. The only variation between the three plots of the Haq *et al.* (1988) curve is in the ^{earliest} lowermost Lower Campanian at the start of sequence CaA, with the curve compared by calibrated age giving the best fit, placing the equivalent of SB CaA earlier than the curves comparing relative stage boundary and biozone positions.

Hancock (1990) reported a trough in sea level at the base of the Campanian, followed by a minor peak during the *Echinocorys truncata* Subzone. These correspond to sequence CaA. He identified another regressive trough at the base of the *G. quadrata* Biozone that correlates with the LmST of sequence CaB. Above this, using nodular chalks and hardgrounds as indicators, he found no readily identifiable regression, although a minor trough in the *G. quadrata gracilis* Subzone was tentatively suggested. This trough correlates broadly with the fall in relative sea-level, identified here, prior to the *G. quadrata* – *B. mucronata* Biozone boundary. In his global summary of eustatic changes for the Campanian, Cooper (1977) identified a number of localities world-wide that show evidence for transgression during the Cretaceous. However the resolution of his data is below that required to make any meaningful comparisons with the relative sea-level curves presented here. More recently, Hancock (1993a) has recognised cycles from the Western Interior of North America that can be correlated with those from Northwest Europe. Shanley and McCabe (1995) reported a decrease in relative sea-level in the early Campanian from the Western Interior Seaway of Utah.

Mortimore and Pomerol (1987 Figure 26) indicated a late Santonian regression that can be correlated with the SB between Sequence CaA and the preceding sequence, Sa (Chapter 3 herein). Their initial Lower Campanian transgressive – regressive cycle corresponds to Sequence CaA identified herein. They also suggested a transgressive event coincident with the *O. pilula* – *G. quadrata* Biozone boundary and another transgressive event followed by regression at the end of

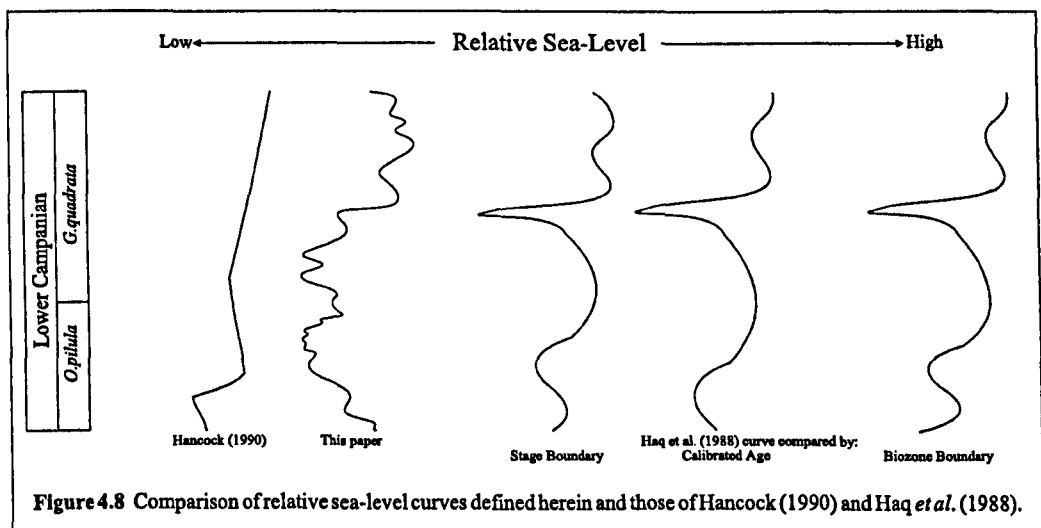


Figure 4.8 Comparison of relative sea-level curves defined herein and those of Hancock (1990) and Haq *et al.* (1988).

the *G. quadrata* Biozone. These correlates broadly with the initial transgression of Sequence CaB and the regression to the SB at the end of Sequence CaB. There is a good correlation between the relative sea-level curves presented here and those published in the literature within the constraints of correlation between the schemes.

STABLE OXYGEN AND CARBON ISOTOPE DATA

Stable oxygen and carbon isotope data are taken from Jenkyns, Gale and Corfield (1994). Values of $\delta^{18}\text{O}$ vary from -1.7 to -3‰ over Sequences CaA and CaB of the Lower Campanian interval from the Trunch borehole (Figure 4.9). During Sequence CaA an inverse relationship is seen between the $\delta^{18}\text{O}$ and relative sea-level curves. As relative sea-level falls during the early Campanian, $\delta^{18}\text{O}$ becomes less negative, rising from -2.5 to -1.8‰. During sequences Ca5 to Ca7, relative sea-level rises corresponding to a decrease in $\delta^{18}\text{O}$ values. This relationship holds true for both the third and second-order curves during CaA. During Sequence CaB, a similar relationship is observed for the third-order cycles, but this breaks down for the second-order relative sea-level curve.

During the ^{early} Lower Campanian, $\delta^{13}\text{C}$ values decrease gradually over sequence CaA to a minor negative excursion (2.1‰) during Sequence Ca9. Above this point, the long-term trend is one of gradually-rising $\delta^{13}\text{C}$, with short-term positive excursions corresponding to the third-order TSTs. This relationship between $\delta^{13}\text{C}$ and relative sea-level has been observed for the Coniacian and Santonian chalks of southern England (Chapters 2 & 3).

The inverse relationship between $\delta^{18}\text{O}$ and relative sea-level is a direct consequence of the fractionation ratio between ^{16}O and ^{18}O being dependent upon temperature. Rising temperatures result in a more negative $\delta^{18}\text{O}$ value, and a corresponding thermal expansion of the water column, hence relative sea-level rise. That this relationship holds true, over the second-order Sequence CaA, suggests that climatically controlled thermal expansion and contraction of the water column was responsible for both the short and long term changes in relative sea-level during this part of the ^{early} Lower Campanian. This pattern also holds true for the short-term sequences during Sequence CaB. However, the absence of such a clear relationship during the longer-term of Sequence CaB suggests a tectonic rather than climatic control for this second-order cycle

TECTONICS

Tectonic influences on chalk sedimentation during the Lower Campanian can be considered on two scales. Localised movements disrupt chalk sedimentation along regional fault-axes, often resulting in anomalous deposition. Global tectonic processes such as variation in the rate of spreading at the mid-ocean ridges combine with longer-term climatic trends to influence pattern of transgression – regression.

Mortimore (1986) recognised a number of periods of tectonic activity in the Culver Cliff succession that he related to the evolution of the Sandown Pericline. Subsequent work (Mortimore and Pomerol, 1997; Mortimore *et al*, in press) has built on this and linked anomalous patterns of sedimentation in the late Santonian – early Campanian to the Wernigerode phase of tectonic activity. They also recognised the Peine phase in the ^{early} Lower – ^{late} Upper Campanian interval, based upon initial observations in Germany (references in Mortimore and Pomerol, 1997).



Figure 4.9 Relative sea-level curve and stable $\delta^{13}\text{C}$ and $\delta^{18}\text{O}$ isotope data. Isotope data reproduced from Jenkyns, Gale and Corfield (1994).

The anomalous, flintless chalk and hardground complex at Culver Cliff (Sequences Sa7 – Ca5) spanning the Santonian – Campanian boundary are restricted to the eastern end of the Isle of Wight. The localisation of this pulsed tectonism allows its effects to be removed from the regional sequence stratigraphical interpretation. The Culver Cliff succession is essentially a deeper water one, occasionally showing sedimentation characteristic of shallow water during episodes of tectonic uplift. Similar patterns are seen at Beauval and Taplow where anomalous hardgrounds are preserved prior to phosphatic chalk deposition.

The mid-Campanian Peine event is characterised by a hardground in some sections — Pr  cy-sur-Oise, Culver Cliff, and Downend near Portsmouth (Gale, 1980). Condensation at this level has been widely attributed to tectonism (Gale, 1980; Mortimore, 1987; Mortimore and Pomerol, 1987, 1997; Mortimore *et al.*, in press). This event, coinciding with a longer-term fall in relative sea-level, enhanced the effects of eustatic change.

Changes in plate dynamics can be invoked as a mechanism for eustatic sea-level changes on a longer timescale. These changes take the form of variations in the rate of sea-floor spreading (Hays and Pitman, 1973) and changes in flexure, especially at passive continental margins (Watts, 1982). An increase in mid ocean ridge activity has been suggested as a mechanism for the Coniacian long-term eustatic cycle (Chapter 2 herein). A gradual decrease in ridge activity characterises the interval from the Campanian to present. Coupled with climatic change, this has resulted in modern relative sea-levels being several hundred metres lower than those of the mid – late Cretaceous. Variations in plate movement on the several million year timescale, thought to be important in terms of eustatic cycles, are below the resolution available from magnetic anomaly data prior to the Campanian, due to the long quiet zone.

DISCUSSION AND CONCLUSIONS

Fourteen third-order cycles of relative sea-level change (Ca1 – Ca14) have been identified during the ~~Lower~~^{Gault} Campanian, stacking to form two second-order cycles (CaA and CaB). Assuming a Milankovitch 400 Ka eccentricity control for the short-term cycles, as suggested for the Coniacian and Santonian (Chapters 2 & 3), Sequence CaA has a duration of 3.2 Ma and CaB 2.4 Ma. This combined duration of 5.6 Ma agrees closely with the Gradstein *et al.* (1995) figure of 5.5 Ma for the Lower Campanian.

The inverse relationship between the third-order cycles of relative sea-level change and $\delta^{18}\text{O}$ suggest that thermal expansion and contraction of the water column, resulting from climatic variation brought about by the Milankovitch 400ka eccentricity cycle, is the underlying controlling mechanism. A similar mechanism has also been suggested as the major control of sedimentation and cyclicity within the Coniacian and Santonian successions, though here the relationship between relative sea-level and $\delta^{18}\text{O}$ was positive, controlled by the effects of evaporation on a salinity-stratified ocean (Chapters 2, 3 & 6).

The direct relationship between relative sea-level change and stable isotope curves (Figure 4.9) holds true during second-order cycle CaA which is interpreted as being due to a cycle of climatic warming and cooling, linked to the establishment of an ocean circulation system in the late Santonian (Chapters 2, 3 & 6 herein), superimposed upon wider-scale plate tectonic movements (Barron, 1986; Srivastava and Tapscott, 1986; Roest and Srivastava, 1991; Wei, 1995; Guiraud and Bosworth, 1997)

During ^{deposition of} sequence CaB, this relationship is less clear. Short-term fluctuations in relative sea-level are matched by corresponding changes in $\delta^{18}\text{O}$, but the long term pattern of relative sea-level change is not followed by the $\delta^{18}\text{O}$ curve. This suggests that whilst temperature fluctuations remain the short-term control on relative sea-level as a result of thermal expansion and contraction of the water column, in the long term it is not a factor. Tectonism is inferred to control the observed changes. During the mid-Campanian, evidence for transgression has been recorded from European, American, African and Indian successions (Hancock and Kauffman, 1979; Hancock, 1990, 1993a). Hancock and Kauffman (1979) argued that the synchronicity and location of the changes strongly indicated an eustatic change, further demonstrated by Hancock (1993). As climate can be ruled out as a mechanism for this change during Sequence CaB, mid-ocean-ridge activity must be considered. The early Campanian is regarded as a period of increased tectonic activity, with a significant, short period of compression at the Santonian – Campanian boundary, followed by more prolonged extension in the Campanian of Africa (Guiraud and Bosworth, 1997).

Chapter 5

Geochemistry

ABSTRACT

Forty-six marl bands from the Coniacian to Lower Campanian of southern England have been examined using geochemical analytical techniques to determine whether they are of volcanic or detrital origin. The results are compared to similar studies from the literature. Analysis by ICP-MS is found to be an effective technique in isolating volcanogenic marls from the chalk whilst analysis by XRD and XRF techniques is inconclusive.

The geochemical results are employed to resolve specific problems of correlation and strengthen the sequence stratigraphical analysis. In association with Chapters 2,3,4 and 6, the data are used to draw wider conclusions regarding volcanism and relative sea-level changes in the ^{Late}Upper Cretaceous oceans.

INTRODUCTION

The general mineralogy of the coccolith-rich chalks from the Upper Cretaceous strata of the Anglo-Paris Basin is well known, with typical compositions given by Hancock (1975), Figure 5.1 herein. The Coniacian to Lower Campanian chalks typically contain regularly-spaced bands of chert. A consistent feature of the chalk is the occurrence of clay minerals concentrated into marl bands; levels where the non-carbonate fraction may be as high as 40%. Many of these marl bands can be traced for hundreds and even thousands of kilometres (Mortimore, 1986) and correlated using wire-line log signatures (Mortimore & Pomerol, 1987). Localised stratigraphic horizons such as hardgrounds are often characterised by phosphatic and glauconitic mineralization. Iron-staining of hardground surfaces is also common, and may also be associated with sponges and

	<i>M. coranguinum</i> Zone, Coniacian	<i>M. testudinarius</i> Zone, Santonian	<i>M. cortestudinarium</i> Zone, Coniacian	<i>G. quadrata</i> Zone, Campanian
SiO ₂	1.15	0.50	0.66	2.50
Al ₂ O ₃	0.021	0.14	0	0.37
Fe ₂ O ₃	0.06	0.05	0.02	0.91
MnO	0.03	0.03	0.033	0.031
MgO	0.25	0.33	1.26	0.50
CaO	54.75	54.96	53.26	52.80
Na ₂ O	0.04	0.16	0.87	0.03
K ₂ O	0.04	0.03	0.074	0.229
P ₂ O ₅	0.09	0.08	0.317	1.529
CO ₂	43.67	43.85	—	—
(CaCO ₃)	98.22	98.55	—	—
Total	100.29	100.13	56.58	58.91

Figure 5.1 Typical chalk compositions. *M. coranguinum* and *M. testudinarius* Biozone values are from Hancock, 1975 (Table 1, Numbers 5 & 10). The *M. cortestudinarium* Biozone sample is from the Parlour Hardground, Langdon Stairs, Kent. The *G. quadrata* Biozone sample is from the hardground at Pr cy-sur-Oise, France. Values as per-centages.

flint bands. Individual pyritic nodules are also found at certain stratigraphic intervals. Phosphatic chalks (>5% P_2O_5) also occur at spatially and temporally localised levels within the basin. These have been studied in detail by Jarvis (1980a, 1980b & 1992) who recorded levels of phosphate of up to 25% at Beauval (Figure 1.1).

Several papers have been published on the geochemistry of marl bands from the chalk in recent years. Gale and Wray (1993) attempted to characterise these horizons by element ratios, plotting the results to define characteristic fields for each marl band. This was then used to suggest correlations, though the technique was later shown to be unreliable (Gale, 1996). Clays of volcanic origin — bentonites — provide useful marker horizons throughout the stratigraphical column; a result of their unique character, widespread distribution and rapid deposition. Bentonitic marls have been identified within European chalk successions by Pacey (1983), Wray (1995) and Wray and Wood (1995) and in the United States by Izett, (1981). Wray (1995) used marl rare earth element (REE) profiles, normalised to a shale standard, to distinguish bentonitic marls from detrital ones.

The marl bands from the Coniacian to Lower Campanian chalk have been analysed in this study to aid the sequence stratigraphical analysis and to improve correlation between sections. In the sequence stratigraphical model, marl is used as an indicator of lower relative sea-level and increased run-off; consequently the identification of bentonites is essential in order to avoid distorting the sequence-stratigraphical interpretation.

EXPERIMENTAL PROCEDURE

Samples were left to air-dry for a period of weeks, subsequently being crushed using an agate pestle and mortar. Cleaning between samples was achieved using de-ionised water. After drying at between 101 and 104 °C in an oven, powders were placed in sample bags and left to cool. These powders were then used for XRD, XRF and ICP-MS analysis.

XRD

Powdered samples were reacted with weak (10%) HCl to remove the bulk of the carbonate component prior to analysing the clay minerals. The residues were collected and oven-dried at between 101 and 104 °C. Smear slides were prepared by settling the powdered sample through methylated spirits on a glass slide. After the slides had air-dried, they were analysed using a Philips PW1130 X-ray Generator / Diffractometer assembly (operating parameters listed in Figure 5.2).

XRF

Several grams of powdered sample were mixed with Morviol glue and compressed to make rock discs. These were analysed with a Philips PW1400 XRF machine using peak and background intensity measurements. This was conducted using the Philips X41 software package and international standards (operating parameters listed in Figure 5.2). Some samples were re-examined after having been treated with ethylene glycol, used to forcibly expand the lattice spacing of 'swelling' clays.



XRD:

Philips PW1130 2kV x-ray generator / diffractometer assembly

Ni filtered Cu radiation (40kV, 30Ma)

Rotation speed: $1^\circ(2\theta) \text{ min}^{-1}$ **XRF:**

Philips PW1400 3kW x-ray fluorescence machine

Rh x-ray tube (80kV, 30Ma)

Analysis by Philips X41 software package utilising international rock standards

ICP-MS:

Perkin Elmer Sciex Elan 6000 inductively-coupled plasma mass spectrometer

Perkin Elmer Software v2 utilising international rock standards

Plasma conditions:

Power: 1100 W

Temperature: 6000 K

Sample introduction:

Cross-flow nebuliser

 1 ml/min^{-1}

Optimisation:

Double charged species <1%

Oxides <3%

Figure 5.2 Operating parameters
for the analytical machines.

ICP-MS

After powdering and drying, 0.1g +/- 0.001g of sample was transferred into a clean teflon vial. 2ml of Aristar HNO₃ were added and allowed to react with the sample. Subsequently, 4ml of Aristar HF were added to each sample. The vials were then left on a hotplate at 130 – 150°C for twenty-four hours. After being allowed to cool, the vials were replaced on the hot plate, without their lids, allowing the solution to evaporate. This process was halted prior to the sample oxidising and the samples were left to cool. Another 1ml of Aristar HNO₃ was added to the vials, and the samples evaporated again as before. The process was repeated with a further 1ml of HNO₃. After cooling, 2.5ml of Aristar HNO₃ was added to each vial, and topped up with 10 – 15ml of de-ionised water. The vials were returned to the hot plate at 130 – 150°C for thirty minutes and allowed to cool. 1.25ml of internal standard was added to each sample which was then transferred to a 50ml polypropylene volumetric flask. After all the sample had been transferred, the flask was made up to 50ml with de-ionised water. After these procedures the solution comprised the sample diluted to 50ml in 3.5% HNO₃ with internal standards at 50ppb. The solutions were diluted with 3.5% Aristar HNO₃ to a ratio of 1:10 immediately prior to being run on the ICP-MS. This procedure gives a 5000-fold dilution of the original rock sample.

The REE data have been chondrite-normalised to allow ready interpretation of the profiles observed. The data have also been normalised to the Cody Shale (United States Geological Survey standard SCo-1) to allow direct comparisons to be made with the Wray (1995a & 1995b) data.

REE APPLICATION

Rare earth elements preserved within the clay minerals of marl bands are invaluable in provenance studies. Though the compositions of lanthanides in minerals are controlled largely by 'crystallo-chemical' factors, they are also greatly influenced by changes in geological environment (Fleischer & Altschuler, 1969). REE profiles of minerals resulting from continental weathering have been shown to exhibit significant similarities (Haskin *et al.*, 1966). During transportation from source to depositional environment many of these elements remain reasonably inert. However, as there is a progressive reduction in the ionic radii of the REE with increasing atomic weight, the heavy rare earth elements (HREE) may be preferentially taken-up by some minerals. Authigenic clays are affected by the REE profile of sea-water which is distinctly different from that of oceanic sediments (Wildeman & Haskin, 1965). Sea-water is characterised by lower proportions of the lighter rare earth elements (LREE) than is the case for a composite shale. The abundance of Ce in sea-water is especially low and it is preferentially extracted from sea-water by its oxidation to the 4⁺ state (Wildeman & Haskin, 1965).

Clay minerals from volcanogenic ash predominantly exhibit the REE profile reflecting their source composition, dominated by a negative Eu anomaly when chondrite-normalised (Izett, 1981). A negative Eu anomaly is not characteristic of shales because of the homogenising effects of erosion and transportation prior to deposition (Haskin & Gehl, 1962). Though the REE are generally free from interference effects, both Ce and Eu may become affected by fractionation relative to the other REE during pre-depositional transportation (Jarvis, 1988). If clay minerals are exposed to sea-water for extended periods of time, they may begin to assimilate the sea-water REE profile. Murray *et al.* (1992) suggested a sub-division of depositional water depth based upon the degree of assimilation suggested by the REE profile.

In a brief review of the application of REE studies, Wray (1995) concludes that the REE profiles of clay minerals from the chalk may originate from three sources — their original profiles reflecting detrital or volcanogenic source, those resulting from carbonate and marine-sourced minerals, and those that have been altered by their interaction with the marine environment.

Jarvis and Jarvis (1985) analysed a number of international standard sediments using ICP-MS and concluded that SCo-1 (Cody Shale) was a good standard to use for normalising sedimentary data. They argued that data normalised to SCo-1 was more readily interpreted than data normalised to an averaged composite shale.

RESULTS

XRF AND XRD

The XRF procedure was used to determine major and minor elemental analyses for samples of white chalk and lithified hardground chalk with the aim of distinguishing between weak phosphatisation and mild iron-staining where not clear in hand specimen. These data are incorporated in the graphic logs for the Coniacian, Santonian and Lower Campanian (Appendix B) and are not reproduced here. Major and minor element data were also used to aid the correlation of marl bands between benches in Shoreham Cement Works Quarry over the late Turonian interval as a test of the potential for this technique as a correlation tool. Over this localised geographical area, absolute elemental values provided a useful correlation tool, though it is unlikely that this technique is viable over increased distances. These are not reproduced herein.

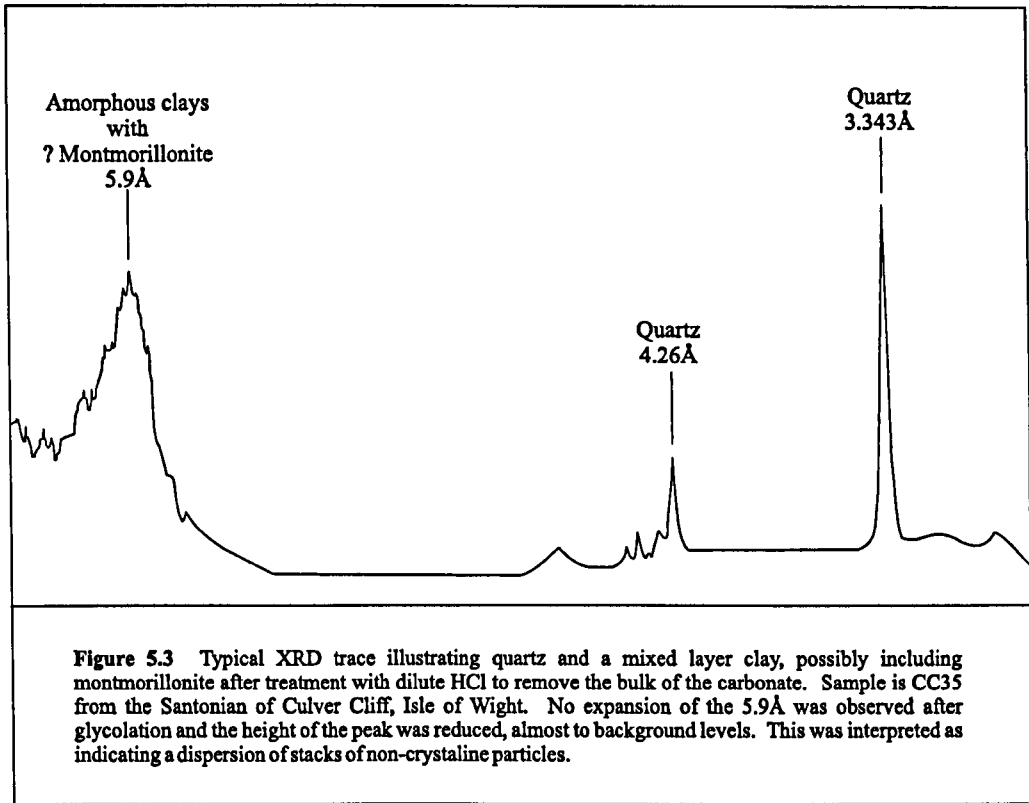


Figure 5.3 Typical XRD trace illustrating quartz and a mixed layer clay, possibly including montmorillonite after treatment with dilute HCl to remove the bulk of the carbonate. Sample is CC35 from the Santonian of Culver Cliff, Isle of Wight. No expansion of the 5.9Å was observed after glycolation and the height of the peak was reduced, almost to background levels. This was interpreted as indicating a dispersion of stacks of non-crystalline particles.

XRD was used in an attempt to distinguish clay minerals that would suggest a volcanic rather than detrital origin, and to isolate a sample set for initial ICP-MS analysis. The XRD results proved inconclusive. Peaks indicating mixed-layer clays were identified (e.g. Figure 5.3), though some of these were only weakly defined. The more prominent ones were treated with ethylene glycol and re-examined. After glycolation, many of the peaks disappeared, indicating the original peaks were the result of clumping together of the amorphous clays to indicate spuriously a mixed-layer clay (e.g. Figure 5.4). In other samples, expansion was evident, but this was not indicative of a particular clay mineral that could be associated with an originally volcanogenic origin such as smectite or montmorillonite. There was no discernible mineralogical pattern linking the marl bands that field evidence suggested might be of volcanic origin. Equally, the ‘suspected’ bentonites identified from field observation were not distinguished from the ‘suspected’ detrital marls. The

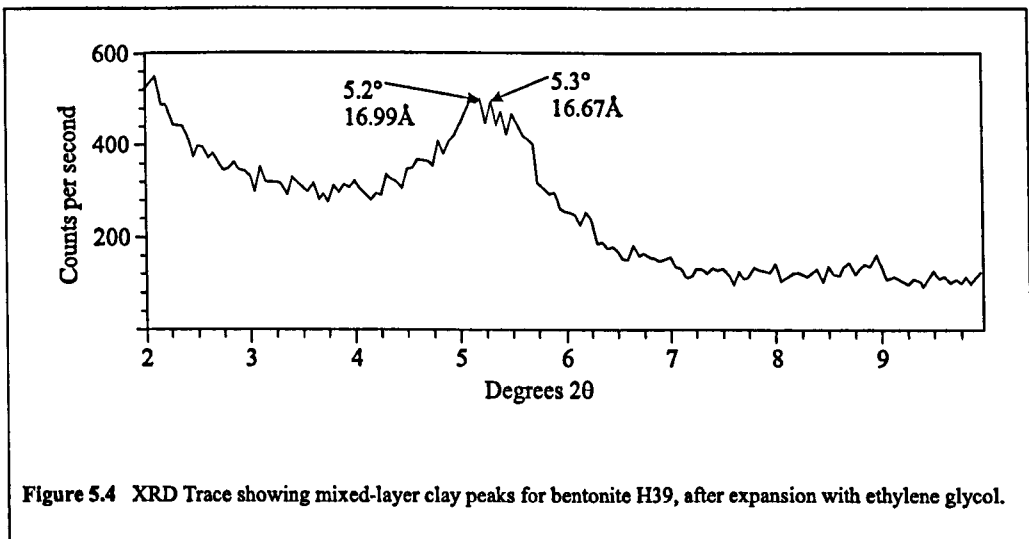
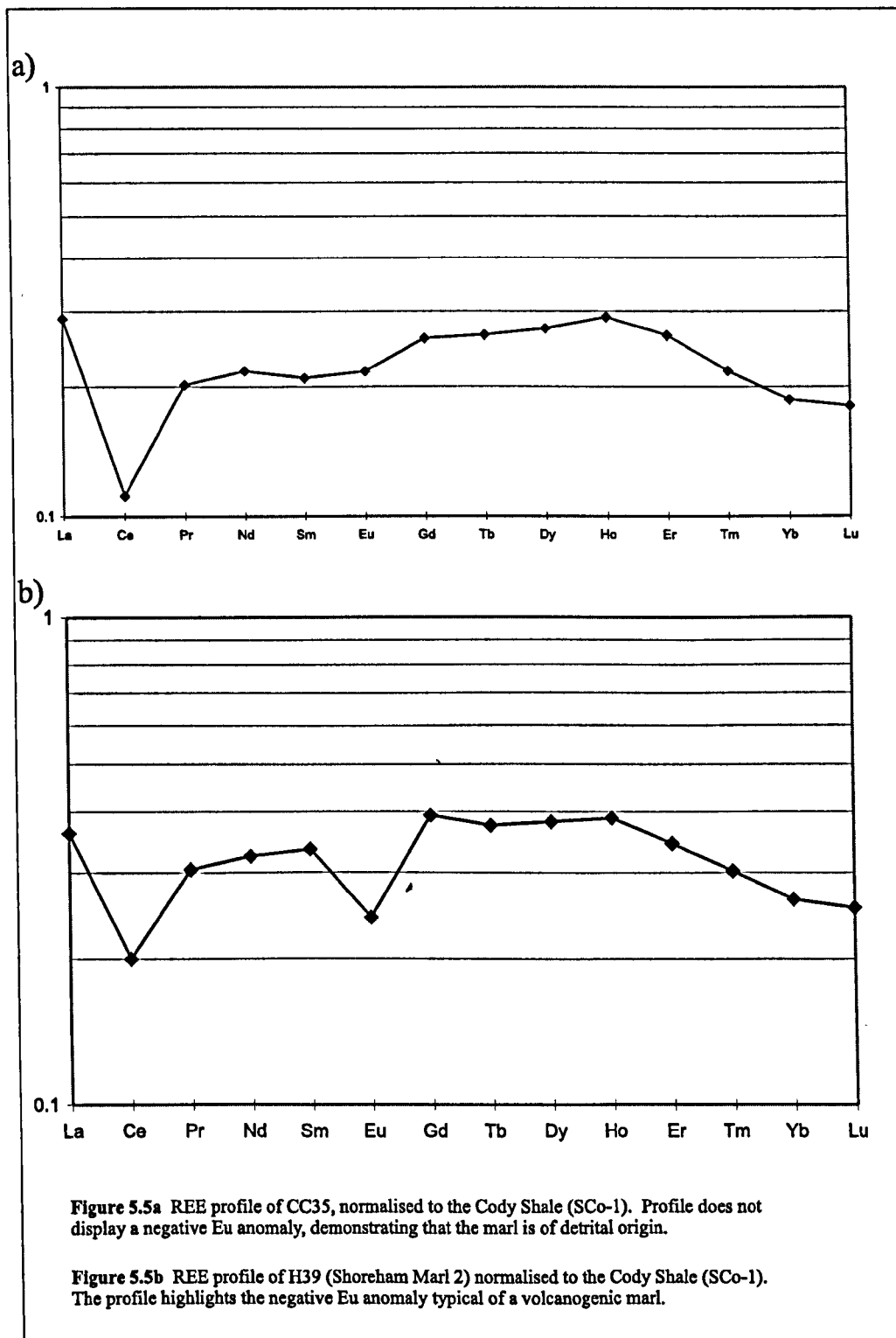


Figure 5.4 XRD Trace showing mixed-layer clay peaks for bentonite H39, after expansion with ethylene glycol.

results obtained here follow those of Wray (1993) in indicating the unreliability of XRD data for the conclusive differentiation between bentonitic and detrital marl bands from the European Cretaceous chalks.



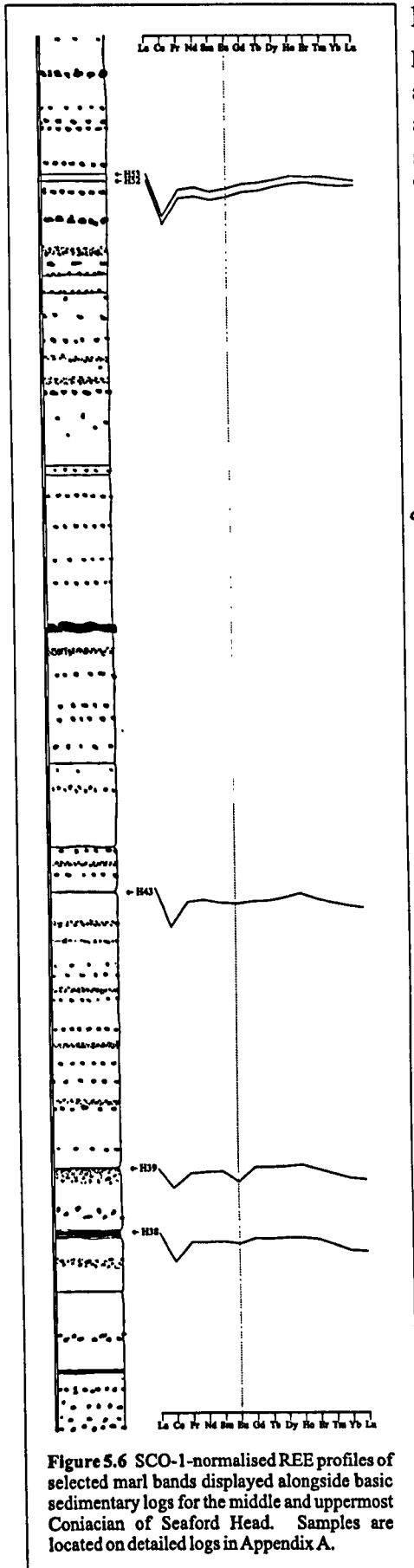


Figure 5.6 SCO-1-normalised REE profiles of selected marl bands displayed alongside basic sedimentary logs for the middle and uppermost Coniacian of Seaford Head. Samples are located on detailed logs in Appendix A.

ICP-MS

Forty-six marl bands from the Coniacian, Santonian and Lower Campanian of southern England were analysed. Of these, two were found to have REE signatures characteristic of a volcanogenic origin. These were samples H82, the Old Nore Marl from Seaford Head and H39, Shoreham Marl 2 from Seaford Head. All the marl bands of the Santonian – Lower Campanian condensed section of Culver Cliff were analysed and all were found to be detrital. All the samples analysed in this study exhibit REE profiles with a negative Ce anomaly when normalised to SCo-1. This contrasts with the Turonian-age samples analysed by Wray (1993) that were not characterised by this anomaly. Work on the Coniacian marls of eastern England (Wray, unpublished abstract, BSRG Dublin, 1996) has also shown a negative Ce anomaly, which Wray explained as being related to increased levels of phosphate in the Coniacian. This and other interpretations are discussed below. The SCo-1 shale-normalised REE profiles are shown alongside sedimentary logs in Figures 5.5a – 5.13. Chondrite-normalised plots are included in Appendix C.

DISCUSSION

Of forty-six marl bands analysed, only two exhibited bentonitic REE profiles. This indicates a probable reduction in volcanic activity during the Coniacian – ^{Early} ~~Lower~~ Campanian, compared with the earlier Cretaceous (Pacey, 1983; Wray, 1995 and Izett, 1981). The two marl horizons identified as bentonites herein are H39 and H82 from the Seaford Head succession. The bentonite commonly found at the *M. cortestudinarium* – *M. coranguinum* Biozone boundary, Shoreham Marl 2 (H39 herein, East Cliff Marl 2 in Kent and Little Wheeton Marl in eastern England) has been correlated in the literature across the main sections of the Anglo-Paris Basin, and into the Anglo-Dutch Basin at Trunch. The Old Nore Marl (a bentonite, sample H82 herein) is a major marker horizon in the Lower Campanian, recognised across a wide geographical area. It is known from Sussex (Mortimore, 1986 and Mortimore & Pomerol, 1987), the Trunch Borehole (Morter & Gallois 1975 & 1976), Precy-sur-Oise, (Mortimore & Pomerol,

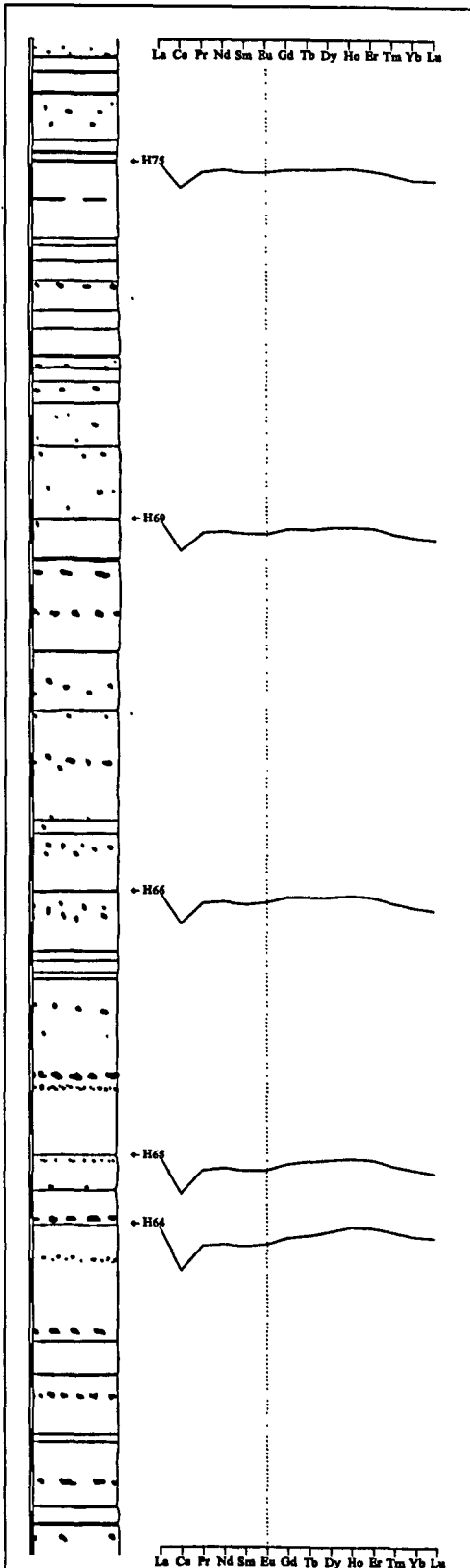


Figure 5.7a SCo-1-normalised REE profiles of selected marl bands displayed alongside basic sedimentary logs for the Lower Campanian of Seaford Head. Samples are located on detailed logs in Appendix A.

1987) and has been reported at Culver Cliff (Mortimore & Pomerol, 1997). The Old Nore was also tentatively placed in the Culver Cliff succession by Jenkyns, Gale and Corfield (1994). The ICP-MS analyses examined in this study show that the Old Nore Marl is not in fact preserved at Culver Cliff. Mortimore and Pomerol (1997) constrained the timing of the hardgrounds in the condensed zone by macrofossil assemblages, and presumably positioned their Old Nore Marl as a consequence of this and of its prominence in the cliff section. The marl band that they correlated with the Old Nore corresponds to samples CC56 and CC104 in this study, exhibiting a clear, detrital profile.

None of the Lower Campanian marls from Culver Cliff analysed in this study display bentonitic

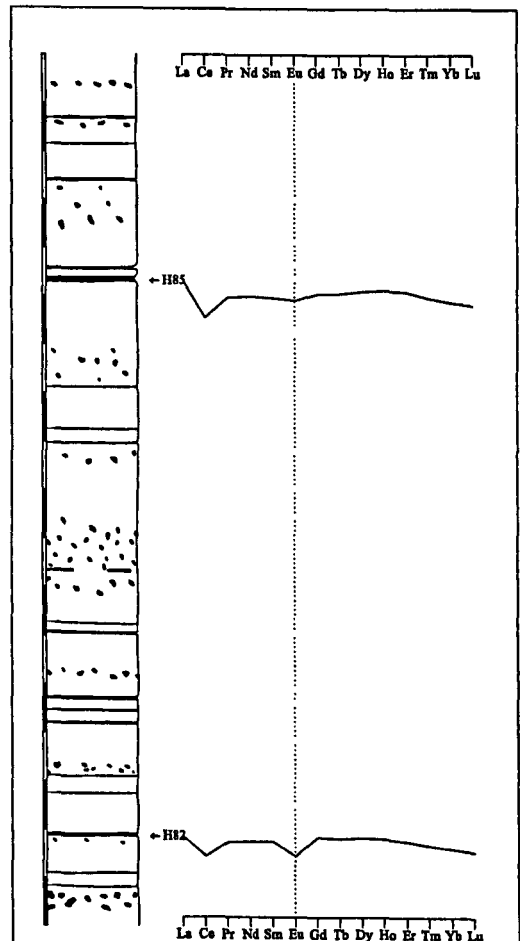


Figure 5.7b SCo-1-normalised REE profiles of selected marl bands displayed alongside basic sedimentary logs for the Lower Campanian of Seaford Head. Samples are located on detailed logs in Appendix A.

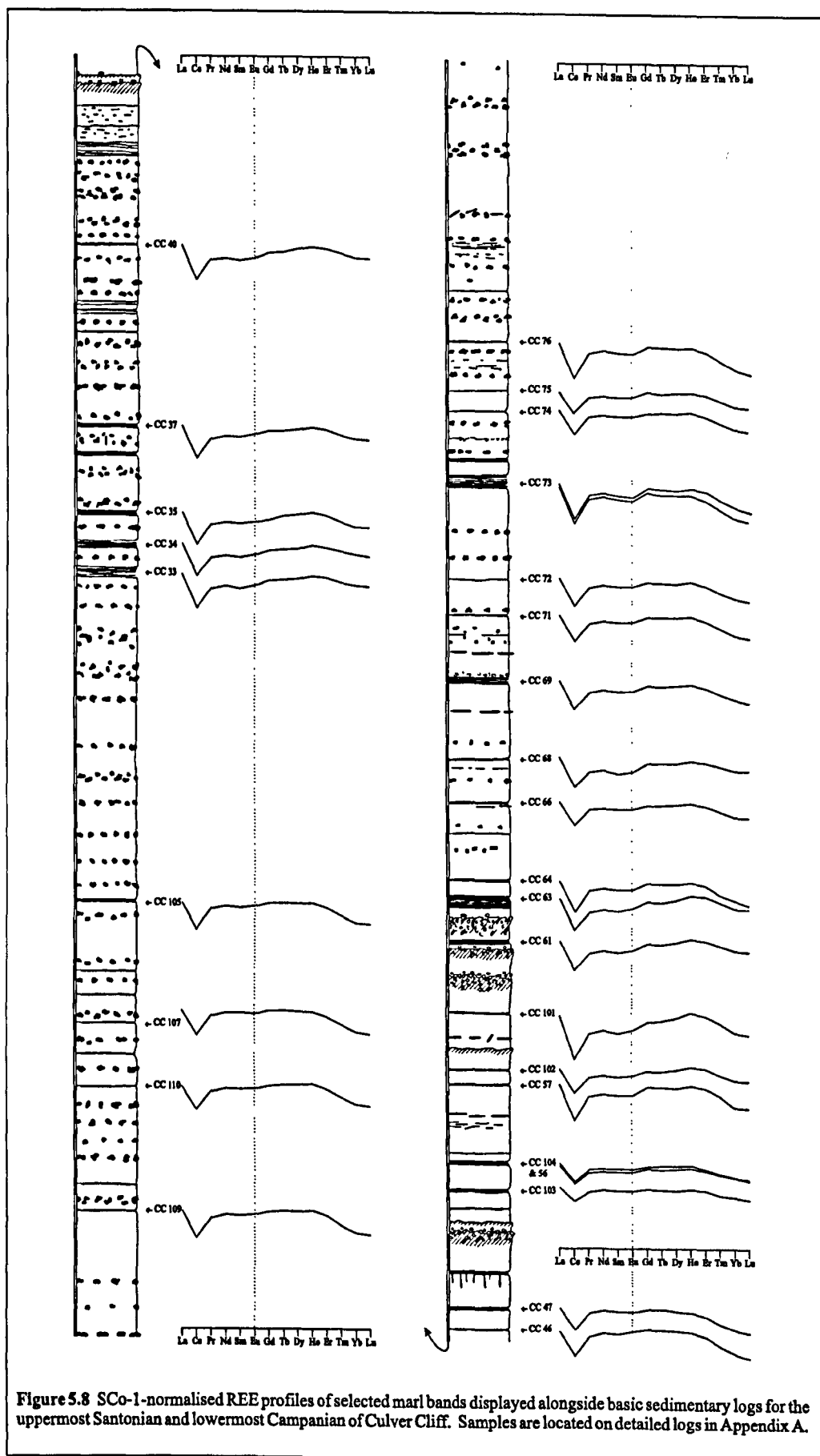


Figure 5.8 SCo-1-normalised REE profiles of selected marl bands displayed alongside basic sedimentary logs for the uppermost Santonian and lowermost Campanian of Culver Cliff. Samples are located on detailed logs in Appendix A.

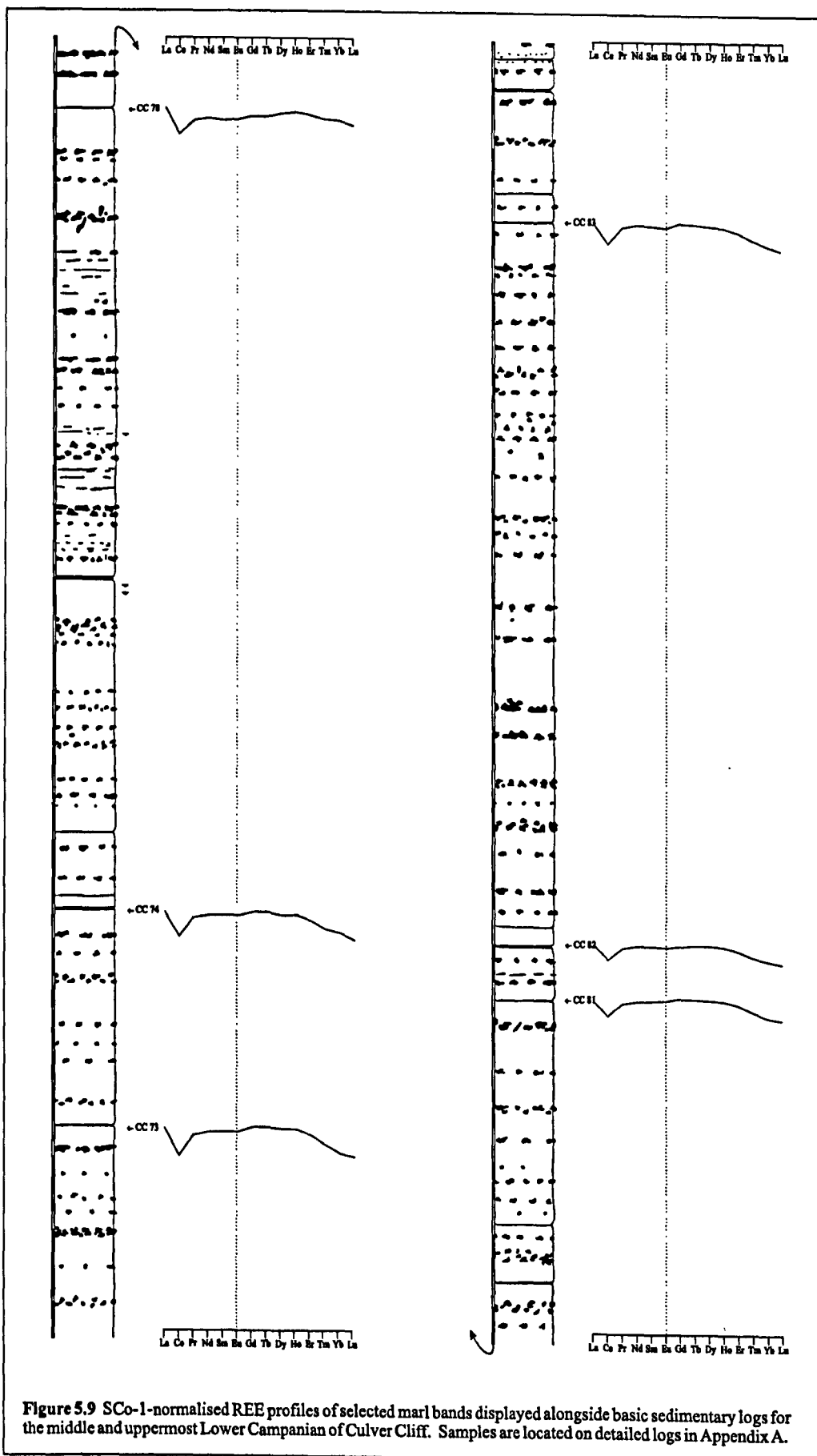


Figure 5.9 SCo-1-normalised REE profiles of selected marl bands displayed alongside basic sedimentary logs for the middle and uppermost Lower Campanian of Culver Cliff. Samples are located on detailed logs in Appendix A.

characteristics, and the conclusion reached herein is that the Old Nore Marl is not preserved at Culver Cliff, presumably having been removed by erosion associated with the development of one of the hardgrounds. From Mortimore and Pomerol's (1997) biostratigraphic data and from the graphical correlation cross-plots herein, the hardground three metres above the prominent marl band CC56/CC104 (Figure 5.8) is suggested to correspond to the stratigraphical level of the Old Nore Marl in the Culver Cliff succession.

Wray (pers. com.) suggested that the negative Ce anomaly displayed by his Coniacian marl bands from eastern England was the result of increased levels of phosphate in the sediment — samples from the Turonian do not display this anomaly. Murray *et al.* (1992) detail variations in the REE signature of cherts which they believe to be the result of differences in the exposure times of these samples to sea-water and ocean-bottom interactions. They identified a number of characteristic sea-water signatures for oceans of varying size, illustrative of deposition after progressively increased distances from source. The SCo1-normalised REE patterns in this paper match those for Murray *et al.*'s (1992) cherts from an 'Atlantic-type' open ocean. These environments are characterised by small ocean basins, wide continental shelves and high levels of terrigenous input. Here, detrital clay minerals were in contact with sea-water for sufficient length of time to allow the sea-water REE profile to start to overprint the original 'continental-weathered' profile. The REE profiles from the Turonian (Wray 1995 and Wray & Wood, 1995) match Murray *et al.*'s (1992) for a continental margin depositional environment. Murray *et al.* (1992) highlight the process of oxidation with a change from Ce (III) to Ce (IV), and an overprinting of the sea-water profile on terrigenous-profile as Ce is depleted. During the Turonian it is probable that the clay minerals were not in contact with the sea-water for a sufficient length of time prior to deposition for their 'continental weathering' profile to be distorted. The increased influence of more of an open-ocean circulation from Coniacian-times fits the upwelling-model of Jarvis (1980a) as a generating mechanism for the Santonian and Campanian phosphorites deposited over structural highs in the Anglo-Paris Basin.

In addition to negative Eu anomalies in SCo-1 and chondrite-normalised REE profiles, simple scatter-plots can be used to discriminate between detrital and volcanogenic marls. Figures 5.10 and 5.11 reinforce the usefulness of a negative Eu anomaly by discriminating between the two end-members using the Eu/Eu* ratio. This is a simple calculation of the Eu anomaly, comparing the chondrite-normalised Eu value to chondrite-normalised Sm and Gd. Ratios of selected other elements may be used, as seen in Figures 5.12 and 5.13. Here, the Ti/Zr ratio is used to separate the volcanogenic marls from the detrital. In Figure 5.12, Sr is used to spread the data along the x-axis, and in Figure 5.13 Th is used for this purpose. The two bentonites have a lower Ti/Zr ratio than the detrital marls.

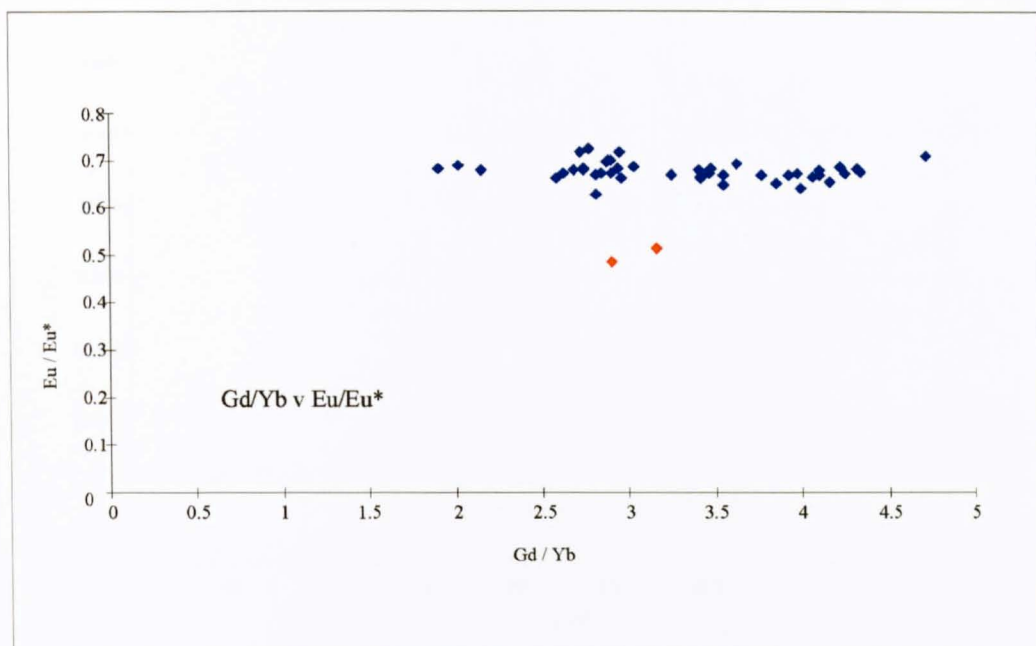


Figure 5.10 Plot showing ratio of Gd/Yb against Eu/Eu*. The two bentonitic samples may be identified by their lower Eu/Eu* ratios and are plotted in red.

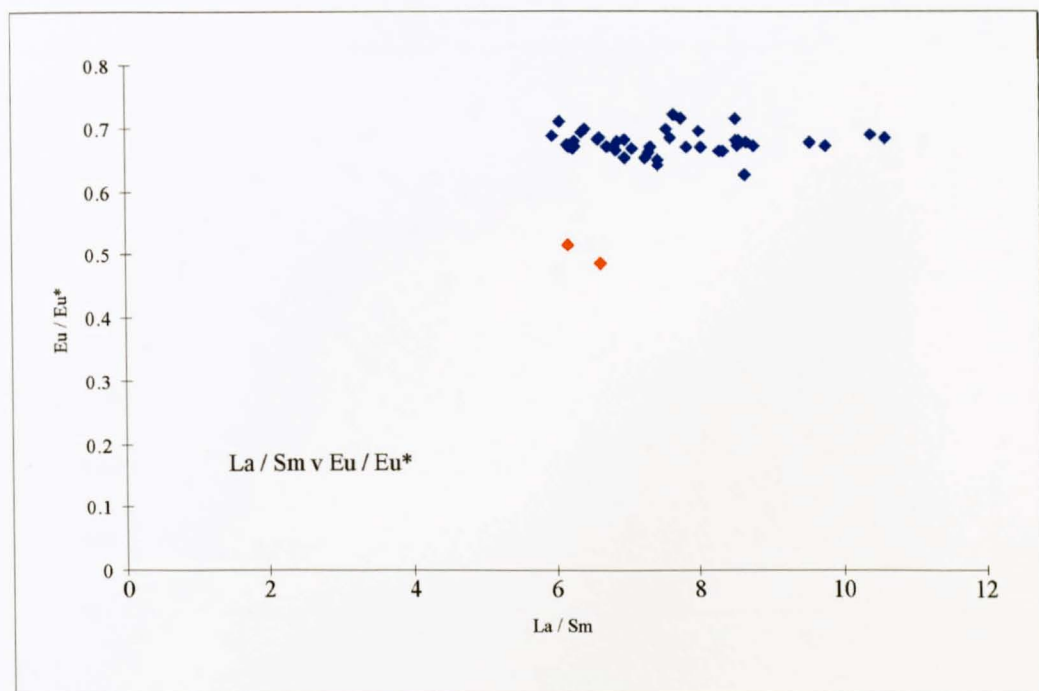


Figure 5.11 Plot showing ratio of La/Sm against Eu/Eu*. The two bentonitic samples may be identified by their lower Eu/Eu* ratios and are plotted in red.

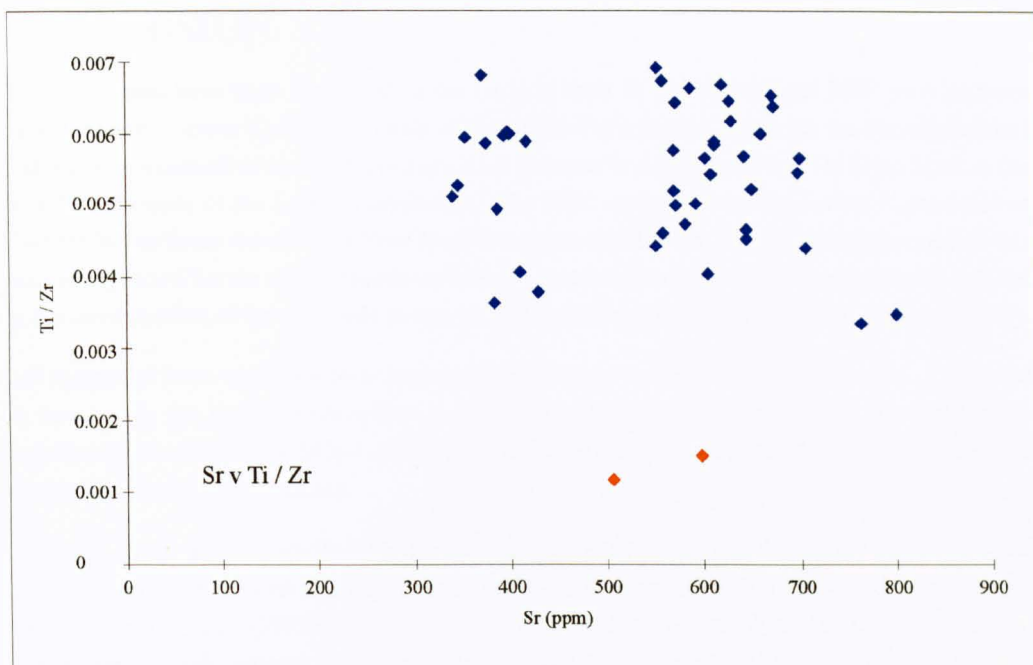


Figure 5.12 Plot showing ratio of Sr against Ti/Zr. The two bentonitic samples may be identified by their lower Ti/Zr ratios and are plotted in red.

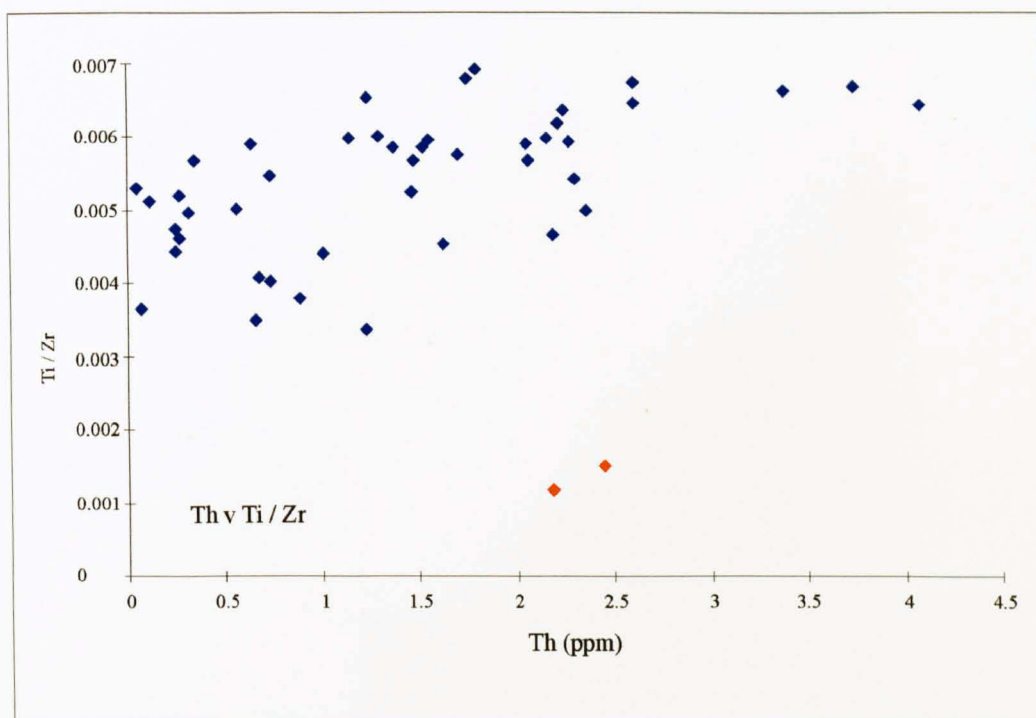


Figure 5.13 Plot showing ratio of Th against Ti/Zr. The two bentonitic samples may be identified by their lower Ti/Zr ratios and are plotted in red.

CONCLUSION

Two bentonites have been identified on the basis of their SCo-1-normalised REE profiles from the Coniacian – Lower Campanian chalk of the Anglo-Paris Basin. These are the Shoreham Marl 2 at the *M. cortestudinarium* – *M. coranguinum* Biozone boundary and the Old Nore Marl in the *O. pilula* Biozone of the Lower Campanian. The REE analyses from the Lower Campanian at Culver Cliff indicate that the Old Nore Marl is not preserved there. The localised absence of this marl is explained herein as a consequence of erosion associated with the tectonic activity that led to the development of hardgrounds in this part of the succession (Mortimore & Pomerol, 1997).

It is suggested that a combination of increased exposure to the sea-water (Murray *et al.*, 1992) and an increase in the levels of phosphate in the sediment (Wray, pers. com.) can account for the negative Ce anomaly in the SCo-1-normalised REE profiles of marl bands derived from the strata above the base of the Coniacian.

Sequence stratigraphical analysis has revealed a relative sea-level rise during the Coniacian, and a subsequent more sudden rise during the middle-Santonian. The data presented here coupled with the Murray *et al.* (1992) ocean-basin model and REE data from Wray (1993) and Wray and Wood (1995) lends support to this interpretation. This deepening of the oceans resulted in a drowning of marginal landmasses, and increased distances between terrigenous source and depocentre, prolonging contact between detrital clay minerals and the sea-water. Increased current-reworking associated with transgression is thought to have delayed deposition, further prolonging clay – sea-water interactions, enhancing the effects of increased levels of phosphate to increase the negative Ce anomaly.

Chapter 6

Conclusions

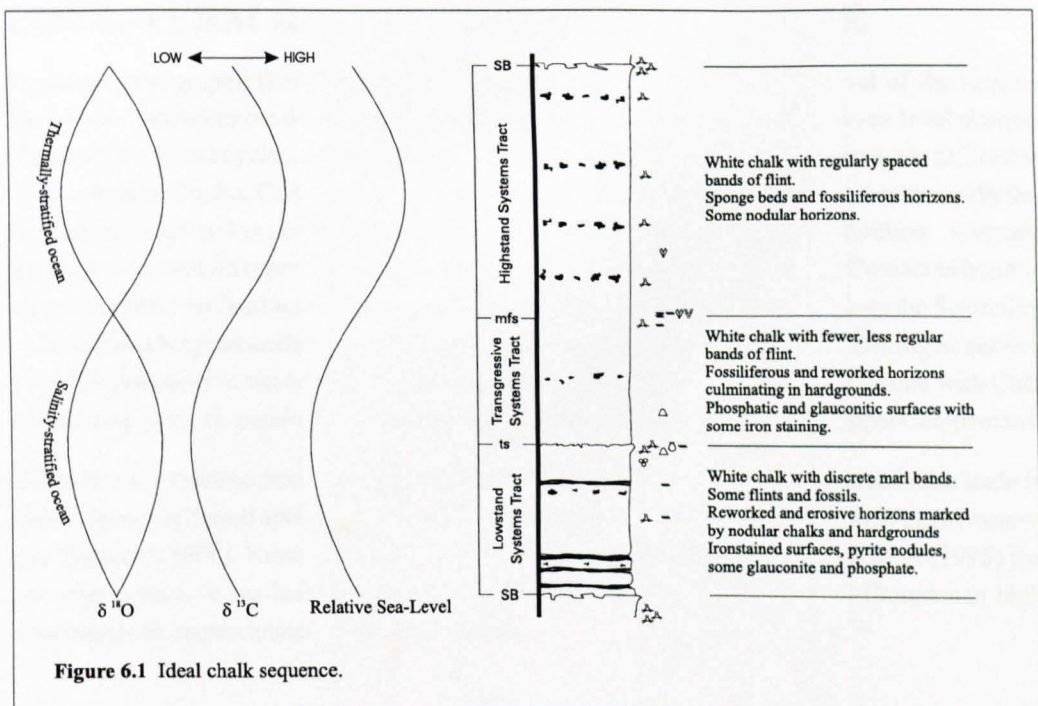
INTRODUCTION

This chapter summarises the research presented in Chapters 1 – 5, and considers some of its wider implications with regard to ^{Upper} Cretaceous climate. Longer-term changes in relative sea-level and stable oxygen and carbon isotope data are assessed and discussed in the light of established ocean state models. Previous chapters have established a model for interpreting pelagic and hemi-pelagic chalk successions in terms of sequence stratigraphy and have presented a sequence stratigraphical framework for the Coniacian – Lower Campanian chalk of the Anglo-Paris and the English part of the Anglo-Dutch Basin. This analysis has enabled the elucidation of a relative sea-level curve. The sequence stratigraphy and relative sea-level curves have been compared with independently-derived stable oxygen and carbon curves (Jenkyns, Gale & Corfield, 1994) to establish the underlying causal mechanisms responsible for the observed trends. The data indicate that the controlling mechanisms have not remained stable, and that changes in the relationship between the data variables suggest that the changing mechanisms are a function of dynamic ocean – atmosphere interactions.

SEQUENCE STRATIGRAPHICAL MODEL

A sequence stratigraphical model is proposed for the Coniacian – Campanian chalk-dominated successions of the Anglo-Paris Basin, Figure 6.1.

During periods of lower relative sea-level, the sequence boundary (SB) in proximal settings is usually defined by a hardground surface that passes into nodular chalk basinwards. The lowermost systems tract (LmST) is characterised by an influx of marls, representing increased terrigenous erosion and run-off, associated with increased exposure. Deposition may be rapid, with associated slumping and sliding arising from slope instability. Bands of chert may be preserved during slower, more prolonged deposition, but are often localised. During periods of higher long-term relative sea-level, the SB may be far less pronounced, often only represented by a hardground or



nodular chalk over structural highs and on the basin margins. Consequently, the SB is a correlative conformity. This is placed, *a priori*, at the base of the lowest marl band where present, or at the base of a unit of unfossiliferous, flint-free chalk overlying characteristic Highstand Systems Tract (HST) deposits, described below.

Hardground and nodular chalk lithologies are also characteristic of higher energy environments and winnowing as the basin margins are flooded and also mark the transgressive surface (ts) in marginal sections and over structural highs. Transgressive surface hardgrounds are often more fossiliferous than those at SBs and may be characterised by phosphatic and glauconitic mineralization, usually associated with less-prominent iron-staining compared to SB hardgrounds. In deeper-water sections, the ts is often represented only by a fossil lag, or reduced clay content represented by a decrease in, or cessation of, discrete marl band preservation. A succession of nodular chinks, representing successive transgressive pulses, may punctuate the transgressive systems tract (TST). The TST is generally more fossiliferous and less marly than the LmST. Chert bands are more common than in the LmST since their occurrence is directly related to bioproductivity and punctuated relative sea-level rise. Pauses in deposition lead to periods of stability at the redox boundary up to a few metres beneath the sediment – water interface (Clayton, 1986) allowing the precipitation of silica.

The maximum flooding surface (mfs) is more discrete than other sequence stratigraphical key surfaces, in both distal and proximal settings. The most characteristic feature of the base of the highstand systems tract (HST) is a change to regularly-spaced flint bands, characterising the deeper-water part of the sequence. The mfs, hard to define in chalk successions, is sometimes represented by a fossiliferous horizon, commonly an iron-stained sponge bed. In some shallow-water sections, especially over tectonically-active structural highs, a winnowed hardground or a glauconitic patina on the hardground surface is taken to represent the mfs. Marl horizons may be preserved in the HST owing to reduced current-winnowing and increased detrital input associated with the commencement of a fall in relative sea-level (Owen, 1996).

LONG-TERM RELATIVE SEA-LEVEL CURVE

Sequence stratigraphical analysis of the Coniacian – Lower Campanian interval of the Anglo-Paris Basin has led to the definition of twenty-nine third-order cycles of relative sea-level change (Figure 6.2). These cycles, average duration 400ka, stack to form four longer-term, second-order cycles, termed Co, Sa, CaA and CaB. Sequence Co, duration 3.2 Ma, largely coincides with the Coniacian Stage and is succeeded by the Santonian Sequence (Sa), 2.8 Ma duration. Overall, Sequences Co and Sa represent a rise in relative sea-level, from the Turonian – Coniacian boundary to the end of the Santonian. Sequence CaA marks a fall in relative sea-level from the Santonian – Campanian Stage boundary to early in the Campanian *G. Quadrata* Biozone. During Sequence CaB, overall relative sea-level is interpreted to rise through the *G. quadrata* Biozone with CaB terminating at the *G. quadrata* – *B. mucronata* Biozone boundary (base of the Upper Campanian).

Differences in relative sea-level (Figure 6.2) are intended to be relative, and no absolute scale is given. However, based upon estimates made by Hays and Pitman (1973), Pitman (1978), Srivastava and Tapscott (1986), Knott, Burchell, Jolley and Fraser (1993) and Cande and Kent (1995) the increase in relative sea-level between the basal Coniacian and the late Lower Campanian high may equate to approximately a hundred metres.

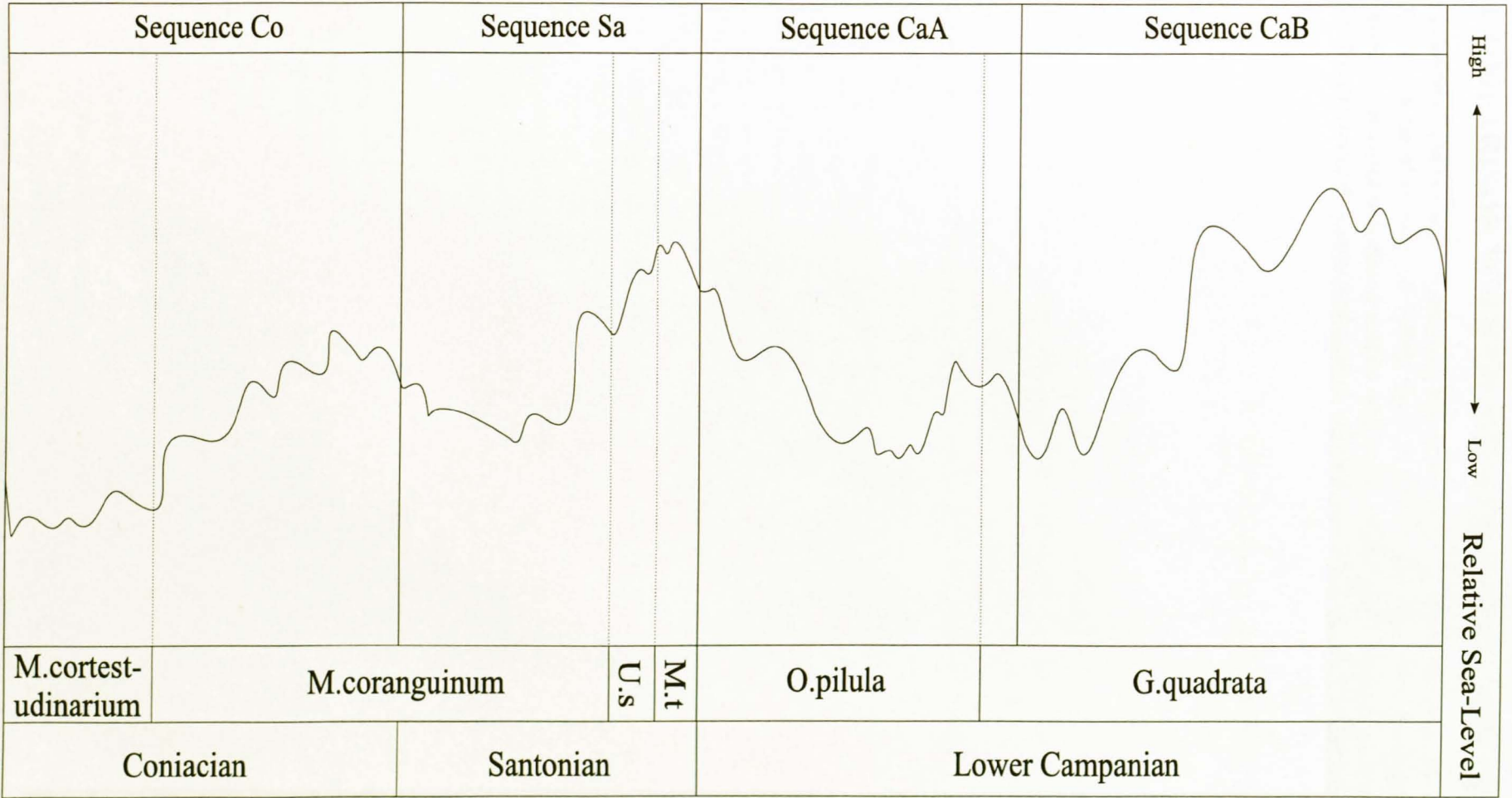


Figure 6.2 Relative sea-level curve for the Coniacian–Lower Campanian. Values are relative, but no absolute values are assigned.

COMPARISON WITH OTHER SEA-LEVEL CURVES

A number of relative sea-level curves have been published for the Upper Cretaceous, often tied to the 'Exxon curve' of Haq *et al.* (1988). Hancock (1993b) argued that there are considerable problems associated with this curve and consequently with subsequent, dependent correlations. Miall (1992) tested the Exxon curve against a randomly generated succession, and found at least a 70% fit, though this disregards variations in the magnitude of relative sea-level changes. He concluded that any correlation with the Exxon curve would invariably succeed, and as such, was pointless. Nonetheless the Exxon work has inspired considerable research into global, eustatic sea-level changes and the relative sea-level curves presented here are considered in the light of the Exxon curve for interest. However, because of the difficulties inherent with the Exxon curve's radiometric, biostratigraphical and stage boundary data, the latter has been replotted for each of the criteria to allow direct comparison to be made using these criteria as the tie-points (Figure 6.3).

When the Haq *et al.* (1988) curve is considered using the position of stage boundaries, the two curves show the opposite during the Coniacian, with the winnowed and condensed lower part of the Coniacian being interpreted as relatively high sea level, followed by a decrease in sea level corresponding to the transgression of Sequence Co identified herein. When the Haq *et al.* curve is considered using calibrated age and then biozone boundary as the tie points, the situation is

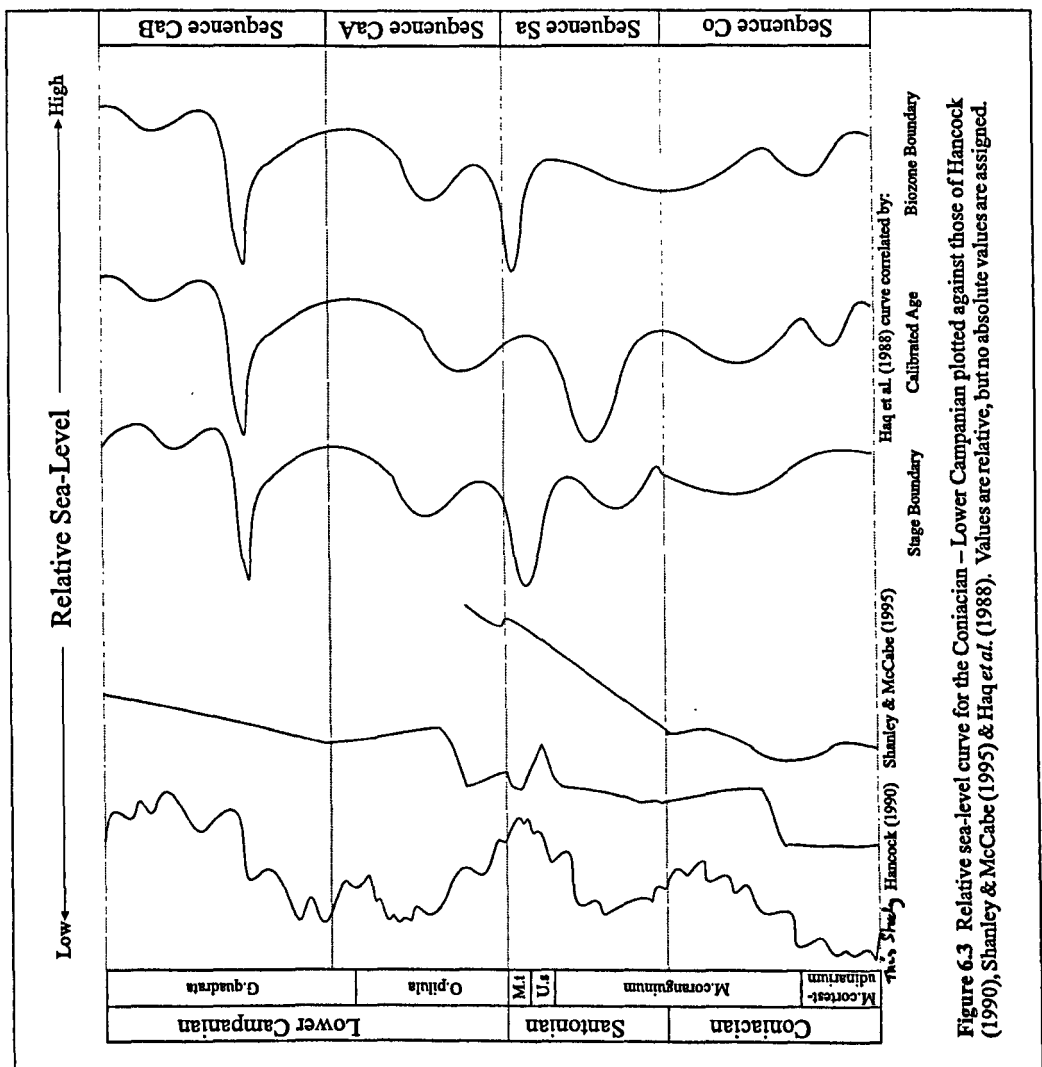


Figure 6.3 Relative sea-level curve for the Coniacian – Lower Campanian plotted against those of Hancock (1990), Stanley & McCabe (1995) & Haq *et al.* (1988). Values are relative, but no absolute values are assigned.

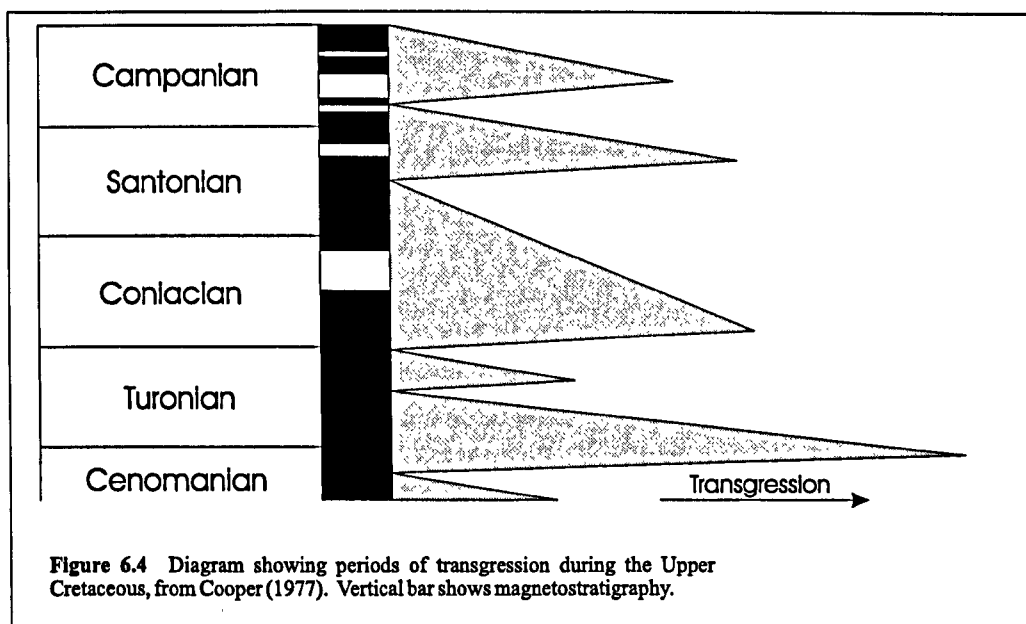
slightly different but the poor correlation between the curves remains. During the Santonian, the comparison by stage boundary produces a closer fit than for the Coniacian, but this is restricted to the lower Santonian, with a regressive low-point in sea level corresponding to the HST of Sequence Sa, herein. However, the fit during the Santonian based upon calibrated age and biozone boundaries is much closer (Figure 6.3).

There is less internal discrepancy between the Haq *et al.* (1988) curves when plotted by stage boundary, calibrated age and biozone boundary during the ~~Lower~~ ^{early} Campanian. The fit between the stage boundary and calibrated age curves and the relative sea-level curve presented herein is reasonable. The decrease in relative sea-level associated with the LmST of CaA is reflected by a similar decrease in sea level in the Haq *et al.* chart. The TST and HST of CaA is matched by a more significant increase in sea-level in the Haq *et al.* curve, not recording a regressive low-point until the TST of CaB in this analysis. The curve herein compares favourably with the Haq *et al.* curve in recognising the late Lower Campanian as a period of high relative sea-level (HST CaB).

Hancock (1990 — Figure 11) constructed a sea-level curve using hardgrounds and nodular chinks as indicators of regressive 'troughs', i.e. low sea-level. This approach is not dissimilar to that used herein with regard to the identification of sequence boundaries. However, the formation of nodular chinks and hardgrounds during some transgressive events, as recognised herein, means that the Hancock (1990) curve requires a degree of modification. Similarly, the 'sea level highstand' is not necessarily placed equidistant between regressive troughs as was the case for Hancock's curve, allowing the definition of asymmetrical relative sea-level curves.

Hancock's (1990) curve is plotted against the relative sea-level curves presented herein in Figure 6.3. He indicated a relative lowstand during the early-to-mid Coniacian, with a mid-to-late Coniacian transgression terminating in another relative lowstand at the beginning of the Santonian, similar to the base of Sequence Sa proposed herein. The early Santonian relative sea-level is higher than that of the early Coniacian. Shanley and McCabe (1995 — Figure 22), working on the Kaiparowits Plateau of Utah have suggested a sequence boundary at the base of the Coniacian, with a subsequent sequence boundary towards the end of the stage (Figure 6.3). A transgressive event precedes a significant sea level rise during the Coniacian. Cooper (1977) lists a number of localities world-wide that indicate the Coniacian is generally transgressive.

In the Santonian, Hancock (1990) recognised a significant peak during the mid *U. socialis* Biozone characterised by relative sea-levels higher than in the previous Cretaceous. The *U. socialis* Biozone peak corresponds to the highest Santonian relative sea-level identified herein. Cooper (1977) lists the localities world-wide which indicate a mid-Santonian transgression. One can interpret his global data-set in terms of a sequence boundary at the Coniacian-Santonian boundary, a prolonged LmST, and a rapid mid-Santonian transgression culminating in a sequence boundary at the top of the Santonian (Figure 6.4). Additionally, in Poland (Marcinowski, 1974) and in Libya (Barr, 1972) Santonian sediments onlap, resting unconformably on Turonian rocks as they do in the Southwest Anglo-Paris Basin (Jarvis and Gale, 1982). The base of the Dessau Limestone in Texas (Young, 1963 reported in Cooper, 1977) is unconformable with the underlying rocks, and this unconformity may correlate with the basal Santonian sequence boundary (SB Sa) defined herein. Jeletzky (1971) reported that the mid-Santonian was strongly transgressive, and represented the maximum extent of the Cretaceous Sea in the Canadian Western Interior Seaway. More recently, work on the Western Interior Seaway of North America by Shanley and McCabe (1995) has also identified a relative sea-level rise that is coincident with the Santonian stage. These suggested sea-level fluctuations during the Santonian tie-in closely with those of Sequence Sa presented here.



Hancock (1990) reported a regressive trough at the base of the Campanian, followed by a minor peak during the Subzone of *Echinocorys truncata*. These correspond to Sequence CaA. He identified another regressive trough at the base of the *G. quadrata* Biozone that correlates well with the LmST of Sequence CaB. Above this, using nodular chalks and hardgrounds as an indication of regression, he found no readily identifiable regression. However, he tentatively suggested a minor trough in the Subzone of *G. quadrata gracilis* that correlates broadly with the fall in relative sea-level, identified here, prior to the *G. quadrata* - *B. mucronata* Biozone boundary. Shanley and McCabe (1995) report a trough in the early Campanian from the Western Interior Seaway of Utah. In his global summary of eustatic changes for the Campanian, Cooper (1977) reports a number of locations in which the mid-Cretaceous appears to be transgressive. However, the resolution of his data is below that required to make any meaningful comparisons with the relative sea-level curves presented here. There is a good correlation between the relative sea-level curves presented here and those published in the literature within the constraints of low resolution correlation between the schemes.

COMPARISON OF THE DATA WITH STABLE ISOTOPE CURVES

$\delta^{13}\text{C}$ CURVE

When the relative sea-level curve, constructed in this study, is compared with the stable carbon isotope ($\delta^{13}\text{C}$) curve (Figure 6.5) a number of relationships are observed. During the Coniacian and Santonian there is a good correlation between the $\delta^{13}\text{C}$ and relative sea-level curves, both in the short-term and long-term. This reflects a positive relationship between organic carbon and changes in relative sea-level. The area of the shallow shelf seas at the continental margins is dramatically affected by comparatively minor changes in relative sea-level. These seas represent a significant proportion of the nutrient-rich photic zone available for photosynthesis and, thus, changes in the $\delta^{13}\text{C}$ curve are related directly to relative sea-level change (Mitchell, Paul & Gale, 1993 and Jenkyns, Gale & Corfield, 1994).

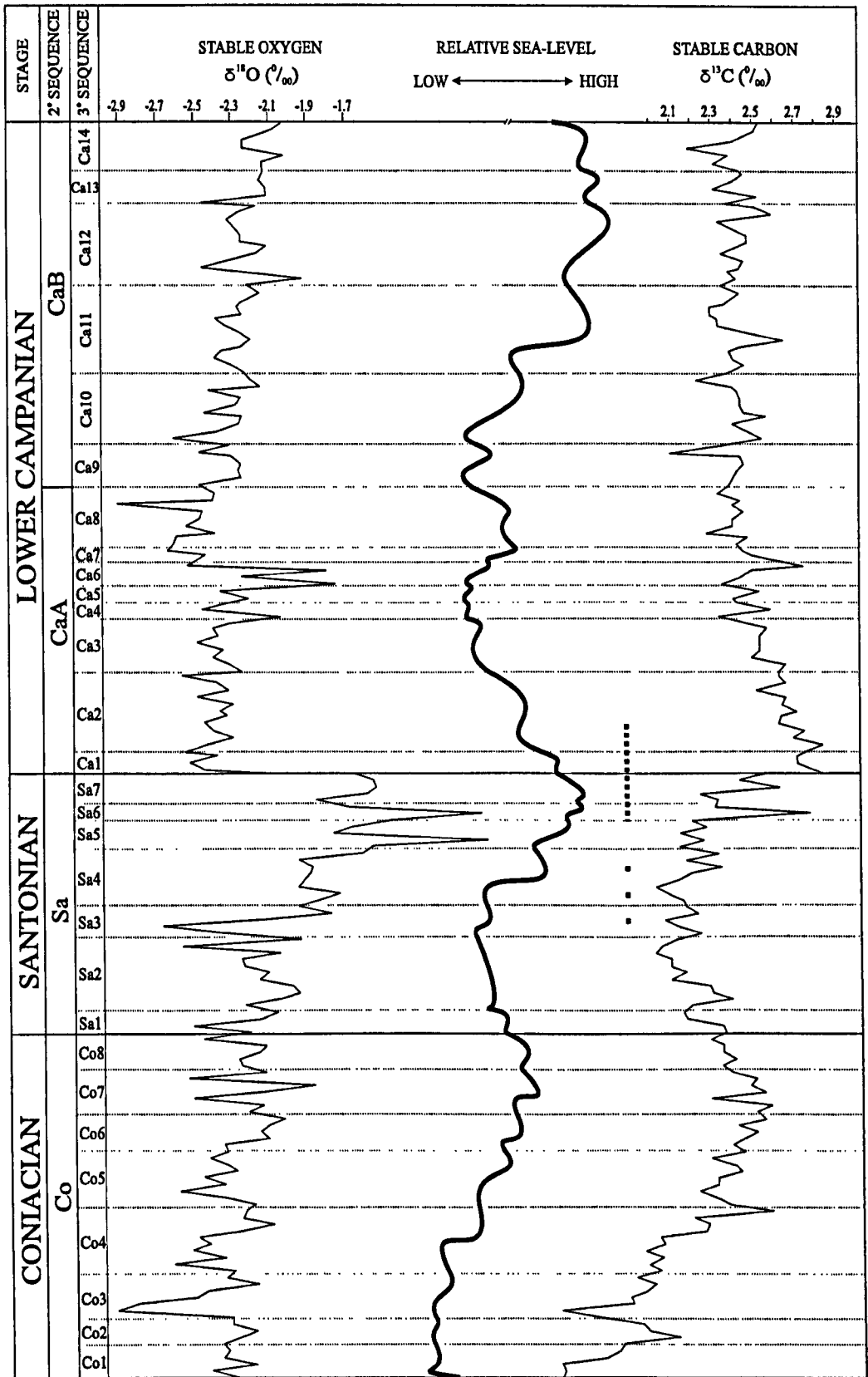


Figure 6.5 Sequence stratigraphy, relative sea-level and stable δ¹⁸O and δ¹³C curves. Stable isotope data replotted from Jenkyns, Gale and Corfield (1994). Periods of phosphate deposition are shown by Spacing of dashes represents relative intensity of phosphorite deposition.

During times of transgression, flooding of continental margins, and subsequent enlargement of the nutrient-rich photic zone, results in an increased $\delta^{13}\text{C}$ ratio (Mitchell, Paul & Gale, 1993 and Jenkyns, Gale & Corfield, 1994). The $\delta^{13}\text{C}$ curve has been taken, additionally, as an indication of rates of transgression rather than absolute levels of sea-level by Jenkyns, Gale and Corfield (1994), a relationship that is evident in the data presented here. The sharp increases in $\delta^{13}\text{C}$ during Sequences Co4, Co5 and Sa4 (Figure 6.5) can be seen to relate to periods of rapid transgression. However, in the case of the Coniacian and Santonian data presented herein, the $\delta^{13}\text{C}$ curve can be seen to also provide a reliable indicator of relative sea-level change.

During the Campanian, the relationship between $\delta^{13}\text{C}$ and relative sea-level is less clear in the longer-term, especially during Sequence CaB, though the relationship remains clear over the course of the short-term cycles. During CaA, the relationship holds true, though the absolute changes in the $\delta^{13}\text{C}$ curve are less significant than the changes in the relative sea-level curve. In the short term, changes in $\delta^{13}\text{C}$ follow those in relative sea-level. The significance of periods of rapid transgression to the $\delta^{13}\text{C}$ ratio is highlighted by the correspondingly prominent $\delta^{13}\text{C}$ excursions, for instance during times Ca6 and Ca11 (Figure 6.5). In the longer term, a decline in the $\delta^{13}\text{C}$ values during Sequences Ca1 to Ca9 follows the long-term decline in relative sea-levels during the early Campanian. A minor increase in the relative sea-level curve is seen during Ca6 – Ca7-time and this is reflected in a correspondingly minor positive shift in $\delta^{13}\text{C}$ values, notably during TST Ca6.

$\delta^{18}\text{O}$ CURVE

During the Coniacian and Santonian, the $\delta^{18}\text{O}$ curve mimics the relative sea-level curve. This positive relationship is observable during the Coniacian, though is less pronounced than during the middle-to-late Santonian where the abrupt rise in relative sea-level is matched by a marked positive $\delta^{18}\text{O}$ excursion (Figure 6.5) The positive relationship between $\delta^{18}\text{O}$ and relative sea-level breaks down, and reverses, at the end of the Santonian, with a distinctive inverse relationship observed between the $\delta^{18}\text{O}$ and relative sea-level curves over the Lower Campanian (Figure 6.5). A pronounced positive $\delta^{18}\text{O}$ excursion corresponds to the low-point in relative sea-level during Ca3 – Ca5-time. The subsequent negative $\delta^{18}\text{O}$ excursion correlates with rising and high relative sea-levels during Sequences Ca6 – Ca8. During Sequence CaB, values of $\delta^{18}\text{O}$ rise by 0.2 ‰ to the end of the Lower-Campanian. This gradual increase in $\delta^{18}\text{O}$ coincides with a steady rise in relative sea-level.

In the short term, a clear positive relationship is observable in the data for the Coniacian and Santonian. Over this interval, negative $\delta^{18}\text{O}$ excursions correlate with LmSTs whilst less-negative $\delta^{18}\text{O}$ excursions correlate with TSTs and HSTs. This relationship is exemplified by the mid – late Coniacian transgressions (Co4 – Co7) that correlate clearly with positive $\delta^{18}\text{O}$ excursions. During the Campanian, the short-term relationship is partially disguised by the low resolution of the isotope data compared to the higher resolution sequence stratigraphical interpretation, though an inverse relationship, following that clearly observable in the long-term, is indicated. The long-term relationship between $\delta^{18}\text{O}$ and relative sea-level is strong during Sequences Sa and CaA, but less so during Sequences Co and CaB.

Ocean circulation varies considerably depending on a number of factors, not least climate. The equator – polar temperature gradient and dominant wind patterns both greatly influence the movement of water masses. These masses are in turn defined by their temperature and salinity characteristics. Plate movement and continental reconfiguration also significantly influence patterns of

circulation, albeit over longer time periods. The relationships observed in the stable oxygen and carbon data, the relative sea-level curves and the lithologies preserved, over the Coniacian – ^{Early} Lower Campanian interval of the Anglo-Paris Basin record apparent changes in the patterns of ocean circulation and consequently in styles of deposition. This relationship, identified between the $\delta^{18}\text{O}$ and relative sea-level curves, is a complicated one and is considered below with respect to tectonics and two extreme end-member models of climate and ocean state — icehouse and greenhouse.

ICEHOUSE STATE

During icehouse conditions, oceans are thermally stratified and characterised by water masses defined by temperature and salinity contrasts, moving under thermohaline circulation (Wilde and Berry, 1986) Circulation is sensitive to a number of external controls such as changes in surface salinity and temperature, often related to Milankovitch cyclicity (Eyles, 1993). Modern oceans are dominated by cold deep-waters, formed at high latitudes, which move towards the equator. Strong thermohaline circulation promotes upwelling of nutrient-rich waters and high bio-diversity along continental margins. Taken to its logical extreme, as exemplified by the Monterey Effect of Vincent and Berger (1985), the enhanced draw-down of atmospheric CO_2 by oceanic photosynthesis accentuates the cycle of intensifying climatic cooling. Vincent and Berger (1985) interpreted the presence of large quantities of organic carbon and phosphorus preserved in the sediment as evidence for palaeo-upwelling and attributed this upwelling to the combined influence of zonal winds and thermocline evolution. The thermocline is further strengthened by an increasing thermal gradient that results from climatic deterioration (Figure 6.6). The Monterey Effect feedback loop breaks down when the nutrient supply becomes depleted. Vincent and Berger (1985) equated the amount of carbon taken out of the ocean-atmosphere system, trapped in sediments by this process, to the total stored in the modern oceanic carbon reservoir.

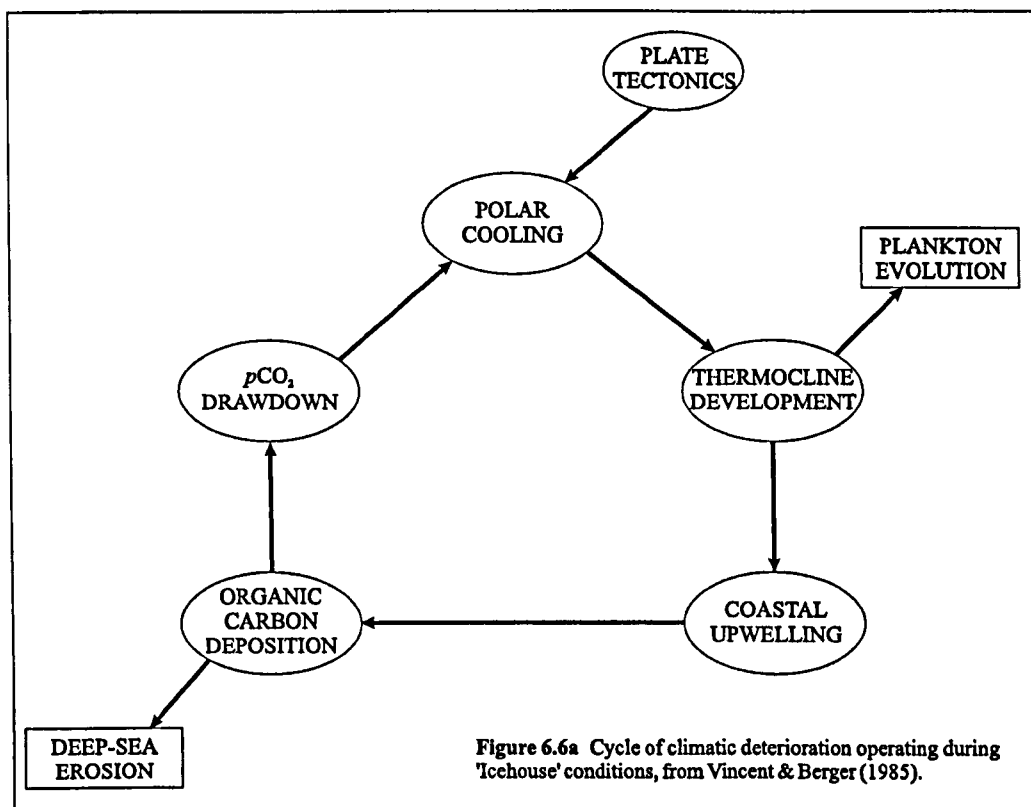
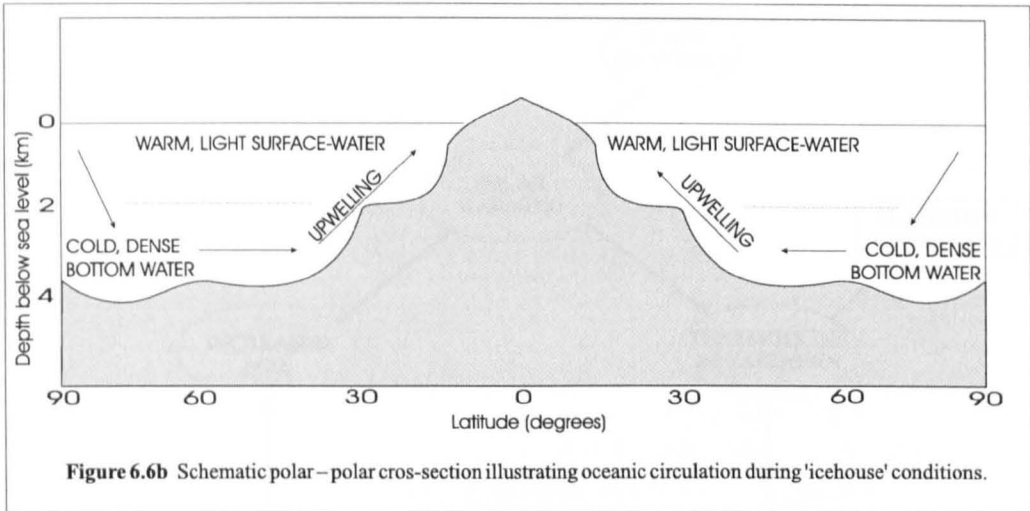


Figure 6.6a Cycle of climatic deterioration operating during 'icehouse' conditions, from Vincent & Berger (1985).



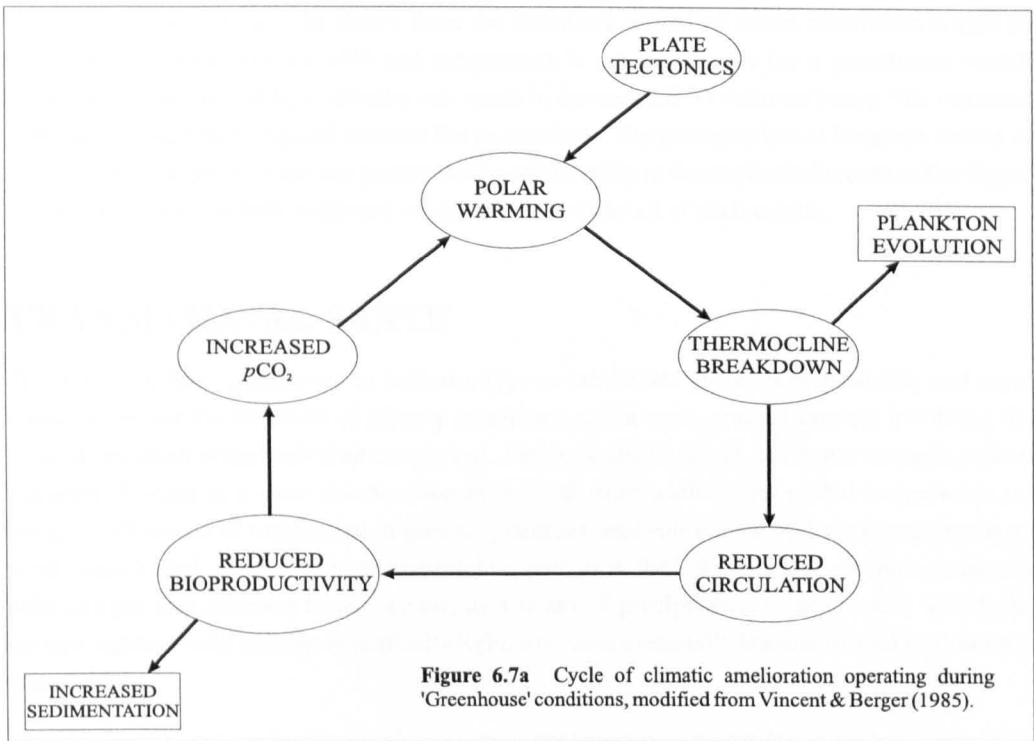
During photosynthesis, isotopically light carbon is removed from the surface photic zone and becomes trapped at depth, beneath the thermocline, where it is oxidised releasing light carbon dioxide. The more efficient the biological cycling, the greater the disparity between shallow and deep water values of $\delta^{13}\text{C}$. Berger and Vincent (1985) argued that as organic carbon has a $\delta^{13}\text{C}$ value of approximately 20‰, a difference of 2‰ between surface and deep waters indicated that 10% of the total dissolved carbon in shallow water had been removed through the settling of organic matter. Consequently they linked higher values of $\delta^{13}\text{C}$ to higher productivity in the oceans. Mitchell, Paul and Gale (1993), Jenkyns, Gale and Corfield (1994) and Chapters 2 – 4 herein have subsequently used the link between productivity and $\delta^{13}\text{C}$ as an indication of relative sea-level changes.

Temperature increases resulting from climatic change will be reflected in $\delta^{18}\text{O}$ values. The standard inverse relationship between temperature and the fractionation of ^{16}O and ^{18}O (Epstein *et al.* 1951) during biogenic calcite precipitation shows that a decrease in $\delta^{18}\text{O}$ values will result from temperature rises. This has been used extensively during the later Tertiary and Quaternary to elucidate a climatic, specifically temperature, signal from biogenic calcite (e.g. Ruddiman, Shackleton & McIntyre, 1986). Conversely, periods of temperature deterioration will be recorded by positive, or less negative, shifts in the stable oxygen ^{isotope} curve. Other factors can disguise this relationship under greenhouse conditions.

GREENHOUSE STATE

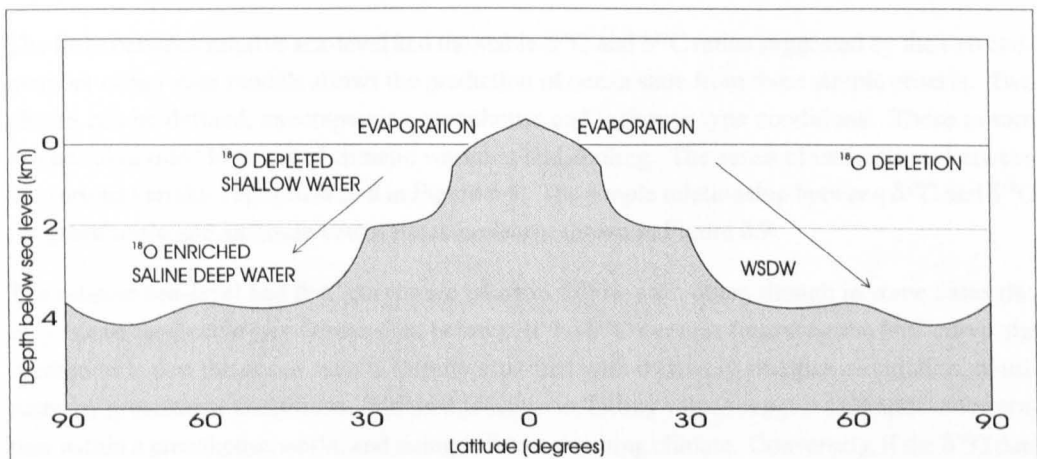
Over greenhouse intervals the oceans behave in a sluggish manner with weak oceanic and atmospheric circulation; a result of reduced polar – equatorial temperature gradients and therefore reduced ocean current activity. This results in a different mode of bottom-water formation to that seen today, with warm, saline bottom water (WSBW) forming in isolated basins dominated by evaporation or on shelves at low latitudes (Brass *et al.*, 1982). These WSBWs moved polewards and may have been modified by interaction with other water-masses at turbulent interfaces, with the result that only major water bodies would preserve their characteristics.

Railsback (1990) proposed a model for the salinity stratified oceans of the Ordovician and Cretaceous, building upon that of Brass *et al.* (1982). Here, evaporation resulted in a warm, saline layer of ^{18}O -rich water that sunk owing to density contrasts and became trapped beneath the pycnocline. The return of ^{16}O to the surface waters, through precipitation, in a world free of land-



ice, resulted in a net depletion of ^{18}O , and consequently, less negative $\delta^{18}\text{O}$ ratios during periods of increased evaporation (Figure 6.7). Wilde and Berry (1982) proposed a similar model allowing for sinking of intermediate – deep-water masses as a result of evaporation, accounting for the development and intensification of oxygen-minimum zones.

An example of these stratified oceanic conditions, favouring the development of anoxia and subsequent deposition of black shales, is seen during the Cenomanian – Turonian boundary interval (Schlanger and Jenkyns, 1976; Jenkyns, 1980). Jewell (1993 & 1996) reported the likelihood of large vertical salinity gradients having been established over a period of just one or two years in the Cretaceous North American Seaway, and that major storms were ineffectual at mixing oxygen at the sediment-water interface in water depths greater than 300m where the salinity gradient exceeded 1 – 2‰.



The obvious conclusion to be drawn from the Railsback model of ocean circulation is that an inverse relationship between $\delta^{18}\text{O}$ and temperature is not sustainable for a greenhouse world. Increased evaporation at low latitudes can result in increased $\delta^{18}\text{O}$ value as heavy ^{18}O , removed from surface waters, is trapped beneath the pycnocline. The precipitation of biogenic calcite in the light-oxygen, photic zone has preserved this relationship in the geological record of the Upper Cretaceous where the bulk sediment — chalk — is composed of such calcite.

TRANSITIONAL STATE

The transition from greenhouse to icehouse-type ocean is one of inherent instability and rapid transition whilst the initiation of salinity stratification is a more gradual process involving the gradual cessation of thermohaline circulation. Deeper water becomes less dense through gradual warming, leading to a slow deterioration in thermal stratification. As global temperature increased, ^{16}O would be evaporated in greater quantities, and subsequently, denser surface waters would start to sink in areas of high evaporation, such as in the low latitudes. As the isotopically light oxygen was returned to the oceans, as a result of precipitation in an ice-free world, the surface waters would become isotopically light, a process eventually leading to a salinity-density stratification.

This gradual transition, between icehouse and greenhouse ocean circulation systems, would be susceptible to external forcing. Work by Woo *et al.* (1992) has suggested that during the mid-Cretaceous, deep waters were derived from a combination both of cold water sinking at high latitudes and moving equatorwards and of conversely flowing warm, saline waters that originated in sub-tropical latitudes.

The transition from greenhouse to icehouse flow is a relatively sudden one. Factors such as basin geometry, Milankovitch cyclicity and nutrient fluxes, discussed below with regard to the mid-late Cretaceous, can break down oceanic salinity stratification rapidly, instigating a renewed thermohaline circulation.

RELATIVE SEA-LEVEL, STABLE ISOTOPES AND OCEAN STATE

The links between relative sea-level and the stable $\delta^{18}\text{O}$ and $\delta^{13}\text{C}$ ratios suggested by the two end-member ocean state models allows the prediction of ocean state from these simple criteria. Two phases can be defined, encompassing greenhouse and icehouse-type conditions. These in turn can be subdivided in terms of climatic warming and cooling. The series of interactions between the various variables are illustrated in Figure 6.8. The simple relationship between $\delta^{13}\text{C}$ and $\delta^{18}\text{O}$ for greenhouse and icehouse ocean states is clearly shown in Figure 6.9.

The relative sea-level and $\delta^{13}\text{C}$ curves are taken to follow each other, though in some cases this may not be applicable (see Discussion, below). If the $\delta^{18}\text{O}$ curve is following the $\delta^{13}\text{C}$ curve, the prediction is that the ocean state is salinity stratified with relatively sluggish circulation, dominated by greenhouse conditions. Within this scenario, falling values suggest a climatic deterioration within a greenhouse world, and rising values a warming climate. Conversely, if the $\delta^{18}\text{O}$ data is mirroring the $\delta^{13}\text{C}$ and relative sea-level curves, an icehouse-type climate is suggested with

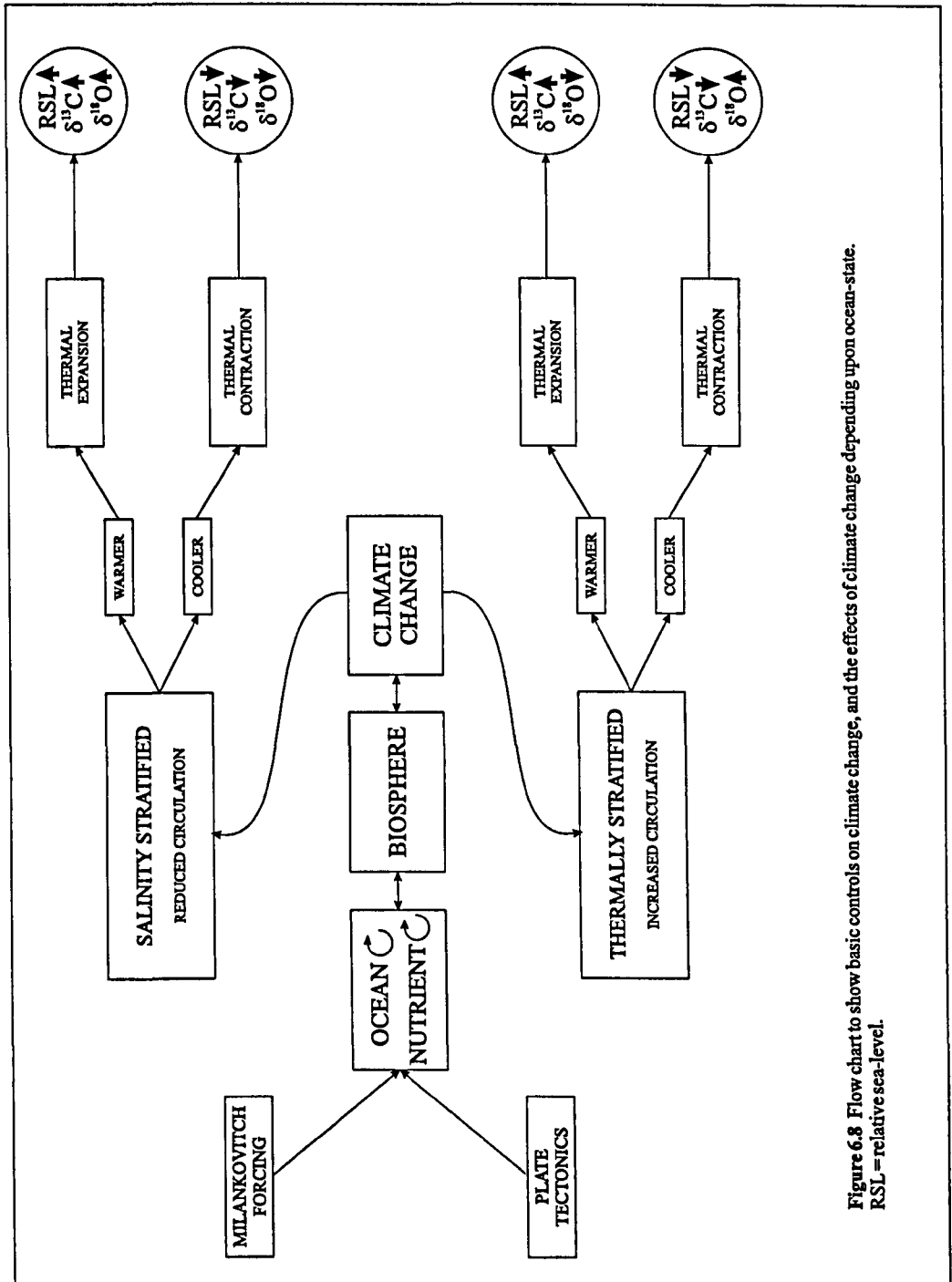


Figure 6.8 Flow chart to show basic controls on climate change, and the effects of climate change depending upon ocean-state. RSL = relative sea-level.

associated thermal stratification and vigorous circulation in the oceans. Rising $\delta^{13}\text{C}$ and falling $\delta^{18}\text{O}$ suggest a warming climate within the constraints of the icehouse world, and falling $\delta^{13}\text{C}$ associated with a rising $\delta^{18}\text{O}$ ratio would indicate further climatic deterioration (Figures 6.8 & 6.10). A threshold level exists between the two ocean states, below which the climatic conditions can fluctuate between warmer and cooler though remaining within the general greenhouse or icehouse climatic phases.

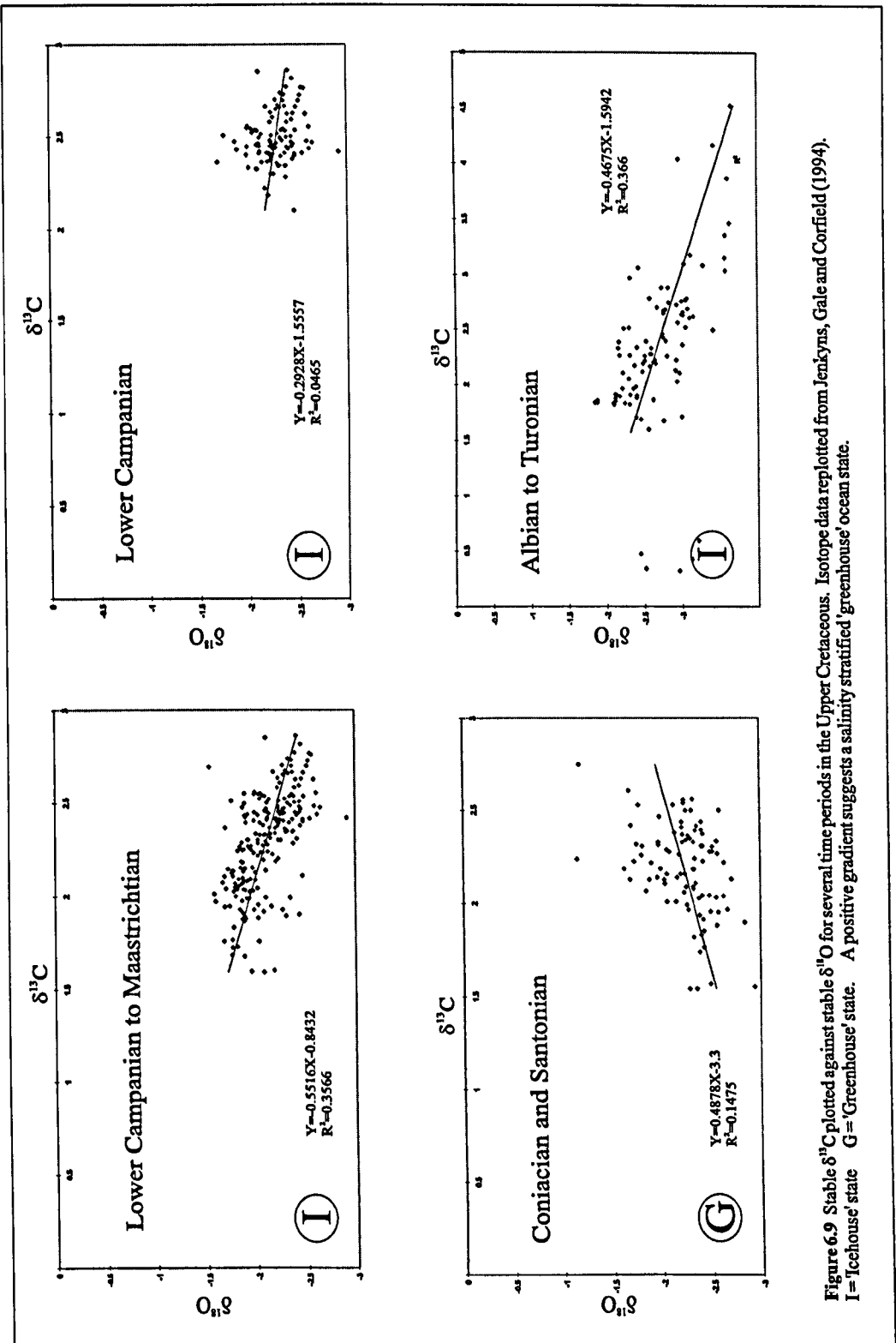


Figure 6.9 Stable $\delta^{13}\text{C}$ plotted against stable $\delta^{18}\text{O}$ for several time periods in the Upper Cretaceous. Isotope data replotted from Jenkyns, Gale and Corfield (1994). I = 'icehouse' state G = 'Greenhouse' state. A positive gradient suggests a salinity stratified 'greenhouse' ocean state.

Such a situation is seen during the Coniacian – Santonian, and during the ^{Early} Lower Campanian. However, the threshold was reached at the Santonian – Campanian boundary with a change from greenhouse to icehouse ocean state. In this case the threshold is likely to have been temperature changes sufficient to increase the polar – equatorial temperature gradient such that a thermohaline circulation became established. This broke down the salinity stratification in the oceans and

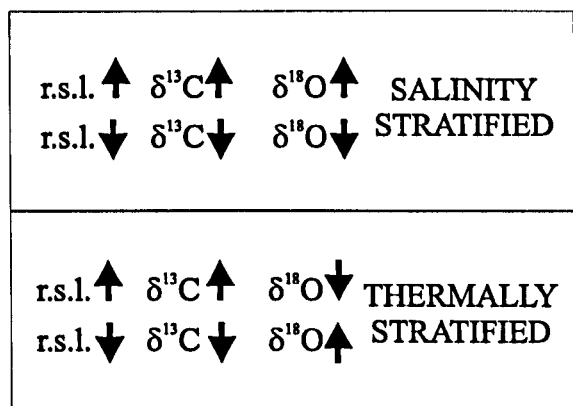


Figure 6.10 Relative sea-level and stable isotope indicators of ocean-state.

higher levels of atmospheric CO_2 (Berner, 1991) with palaeogeographical and palaeorographical changes thought insufficient to have caused the warming (Barron and Washington, 1984).

Despite occasional Victorian allusions to the possibility of sea-ice (Goodwin-Austen, 1858; Martin, 1897 and Stebbing, 1897) a vast majority of the subsequent literature has postulated the apparent non-glacial nature of the ^{late}Upper Cretaceous — one of the warmest periods in Earth history. However, a growing body of recent publications has discussed the probability that the climate was rather more seasonal than had previously been supposed, with temperatures dropping significantly below freezing during high-latitude winters (Spicer, Rees & Chapman, 1993 and d'Hondt & Arthur, 1996). Evidence from high-latitude flora (Spicer & Parish, 1990) supports the Victorian observations that erratic blocks within the chalk may be the result of seasonal ice-rafting. Jeans *et al.* (1991) have identified what they see as a probable glacial interval at the Cenomanian – Turonian boundary, coinciding with a major positive excursion in the stable carbon isotope curve (Gale *et al.*, 1993 and Jenkyns, Gale & Corfield, 1994). Between this interval and the late Cretaceous climatic deterioration in the Maastrichtian, there is no evidence for such a dramatically cool climate, though it is likely that some equatorial – polar temperature gradient existed, albeit one that was less steep than that at the present day.

There is a positive correlation between $\delta^{18}\text{O}$ and relative sea-level during the Coniacian and Santonian, suggesting a salinity-stratified ocean state indicative of the greenhouse phase. At the end of the Santonian, the relationship between $\delta^{18}\text{O}$ and relative sea-level reverses, indicating movement through the threshold criteria to an icehouse phase characterised by thermohaline circulation in the ocean.

Data from the Coniacian and Santonian suggest a salinity stratified ocean where evaporation at the low latitudes concentrated ^{18}O into dense saline waters that were trapped beneath the pycnocline in poleward moving water masses. Precipitation concentrated ^{16}O in the surface waters, resulting in a $\delta^{18}\text{O}$ ratio heavier than expected from global temperature estimates. Enlargement and reduction of the shallow shelf sea area is recorded in the $\delta^{13}\text{C}$ curve, a consequence of expansion and contraction of the marine biosphere controlled by relative sea-level change. At the end of the Santonian, upwelling and a dynamic ocean basin reorder the ocean circulation system and initiate a thermohaline circulation. This corresponds to a major change in sedimentation (Jarvis, 1980a, 1980b and 1992) with the precipitation of rich phosphorite deposits on structural highs in the Anglo-Paris Basin (Sequences Sa6 – Ca6 herein). The initiation of oceanic circulation appears a widespread phenomenon during the late Santonian – early Campanian with rich phosphorites being deposited around the world (Northolt & Jarvis, 1990).

generated the upwelling water masses responsible for the precipitation of phosphorite deposits in the Anglo-Paris Basin.

DISCUSSION

The ^{late}Upper Cretaceous is well known as a period of warm climate and high eustatic sea-level. Barron (1983) put mean global temperatures in the range 6 – 14 °C warmer than the present day based upon palaeontological and isotopic data. Such temperatures have been attributed to

Jarvis (1980a and 1992) has linked the deposition of these phosphorites to increased bioproductivity in the Anglo-Paris Basin which he attributed to the upwelling of cold, nutrient-rich waters at the continental margin. The likelihood of the existence of an upwelling system in the late Santonian is further indicated by the inverse relationship identified herein between $\delta^{18}\text{O}$ values and short-term relative sea-level change. In the late Santonian, increases in temperature are mirrored by a negative shift in the $\delta^{18}\text{O}$ curve, as typified in the icehouse model outlined above. These data indicate a breakdown in the relatively sluggish, salinity-stratified greenhouse ocean characterised by reverse circulation followed by a return to an icehouse-type ocean exhibiting thermohaline circulation. Such a change in ocean-state would be a logical result of the initiation of an upwelling system. The relationship between relative sea-level, based upon the $\delta^{13}\text{C}$ curve of Jenkyns, Gale and Corfield (1994), and $\delta^{18}\text{O}$ for the Late Campanian suggests that open-ocean circulation was a persistent feature of the post-Santonian ~~Upper~~ Cretaceous oceans; a likely precursor to the end Cretaceous climatic deterioration.

The long-term relationship between $\delta^{18}\text{O}$ and relative sea-level in the Coniacian is not as pronounced as it is in the Santonian or ~~Lower~~ Campanian, suggesting a possible tectonic control on the second-order relative sea-level cyclicity. This agrees with a number of authors working on volumetric changes in mid-ocean ridge volume over this interval (Srivastava & Tapscott, 1986; Barron, 1987; Roest & Srivastava, 1991; Wei, 1995 and Guiraud & Bosworth, 1997). The clear, positive relationship between $\delta^{18}\text{O}$ and longer-term relative sea-level during the Santonian suggests that climatic factors dominated the long-term rise in relative sea-level; temperature becomes the dominant control on $\delta^{18}\text{O}$, with the stable isotope curve mirroring the relative sea-level curve. This relationship holds true for Sequence CaA of the Lower Campanian. The $\delta^{13}\text{C}$ curve remains a proxy for relative sea-level, but the relationship is less pronounced than for the Coniacian – Santonian interval. In the latter-half of the Lower Campanian, Sequence CaB, the relationship between the $\delta^{18}\text{O}$ and the relative sea-level curves is also less clear. Third-order cycles of relative sea-level change are reflected in the $\delta^{18}\text{O}$ data, but the longer term trend is partially obscured. This suggests a longer-term tectonic control for the relative sea-level change during the late Campanian, such as that suggested for the Coniacian.

Climatic modelling by Barron and Peterson (1989) has suggested that the mid-Cretaceous ocean was sufficiently sensitive to continental configuration, climate and sea level to limit the validity of the use of modern analogues in studying past patterns of circulation. They postulate that a westward-flowing circumglobal Tethyan current may not be viable, preferring an eastward primary flow, with oceanic circulation being greatly influenced by dynamic basin geometries. It is possible, therefore, that the continued opening of the North Atlantic had caused a sufficient change in ocean dynamics to allow the influx of nutrient-rich waters into the Anglo-Paris Basin, associated with upwelling at the end of the Santonian. Upwelling is a major oceanic variable directly influenced by Milankovitch-type cyclicity (Barron, Arthur & Glancy, 1988). Milankovitch cyclicity directly affects the distribution of incoming solar radiation, and consequently, the equator-pole temperature gradient that is responsible for atmospheric wind intensity. These winds and contrasts between marine and land temperatures have a major influence upon upwelling at the regional scale. Barron, Arthur and Glancy (1988) argue that these regional effects, including the effects of monsoon circulations and winter storms, can be translated to the global scale, influencing the type and location of deep-water formation.

The change in ocean circulation is recorded in the relationship between relative sea-level change and stable isotope records from the late Santonian to the early Campanian a period of upwelling and rapid transition. It is probable that the instigation of an upwelling system controlled and

dictated the change in ocean circulation, initiated by continued changes in basin geometry associated with the opening of the North Atlantic Ocean, and Milankovitch cyclicity.

POSSIBLE WIDER IMPLICATIONS

Prior to the Coniacian, the relationship between $\delta^{13}\text{C}$ and relative sea-level is unclear. Gale (1996) has published a sequence stratigraphical interpretation of the Turonian of southern England and Owen (1996) has done the same for the Cenomanian of the Anglo-Paris, Aquitaine and Munster Basins. Jenkyns, Gale and Corfield (1994) concluded that there appeared to be no clear relationship between their isotope data and the sea-level curves from the literature that they considered.

The stable $\delta^{18}\text{O}$ and $\delta^{13}\text{C}$ curves of Jenkyns, Gale and Corfield (1994) indicate that if $\delta^{13}\text{C}$ is taken as a proxy for relative sea-level, an icehouse-type circulation model could be applied to the Cenomanian – Turonian demonstrating the expected inverse relationship between $\delta^{18}\text{O}$ and temperature. However, the $\delta^{13}\text{C}$ ratio can not be treated in this simplistic manner prior to the Coniacian. Jenkyns (1980) has discussed a number of oceanic anoxic events during the Cenomanian – Turonian, exemplified by the exceptional preservation of organic matter on the sea floor. Warm oceans and high sea levels have been invoked as a mechanism for the oceanic anoxic events that preserve black shales in deep water sediments, most notably in the Cenomanian – Turonian (Jenkyns, 1980). During these intervals, large amounts of organic carbon were trapped beneath a redox boundary elevated above the ocean floor. This resulted in the removal of organic carbon from the biosphere and its subsequent preservation. Jeans *et al.* (1991) discuss the possibility of terrestrial carbon being involved during the Cenomanian – Turonian $\delta^{13}\text{C}$ excursion, characterised by $\delta^{13}\text{C}$ values averaging 4‰ higher than marine values (Herbin *et al.* 1986). Jeans *et al.* (1991) argued that not only would the presence of terrigenous organic carbon have intensified the $\delta^{13}\text{C}$ excursion, but that it could have been a trigger in the development of anoxia.

Hancock (1990) concluded that the Cenomanian – Turonian black shales were deposited during regression, a proposition supported by Jeans *et al.* (1991) who specified that the peak $\delta^{13}\text{C}$ excursion coincides with maximum regression. If this is the case, it suggests that the greenhouse ocean relationship between $\delta^{18}\text{O}$ and temperature, invoked for the Coniacian and Santonian, is valid for the Cenomanian – Turonian with the proviso that this regression was climatically-controlled. Equally this highlights that $\delta^{13}\text{C}$ can not be used as a proxy for relative sea-level whilst the conditions for extraordinary organic carbon preservation exist. The conclusions of Hancock (1990) and Jeans *et al.* (1991) are at odds with Schlanger's and Jenkyns's (1976) original explanation for the occurrence of OAEs. Jenkyns and Schlanger suggested transgression associated with a reduced supply of cold oxygenated water to the deep oceans as a mechanism for anoxic events. Sediments characteristic of anoxia were recorded from settings as diverse as oceanic plateaux and basins, continental margins and shallow shelf-seas, suggesting that simple bathymetry was not a controlling factor. Geographically-variable anoxia could be the result of increased organic matter accumulation in locally restricted settings, a probable characteristic of a salinity stratified ocean. Such a view was expounded by Jeans *et al.* (1991) who argued that the premise of the existence of OAEs is not supported by the evidence. They suggested that the stable isotope excursions could be explained by widespread regression, restricted ocean circulation, lower ocean temperatures and the enhanced input of terrestrial organic matter.

In effect it is likely that no single set of circumstances can be invoked for the occurrence of such isotope excursions. The attribution of the isotope excursions to a combination of changes in

relative sea-level, restricted oceanic circulation and changes in temperature is in accordance with the data presented herein for the Coniacian – Santonian interval. However, the non-existence of OAEs is not a prerequisite of such an interpretation. Indeed, oceanic anoxia is required as a mechanism for the preservation of the large accumulations of organic carbon over the Cenomanian – Turonian interval. Anoxia is a logical result of a degree of stagnation associated with a salinity-stratified, reduced-circulation ocean system. Equally, a transgression triggering upwelling at the continental margins, though a method of introducing increased nutrient supply, is not required to increase bioproductivity. An increase in the area of the shallow shelf seas can be invoked as a mechanism for such an increase in bioproductivity without the need for wholesale upwelling. Similarly, a fall in relative sea-level, exposing greater areas of landmass to precipitation and run-off, can introduce more nutrients to the surface waters, promoting increased bioproductivity. The relationships observed during the Santonian – Lower Campanian interval would suggest that OAEs and widespread regression are not mutually exclusive.

CONCLUSIONS

- Sequence stratigraphy is applicable to pelagic and hemi-pelagic biogenic successions such as the chalk of Northwest Europe.
- An ideal sequence cycle is defined (Figure 6.1) for application to the chalk.
- The Coniacian – Lower Campanian chalk of Northwest Europe displays a short-term, third-order cyclicity probably related to the 400ka Milankovitch eccentricity cycle.
- A number of longer-term, second-order cycles, several Ma duration, are identifiable, controlled by wider tectonism or a combination of tectonism and climate.
- Relative sea-level curves may be defined from the sequence stratigraphical interpretation giving an order of magnitude higher resolution than available in the literature.
- Stable $\delta^{18}\text{O}$ data can not be used as a reliable indicator of temperature in a greenhouse world.
- Relative sea-level, stable $\delta^{18}\text{O}$ and stable $\delta^{13}\text{C}$ curves can be used to predict ocean-state in the Upper Cretaceous.
- The Coniacian and Santonian exhibited greenhouse conditions characterised by a salinity stratified ocean.
- The Lower Campanian was an icehouse world characterised by a thermally stratified ocean.
- A threshold between greenhouse and icehouse conditions was crossed at the end of the Santonian, leading to the initiation of a thermohaline circulation and the deposition of phosphatic chalk.

**PAGE
NUMBERING
AS ORIGINAL**

References

- BARR, F. T. 1972. Cretaceous biostratigraphy and planktonic foraminifera of Libya. *Micropalaeontology* **18** 1 – 46.
- BARRON, E. J. 1983. A warm equable Cretaceous: the nature of the problem. *Earth Science Reviews* **19** 305 – 338.
- BARRON, E. J. 1984. The role of geographic variables in explaining palaeoclimates: Results from Cretaceous climatic model sensitivity studies. *Journal of Geophysical Research* **89** D1 1267 – 1279.
- BARRON, E. J. 1986. Physical palaeoceanography: a status report. In Hsu, K. J. (ed) *Mesozoic and Cenozoic oceans, AGU/GSA Geodynamics Series* **15** 1 – 9.
- BARRON, E. J. 1987. Cretaceous plate tectonic reconstructions. *Palaeogeography, palaeoclimatology, palaeoecology* **59** 3 – 29.
- BARRON, E. J. & PETERSON, W. H. 1989. Model simulation of the Cretaceous ocean circulation. *Science* **244** 684 – 686.
- BARRON, E. J., ARTHUR, M. A. & KAUFFMAN, E. G. 1985. Cretaceous rhythmic bedding sequences — a plausible link between orbital variations and climate. *Earth and Planetary Science Letters* **72** 327 – 340.
- BARRON, E. J., ARTHUR, M. A. & GLANCY, T. J. 1988. Climate model perspective for pre-Pleistocene milankovitch forcing. *AAPG Bulletin* **72** 158.
- BERGER, A. & LOUTRE, M. F. 1994. Astronomical forcing through geological time. *Special Publication of the International Association of Sedimentologists* **19** 15 – 24.
- BERGER, W. H. & VINCENT, E. 1986. Deep-sea carbonates: reading the carbon isotope signal. *Geologische Rundschau* **75** 246 – 269.
- BERNER, R. A. 1991. A model for atmospheric CO₂ over Phanerozoic time. *American Journal of Science* **291** 339 – 376.
- BIRKELUND, T., HANCOCK, J. M., HART, M. B., RAWSON, P. F., REMANE, J., ROBASZYNSKI, F., SCHMID, F. & SURLYK, F. 1984. Cretaceous Stage boundaries — Proposals. *Bulletin of the Geological Society of Denmark* **33** 3 – 20.
- DE BOER, P. L. & SMITH, D. G. 1994. Orbital forcing and cyclic sequences. *Special Publication of the International Association of Sedimentologists* **19** 1 – 14.

- BRALOWER, T. J., LECKIE, R. M., SLITER, W. V. & THIERSTEIN, H. R. 1995. An integrated Cretaceous microfossil biostratigraphy. In Berggren, W. A. (ed) *Geochronology, time scales and global stratigraphic correlation*. Society of Economic Palaeontologists and Mineralogists Special Publication 54, Tulsa, 1995.
- BRASS, G. W., SALTZMAN, E., SOUTHAM, J. R. & PETERSON, W. H. 1982. Warm saline bottom water in the ancient ocean. *Nature* 296 620 – 623.
- BRISTOW, R., MORTIMORE, R. & WOOD, C. 1987. Lithostratigraphy for mapping the chalk of southern England. *Proceedings of the Geologists' Association* 108 293 – 316.
- BROMLEY, R. G. & GALE, A. S. 1982. The lithostratigraphy of the English Chalk Rock. *Cretaceous Research* 3 273 – 306.
- BROMLEY, R. G., SCHULZ, M. G. & PEAKE, N. B. 1975. Paramoudras: Giant flints, long burrows and the early diagenesis of chalks. *Det Kongelige Danske Videnskabernes Selskab Biologiske Skrifter* 20 10 31pp.
- CANDE, S. C. & KENT, K. V. 1995. Revised calibration of the geomagnetic polarity timescale for the Late Cretaceous and Cenozoic. *Journal of Geophysical Research* 100 B4 6093 – 6095.
- CARNEY, J. L. & PIERCE, R. W. 1995. Graphic correlation and composite standard databases as tools for the exploration biostratigrapher. In Mann, K. O. & Lane, H. R. (Eds.) *Graphic Correlation*. Society of Economic Palaeontologists and Mineralogists Special Publication 53 23 – 43.
- CHADWICK, R. A. 1986. Extension tectonics in the Wessex basin, southern England. *Journal of the Geological Society* 143 465 – 488.
- CHRISTENSEN, W. K. 1990. Upper Cretaceous belemnite stratigraphy of Europe. *Cretaceous Research* 11 371 – 386.
- CLOETINGH, S. 1988. Intraplate stresses: A tectonic cause of third-order cycles in apparent sea-level? In Wilgus, C. K. *et al.* (eds) *Sea-level changes: an integrated approach*.

- Society of Economic Palaeontologists and Mineralogists Special Publication **42** 19 – 29.
- COE, A. L. 1996. Unconformities within the Portlandian Stage of the Wessex Basin and their sequence-stratigraphical significance. From Hesselbo, S. P. & Parkinson, D. N.(eds) *Sequence Stratigraphy in British Geology*, Geological Society Special Publication **103** 109 – 143.
- COOPER, M. R. 1977. Eustasy during the Cretaceous: Its implications and importance. *Palaeogeography, palaeoclimatology, palaeoecology* **22** 1 – 60.
- DITCHFIELD, P. & MARSHALL, J. D. 1989. Isotopic variation in rhythmically bedded chalks: Palaeotemperature variation in the Upper Cretaceous. *Geology* **17** 842 – 845.
- EPSTEIN, S., BUCHSBAUM, R., LOWENSTAM, H. & UREY, H. 1951. Carbonate-water isotopic temperature scale. *Bulletin of the Geological Society of America* **62** 417 – 426.
- EYLES, N. 1993. Earth's glacial record and its tectonic setting. *Earth-Science Reviews* **35** 1 – 248.
- FISCHER, A. G. 1993. Cyclostratigraphy of Cretaceous chalk – marl sequences. In Caldiwell, W. G. E. & Kauffman, E. G. (eds), Evolution of the Western Interior Basin, *Geological Association of Canada Special Paper* **39** 283 – 295.
- FLEISCHER, M. & ALTSCHULER, Z. S. 1969. The relationship of the rare-earth element composition of minerals to geological environment. *Geochimica e Cosmochimica Acta* **33** 725 – 732.
- GALE, A. S. 1980. Penecontemporaneous folding, sedimentation and erosion in Campanian Chalk near Portsmouth, England. *Sedimentology* **27** 137 – 51.
- GALE, A. S. 1990. A Milankovitch scale for Cenomanian time. *Terra Nova* **1** 420 – 425.
- GALE, A. S. 1995. Cyclostratigraphy and correlation of the Cenomanian of western Europe. In House, M. R. & Gale, A. S.(eds), *Orbital forcing timescales and cyclostratigraphy*, Geological Society Special Publication **85** 177 – 197.

- GALE, A. S. 1996. Turonian correlation and sequence stratigraphy of the Chalk in southern England. From Hesselbo, S. P. & Parkinson, D. N.(eds) *Sequence Stratigraphy in British Geology*, Geological Society Special Publication 103 177 – 195.
- GALE, A. S. & WOODROOF, P. B. 1981. A Coniacian ammonite from the 'Top Rock' in the Chalk of Kent. *Geological Magazine* 118 557 – 560.
- GALE, A. S., WOOD, C. J. & BROMLEY, R. G. 1987. The lithostratigraphy and marker bed correlation of the White Chalk (Late Cenomanian-Campanian) of southern England. *Mesozoic Research* 1 107 – 18.
- GALE, A. S., JENKYNS, H. C., KENNEDY, W. J. & CORFIELD, R. M. 1993. Chemostratigraphy v biostratigraphy: Data from around the Cenomanian – Turonian boundary. *Journal of the Geological Society* 150 29 – 32.
- GALE, A. S., MONTGOMERY, P., KENNEDY, W. J., HANCOCK, J. M., BURNETT, J. A. & MCARTHUR, J. M. 1996. Definition and global correlation of the Santonian – Campanian boundary. *Terra Nova* 7 611 – 622.
- GALLOIS, R. W. & MORTER, A. A. 1975. Unpublished IGS report on the lithology of the Trunch Borehole.
- GALLOIS, R. W. & MORTER, A. A. 1976. IGS boreholes 1975. IGS report 76/10.
- GODWIN-AUSTEN, R. 1858. On a boulder of granite found in the White Chalk near Croydon, and the extraneous rocks from that formation. *Quarterly Journal of the Geological Society of London* 14 252 – 266.
- GRADSTEIN, F. M., AGTERBERG, F. P., OGG, J. G., HARDENBOL, J., VAN VEEN, P., THIERRY, J. & HUANG, Z. 1994. A Mesozoic time scale. *Journal of Geophysical Research* 99 B12 24,051 – 24,074.
- GRADSTEIN, F. M., AGTERBERG, F. P., OGG, J. G., HARDENBOL, J., VAN VEEN, P., THIERRY, J. & HUANG, Z. 1995. A Triassic, Jurassic and Cretaceous Timescale. In *Geochronology, time scales and global stratigraphic correlation*, Society of Economic Palaeontologists and Mineralogists Special Publication 54 95 – 126.

- GUIRAUD, R. & BOSWORTH, W. 1997. Senonian basin inversion and rejuvenation of rifting in Africa and Arabia: synthesis and implications to plate-scale tectonics. *Tectonophysics* **282** 39 – 82.
- HANCOCK, J. M. 1975. The petrology of the Chalk. *Proceedings of the Geologists' Association* **86** 499 – 535.
- HANCOCK, J. M. 1990. Sea-level changes in the British region during the late Cretaceous. *Proceedings of the Geologists' Association* **100** 565 – 94.
- HANCOCK, J. M. 1993a. Transatlantic correlations in the Campanian – Maastrichtian stages by eustatic changes in sea level. In Hailwood & Kidd (eds) High Resolution Stratigraphy, *Geological Society Special Publication* **70** 241 – 256.
- HANCOCK, J. M. 1993b. Comments on the EXXON cycle chart for the Cretaceous system. *Cuadernos de Geologica Iberica* **17** 57 – 78.
- HANCOCK, J. M. & KAUFFMAN, E. G. 1979. The great transgressions of the late Cretaceous. *Journal of the Geological Society* **136** 175 – 186.
- HANCOCK, J. M. & GALE, A. S. 1996. The Campanian Stage. *Bulletin de l'Institut Royal des Sciences Naturelles de Belgique. Sciences de la Terre* **66 – Supp.** 103 – 109.
- HAQ, B. U., HARDENBOL, J. & VAIL, P. R. 1988. Mesozoic and Caenozoic chronostratigraphy and cycles of sea-level change. In Wilgus, C.K. *et al.* (eds) *Sea-level Changes: an Integrated Approach*. Society of Economic Palaeontologists and Mineralogists Special Publication **42** 71 – 108.
- HARLAND, W. B., COX, A. V., LLEWELLYN, P. G., PICKTON, C. A. G., SMITH, A. G. & WALTERS, R. 1982. A Geologic Timescale. Cambridge University Press, Cambridge, 131pp.
- HARLAND, W. B., ARMSTRONG, R. L., COX, A. V., CRAIG, I. E., SMITH A. G. & SMITH D. G. 1989. A Geologic Timescale. Cambridge University Press, Cambridge, 265pp.
- HART, M. B. 1987. Orbitally Induced cycles in the chalk facies of the United Kingdom.

- Cretaceous research* 8 335 – 348.
- HART, M. B., BAILEY, H. W., CRITTENDEN, S., FLETCHER, B. N., PRICE, R. J. & SWIECICKI, A. 1989. Cretaceous. In Jenkyns, D.G. & J.W. Murray (eds), *Stratigraphical Atlas of fossil foraminifera*, 2nd Ed. Chapter 7, 273 – 371. Chichester, England.
- HASKIN, L. A. & GEHL, M. A. 1962. The rare-earth distribution in sediments, *Journal of Geophysical Research* 67 2537 – 2541.
- HASKIN, L. A., WILDEMAN, T. R., FREY, F. A., COLLINS, K. A. KEEDY, C. R. & HASKIN, M. A., 1966. Rare-earths in sediments. *Journal of Geophysical Research* 71 6091 – 6105.
- HAY, W. W. 1993. Physical oceanography and water masses in the Cretaceous Western Interior Seaway. In Caldiwell, W. G. E. & Kauffman, E. G. (eds), Evolution of the Western Interior Basin, *Geological Association of Canada Special Paper* 39 297 – 318.
- HAYS, J. D., PITMAN III, W. C. 1973. Lithospheric plate motion, sea level changes and climatic and ecological consequences. *Nature* 246 November 2, 1973.
- HERBIN, J. P., MONTADERT, L., MULLER, C., GOMEZ, R., THUROW, J. & WIEDMANN, J. 1986. Organic-rich sedimentation at the Cenomanian-Turonian boundary in oceanic and coastal basins in the North Atlantic and Tethys. In Summerhayes, C. P. and Shackleton, N. J. North Atlantic palaeoceanography, *Geological Society Special Publication* 21 389-422.
- HESELBO, S. P. & PARKINSON, D. N. 1996. Sequence stratigraphy in British Geology. *Geological Society Special Publication* 103.
- D'HONDT, S. ^{and Arkani, M. A.} 1996. Late Cretaceous oceans and the cool tropic paradox. *Science* 271 1838 – 1841.
- HOUSE, M. R. 1995. Orbital forcing timescales: an introduction. In House, M. R. & Gale A. S. (eds), *Orbital Forcing Timescales and Cyclostratigraphy*, Geological Society Special

- Publication 85 1 – 18.
- HOWELL, J. A. & AITKEN J. F. ^(eds) 1996. High resolution sequence stratigraphy: innovations and applications. *Geological Society Special Publication* 104.
- HUNT, D. & TUCKER, M. E. 1993. Sequence stratigraphy of carbonate shelves with an example from the mid-Cretaceous (Urgonian) of south-east France. *Special Publication of the International Association of Sedimentologists* 18, 307 – 341.
- IZETT, G. A. 1981. Volcanic ash beds - recorders of the Upper Cenozoic silicic pyroclastic volcanism in the western United States. *Journal of Geophysical Research* 86 200.
- JARVIS, I. 1980a. Unpublished D. Phil. Thesis, University of Oxford.
- JARVIS, I. 1980b. The initiation of phosphatic chalk sedimentation — the Senonian (Cretaceous) of the Anglo-Paris Basin. *Society of Economic Mineralogists and Palaeontologists Special Publication* 29 167 – 192.
- JARVIS, I. 1980c. Geochemistry of phosphatic chalks and hardgrounds from the Santonian to early Campanian (Cretaceous) of northern France. *Journal of the Geological Society* 137 705 – 721.
- JARVIS, I. 1992. Sedimentology, geochemistry and origin of phosphatic chalks: the Upper Cretaceous deposits of Northwest Europe. *Sedimentology* 39 55 – 97.
- JARVIS, I. & WOODROOF, P. B. 1981. The phosphatic chalks and hardgrounds of Boxford and Winterbourne, Berkshire - two tectonically controlled facies in the late Coniacian to early Campanian (Cretaceous) of southern England. *Geological Magazine* 118 175 – 187.
- JARVIS, I. & JARVIS, K. E. 1985. Rare-earth element geochemistry of standard sediments: a study using inductively coupled plasma spectrometry. *Chemical Geology* 53 335 – 344.
- JARVIS, I. & TOCHER, B. A. 1987. Field Meeting: the Cretaceous of south east Devon, 14th - 16th March, 1986. *Proceedings of the Geologists' Association* 98 51 – 66.
- JARVIS, I., GALE, A. S. & CLAYTON, C. 1982. Litho- and biostratigraphical observations

- on the type sections of the Craie-de-Villedieu Formation (Upper Cretaceous, western France). *Newsletters on Stratigraphy* **11** 64 – 82.
- JARVIS, K. E. 1988. Inductively coupled plasma mass spectrometry: a new technique for the rapid or ultra-trace level determination of the rare-earth elements in geological materials. *Chemical Geology* **68** 31 – 39.
- JEANS, C. V., LONG, D., HALL, M. A., BLAND, D. J. & CORNFORD, C. 1991. The geochemistry of the Plenus Marls at Dover, England: evidence of fluctuating oceanographic conditions and of glacial control during the development of the Cenomanian – Turonian $\delta^{13}\text{C}$ anomaly. *Geological Magazine* **128** 603 – 632.
- JELETZKY, J. A. 1971. Marine Cretaceous biotic provinces and palaeogeography of western and Arctic Canada illustrated by a detailed study of ammonites. *Paper of the Geological Survey of Canada* **70** 1 – 92.
- JENKYNS, H. C. 1980. Cretaceous anoxic events: from continents to oceans. *Journal of the Geological Society* **137** 171 – 188.
- JENKYNS, H. C., GALE, A. S. & CORFIELD, R. M. 1994. Carbon- and oxygen-isotope stratigraphy of the English Chalk and Italian Scaglia and its palaeoclimatic significance. *Geological Magazine* **131** 1 – 34.
- JEWELL, P. W. 1993. Water column stability, residence times and anoxia in the Cretaceous North American seaway. *Geology* **21** 579 – 582.
- JEWELL, P. W. 1996. Circulation, salinity and dissolved oxygen in the Cretaceous North American Seaway. *American Journal of Science* **296** 1093 – 1125.
- KARNER, G. D., LAKE, S. D. & DEWEY, J. F. 1987. The thermal and mechanical development of the Wessex Basin, southern England. From Coward, M. P., Dewey, J. F. & Hancock, P. L. (eds), 1987. *Continental Extensional Tectonics*, Geological Society Special Publication **28** 517 – 536.
- KENNEDY, W. J. 1984. Ammonite faunas and the 'standard zones' of the Cenomanian to Maastrichtian stages in their type areas, with some proposals for the definition of stage

- boundaries by ammonites. *Bulletin of the Geological Society of Denmark* **33** 147 – 161.
- KNOTT, S. D., BURCHELL, M. T., JOLLEY, E. J. & FRASER, A. J. 1993. Mesozoic to Cenozoic plate reconstructions of the North Atlantic and hydrocarbon plays of the Atlantic margins. From Parker, R. J. (ed) *Petroleum Geology of north-west Europe*. Proceedings of the 4th Conference. Geological Society, London. 953 – 974.
- KRISTOFFERSEN, Y. 1978. Sea-floor spreading and the early opening of the North Atlantic. *Earth and Planetary Science Letters* **38** 273 – 290.
- LAKE, S. D. & KARNER, G. D. 1987. The structure and evolution of the Wessex Basin, southern England: an example of inversion tectonics. *Tectonophysics* **137** 347 – 378.
- LAKE, R. D., MORTIMORE, R. N. & WOOD, C. J. 1987. Chapter 7 — Cretaceous: Chalk. In: *Geology of the Country around Lewes*. British Geological Survey Memoir Sheet 319.
- LAKE, R. D., MORTIMORE, R. N. & WOOD, C. J. 1988. Chapter 6 — Cretaceous: Chalk. In: *Geology of the Country around Brighton and Worthing*. British Geological Survey Memoir Sheet 318.
- LAMODA, M. A. & HANCOCK, J. M. 1996. The Santonian Stage and its substages. *Bulletin de l'Institut Royal des Sciences Naturelles de Belgique, Sciences de la Terre* **66-Supp.** 95 – 102.
- MCARTHUR, J. M., KENNEDY, W. J., GALE, A. S., THIRLWALL, M. F., CHEN, M., BURNETT, J. & HANCOCK, J. M. 1992. Strontium isotope stratigraphy in the late Cretaceous: Intercontinental correlation of the Campanian – Maastrichtian boundary. *Terra Nova* **4** 385 – 393.
- MCARTHUR, J. M., THIRLWALL, M. F., GALE, A. S., KENNEDY, W. J., BURNETT, J. A., MATTEY, D., LORD, A. R. 1993. Strontium isotope stratigraphy for the late Cretaceous: a new curve based on the English Chalk. In Hailwood, E. A. & Kidd, R. B. 1993. *High Resolution Stratigraphy*, Geological Society Special Publication **70**

- 195 – 209.
- MARCINOWSKI, R. 1974. The transgressive Cretaceous (Upper Albian through Turonian) deposits of the Polish Jura Chain. *Acta Geologica Polonica* **24** 117 – 220.
- MARTIN, E. A. 1897. Foreign boulders in the chalk. *Geological Magazine* **4** 169 – 170.
- MIALL, A. D. 1992. Exxon global cycle chart: An event for every occasion? *Geology* **20** 787 – 790.
- MITCHELL, S. F., PAUL, C. R. C. & GALE, A. S. 1993. Carbon isotopes and sequence stratigraphy. In Howell, J. A. & Aitken, J. F. (eds) *High Resolution Sequence Stratigraphy: Innovations and Applications*, Geological Society Special Publication **104** 11 – 24.
- MITCHUM, R. M. 1977. Seismic stratigraphy and global changes of sea-level, Part 1: Glossary of terms used in seismic stratigraphy. In Payton, C. E. (ed) *Seismic Stratigraphy — Applications to Hydrocarbon Exploration*. American Association of Petroleum Geologists' Memoir **26** 205 – 212.
- MORTIMORE, R. N. 1983. The stratigraphy and sedimentation of the Turonian – Campanian in the Southern Province of England. *Zitteliana* **10** 27 – 41.
- MORTIMORE, R. N. 1986. Stratigraphy of the Upper Cretaceous White Chalk of Sussex. *Proceedings of the Geologists' Association* **97** 97 – 139.
- MORTIMORE, R. N., 1987. Controls on Upper Cretaceous sedimentation in the South Downs, with particular reference to flint distribution. In Sieveking, G. de C. & Hart, M. B. *The Scientific Study of Flint and Chert*, Cambridge University Press, 1987. 21 – 42.
- MORTIMORE, R. N. & POMEROL, B. 1987. Correlation of the Upper Cretaceous white chalk (Turonian to Campanian) in the Anglo-Paris Basin. *Proceedings of the Geologists' Association* **98** 97 – 143.
- MORTIMORE, R. N. & POMEROL, B. 1991. Upper Cretaceous tectonic disruptions in a placid chalk sequence in the Anglo-Paris Basin. *Journal of the Geological Society*

- 148 391 – 404.
- MORTIMORE, R. N. & POMEROL, B. 1997. Upper Cretaceous tectonic phases and end Cretaceous inversion in the Chalk of the Anglo-Paris Basin. *Proceedings of the Geologists' Association* **108** 231 – 255.
- MURRAY, R. W., BUCHHOLTZ TEN BRINK, M. R., GERLACH, D. C., RUSS, G. P. III & JONES, D. L. 1992. Interoceanic variation in rare earth, major and trace element depositional chemistry of chert: Perspectives gained from the DSDP and ODP record. *Geochimica et Cosmochimica Acta* **56** 1897 – 1913.
- NEAL, J. E., STEIN, J. A. & GAMBER, J. H. 1995. Integration of the graphic correlation methodology in a sequence stratigraphic study: Examples from the North Sea Paleogene sections. In Mann, K. O. & Lane, H. R. (Eds.) *Graphic Correlation*. Society of Economic Paleontologists and Mineralogists Special Publication **53**, 95 – 113.
- NORTHOLT, A. J. G. & JARVIS, I. 1990. Phosphorite research and development. *Geological Society Special Publication* **52**.
- OBRADOVICH, J. D. & COBBAN, W. A. 1976. A time-scale for the late-Cretaceous of the Western Interior of North America. *Geological Society of Canada Special Paper* **13** 31 – 54.
- OSBORNE - WHITE, H. J. 1921. A short account of the geology of the Isle of Wight. *British Geological Survey Memoir*.
- OWEN, D. 1996. Interbasinal correlation of the Cenomanian Stage; testing the lateral continuity of sequence boundaries. From Howell, J. A. & Aitken J. F. (eds), *High Resolution Sequence Stratigraphy: Innovations and Applications*, Geological Society Special, Publication **104** 269 – 293.
- PACEY, N. R. 1983. Bentonites in the chalk of central eastern England and their relation to the opening of the northeast Atlantic. *Earth and Planetary Science Letters* **67** 48 – 60.

- PITMAN III, W. C. 1978. Relationship between eustacy and stratigraphic sequences of passive margins. *Geological Society of America Bulletin* **89** 1389 – 1403.
- POMEROL, B. 1985. The Turonian-Senonian (Coniacian) Boundary in the Anglo-Paris Basin, its correlation with the Turonian-Coniacian Boundary as defined in Southern France. *Newsletters on Stratigraphy* **14** 81 – 95.
- POMEROL, B. 1989. Tectonique et sédimentation. Exemples dans le sud du Bassin de Paris. *Géologie de la France* **3** 63 – 69.
- POMEROL, B. & MORTIMORE, R. N. 1990. Lithostratigraphie et cycles sédimentaires dans la Craie du bassin Anglo-Parisien. *Comptes Rendus Académie Science Paris*, **310** II 553 – 558.
- POMEROL, B., LAMBERT, B. & MANIVIT, H. 1985. Biozones de nannoplankton calcaire dans les craies stratotypiques du Campanien et du Sénonien. Implications biostratigraphiques. *Comptes Rendus Académie Science Paris*, **301** II 177 – 182.
- POMEROL, B., BAILEY, H. W., MONCIARDINI, C. & MORTIMORE, R. N. 1987. Lithostratigraphy and biostratigraphy of the Lewes and Seaford Chalks: A link across the Anglo-Paris Basin at the Turonian-Senonian boundary. *Cretaceous Research* **8** 289 – 304.
- PRATT, L. M., ARTHUR, M. A., DEAN, W. E. & SCHOLLE, P. A. 1993. Palaeo-oceanographic cycles and events during the late-Cretaceous in the Western Interior Seaway of North America. In Caldiwell, W. G. E. & Kauffman, E. G. (eds), Evolution of the Western Interior Basin, *Geological Association of Canada Special Paper* **39** 333 – 353.
- RAILSBACK, L. B. 1990. Influence of changing deep ocean circulation on the Phanerozoic oxygen isotope record. *Geochimica et Cosmochimica Acta* **54** 1501 – 1509.
- RAWSON, P. F., CURRY, D., DILLEY, F. C., HANCOCK, J. M., KENNEDY, W. J., NEALE, J. M., WOOD, C. J & WORSSAM, B. C. 1978. A correlation of Cretaceous rocks in the British Isles. *Special Report of the Geological Society* **9** 70pp.
- RENARD, M. 1986. Pelagic carbonate chemostratigraphy (Sr, Mg, ¹⁸O, ¹³C). *Marine*

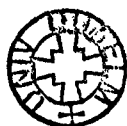
- Micropalaeontology* **10** 117 – 164.
- RESEARCH ON CRETACEOUS CYCLES RESEARCH GROUP 1986. Rhythmic bedding in Upper Cretaceous pelagic carbonate sequences: Varying sedimentary response to climatic forcing. *Geology* **14** 153 – 156.
- ROBASZYNSKI, F. & AMÉDRO F. 1980. Synthèse biostratigraphique de l'Aptien et Santonien du Boulonnais à partir de sept groupes paléontologiques. *Revue de Micropaléontologie* **22** 195 – 321.
- ROBASZYNSKI, F. & AMÉDRO F. 1986. The Cretaceous of the Boulonnais (France) and a comparison with the Cretaceous of Kent (United Kingdom). *Proceedings of the Geologists' Association* **97** 171 – 208.
- ROBASZYNSKI, F. & AMÉDRO F. 1986. Report of a field meeting to the Cretaceous of the Boulonnais, northern France 28 – 30/9/1984. *Proceedings of the Geologists' Association* **97** 209 – 212.
- ROBINSON, N. D. 1986. Lithostratigraphy of the Chalk Group of the North Downs, south-east England. *Proceedings of the Geologists' Association* **97** 141 – 170.
- ROBINSON, N. D. 1988. Upper Cretaceous Chalk in the North and South Downs, England: a reply. *Proceedings of the Geologists' Association* **98** 87 – 93.
- ROEST, W. R. & SRIVASTAVA, S. P. 1991. Kinematics of the plate-boundaries between Eurasia, Iberia and Africa in the North Atlantic from the Late Cretaceous to the present. *Geology* **19** 613 – 616.
- ROWE, A. W. 1902. The Zones of the White Chalk of the English Coast: I. Kent and Sussex. *Proceedings of the Geologists' Association* **16** 289 – 368.
- ROWE, A. W. 1903. The Zones of the White Chalk of the English Coast: II. Dorset. *Proceedings of the Geologists' Association* **17** 1 – 76.
- ROWE, A. W. 1904. The Zones of the White Chalk of the English Coast: III. Devon. *Proceedings of the Geologists' Association* **18** 1 – 51.
- ROWE, A. W. 1905. The zones of the White Chalk of the English Coast: IV. Yorkshire. *Proceedings of the Geologists' Association* **18** 193 – 296.

- ROWE, A. W. 1908. The Zones of the White Chalk of the English Coast: V. Isle of Wight. *Proceedings of the Geologists' Association* **20** 209 – 352.
- RUDDIMAN, W. F., SHACKLETON, N. J. & McINTYRE, A. 1986. North Atlantic sea-surface temperatures for the last 1.1 million years. In Summerhayes, C. P. & Shackleton, N. J. (eds) North Atlantic Palaeoceanography, *Geological Society Special Publication* **21** 155 – 173.
- SARG, J. F. 1988. Carbonate sequence stratigraphy. From Wilgus, C. *et al.* (eds) *Sea-Level Changes — An Integrated Approach*. Society of Economic Palaeontologists and Mineralogists Special Publication **42**, 155 – 181.
- SCHLAGER, W. 1991. Depositional bias and environmental change — important factors in sequence stratigraphy. *Sedimentary Geology* **70** 109 – 130.
- SCHLANGER, S. O. & JENKYN, H. C. 1976. Cretaceous oceanic anoxic events: causes and consequences. *Geologie en Mijnbouw* **55** 179 – 184.
- SCHOLLE, P. A. & ARTHUR, M. A. 1980. Carbon isotope fluctuations in Cretaceous pelagic limestones: Potential stratigraphic and petroleum exploration tool. *American Association of Petroleum Geologists' Bulletin* **64** 67 – 87.
- SHANLEY, K. W. & McCABE, P. J. 1995. Sequence stratigraphy of Turonian – Santonian strata, Kaiparowits Plateau, southern Utah, U.S.A. Implications for regional correlation and foreland basin evolution. In Wagoner, J. C. VAN & BERTRAM, G. T. (eds). Sequence stratigraphy of foreland basin deposits. *AAPG Memoir* **64** 103 – 136.
- SHEPHARD-THORN, E. R. 1988. *Geology of the Country around Ramsgate and Dover*. British Geological Survey memoir Sheets 274 / 290.
- SMITH, A. J. & CURRY, D. 1975. The structure and geological evolution of the English Channel. *Philosophical Transactions of the Royal Society, London* **A279** 3 – 20.
- SPAETH, C., HOEFS, J. & VETTER, U. 1971. Some aspects of isotopic composition of belemnites and related palaeotemperatures. *Bulletin of the Geological Society of America* **82** 3139 – 3150.

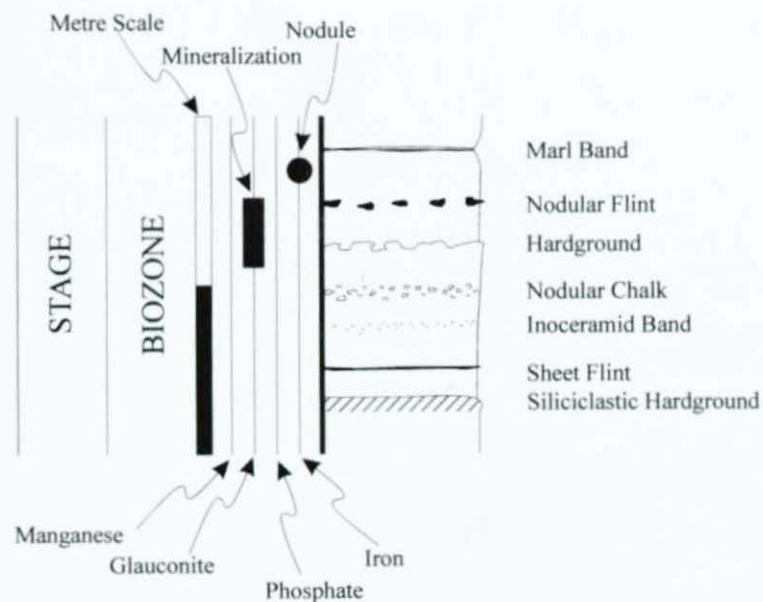
- SPICER, R. A. & PARRISH, J. T. 1990. Late-Cretaceous – early-Tertiary palaeoclimates of northern high latitudes: a quantitative view. *Journal of the Geological Society of London* **147** 329 – 341.
- SPICER, R. A., REES, P. McA & CHAPMAN, J. I. 1993. Cretaceous phytogeography and climate signals. *Philosophical Transactions of the Royal Society of London* **B341** 277 – 286.
- SRIVASTAVA, S. P. & TAPSCOTT, C. R. 1986. Plate kinematics of the North Atlantic. In *The Geology of North America Vol. M. The Western North Atlantic Region*. Chapter 23. The Geological Society of America, 1986.
- STEBBING, W. P. D. 1897. On two boulders of granite from the Middle Chalk of Betchworth, Surrey. *Quarterly Journal of the Geological Society of London* **53** 213 – 220.
- TEIS, R. V., CHUPAKHIN, M. S. & NAIDIN, D. P. 1957. Determination of palaeotemperatures from the isotopic composition of oxygen in calcite of certain cretaceous fossil shells from Crimea. *Geochemistry* **4** 323 – 329.
- TRÖGER, K. A. 1989. Problems of Upper Cretaceous inoceramid biostratigraphy and palaeobiology in Europe and western Asia. In Wiedmann, J. (ed) *Cretaceous of the Western Tethys*. 3rd International Cretaceous Symposium, 1987, Tubingen, Stuttgart, 1989. 911 – 930.
- UREY, H. C., LOWENSTAM, H. A., EPSTEIN, S. & MCKINNEY, C. R. 1951. Measurement of palaeotemperatures and temperatures of the Upper Cretaceous of England, Denmark, and the south-eastern United States. *Bulletin of the Geological Society of America* **62** 399 – 416.
- VAIL, P. R., AUDEMARD, F., BOWMAN, S. A., EISNER, P. N. & PEREZ-CRUZ, C. 1991. The Stratigraphic Signatures of Tectonics, Eustasy and Sedimentology — an Overview. Ch. 6.1 in Einsele *et al.* (eds), *Cycles and Events in Stratigraphy*. Springer-Verlag Berlin, Heidelberg 1991.
- VAIL, P. R., MITCHUM, R. M. & THOMPSON, S. III 1977. Seismic stratigraphy and global changes of sea-level, Part 4: Global cycles of relative changes of sea-level. In

- Payton, C. W. (Ed), *Seismic stratigraphy — Applications to Hydrocarbon exploration: American Association of Petroleum Geologists' Memoir* 26 83 – 97.
- VINCENT, E. & BERGER, W. H. 1985. Carbon dioxide and polar cooling in the Miocene: The Monterey Hypothesis. In Sundquist E. T. & Broecker, W. S. (eds) *The Carbon Cycle and Atmospheric CO₂: Natural Variations Archean to Present. Geophysical Monograph* 32.
- VAN WAGONER, J. C., POSAMENTIER, H. W., MITCHUM, R. M., VAIL, P. R., SARG, J. F., LOUITT, T. S. & HARDENBOL, J. 1988. An overview of the fundamentals of sequence stratigraphy and key definitions. From Wilgus, C. *et al.* (eds) *Sea-Level Changes — An Integrated Approach*. Society of Economic Palaeontologists and Mineralogists Special Publication 42 39 – 45.
- WATTS, A. B. 1982. Tectonic subsidence, flexure and global changes of sea-level. *Nature* 297 470 – 475. 10th June 1982.
- WEI, W. 1995. Revised age calibration points for the geomagnetic polarity timescale. *Geophysical Research Letters* 22 957 – 960.
- WESTHEAD, R. K. & WOODS, M. A. 1994. Anomalous Turonian-Campanian Chalk deposition in south Dorset; the influence of inherited pre-Albian structures. *Proceedings of the Geologists' Association* 105 81 – 89.
- WILDE, P. & BERRY, W. B. N. 1982. Progressive ventilation of the oceans - potential for return to anoxic conditions in the post- Paleozoic. In: Schlanger, S.O. (ed) *Nature and Origin of Cretaceous Carbon-rich facies*. 209 – 224.
- WILDE, P. & BERRY, W. B. N. 1986. The role of oceanographic factors in the generation of global bio- events. In Walliser, O. H., *Global bio-events*. Proceedings of the first meeting of IGCP Project 216, 75 – 91.
- WILDEMAN, T. R. & HASKIN, L. A. 1965. Rare-earth elements in ocean sediments. *Journal of Geophysical Research* 70 2905 – 2910.
- WILLIAMS, D. F., 1988. Evidence for and against sea-level changes from the stable isotope

- record of the Cenozoic. In Wilgus, C.K. *et al.* *Sea-Level Changes - An Integrated approach*, . Society of Economic Palaeontologists and Mineralogists Special Publication 42 31 – 36.
- WOO, K. S., ANDERSON, T. F., RAILSBACK, L. B. & SANDBERG, S. A. 1992. Oxygen isotopic evidence for high salinity surface seawater in the mid-Cretaceous Gulf of Mexico: implications for warm, saline deepwater formation. *Palaeoceanography* 7 673 – 685.
- WRAY, D. S. 1995. Origin of clay-rich beds in Turonian chalks from Lower Saxony, Germany — A REE study. *Chemical Geology* 119 161 – 173.
- WRAY, D. S. & WOOD, C. J. 1995. Geochemical identification and correlation of tuff layers in Lower Saxony, Germany. *Berliner geowiss. Abh.* E16 215 – 225.
- WRIGHT, E. K. 1987. Stratification and palaeocirculation of the late Cretaceous Western Interior Seaway of North America. *Geological Society of America Bulletin* 99 480 – 490.
- ZIEGLER, P. A. 1988. Evolution of the Arctic – North Atlantic and the Western Tethys. *AAPG Memoir* 43.
- ZIEGLER, P. A. 1990. Geological Atlas of Western and Central Europe. 1990.



Key to logs (Chapters 1 – 6 and Appendices A, B & D)



- | | |
|---------------------|--------------------------|
| △ Echinoid | ⊗ Abundant fossil debris |
| ∟ Echinoid Spine | ∇ Sponge |
| ○ Bivalve | ⊖ Porispherid sponge |
| — Inoceramid debris | ⊕ Bryozoa |
| ∪ Brachiopod | ☆ Crinoid |
| — Belemnite | ⊕ Gastropod |
| ⊙ Ammonite | ∪ Serpulid |
| ∞ Fish debris | ⊕ Coral |

∟ *Thalassinoides*

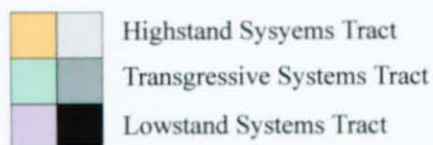
∞ *Planolites*

∞ *Chondrites*

∞ *Zoophycos*

∇ Borings

● Nodules



Localities are described in Chapters 2 – 4 under the following sequence headings.

Beauval:	Sequences Sa1 – Sa7
Charnage Down:	Sequences Co1 & Co2
Compton Abbas:	Sequences Co1 & Co2
Coquelles:	Sequences Sa1 – Sa3
Culver Cliff:	Sequences Co1 – Ca14
East Kent Coast:	Sequences Co1 – Sa7
Loir:	Sequences Co1 – Sa7
Pinhay:	Sequences Co1 – Co4
Précy-sur-Oise:	Sequences Ca3 – Ca14
Reed:	Sequences Co1 & Co2
Seaford Head:	Sequences Co1 – Ca9
Shoreham Cement Works:	Sequences Co2 – Co6
Taplow:	Sequences Sa4 – Sa7
Triguères:	Sequences Co4 – Co7
Trunch borehole:	Sequences Co1 – Ca14

